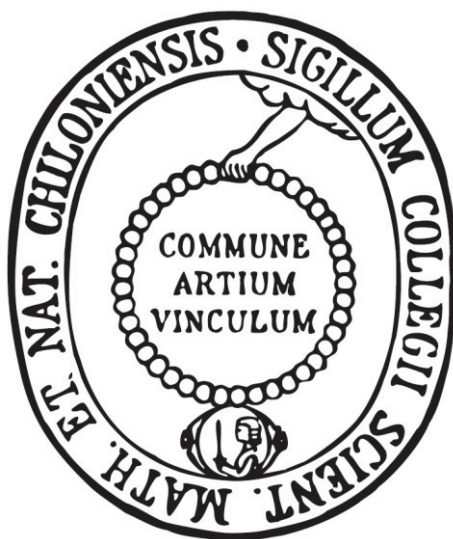

Main Group Heterocycles for Semiconducting Polymers



Dissertation

zur Erlangung des Doktorgrades

der Mathematisch-Naturwissenschaftlichen Fakultät

der Christian-Albrechts-Universität zu Kiel

vorgelegt von

Julian Linshöft

Kiel 2014

1. Gutachterin: Prof. Dr. Anne Staubitz

2. Gutachter: Prof. Dr. Ulrich Lüning

Tag der mündlichen Prüfung: 24. November 2014

Zum Druck genehmigt: 24. November 2014

gez. Prof. Dr. Wolfgang J. Duschl, Dekan

Die vorliegende Arbeit wurde unter Anleitung von
Prof. Dr. Anne Staubitz
am Otto-Diels-Institut für Organische Chemie
der Christian-Albrechts-Universität zu Kiel
in der Zeit von Mai 2011 bis Oktober 2014 angefertigt.

Hiermit erkläre ich, Julian Linshöft, an Eides statt, dass ich die vorliegende Dissertation selbstständig und nur mit den angegebenen Hilfsmitteln angefertigt habe. Inhalt und Form dieser Arbeit sind, abgesehen von der Beratung durch meine Betreuerin Prof. Dr. Anne Staubitz, durch mich eigenständig erarbeitet und verfasst worden. Die Arbeit entstand unter Einhaltung der Regeln guter wissenschaftlicher Praxis der Deutschen Forschungsgemeinschaft. Weder die gesamte Arbeit noch Teile davon habe ich an anderer Stelle im Rahmen eines Prüfungsverfahrens eingereicht. Dies ist mein erster Promotionsversuch.

Kiel, den 2. Oktober 2014

(Julian Linshöft)

Danksagung

An dieser Stelle möchte ich mich bei all denen bedanken, die dazu beigetragen haben, dass ich diese Arbeit fertigstellen konnte.

Dazu gehört an erster Stelle die Unterstützung, die in direktem Zusammenhang zu dieser Arbeit steht: Vielen Dank an Prof. Dr. Anne Staubitz! Danke für das spannende und fordernde Thema sowie die ausgezeichnete und immer sehr engagierte Betreuung und Beratung. Vielen Dank für das Vertrauen in mich und all die gewährten Freiheiten.

Ein großes Dankeschön geht auch an die Deutsche Bundesstiftung Umwelt (DBU), die meine Promotion über 3 Jahre finanziert hat. Die Seminare (und die Verleihungen der Umweltpreise, Woche der Umwelt, ...) jedes Jahr waren nicht nur sehr lehrreich, sondern haben wirklich viel Spaß gebracht und ich habe viele nette Menschen kennengelernt.

Prof. Dr. Ulrich Lüning möchte ich für die Übernahme des Zweitgutachtens danken. Diese Arbeit wäre außerdem nicht möglich gewesen ohne die Mitarbeiter dieses Instituts: Danke, dass ihr immer so bereitwillig und hervorragend geholfen habt, auch wenn man mal bei einem „Spezialfall“ Hilfe benötigte. Vielen Dank an Prof. Dr. Frank Sönnichsen für die Hilfe bei dem einen oder anderen verwirrenden Spektrum, und dafür, dass Sie immer bereitwillig neue Kerne eingerichtet haben. Danke an die gesamte spektroskopische Abteilung für die Messungen all dieser Spektren! Vielen Dank auch an Prof. Dr. Christian Näther und seine Mitarbeiter für die Röntgenstrukturanalysen. Ich danke außerdem Tobias Tellkamp für das Korrekturlesen dieser Arbeit. I would like to thank Dr. Paul Gates for all the high resolution mass spectra. Many thanks to my interns Stephan Segler, Evan Baum, Andreas Hussain and Nils Lüdecke: thanks for all your work and the fun time we spent together!

Den gesamten Arbeitskreisen Staubitz und Sönnichsen danke ich für die sehr schöne und witzige Zeit, die wir beim Arbeiten, beim Essen und auch zwischendurch miteinander verbracht haben. Meiner Laborkollegin Annika Heinrich möchte ich zusätzlich für die sehr gute Zusammenarbeit über all die Jahre in unserem kleinen Labor danken.

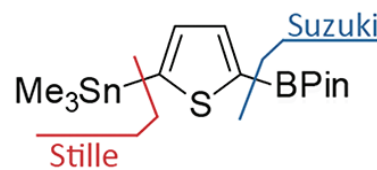
Viele Leute haben mich auch eher indirekt beim Gelingen dieser Arbeit unterstützt: immer wenn ich Abwechslung brauchte, habt ihr für sie gesorgt – und zum Glück auch dann, wenn man eigentlich gar keine Abwechslung brauchte :) Vielen lieben Dank an meine Freunde für die wundervolle Zeit! Danke an meine Familie für den Rückhalt und das Verständnis, wenn ich mal keine Zeit für euch hatte.

Grace, ich habe keine Ahnung, wer ich wäre, wo ich wäre und wie ich wäre, wenn ich dich nicht (kennengelernt) hätte. Vielen Dank, dass ich es nicht herausfinden musste :)

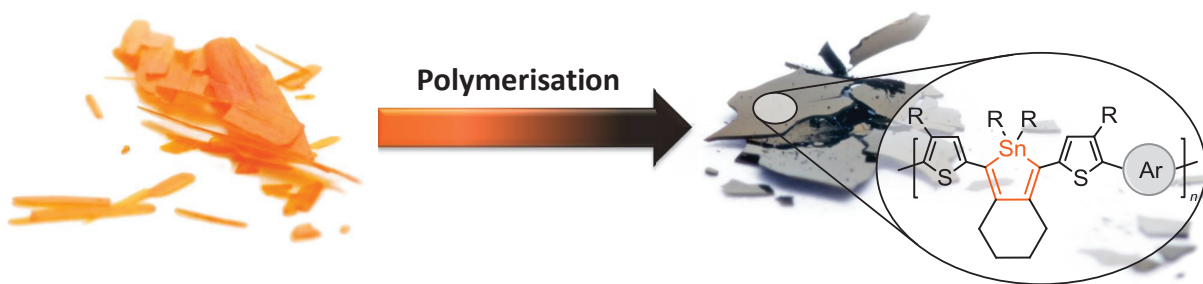
Achja, und vielen Dank an den/die Mitarbeiter/in aus dem Studierendensekretariat: hätten Sie damals nicht so eine nette Antwortkarte geschrieben, dass meine Bewerbungsunterlagen für den Studiengang gut angekommen sind, hätte ich vielleicht einen anderen Studienort gewählt.

Zusammenfassung

In dieser Arbeit wurde das Konzept der Nucleophil-selektiven Kreuzkupplung entwickelt und auf Thiophen, welches ein klassischer Baustein für halbleitende Polymere ist, angewendet. Zwei Metallfunktionalitäten unterschiedlicher



Reaktivität wurden an den Heteroaromaten angebracht - eine Zinn-Gruppe und ein Borester. Diese neue Verbindung ermöglichte Nucleophil-selektive Kreuzkupplungsreaktionen in hohen Ausbeuten: Im ersten Schritt läuft die Stille-Reaktion ab, während im zweiten Schritt nach der Zugabe eines weiteren Elektrophils, Wasser und einer Base die Suzuki-Kreuzkupplung stattfindet. Die Vielseitigkeit der Reaktion wurde an Hand von elektronenneutralen, elektronenreichen und elektronenarmen Elektrophilen gezeigt.



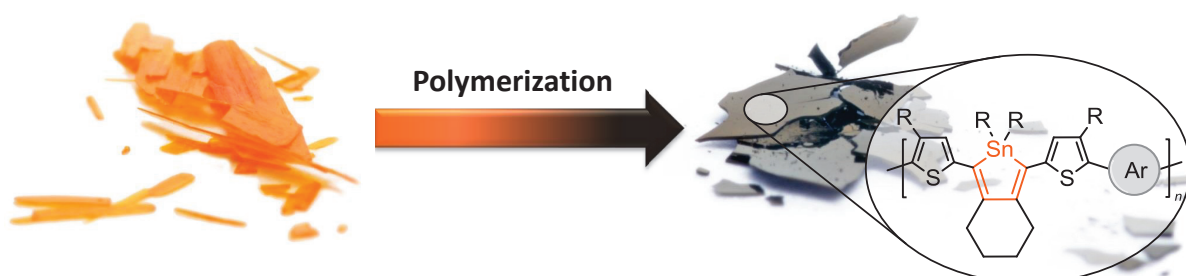
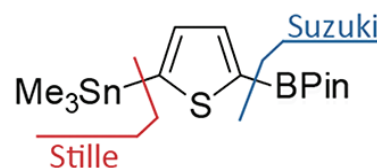
Eine Syntheseroute zu Stannolmonomeren des AA-Typs wurde entwickelt und das erste stannolhaltige halbleitende Polymer wurde hergestellt. Für die Polymerisation wurde die Stille-Kreuzkupplung verwendet, wobei das Problem, dass der Stannolring unter diesen Reaktionsbedingungen reagieren könnte, durch sterische Abschirmung des Stannolrings verhindert wurde. Dies führte zu einer Nucleophil-selektiven Kreuzkupplung, die zwischen zwei Zinnfunktionalitäten unterscheiden kann. Der Erfolg der Polymerisation wurde durch NMR-Spektroskopie, MALDI Massenspektrometrie, GPC und UV/Vis Messungen bestätigt. Die Stannole haben sich als Heterocyclen mit einem hohen Potential für halbleitende Polymere herausgestellt, da sie starke bathochrome Verschiebungen in den Absorptionsspektren zeigen.

Ein Stannolmonomer vom AB-Typ wurde für eine Kettenwachstumspolymerisation hergestellt und polymerisiert. Das erhaltene Polymer war schwerlöslich und eine Untersuchung der Kinetik war nicht möglich.

Wichtige Schritte auf dem Weg zum ersten Polymer mit einem antiaromatischen Borol wurden unternommen. Hierfür wurde ein stark abgeschirmtes Zirconacyclopentadien regioselektiv hergestellt.

Abstract

The concept of nucleophile selective cross-coupling reactions was developed for thiophene, a motif that is typically used in semiconducting polymers. Two metal functional groups of different reactivity were attached to the heteroaromatic compound, a stannyl group and a boronic ester. This new compound allowed high yielding, fully nucleophile selective cross-coupling reactions, where the Stille reaction occurs first, and in a second step, after adding another electrophile, water and a base, the Suzuki cross-coupling reaction takes place. The versatility of the reaction was shown with electron rich, electron neutral and electron poor electrophiles.



A synthetic route to AA-type stannole monomers was developed, and the first stannole containing semiconducting polymer was synthesized. The Stille cross-coupling reaction was used for the polymerization, and the problem that the stannole ring could react under these conditions was eliminated by steric shielding of the stannole ring. This led to nucleophile selective cross-coupling reactions that distinguish between two stannyl functionalities. The success of the polymerization was proved by NMR spectroscopy, MALDI spectrometry, GPC and UV/Vis measurements. The stannoles have a high potential as heterocycles for semiconducting polymers, as they caused strong bathochromic shifts in the absorption spectra.

An AB-type stannole monomer for a polymerization that may proceed via a chain-growth mechanism was developed and polymerized. The obtained polymer was poorly soluble and an investigation of the kinetics was impossible.

Major steps on the way to the first polymer containing an antiaromatic borole were undertaken. For this purpose, the regioselective formation of a highly shielded zirconacyclopentadiene was achieved.

Abbreviations

ATR	attenuated total reflectance
calcd.	calculated
COSY	correlated spectroscopy
Cp	cyclopentadienyl
CV	column volume
d	doublet (NMR)
DCM	dichloromethane
DMF	dimethylformamide
DMSO	dimethyl sulfoxide
EI	electron ionization
ESI	electrospray ionization
FT	Fourier transform
GPC	gel permeation chromatography
HH	head-to-head
HMBC	heteronuclear multiple bond coherence
HOMO	highest occupied molecular orbital
HRMS	high resolution mass spectrometry
HSQC	heteronuclear single quantum coherence
HT	head-to-tail
IR	infrared
LDA	lithium diisopropylamide
LUMO	lowest unoccupied molecular orbital
m	medium (concerning the intensity) (IR)
m	multiplet (NMR)
M.p.	melting point
MALDI	matrix-assisted laser desorption/ionization
MW	microwave
NIS	<i>N</i> -iodosuccinimide
NMR	nuclear magnetic resonance
OFET	organic field effect transistor
OLED	organic light emitting diode
ORTEP	oak ridge thermal ellipsoid plot
OSC	organic solar cell
P3AT	poly(3-alkyl)thiophene
PA	polyacetylene
PDI	polydispersity index
PE	polyethylene
PEDOT	polyethylene dioxythiophene
PPP	polyparaphenylene
PPV	polyparaphenylene vinylene
PPy	polypyrrole
pyr	pyridine
R _f	retardation factor
RFID	radio frequency identification
rr	regioregular
s	strong (concerning the intensity) (IR)
s	singlet (NMR)
TEA	triethylamine
THF	tetrahydrofuran
TLC	thin layer chromatography
TMS	tetramethylsilane

TOF	time-of-flight
TT	tail-to-tail
UV	ultraviolet
Vis	visible

Abbreviations for building blocks in polymer names:

B	benzothiadiazole
St	stannole
T	thiophene

A Guide to this Thesis

This thesis is divided into 5 chapters (see table of contents). Most of the results in this thesis have been published in peer reviewed journals, and the original publications can be found in the subsections of chapter 3, “Results and Discussion”. The “Supporting Information” that belongs to each publication, including all the experimental data, can be found in the subsections of chapter 5, “Experimental Section”. As every publication has its own introduction, chapter 1 (“Introduction”) provides some general information on the topic of semiconducting polymers.

A continuous numbering of all molecules in this thesis was impossible, since every publication has its own numbering. To avoid that a molecule has two different numbers, molecules from a publication are described as “**PX-Y**” in the text, where P stands for “publication”, with X = number of subsection where the publication appears and Y = number of the molecule in the respective publication. For example, one stannole monomer has the number **9** in *Angew. Chem.* **2014**. This publication can be found in subsection 2 of “Results and Discussion”, so the numbering used in the other parts of the thesis is **P2-9**.

Table of Contents

1 Introduction.....	1
1.1 Semiconducting Polymers	2
1.2 Syntheses of Semiconducting Polymers.....	6
1.3 Boroles.....	9
2 Objectives	11
3 Results and Discussion.....	13
3.1 Chemoselective Cross-Coupling Reactions (<i>Org. Lett.</i> 2012 , <i>14</i> , 5644-5647).....	13
3.2 Group 14/16 Heterocycles for Polycondensation Polymers	18
3.2.1 Stannole Containing Polymers	18
3.2.1.1 Stannole-Thiophene Copolymers (<i>Angew. Chem.</i> 2014 , <i>asap</i>).....	18
3.2.1.2 Stannole-Thiophene-Benzothiadiazole Copolymers	31
3.2.2 Further Comparison of Stannole Containing Polymers (<i>Acta Cryst.</i> 2014 , <i>E70</i> , o1133-o1134).....	33
3.3 Stannole Monomers for Chain Growth Polymerizations	39
3.4 Rosenthal's Zirconocene – a Versatile Reagent (<i>Synlett</i> 2014 , <i>asap</i>)	46
3.5 Boroles.....	49
4 Summary and Outlook.....	54
5 Experimental Section.....	58
5.1 Supporting Information for <i>Org. Lett.</i> 2012 , <i>14</i> , 5644-5647	58
5.2 Supporting Information for <i>Angew. Chem.</i> 2014 , <i>asap</i>	95
5.3 Supporting Information for <i>Acta Cryst.</i> 2014 , <i>E70</i> , o1133-o1134.....	137
5.4 General Methods and Materials for Unpublished Syntheses	137
5.4.1 Analyses	151
5.4.2 Chemicals.....	152
5.4.3 Solvents	153

5.4.4 Chromatography	153
5.5 Unpublished Syntheses	154
5.5.1 4,7-Bis(trimethylstannyl)benzo[c][1,2,5]thiadiazole (2).....	154
5.5.2 1,3-Bis(4-hexyl-5-(trimethylstannyl)thiophen-2-yl)-2,2-diphenyl-4,5,6,7-tetra- hydro-2 <i>H</i> -benzo[c]stannole (3)	155
5.5.3 7,7'-(5,5'-(2,2-Diphenyl-4,5,6,7-tetrahydro-2 <i>H</i> -benzo[c]stannole-1,3-diyl)bis- (3-hexylthiophene-5,2-diyl))bis(4-bromobenzo[c][1,2,5]thiadiazole) (TSStTB with $n = 1$).....	157
5.5.4 Polymer TTTT	159
5.5.5 2-(5-Iodothiophen-2-yl)-4,4,5,5-tetramethyl-1,3,2-dioxaborolane (6).....	160
5.5.6 4,4,5,5-Tetramethyl-2-(5-(octa-1,7-diyn-1-yl)thiophen-2-yl)-1,3,2-dioxa- borolane (7)	161
5.5.7 2-(5-(8-(5-Bromo-4-hexylthiophen-2-yl)octa-1,7-diyn-1-yl)thiophen-2-yl)- 4,4,5,5-tetramethyl-1,3,2-dioxaborolane (8)	162
5.5.8 1-(5-Bromo-4-hexylthiophen-2-yl)-2,2-diphenyl-3-(5-(4,4,5,5-tetramethyl- 1,3,2-dioxaborolan-2-yl)thiophen-2-yl)-4,5,6,7-tetrahydro-2 <i>H</i> -benzo[c]- stannole (10).....	163
5.5.9 Polymer TSSt	165
5.5.10 3-Hexyl-2-iodothiophene (11)	166
5.5.11 2-(4-Hexyl-5-iodothiophen-2-yl)-4,4,5,5-tetramethyl-1,3,2-dioxa- borolane (12)	167
5.5.12 3-Hexyl-2-(octa-1,7-diyn-1-yl)thiophene (14)	168
5.5.13 2-Bromo-3-hexyl-5-(8-(3-hexylthiophen-2-yl)octa-1,7-diyn-1-yl)- thiophene (15)	169
5.5.14 1-(5-Bromo-4-hexylthiophen-2-yl)-3-(3-hexylthiophen-2-yl)-2,2-diphenyl- 4,5,6,7-tetrahydro-2 <i>H</i> -benzo[c]stannole (16)	170
5.5.15 ((2,6-Dimethylphenyl)ethynyl)trimethylsilane (27).....	172
5.5.16 2-Ethynyl-1,3-dimethylbenzene (28).....	173

5.5.17	2-Bromo-5-((2,6-dimethylphenyl)ethynyl)-3-hexylthiophene (29)	174
5.5.18	2-((2,6-Dimethylphenyl)ethynyl)-4-hexylthiophene (30).....	175
5.5.19	3,4-Bis(2,6-dimethylphenyl)-2,5-bis(4-hexylthiophen-2-yl)-Cp ₂ ZrC ₄ (31).....	176
5.6	Single Crystal Data	177
5.6.1	3,4-Bis(2,6-dimethylphenyl)-2,5-bis(4-hexylthiophen-2-yl)-Cp ₂ ZrC ₄ (31).....	177
References	186

1 Introduction

Organic electronics, also called plastic electronics, offer major advantages over traditional inorganic electronics, because the best of two worlds can be combined: the electronic properties that are normally known from metals or semimetals, and the material properties of plastic. Thus, some general key advantages of organic electronics are that they can be produced as very thin films, and as lightweight, mechanically flexible materials.^[1] They offer the possibility to process them from solution in the form of inks by printing technologies, and they have the potential for cheap large-scale production.^[2] This leads not only to improved and cheaper materials, but new possibilities for applications are also created. How the strengths of organic electronics can be exploited show some examples of technologies that already exist or will be available in near future:

Organic light emitting diodes (OLEDs)^[3] are implemented in, for example, displays of smartphones. The mechanical flexibility of organic electronics will now be used to produce bent displays, extending the functionality of these devices (Figure 1, left).^[4] The low costs of organic electronics make it possible to produce radio frequency identification (RFID) tags (e. g. based on organic field effect transistors (OFETs)^[5]) for single-use: they can be used to label, identify and track products via radio waves, replacing the bar code.^[6] A new field of application has also been opened with organic solar cells (OSCs):^[7] in contrast to their inorganic counterparts, they can not only be produced very thin, lightweight and flexible, but also with a high degree of transparency, allowing applications like transparent car roofs or architectural windows, which are able to produce electricity. The company Heliatek is planning to establish a large scale market production in 2015.^[8]



Figure 1. Samsung uses the flexibility of OLEDs for bended displays, and the transparency of OSCs could find an application in for example car glass roofs (picture credits: press material Samsung^[9] and Heliatek^[10]).

In general, organic electronics can be made out of small molecule or polymeric semiconductors. Small molecule devices can generally be prepared in high purities by vacuum deposition techniques, while polymeric systems can be processed very easily by low-cost solution based techniques like spin-coating or ink-jet printing.^[2b]

1.1 Semiconducting Polymers

In 2000, the Nobel Prize for chemistry was awarded to Alan J. Heeger, Alan G. MacDiarmid and Hideki Shirakawa for the discovery and development of conducting polymers.^[11] They investigated polyacetylene (PA), a compound that was already known but had displayed no conductivity so far. By treatment of polyacetylene with vapors of iodine, bromine or chlorine, the material was oxidized and became conductive. This so-called “doping” led to a conductivity that is nearly comparable with the conductivity of inorganic metals,^[12] and intense interest in using these materials for electronic devices arose.^[13]

How is it possible that plastic becomes conductive, while it is normally used as an insulating material?

The electrical conductivity of solids can be explained by the band theory. A band consists of several closely spaced energy levels and can be partially, completely or not filled with electrons. Depending on the material, three different cases can be considered (Figure 2): In a material with a band gap of $E_g \approx 0$ eV, i. e. without a band gap, the electrons of the levels with the highest energy can easily be excited to unoccupied states of slightly higher energy, and the separated charges can move through the material – such a material is a conductor. In semiconductors, the highest band with electrons in the ground state is completely filled and called valence band. Separated by a band gap of $E_g < 3$ eV, an unoccupied band, called conduction band, is located higher in energy. Therefore, electrons need irradiation or thermal energy to overcome this gap and to lead to conduction in the semiconductor. However, the gap in insulators is too high ($E_g > 3$ eV) and cannot be overcome without damaging the material.^[14]

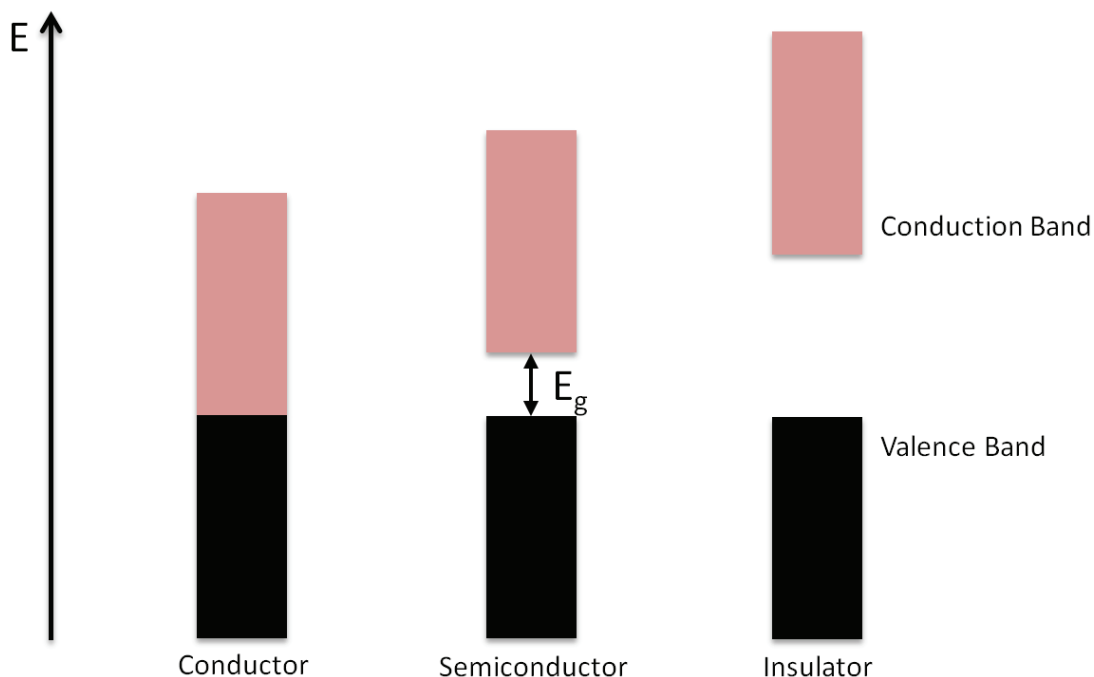


Figure 2. A conductor has no band gap, a semiconductor has a band gap of $E_g < 3$ eV and an insulator has a high band gap of $E_g > 3$ eV.

A standard insulating material like polyethylene (PE; used for plastic bags, bottles etc.) has a very high band gap of $E_g > 8$ eV,^[15] but doped polyacetylene is able to transport charges. The reason for this different behavior is the structure: the backbone of PE consists of carbon atoms that are connected by a single bond, while the carbon atoms of PA are connected by alternating single and double bonds (Figure 3).



Figure 3. Structures of insulating polyethylene and (semi)conducting polyacetylene.

The carbon atoms in polyacetylene are sp^2 -hybridized, which means that every carbon atom has three sp^2 -orbitals (forming three σ -bonds) and one p_z orbital (forming π -bonds). When the p_z orbitals of two carbon atoms are combined, they both split up into a bonding π (HOMO, highest occupied molecular orbital) and one antibonding π^* (LUMO, lowest unoccupied molecular orbital) molecular orbital (Figure 4). The two electrons occupy the orbital with the lower energy, the HOMO. When these molecular orbitals of such an ethylene motif are combined with the molecular orbitals of another ethylene motif, they split up again, forming two π and two π^* orbitals.

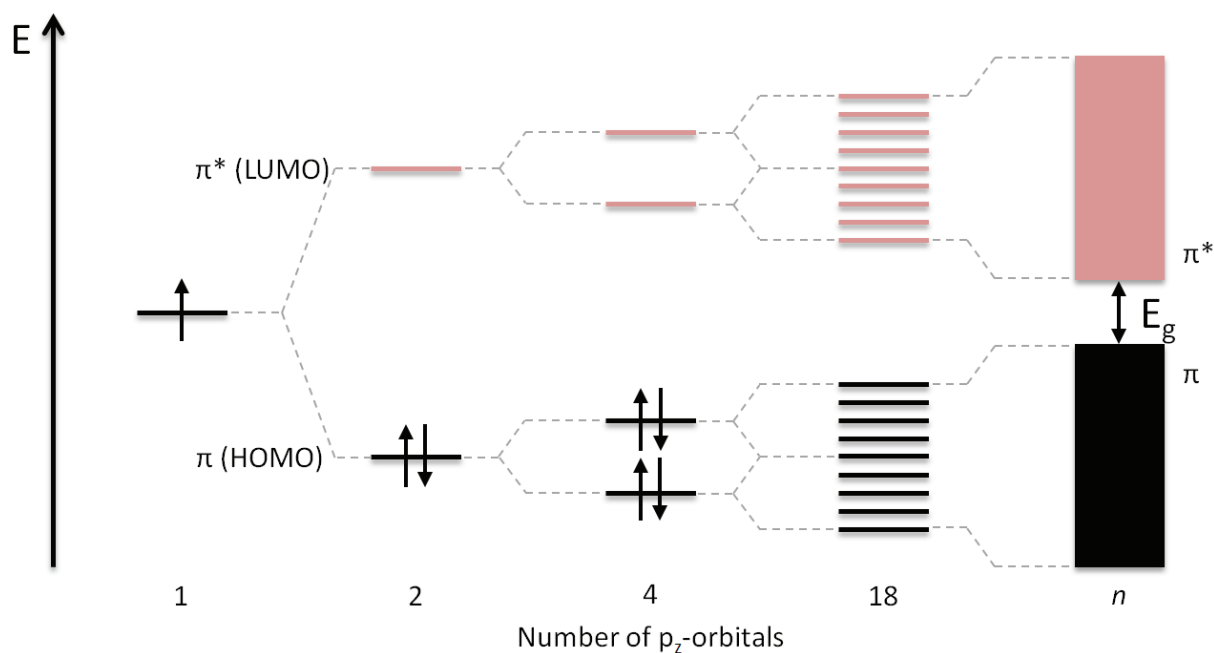


Figure 4. Schematic energy diagram: the combination of p_z -orbitals of sp^2 -hybridized carbon atoms leads towards smaller and smaller HOMO-LUMO gaps, until band structures are formed in semiconducting polymers.^[14]

When this process is repeated for all orbitals of a long polymer chain, it results in several closely spaced energy levels, forming a band like structure. The band that derived from the bonding π -orbitals (HOMOs) is equivalent to the valence band and is completely filled with electrons, while the band derived from the π^* -orbitals (LUMOs) can be considered as the unoccupied conduction band. Following this reasoning, one would expect that the band gap disappears for PA of high molecular weight. However, PA is a semiconductor: instead of a complete delocalization of the π -electrons, a bond-length alternation is found, which causes a small band gap E_g , separating the valence and conduction band. This is due to the Peierls distortion, which makes it energetically favorable to distort the geometry of the polymer backbone from entirely equal carbon-carbon bond lengths and to limit electron delocalization.^[16] Thus, PA is intrinsically not conductive. By oxidative doping with halogens, electrons are removed from the polymer and holes are created. A neighboring electron can move to this hole, and a new hole is created at the former position of the electron. By this process, the charges can move through the material, a new band is created near the conduction band (in the former band gap) and the material becomes conductive.

For typical semiconductor optoelectronic devices like organic solar cells or organic light emitting diodes, (semi)conducting polymers are not used in a permanently doped form; instead, a band gap is required and the properties of a “real synthetic metal” are undesired.

Different aromatic systems were investigated towards their use in semiconducting polymers, for example in polyparaphenylene,^[17] polyparaphenylene vinylene,^[18] polythiophene,^[19] polypyrrole,^[20] and polyethylene dioxythiophene^[21] (Figure 5).

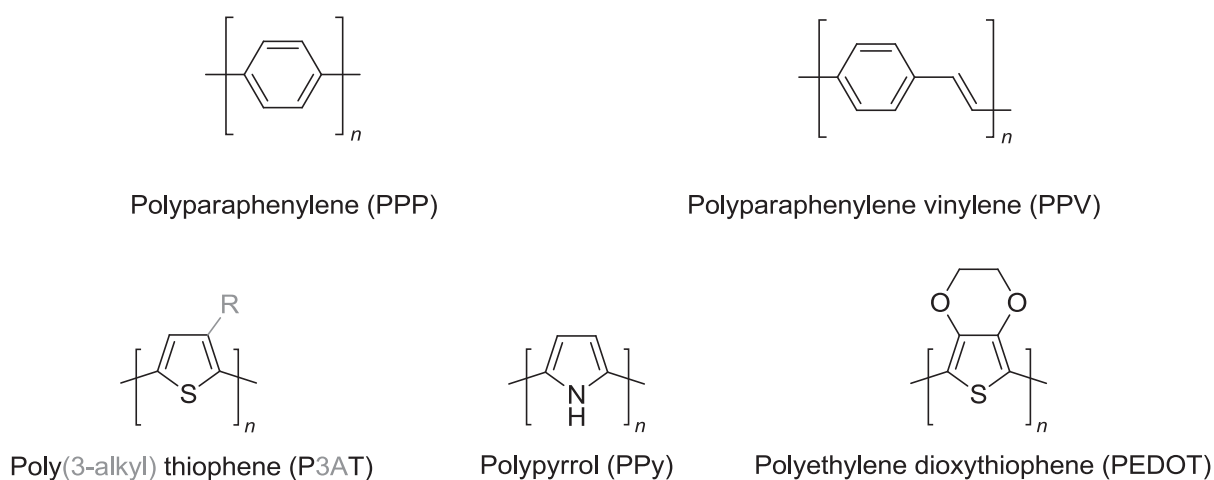


Figure 5. Some of the basic, more important semiconducting polymers.

Thiophene-based polymers emerged to be among the most promising ones for solar cells, because of their high stability, very good solubility of substituted derivatives, their processability and their comprehensive functionalization possibilities.^[22] The polymers are connected via the 2,5-positions, and the 3/4 positions are usually used for attaching solubilizing chains, for example *n*-hexyl chains in the prominent example of poly(3-hexylthiophene).^[7a]

Depending on the application, the band gap has to be adjusted to different levels. For this purpose, further advantages of organic materials come into play: they are highly adjustable in their structure, and the monomers can be varied with an infinitely wide range of functionalization possibilities. For highly efficient organic solar cells, a low band gap is needed to harvest the photons of the sun.^[23] In addition, the morphology of the material plays a critical role, e. g. for the charge carrier mobility.^[7a] The latest generation of semiconducting polymers addresses the problem of a low band gap by the combination of electron rich and electron deficient heterocycles, a common principle to lower E_g (Figure 6).^[24]

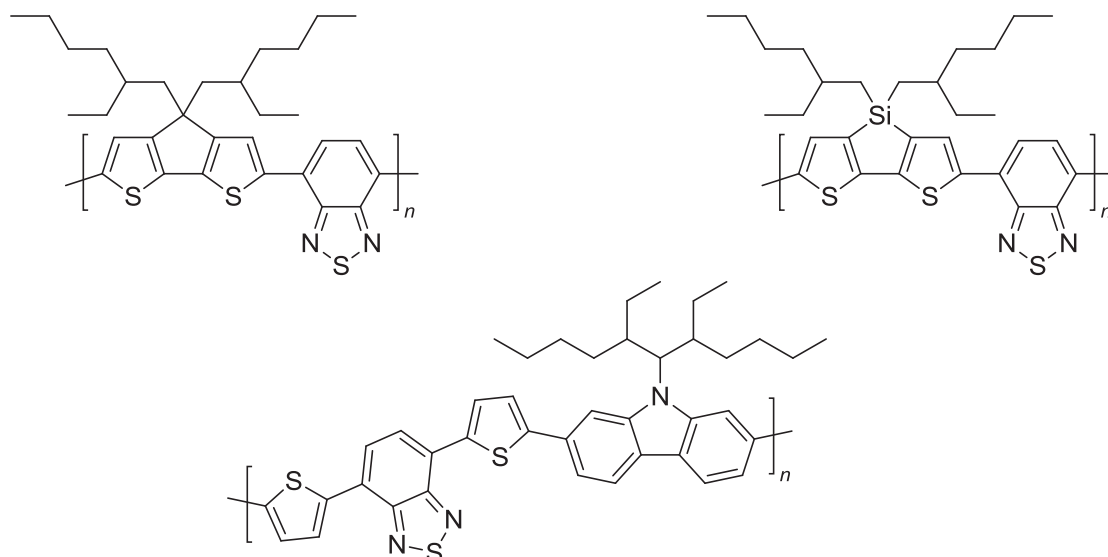


Figure 6. Some examples of the latest generation, low band gap semiconducting polymers.^[25]

1.2 Syntheses of Semiconducting Polymers

Different methods for the preparation of semiconducting polymers were used over the last decades. Polythiophenes were initially prepared without any substituents by Kumada type cross-coupling reactions, leading to insoluble polymers without the possibility to process the material.^[26] Later, thiophenes with flexible alkyl chains in the 3 position were used for polymerization.^[27] They were also prepared by cross-coupling methods or oxidative polymerization, and it was possible to obtain soluble poly(3-alkylthiophene)s (see also Figure 5). Although this addresses the solubility problem, it created a new one that arose with the flexible alkyl chains: regioirregular polymers were obtained. For example, oxidative electropolymerization or oxidative chemical polymerization with iron trichloride created random couplings of the monomers, and not only head-to-tail (HT), but also head-to-head (HH) and tail-to-tail (TT) couplings were found (Figure 7).^[28]

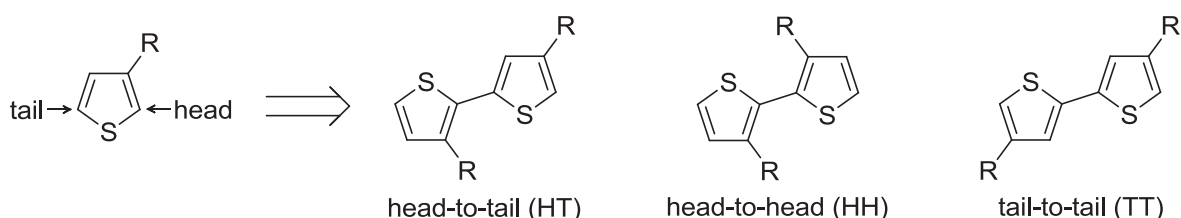
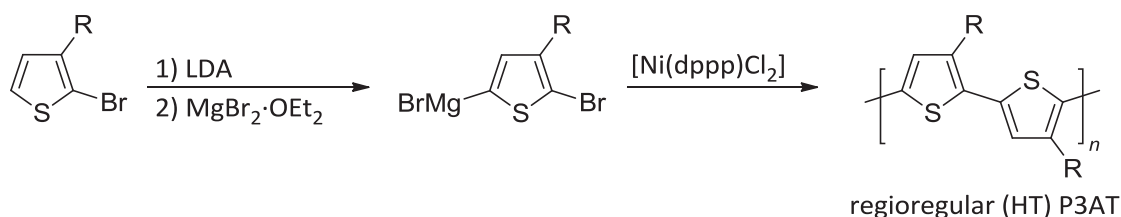


Figure 7. The three different possibilities for the coupling of two thiophene rings are shown.

The consequence of this regioirregularity is a sterical hindrance between the alkyl chains, which leads to a twisted structure of the polymers backbone and a shortened π -conjugation.^[19] In 1992, McCullough and Yokozawa developed independently a new synthetic method:^[29] 2-bromo-3-alkylthiophene was treated with LDA, leading to selective lithiation in the 5 position (Scheme 1). Transmetalation with $\text{MgBr}_2 \cdot \text{OEt}_2$ (or ZnCl_2) led to the respective Grignard or organozinc species, which was polymerized *in situ* with a $[\text{Ni}(\text{dppp})\text{Cl}_2]$ catalyst, and poly(3-alkylthiophene)s with high regioregularities were isolated.



Scheme 1. Cross-coupling method for the preparation of regioregular P3AT with HT couplings, developed by McCullough.^[29]

Not only was the problem of regioirregularity eliminated by using this method, but other extremely advantageous properties were also observed: it was possible to control the molecular weight of the polymers by the amount of the catalyst or by quenching the reaction at a specific time, narrow molecular weight distributions (measured by the polydispersity index, PDI) were achieved, and control over the end groups and access to block copolymers were gained. The polymerizations were carried out by transition-metal catalyzed cross-coupling reactions, formally polycondensations, which are expected to proceed via a step-growth mechanism. However, the observed advantages were all characteristic of a (living) chain growth mechanism, and it could be shown that these reactions actually proceed via such a mechanism.^[30] The reason for this lies in the fact that the nickel catalyst, after the reductive elimination, stays on the polymer chain as an associated pair, without getting transferred to another polymer chain.^[30b]

Later, related methods were reported, using slightly different starting materials and/or reagents.^[30a, 31] With all these new synthetic methods, great progress was made in the field of semiconducting polymers, as these regioregular poly(3-alkylthiophene)s (rrP3ATs) showed dramatically enhanced electrical properties, caused by the well-defined polycrystalline structure.^[32]

The semiconducting polymers of the latest generation are much more complex systems, consisting of different heterocyclic species (compare Figure 6). Virtually all these polymers are prepared by step growth polymerizations using palladium cross-coupling reactions between two different monomers: one monomer is functionalized with two halides, the other one with two metals, mostly trialkyl tin groups or boronic acids/esters (Figure 8). This method allows an easy access to polymers with a variety of differently combined heterocycles, but due to the step growth kinetics, disadvantages like e. g. high PDIs, no regioregularity and the difficulty to achieve very high molecular weights have to be accepted.

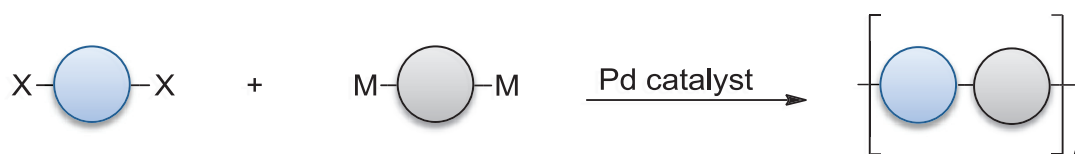
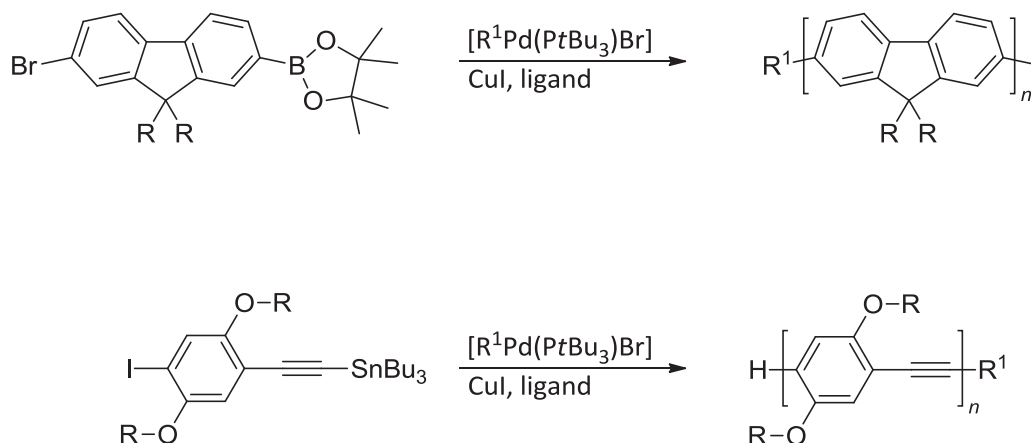


Figure 8. Common preparation method for more complex polymers by step-growth polymerization.

It would be desirable to transfer the advantages of a (living) chain growth polymerization to the preparation of these more complex semiconducting polymers with different heterocycles. The fundamental condition for this is to use only one monomer of the type X-heterocycle1-heterocycle2-M (with X = halogen, M = metal) for the polymerization. Metals like magnesium or zinc, which can be polymerized *in situ* with nickel catalysts, do not allow to purify or isolate the respective monomers because of their instability, making it difficult to use clean monomers. When tin or boron is used as the metal component, the monomers can be purified and isolated. However, the synthesis of appropriate molecules is difficult and elaborate. This is presumably one reason why only very few monomers are known that proceed via a chain growth Stille or Suzuki polymerization: apart from thiophenes,^[31c] only fluorenes,^[33] fluorene-benzothiadiazoles^[34] and polyparaphenylenes^[35] were reported (for two examples, see Scheme 2).



Scheme 2. Two examples for palladium catalyzed cross-coupling reactions, proceeding via chain growth mechanisms.^[33a, 35b]

1.3 Boroles

An often used electron deficient building block for the donor-acceptor approach of semiconducting polymers is benzothiadiazole (Figure 6). However, an example for a much more electron deficient heterocycle is the antiaromatic borole (Figure 9).

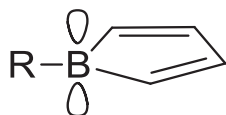


Figure 9. Four π -electrons and the unoccupied p_z -orbital make the borole antiaromatic.

This five-membered ring consists of a butadiene backbone that is connected by a boron atom.^[36] Boron as a group 13 element forms three σ -bonds, and has one unoccupied p_z -orbital. This p_z -orbital leads in combination with the four π -electrons of the butadiene backbone to an antiaromatic system, which is responsible for the unique spectroscopic properties. Most boroles have strongly alternating bond lengths, leading to degenerated energy levels and a singlet ground state (Figure 10); therefore, they are better described as boron bridged dienes rather than antiaromatic. The HOMO is doubly occupied, with a very small energy gap to the LUMO. This leads to the characteristic blue or green color of boroles. The low lying LUMO can easily react with even weak Lewis bases like ethers, leading to a strong hypsochromic shift in the absorption spectrum compared to an uncomplexed borole.^[37] Additionally, boroles are prone to Diels-Alder reactions and chemical reductions.^[36]

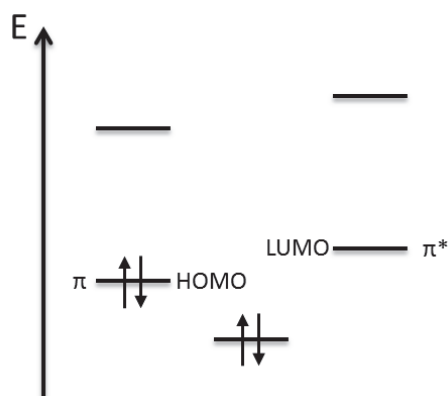


Figure 10. Schematic energy level diagram for a borole.

In 1969, the first synthesis of a borole derivative was reported, pentaphenylborole (Figure 11, left).^[38] This blue solid was prepared by reaction of a stannole precursor with phenylboron dichloride,^[39] until now, the tin-boron exchange is still the most important synthetic method for boroles.^[36] The highly air- and moisture sensitive pentaphenylborole has been used for some fundamental reactivity studies^[40] and remained the only example of a free, non-annulated borole until 2008. From then on, mainly functionalizations at the boron center were carried out, for example pentaphenylboroles with halides^[37, 41] or different aromatic rings^[42] were synthesized.^[43] Only two other examples of antiaromatic boroles are known to date with substituents at the carbon backbone that are not phenyl rings: a perfluorinated species and a tetrathienyl-substituted borole (Figure 11, middle and right).^[44]

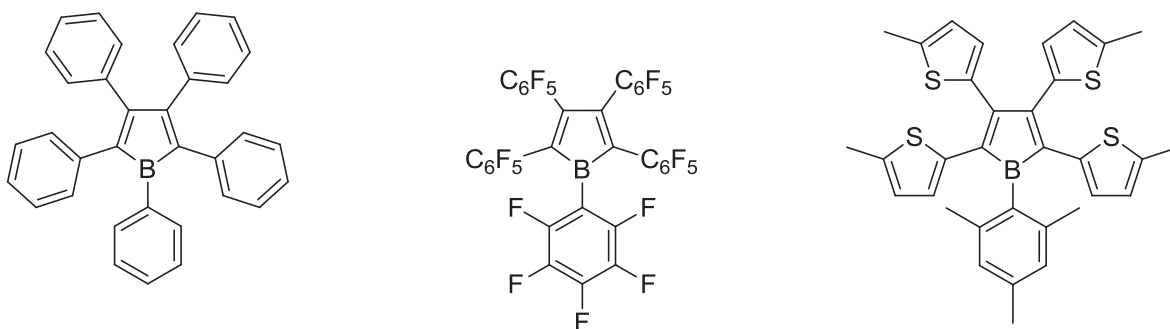


Figure 11. Until now, only three different species are known as substituents for the carbon framework of antiaromatic boroles: phenyl, pentafluorophenyl and thienyl-substituents.

2 Objectives

Thiophene has been established as one of the basic building blocks for semiconducting polymers (see chapter 1.1). By its functionalization and its combination with other heterocycles, the properties of the resulting polymers can be adjusted and tuned. The variety and accessibility of resulting monomers strongly depends on the available synthetic methods. In order to expand the synthetic methods for thiophene building blocks, nucleophile selective cross-coupling reactions should be developed (Figure 12): the thiophene heterocycle should contain two metals of different functionality, allowing only one metal to react under a first set of reaction conditions, while the second one reacts later under slightly different conditions (see chapter 3.1). Further development to nucleophile and electrophile selective cross-coupling reactions would yield a molecule that contains a metal and a halogen functional group. These AB-type compounds could be used as monomers for chain growth (living) polymerizations (compare introduction, chapter 1.2).^[45]



Figure 12. The development of nucleophile selective cross-coupling reactions should give access to a variety of thiophenes.

Especially the combination of thiophenes with other heterocycles has led to distinct improvements in device performances. However, one heterocycle has never been incorporated into a semiconducting polymer so far: a stannole. This was surprising, because related group 14 heteroles like siloles showed very promising results in device performances. Thus, difunctionalized stannole monomers (AA-type) were to be prepared, and the resulting polymers were to be investigated (see Figure 13 and chapter 3.2).

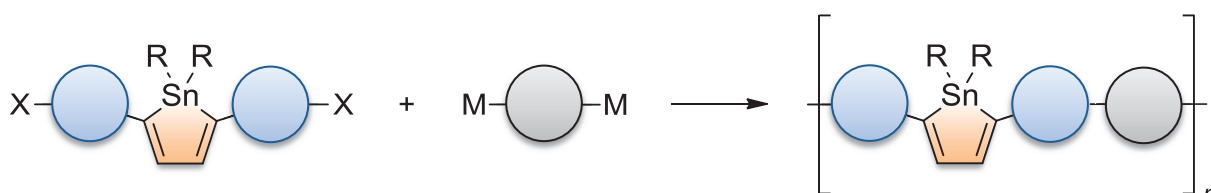


Figure 13. Stannole containing polymers should be synthesized for the first time, using difunctionalized stannole monomers.

Instead of using difunctionalized AA-type stannole monomers in a copolymerization, using only one AB-type stannole monomer for the polymerization would be an alternative approach. In the case of other (hetero)cyclic monomers for semiconducting polymers, this has led to a chain-growth, or even to a living chain-growth polymerization, with all the associated advantages (compare introduction, chapter 1.2). Therefore, it was envisaged to prepare also stannole monomers with a metal functional group and a halide in only *one* molecule (AB-type, Figure 14), which would allow the direct cross-coupling polymerization without another comonomer (see chapter 3.3).

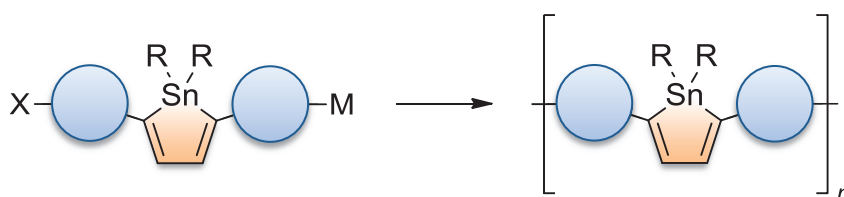


Figure 14. A stannole monomer that already contains all functional groups that are needed for a polymerization should be synthesized.

An antiaromatic borole is another example of a heterocycle that has never been incorporated into a polymer so far. The realization would be very interesting, not only from a fundamental point of view, but also because borole containing polymers may lead to very low band gaps.^[46] Because stannoles are the most common precursors for boroles, and stannole polymers have not been described, no borole containing polymer has been realized so far. Thus, after gaining access to stannole containing polymers, it was envisaged to prepare borole containing polymers (see Figure 15 and chapter 3.5).

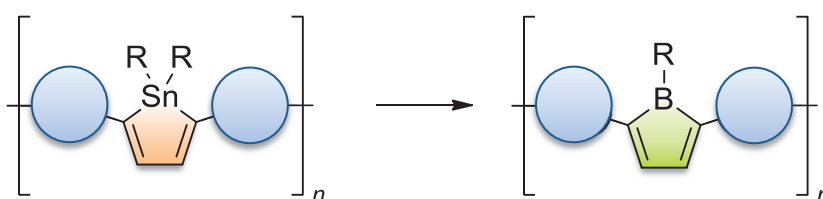


Figure 15. Would it be possible to prepare borole containing polymers?

3 Results and Discussion

3.1 Chemoselective Cross-Coupling Reactions

“Chemoselective Cross-Coupling Reactions with Differentiation between Two Nucleophilic Sites on a Single Aromatic Substrate”

J. Linshoef, A. C. J. Heinrich, S. A. W. Segler, P. J. Gates, A. Staubitz, *Org. Lett.* **2012**, *14*, 5644-5647.

Reprinted with permission from ACS Publications. © 2012 American Chemical Society.

DOI: 10.1021/ol302571t

This communication was highlighted in “*Synfacts*”: P. Knochel, N. M. Barl, *Synfacts* **2013**, *9*, 0204.

A new thiophene building block, containing both a stannyl group and a boronic ester, was prepared. From this starting material, a general, nucleophile-selective one-pot reaction was developed, exploiting the different reactivities of the Stille and Suzuki–Miyaura cross-coupling reactions. A series of aromatic electrophiles were used to demonstrate the high functional group tolerance.

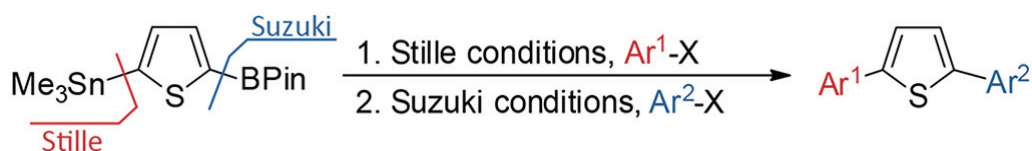


Figure 16. A nucleophile selective one-pot cross-coupling reaction was developed.

Scientific contribution to this paper

In this project, I carried out all syntheses and the experimental work, with the following support by the coauthors: A. Heinrich and I worked together on the synthesis and optimization of the stannyl/boronic ester thiophene **P1-1b**. S. Segler worked under my guidance on the optimization of some reaction conditions during a “F3” internship. P. Gates recorded all high resolution mass spectra. A. Staubitz and I wrote the article together.

Chemoselective Cross-Coupling Reactions with Differentiation between Two Nucleophilic Sites on a Single Aromatic Substrate

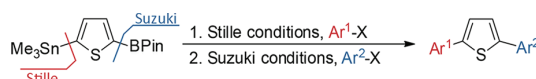
Julian Linshoef, Annika C. J. Heinrich, Stephan A. W. Segler, Paul J. Gates,[†] and Anne Staubitz*

Otto-Diels-Institut für Organische Chemie, Universität Kiel,
Otto-Hahn-Platz 4, 24118 Kiel, Germany

astaubitz@oc.uni-kiel.de

Received September 18, 2012

ABSTRACT



A new thiophene building block, containing both a stannyl group and a boronic ester, was prepared. From this starting material, a general, nucleophile-selective one-pot reaction was developed, exploiting the different reactivities of the Stille and Suzuki–Miyaura cross-coupling reactions. A series of aromatic electrophiles were used to demonstrate the high functional group tolerance.

Transition metal catalyzed cross-coupling reactions (CCRs) are among the most powerful tools in synthesis.¹ They are crucial for the preparation of many complex organic natural products,² pharmaceuticals, and agrochemicals.³ In all these fields, heterocycles play an important role but thiophenes are unquestionably the most impactful.⁴

[†] School of Chemistry, University of Bristol, Bristol BS8 1TS, U.K.

(1) (a) Hartwig, J. F. *Organotransition metal chemistry: from bonding to catalysis*; University Science Books: Sausalito, CA, 2010. (b) Johansson Seechurn, C. C. C.; Kitching, M. O.; Colacot, T. J.; Snieckus, V. *Angew. Chem., Int. Ed.* **2012**, *51*, 5062. (c) Meijere, A. d.; Stang, P. J. *Metal-Catalyzed Cross-Coupling Reactions*, 2nd ed.; Wiley-VCH: Weinheim, 2004. (d) Suzuki, A. *Angew. Chem., Int. Ed.* **2011**, *50*, 6722.

(2) Nicolaou, K. C.; Bulger, P. G.; Sarlah, D. *Angew. Chem., Int. Ed.* **2005**, *44*, 4442.

(3) (a) King, A. O.; Yasuda, N. *Top. Organomet. Chem.* **2004**, *6*, 205. (b) Magano, J.; Dunetz, J. R. *Chem. Rev.* **2011**, *111*, 2177. (c) Torborg, C.; Beller, M. *Adv. Synth. Catal.* **2009**, *351*, 3027.

(4) (a) Barbarella, G.; Melucci, M.; Sotgiu, G. *Adv. Mater.* **2005**, *17*, 1581. (b) Baxter, A.; Brough, S.; Cooper, A.; Floettmann, E.; Foster, S.; Harding, C.; Kettle, J.; McNally, T.; Martin, C.; Mobbs, M.; Needham, M.; Newham, P.; Paine, S.; St-Gallay, S.; Salter, S.; Unitt, J.; Xue, Y. *Bioorg. Med. Chem. Lett.* **2004**, *14*, 2817. (c) Majumdar, K. C.; Chattopadhyay, S. K. *Heterocycles in Natural Product Synthesis*; Wiley-VCH: New York, 2011. (d) Nakano, H.; Cantrell, C. L.; Mamonov, L. K.; Osbrink, W. L. A.; Ross, S. A. *Org. Lett.* **2011**, *13*, 6228. (e) Rossi, R.; Carpita, A.; Lezzi, A. *Tetrahedron* **1984**, *40*, 2773. (f) Sperry, J. B.; Wright, D. L. *Curr. Opin. Drug Discovery Dev.* **2005**, *8*, 723.

(5) (a) Mishra, A.; Ma, C.-Q.; Bäuerle, P. *Chem. Rev.* **2009**, *109*, 1141. (b) Perepichka, I. F.; Perepichka, D. F. *Handbook of Thiophene-based Materials: Applications in Organic Electronics and Photonics*; Wiley-VCH: Weinheim, 2009.

The incorporation of thiophene into organic semiconducting materials for example is a highly active research area.⁵ Thiophenes and their derivatives are arguably the most important monomers for semiconducting polymers⁶ and oligomers^{5a,7} which find already widespread use in, for example, plastic solar cells^{6a,8} and organic field effect transistors.^{5a,7a,c,9} The exploration of their chemistry, in particular their efficient functionalization, is therefore of great urgency.

The electrophiles used in CCRs have different reactivity, which depends on the leaving group. Typically, a gradual decrease in reactivity is observed for electrophiles containing

(6) (a) Thompson, B. C.; Fréchet, J. M. J. *Angew. Chem., Int. Ed.* **2008**, *47*, 58. (b) Roncali, J. *Chem. Rev.* **1992**, *92*, 711. (c) Osaka, I.; McCullough, R. D. *Acc. Chem. Res.* **2008**, *41*, 1202. (d) Marsella, M. J.; Swager, T. M. *J. Am. Chem. Soc.* **1993**, *115*, 12214.

(7) (a) Murphy, A. R.; Fréchet, J. M. J. *Chem. Rev.* **2007**, *107*, 1066. (b) Katz, H. E.; Bao, Z.; Gilat, S. L. *Acc. Chem. Res.* **2001**, *34*, 359. (c) Ramakrishna, G.; Bhaskar, A.; Bauerle, P.; Goodson, T., III. *J. Phys. Chem. A* **2008**, *112*, 2018.

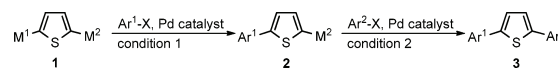
(8) (a) Wong, W. W. H.; Ma, C.-Q.; Pisula, W.; Yan, C.; Feng, X.; Jones, D. J.; Müllen, K.; Janssen, R. A. J.; Bäuerle, P.; Holmes, A. B. *Chem. Mater.* **2009**, *22*, 457. (b) Zhang, F.; Wu, D.; Xu, Y.; Feng, X. *J. Mater. Chem.* **2011**, *21*, 17590. (c) Thomas, K. R. J.; Hsu, Y.-C.; Lin, J. T.; Lee, K.-M.; Ho, K.-C.; Lai, C.-H.; Cheng, Y.-M.; Chou, P.-T. *Chem. Mater.* **2008**, *20*, 1830. (d) Loewe, R. S.; Khersonsky, S. M.; McCullough, R. D. *Adv. Mater.* **1999**, *11*, 250. (e) Krebs, F. C. *Polymer Photovoltaics: A Practical Approach*; SPIE: Bellingham, 2008.

(9) (a) Wang, S.; Kiernowski, A.; Pisula, W.; Müllen, K. *J. Am. Chem. Soc.* **2012**, *134*, 4015. (b) Ong, B. S.; Wu, Y.; Li, Y.; Liu, P.; Pan, H. *Chem.—Eur. J.* **2008**, *14*, 4766.

the leaving groups $I > OTf > Br \gg Cl$.¹⁰ This difference in reactivity has enabled the development of selective CCRs with respect to the electrophile.¹¹ In contrast, nucleophile-selective CCRs have rarely been reported and the few reports that do exist are largely associated with nonaromatic compounds.¹² There are only a few examples in which the difference in reaction rate between Stille and Suzuki–Miyaura cross-coupling has been used¹³ and only one example of a chemoselective CCR involving an aromatic compound containing both tin- and boron-based substituents at the same molecule.¹⁴ In that particular case, the benzene derivative *para*-Bu₃Sn–C₆H₄–B(OR)₂ was cross-coupled with two protected nucleosides for boron neutron capture therapy, but generality was not demonstrated. One possible reason for the striking neglect of nucleophile selective CCRs is that methods for preparing appropriate aromatic starting materials containing two different nucleophilic groups are very rare in the literature.¹⁴ These starting materials could be used for comparing the reactivity of different metal groups, M¹ and M² (**1**, Scheme 1), in CCRs and could

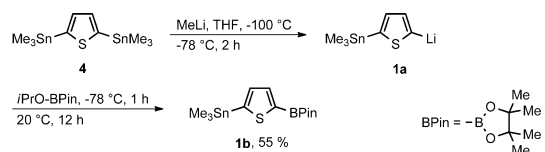
facilitate the preparation of novel molecules and materials that were not accessible before. A particularly intriguing prospect in this context would be the development of reactions that are both electrophile- and nucleophile-selective at the same time, for which work is ongoing in our laboratories.

Scheme 1. General Procedure for Chemoselective CCRs



Herein, we report the synthesis of a thiophene derivative containing both tin- and boron-based substituents and its use in the first systematic study of nucleophile-selective CCRs involving aromatic compounds. This presents a major challenge, as the nucleophilic groups are in chemically identical environments and chemoselectivity could only be derived from the nucleophilic group itself, not from any neighboring effects. We also show that the reaction products, which contain the unreactive nucleophilic metal component, can be used, in situ, in subsequent CCRs involving a second electrophile Ar²–X (Scheme 1).

Scheme 2. Synthesis of Thiophene **1b** (Pin = pinacol)



Thiophene **1b** was prepared in a one-pot reaction of bis-(stannylium) thiophene **4**¹⁵ through monolithiation and in situ Li–B exchange (Scheme 2). Purification of the crude product turned out to be challenging due to contaminations with the starting material **4** and bis(borylated) thiophene. The desired product **1b** was unstable to silica gel chromatography, but it could be purified by fractional sublimation and was eventually isolated in good yields and could be stored in air at 5 °C for at least 5 months without noticeable decomposition.

To establish reaction conditions for a chemoselective CCR, we used 1-bromo-4-nitrobenzene (**5a**) as a test substrate and Pd(PPh₃)₄ as a catalyst in toluene at 110 °C. After 16 h, we obtained product **2a** in 70% yield following isolation (Table 1, entry 6). The isolated product was used as a calibrant for the development of a GC method for reaction monitoring and optimization. The conversion and the yield were highly dependent on the solvent and temperature. At 110 °C, although conversion for the reactions conducted in all solvents was essentially quantitative, the corresponding yields were significantly lower, owing to the formation of unidentified byproducts. The use of toluene and dioxane gave superior yields (83% and 80% respectively, Table 1). DMF was

(15) Seitz, D. E.; Lee, S. H.; Hanson, R. N.; Bottaro, J. C. *Synth. Commun.* **1983**, *13*, 121.

(10) Miyaura, N.; Suzuki, A. *Chem. Rev.* **1995**, *95*, 2457.

(11) (a) Aranyos, A.; Old, D. W.; Kiyomori, A.; Wolfe, J. P.; Sadighi, J. P.; Buchwald, S. L. *J. Am. Chem. Soc.* **1999**, *121*, 4369. (b) Bonnamour, J.; Piedrafita, M.; Bolm, C. *Adv. Synth. Catal.* **2010**, *352*, 1577. (c) Boyer, A.; Isono, N.; Lackner, S.; Lautens, M. *Tetrahedron* **2010**, *66*, 6468. (d) Cho, G. Y.; Rémy, P.; Jansson, J.; Moessner, C.; Bolm, C. *Org. Lett.* **2004**, *6*, 3293. (e) Kienle, M.; Unsinn, A.; Knochel, P. *Angew. Chem., Int. Ed.* **2010**, *49*, 4751. (f) Lou, S.; Fu, G. C. *J. Am. Chem. Soc.* **2010**, *132*, 1264. (g) Mariampillai, B.; Herse, C.; Lautens, M. *Org. Lett.* **2005**, *7*, 4745. (h) Martin, R.; Rivero, M. R.; Buchwald, S. L. *Angew. Chem., Int. Ed.* **2006**, *45*, 7079. (i) Mosrin, M.; Knochel, P. *Chem.—Eur. J.* **2009**, *15*, 1468. (j) Shen, Q.; Hartwig, J. F. *J. Am. Chem. Soc.* **2007**, *129*, 7734. (k) Wang, Y. F.; Deng, W.; Liu, L.; Guo, Q. X. *Chin. Chem. Lett.* **2005**, *16*, 1197. (l) Wu, X.-F.; Anbarasan, P.; Neumann, H.; Beller, M. *Angew. Chem., Int. Ed.* **2010**, *49*, 7316. In this context, the chain growth Suzuki–Heck polymerization is of interest, where dibromoaryl monomers react with potassium vinyl trifluoroborate (Suzuki step) followed by a Heck reaction which carries the chain growth (Heck step) in a one-pot reaction: (m) Grisorio, R.; Mastroianni, P.; Nobile, C. F.; Romanazzi, G.; Suranna, G. P.; Gigli, G.; Pilego, C.; Ciccarella, G.; Cosma, P.; Acierno, D.; Amendola, E. *Macromolecules* **2007**, *40*, 4865. (n) Grisorio, R.; Suranna, G. P.; Mastroianni, P. *Chem.—Eur. J.* **2010**, *16*, 8054.

(12) (a) Pawluć, P.; Hreczycho, G.; Suchecki, A.; Kubicki, M.; Marciniak, B. *Tetrahedron* **2009**, *65*, 5497. (b) Denmark, S. E.; Tymonko, S. A. *J. Am. Chem. Soc.* **2005**, *127*, 8004. (c) Cai, M.-Z.; Zhou, Z.; Wang, P.-P. *Synthesis* **2006**, *2006*, 789. (d) Sorg, A.; Brückner, R. *Angew. Chem., Int. Ed.* **2004**, *43*, 4523. (e) Cai, M.-Z.; Wang, Y.; Wang, P.-P. *J. Organomet. Chem.* **2008**, *693*, 2954. (f) Iannazzo, L.; Vollhardt, K. P. C.; Malacria, M.; Aubert, C.; Gandon, V. *Eur. J. Org. Chem.* **2011**, *2011*, 3283. (g) Ogima, M.; Hyuga, S.; Hara, S.; Suzuki, A. *Chem. Lett.* **1989**, 1959. (h) Malan, C.; Morin, C. *Synlett* **1996**, 167. (i) Pihko, P. M.; Koskinen, A. M. P. *Synlett* **1999**, 1966.

(13) (a) Henze, O.; Parker, D.; Feast, W. J. *J. Mater. Chem.* **2003**, *13*, 1269. (b) Lehmann, U.; Henze, O.; Schlüter, A. D. *Chem.—Eur. J.* **1999**, *5*, 854. (c) Manickam, G.; Schlüter, A. D. *Eur. J. Org. Chem.* **2000**, 3475. (d) Zhang, X.; Tian, H.; Liu, Q.; Wang, L.; Geng, Y.; Wang, F. *J. Org. Chem.* **2006**, *71*, 4332. (e) Lehmann, U.; Schlüter, A. D. *Eur. J. Org. Chem.* **2000**, 3483. (f) Manickam, G.; Schlüter, A. D. *Synthesis* **2000**, 442. (g) Tortosa, M.; Yakelis, N. A.; Roush, W. R. *J. Org. Chem.* **2008**, *73*, 9657. (h) Lee, S. J.; Anderson, T. M.; Burke, M. D. *Angew. Chem., Int. Ed.* **2010**, *49*, 8860. (i) Singidi, R. R.; RajanBabu, T. V. *Org. Lett.* **2010**, *12*, 2622. (j) Coleman, R. S.; Lu, X. *Chem. Commun.* **2006**, 423. (k) Coleman, R. S.; Walczak, M. C.; Campbell, E. L. *J. Am. Chem. Soc.* **2005**, *127*, 16038. (l) Coleman, R. S.; Walczak, M. C. *Org. Lett.* **2005**, *7*, 2289. (m) Coleman, R. S.; Walczak, M. C. *J. Org. Chem.* **2006**, *71*, 9841. (n) Fujii, S.; Chang, S. Y.; Burke, M. D. *Angew. Chem., Int. Ed.* **2011**, *50*, 7862. (o) Tortosa, M.; Yakelis, N. A.; Roush, W. R. *J. Am. Chem. Soc.* **2008**, *130*, 2722. (p) Lee, S. J.; Gray, K. C.; Paek, J. S.; Burke, M. D. *J. Am. Chem. Soc.* **2008**, *130*, 466.

(14) Yamamoto, Y.; Seko, T.; Nemoto, H. *J. Org. Chem.* **1989**, *54*, 4734.

not a suitable solvent, and THF, acetonitrile, and pyridine also gave low yields (see Supporting Information (SI)).

Table 1. Optimization Studies for Chemoselective CCRs with Varying Solvent and Temperature^a

entry	solvent	temp [°C]	conv ^b [%]	yield ^c [%]
1	dioxane	65	20	18
2	dioxane	110	>99	80
3	DMF	65	95	75
4	DMF	110	>99	23
5	toluene	65	16	11
6	toluene	110	>99	83 ^d

^a **5a** (1.0 equiv), **1b** (1.1 equiv), Pd(PPh₃)₄ (5 mol %). ^b Conversion; based on **5a**. ^c Determined by GC (multiple point internal standard method). ^d Yield of isolated product: 70%.

To establish mild conditions that minimize the formation of byproducts, we tested a variety of catalysts for the reaction in toluene (Table 2) and dioxane (see SI). By reducing the reaction time from 16 to 5 h, not only was the starting material completely consumed but also the product was obtained in essentially quantitative yield (Table 2, entry 2). [Pd(dppe)Cl₂]¹⁶ was a poorer catalyst than [Pd(PPh₃)₄]: even after a reaction time of 72 h, the yield was only 61% (Table 2, entries 3–5). Although the use of [Pd(PrBu₃)₂], [Pd(dppf)Cl₂], and Pd(OAc)₂/SPhos¹⁶ resulted in excellent conversions at 110 °C, decomposition of the product was most likely the problem (Table 2, entries 6–14). However, when using the Pd(OAc)₂/SPhos catalyst, this problem could be avoided by reduction of the reaction time to 80 min (Table 2, entry 12). To ensure that the cross-coupling was compatible with temperature-sensitive compounds, we optimized the reaction also at a lower temperature. When the reaction was carried out at 65 °C for 4 h, the product **2a** was obtained in 98% yield (Table 2, entry 18). However, when we attempted to isolate the product by using column chromatography or sublimation, we were unable to obtain the product without contamination with the SPhos ligand. To simplify the purification of the product, the loading of the Pd(OAc)₂/SPhos catalyst was reduced to 1 mol % and, following the reaction at 65 °C over the course of 18 h, the product was obtained in excellent yield (Table 2, entry 19; for further details, see the SI).

With optimized conditions established, the scope of the reaction was explored by using a variety of (hetero)aryl bromides (Table 3). To avoid the potential for product decomposition, reactions were performed at 65 °C. The use of electron-deficient benzene and furan derivatives gave good to excellent yields of the corresponding products (76–98%; Table 3, entries 1–3 and 6–8). However, close to no conversion was observed when 2- or 3-bromopyridine was used (Table 3, entries 4 and 5) and only trace

(16) dppe = 1,2-bis(diphenylphosphino)ethane; dppf = 1,1'-bis(diphenylphosphino)ferrocene; SPhos = 2-dicyclohexylphosphino-2',6'-dimethoxybiphenyl.

Table 2. Chemoselective Cross-Coupling with Varying Catalyst, Reaction Time, and Temperature^a

entry	catalyst	t [h]	temp [°C]	conv ^b [%]	yield ^c [%]
1	[Pd(PPh ₃) ₄]	1.33	110	95	81
2	[Pd(PPh ₃) ₄]	5	110	>99	>99
3	[Pd(dppe)Cl ₂]	16	110	41	41
4	[Pd(dppe)Cl ₂]	50	110	60	57
5	[Pd(dppe)Cl ₂]	72	110	95	61
6	[Pd(PrBu ₃) ₂]	1.33	110	>99	66
7	[Pd(PrBu ₃) ₂]	5	110	>99	50
8	[Pd(PrBu ₃) ₂]	16	110	>99	18
9	[Pd(dppf)Cl ₂]	1.33	110	>99	90
10	[Pd(dppf)Cl ₂]	5	110	>99	85
11	[Pd(dppf)Cl ₂]	16	110	>99	37
12	Pd(OAc) ₂ /SPhos	1.33	110	>99	>99
13	Pd(OAc) ₂ /SPhos	5	110	>99	86
14	Pd(OAc) ₂ /SPhos	16	110	>99	25
15	Pd(OAc) ₂ /SPhos	0.17	65	22	21
16	Pd(OAc) ₂ /SPhos	1.33	65	67	66
17	Pd(OAc) ₂ /SPhos	3	65	88	87
18	Pd(OAc) ₂ /SPhos	4	65	>99	98
19	Pd(OAc) ₂ /SPhos	18	65	>99	>99 ^d

^a **5a** (1.0 equiv), **1b** (1.1 equiv), Pd source (5 mol %), SPhos (10 mol % for entries 12–18). ^b Conversion; based on **5a**. ^c Determined by GC (multiple point internal standard method). ^d 1 mol % Pd(OAc)₂, 2 mol % SPhos. dppe = 1,2-bis(diphenylphosphino)ethane; dppf = 1,1'-bis(diphenylphosphino)ferrocene; SPhos = 2-dicyclohexylphosphino-2',6'-dimethoxy-biphenyl.

amounts of the corresponding products were observed by GC/MS. Increasing the reaction temperature to 110 °C did not improve the yield of product in the case of 2-bromopyridine; however, we found that 3-bromopyridine reacted smoothly within 6 h under these conditions, giving **2e** in 81% yield upon isolation (Table 3, entry 5).

The origin of this behavior could be the deactivation of the catalyst through its binding with the N-atom of the substrate.¹⁷ The use of electron-neutral electrophiles, such as bromobenzene and 1-bromonaphthalene, also gave the corresponding products in good yields, 83% and 91%, respectively; however, the use of 1-bromonaphthalene required a longer reaction time (40 h) for completion (Table 3, entries 9 and 10), presumably owing to steric hindrance. Furthermore, electron-rich aryl bromides could also be employed as electrophiles for the nucleophile-selective CCR (Table 3, entries 11–13); however, the use of amine **5k** gave the product in moderate yield.¹⁸ In all the reactions, the transformation was fully chemoselective with respect to the stannyl and boronic ester functional groups. The reason for this is that, in the case of Suzuki reactions, a base has to be added for the reaction to take place.

(17) Solano, C.; Svensson, D.; Olomi, Z.; Jensen, J.; Wendt, O. F.; Wärnmark, K. *Eur. J. Org. Chem.* **2005**, 3510.

(18) The tertiary amine **5k** showed a low yield of 37% due to a low conversion. Longer reaction times and reflux conditions did not lead to higher conversion. A reason could be the binding of the amine to the Pd. For more information about tertiary amines used as ligands for Pd, see: (a) Li, J.-H.; Liu, W.-J. *Org. Lett.* **2004**, *6*, 2809. (b) Li, Y.; El-Sayed, M. A. *J. Phys. Chem. B* **2001**, *105*, 8938.0.

Table 3. Stille CCR of (Hetero)aryl Bromides with **1b**^a

$$\mathbf{1b} + \text{Ar-Br} \xrightarrow[\text{toluene, 65 } ^\circ\text{C, 18 h}]{\text{Pd(OAc)}_2/\text{SPhos}} \text{Ar-S-BPin}$$

$$\mathbf{5a-m} \qquad \qquad \qquad \mathbf{2a-m}$$

entry	(hetero)aryl-Br	product	yield ^b [%]
1			98
2			84
3			81
4			0/0 ^c
5			0/81 ^c
6			95
7			76
8			87
9			83
10			91 ^d
11			37
12			89
13			66

^a Pd(OAc)₂ (1 mol %), SPhos (2 mol %). ^b Yields of isolated products. ^c 6 h, reflux. ^d 40 h, 65 °C.

The latest analysis on the effect of OH⁻ ions has shown their role to be threefold: First, they are reagents for the formation of the reactive *trans*-[ArPd(OH)(L)₂] from the unreactive *trans*-[ArPd(X)(L)₂], the product of oxidative addition. Second, the reductive elimination step is also accelerated by the reaction of OH⁻ with *trans*-[ArPdAr'(L)₂]. Third, the addition of a base can also have a retarding effect by the formation of Ar'B(OH)₄⁻.¹⁹

Because the Pd(OAc)₂/SPhos catalyst is also known to be very effective for Suzuki–Miyaura CCRs,²⁰ we envisioned

(19) Amatore, C.; Jutand, A.; Le Duc, G. *Chem.—Eur. J.* **2011**, *17*, 2492.

that the boronic ester products in the above nucleophile-selective CCRs could react with a second electrophile in a one-pot transformation. This was accomplished by adding 5-bromofurfuraldehyde as the second electrophile, water, and K₃PO₄ as a base to the reaction mixture upon completion of the Stille CCR and subsequently stirring the reaction mixture at 100 °C for 3 h. The yields of the products **3** were uniformly high for different aryl bromides (Table 4).

Table 4. Chemoselective One-Pot Successive CCRs of Thiophene **1b**^a

$$\mathbf{1b} + \text{Ar-Br} \xrightarrow{\text{i)}} \text{Ar-S-BPin} \xrightarrow{\text{ii)}} \text{Ar-S-O-CHO}$$

$$\mathbf{5} \qquad \qquad \qquad \mathbf{2a,i,l} \qquad \qquad \qquad \mathbf{3a-c}$$

entry	aryl bromide	product	yield ^b [%]
1			84
2			76
3			70

^a (i) **1b** (1.0 equiv), **5** (1.0 equiv), Pd(OAc)₂ (1 mol %), SPhos (2 mol %), toluene, 65 °C, 18 h. (ii) 5-Bromofurfuraldehyde (1.0 equiv), K₃PO₄ (2.0 equiv), water, 100 °C, 3 h. ^b Yields of isolated products.

In conclusion, we prepared a thiophene dinucleophile **1b** with both a trialkyltin group and a boronic ester at the 2 and 5-positions, respectively. With this compound, we established conditions for nucleophile-selective CCRs, that is, conditions that allow a selective Stille CCR involving substrates that contain a boronic ester substituent. The resulting products, which contain the boronic ester group, were used in the same pot in a subsequent Suzuki–Miyaura CCR. We are currently developing efficient syntheses of a wide variety of aryl and heteroaryl substrates containing both tin- and boron-based substituents for their employment in nucleophile-selective CCRs.

Acknowledgment. This work was supported by the Fonds der Chemischen Industrie (FCI). J.L. and A.H. thank the Deutsche Bundesstiftung Umwelt (DBU) for a Ph.D. scholarship.

Supporting Information Available. Experimental procedures, all GC optimization reactions, and NMR spectra. This material is available free of charge via the Internet at <http://pubs.acs.org>.

(20) (a) Walker, S. D.; Barder, T. E.; Martinelli, J. R.; Buchwald, S. L. *Angew. Chem., Int. Ed.* **2004**, *43*, 1871. (b) Barder, T. E.; Walker, S. D.; Martinelli, J. R.; Buchwald, S. L. *J. Am. Chem. Soc.* **2005**, *127*, 4685. (c) Barder, T. E.; Biscoe, M. R.; Buchwald, S. L. *Organometallics* **2007**, *26*, 2183.

The authors declare no competing financial interest.

3.2 Group 14/16 Heterocycles for Polycondensation Polymers

3.2.1 Stannole Containing Polymers

3.2.1.1 Stannole-Thiophene Copolymers

“Highly Tin Selective Stille Coupling: Synthesis of a Polymer Containing a Stannole in the Main Chain” and, respectively, “Hoch Zinn-selektive Stille-Kupplung: Polymersynthese mit einem Stannol in der Hauptkette”

J. Linshoef, E. J. Baum, A. Hussain, P. J. Gates, C. Näther, A. Staubitz, *Angew. Chem. Int. Ed.* **2014**, *asap*; *Angew. Chem.* **2014**, *asap*.

Reprinted with permission from John Wiley and Sons. © 2014 WILEY-VCH Verlag GmbH & Co. KGaA, Weinheim.

DOI: 10.1002/anie.201407377; 10.1002/ange.201407377

A stannole monomer is prepared and employed in a highly tin-selective Stille coupling, giving a well-defined and non-annulated stannole-containing polymer, the first example from this class of π -conjugated polymers. Compared to polythiophenes, a strong bathochromic shift in the absorption spectrum was observed.

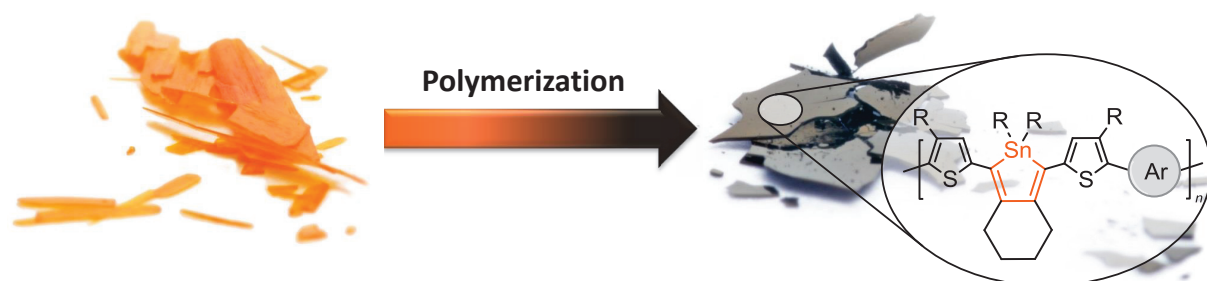


Figure 17. A synthetic route to stannole monomers was developed, leading to the first stannole containing polymer.

Scientific contribution to this paper

In this project, I carried out all syntheses and the experimental work, with the following support of the coauthors: E. Baum worked under my guidance on the synthesis and optimization of the thiophene linked octadiyne **P2-6b** during a DAAD RISE internship. A. Hussain reproduced some of the synthesized compounds during an internship. P. Gates recorded most of the high resolution mass spectra. C. Näther carried out the X-ray crystallography measurement. A. Staubitz and I wrote the article together.

Nucleophile-Selective Cross-Coupling

Highly Tin-Selective Stille Coupling: Synthesis of a Polymer Containing a Stannole in the Main Chain**

Julian Linshoef, Evan J. Baum, Andreas Hussain, Paul J. Gates, Christian Näther, and Anne Staubitz*

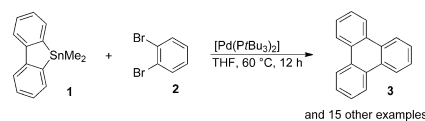
Abstract: The incorporation of heavier Group 14 element heteroles into semiconducting polymers leads to unusual optoelectronic properties. However, polymers containing stannoles have not been accessible to date. We report a synthetic route to a well-defined, stannole-containing polymer, the first example of this class of π -conjugated polymers. This route was made possible by developing difunctionalized stannole monomers and highly tin-selective Stille coupling reactions that leave the tin in the stannole untouched. Compared to poly(3-*n*-hexylthiophene), the resulting polymer displays a remarkable bathochromic shift in its absorption.

The formal replacement of the methylene group in cyclopentadienes by heavier Group 14 elements drastically changes their electronic properties.^[1] With the incorporation of Si, Ge, or Sn the two σ^* -orbitals of the exocyclic E–R bonds (with E = Si, Ge, Sn) are much lower in energy than those of C–R bonds, allowing efficient mixing with the π^* -orbital of the diene system. This mixing distinctly lowers their LUMO levels compared to carbon cyclopentadienes.^[1b,d,e] Therefore, these higher Group 14 heteroles are interesting heterocycles for incorporation into semiconducting polymers: They are expected to have low band gaps and to display novel charge-transporting properties.^[2] Sila- and germafluorenes have been incorporated in polymers^[3] as have siloles and germales,^[4] which led to distinct improvements in device performances.^[5] Furthermore, Group 14 heteroles were also incorporated as 1,1-bridged heteroles.^[1b,6] As far as tin is concerned, there is some work on stannafluorenes,^[7] but the chemistry of stannoles is much less studied.^[1e,8]

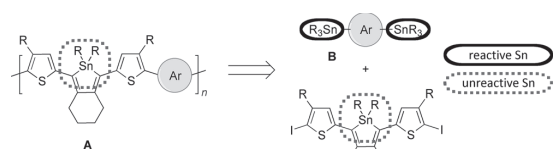
To date, no stannole has been published that contains a reactive halogen functional group that could be used for

cross-coupling reactions—on either the dienyl ring itself or on any further aromatic substituents on this ring. The problem is that stannacycles themselves are very versatile nucleophilic compounds in Stille cross-coupling reactions. Indeed, stannoles may be viewed as cyclic vinyl tin compounds that are regularly used in cross-coupling reactions^[10] and which, depending on the reaction conditions, can be even more reactive than aryl tin compounds.^[11] The recently reported reactivity of the related stannafluorenes illustrates the problem of being able to use reactive organo tin compounds in cross-coupling reactions, if reactions at the tin center are not wanted: it was shown that stannafluorenes **1** react cleanly with dibromobenzenes **2** to give triphenylenes **3** in high yields (Scheme 1).^[9,12]

Herein, we demonstrate the first highly nucleophile selective Stille reaction, differentiating between an endo- and two exocyclic tin functional groups (Scheme 2). This



Scheme 1. The reaction of stannafluorenes **1** with di-electrophiles **2** can lead to cross-coupled products **3** (in this example, isolated in 87% yield).^[9]



Scheme 2. Tin-selective cross-coupling reactions allow the synthesis of stannole containing polymers.

allowed the synthesis of the first well-defined non-annulated stannole-containing polymer of type **A** (Scheme 2), which shows a strong bathochromic shift compared to the related poly(3-*n*-hexylthiophene) (P3HT). To synthesize a monomer of type **C**, two major challenges had to be overcome: First, a synthetic route had to be developed to prepare a stannole monomer that contained electrophilic functional groups (bromides or iodides) on the carbon scaffold for the subsequent polymerization. The second issue was to protect the Sn center in the heterocycle so that it would be stable under polymerization conditions. We envisioned that this

[*] J. Linshoef, E. J. Baum, A. Hussain, Prof. Dr. A. Staubitz
Otto-Diels-Institut für Organische Chemie, Universität Kiel
24098 Kiel (Germany)
E-mail: astaubitz@oc.uni-kiel.de

Prof. Dr. C. Näther
Institut für Anorganische Chemie, Universität Kiel
24098 Kiel (Germany)

Dr. P. J. Gates
School of Chemistry, University of Bristol
Bristol BS8 1TS (UK)

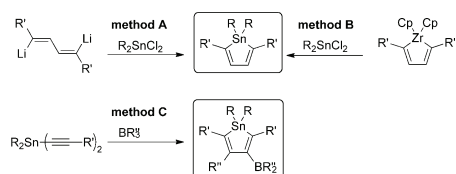
[**] J.L. thanks the Deutsche Bundesstiftung Umwelt (DBU) for a Ph.D. scholarship. E.J.B. thanks the Deutsche Akademische Austauschdienst (DAAD) for a RISE scholarship. We thank Dr. Franz J. Mayer from Bruker Daltonik GmbH for the measurement of MALDI-TOF spectra of our polymer TS1T.

Supporting information for this article is available on the WWW under <http://dx.doi.org/10.1002/anie.201407377>.

could be achieved based on a kinetically deactivated tin center in the stannole monomer.

The reactivity and functionalization possibilities of stannoles are almost entirely unexplored. Crucially, there is no report of stannoles that are substituted with bromides or iodides. This does not only concern bromide/iodide substituents on the ring, but also, no stannoles with brominated/iodinated aryl substituents have been synthesized.

There are three established methods for the preparation of stannoles: Generally, they can be prepared by synthesizing a dilithiated butadiene species in situ and then quenching it with R_2SnCl_2 [8a,13] (method A, Scheme 3). The second route

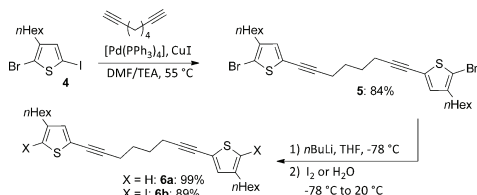


Scheme 3. Common preparation methods for stannoles.

involves a Zr–Sn exchange^[1e,14] of zirconacyclopentadienes with R_2SnCl_2 (method B). Another possibility is the 1,1-carbaboration of activated tin diacetylides, also known as Wrackmeyer reaction, which generally gives the desired stannoles in high yields (method C).^[15]

Because the presence of halides ($R' = -Ar-X$; Scheme 3) is essential for the intended monomer, a route via a dilithiated butadiene is problematic owing to potential unselective halogen–lithium exchange reactions. Although method C is an excellent and straightforward route for the synthesis of stannoles (and other heteroles),^[16] it was not pursued at this stage because it would result in a boron atom in the 3 or 4 position. Such an asymmetric monomer would be expected in the subsequent polycondensation to lead to a regioirregular polymer.

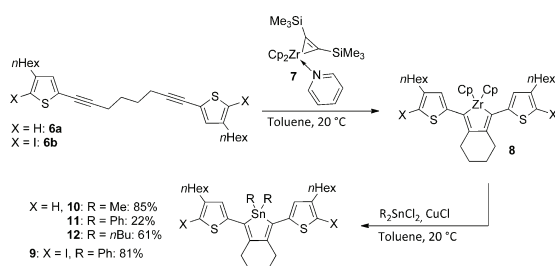
Therefore, a zirconacyclopentadiene was envisaged as a stannole precursor, flanked by two halide substituted 3-*n*-hexylthiophenes. For this route, the octadiyne linked bis(thiophene) **5** was prepared in an electrophile selective Sonogashira cross-coupling reaction, without observing any unselective coupling reaction with the bromide (Scheme 4). Bromine–lithium exchange and subsequent quenching with water or iodine at -78°C led to the protonated and iodinated species **6a** and **6b**, respectively. The bromide–iodide



Scheme 4. Synthesis of thiophene-flanked octadiyne **6**.

exchange was carried out because of the higher reactivity of iodides in cross-coupling reactions,^[17] thus facilitating a later polymerization process.

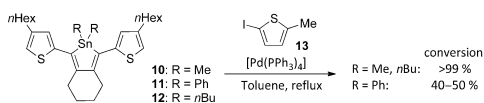
The commonly used reagent for the formation of zirconacyclopentadienes from diynes is the in situ prepared Negishi reagent.^[18] However, this highly reactive reagent is problematic for halide-functionalized compounds, because it is capable of C–X insertion reactions.^[19] A much milder reagent is Rosenthal's zirconocene,^[20] which has been used for a bromide-functionalized zirconacyclopentadiene.^[4a] Because of these advantageous properties, Rosenthal's zirconocene **7** was used in a reaction with **6** in toluene at 20°C for 18 h, giving a dark red solution (Scheme 5). Copper chloride



Scheme 5. Synthesis of a variety of stannoles by a zirconacyclopentadiene one-pot procedure.

promotes the Zr–Sn exchange not only in THF,^[14a–c] but also in toluene, making it possible to carry out the reaction as a simple one-pot procedure: The air- and moisture-sensitive zirconacyclopentadiene **8** was directly transformed into the corresponding stannoles within 3 h, using R_2SnCl_2 (with $R = \text{Me}, n\text{Bu}, \text{Ph}$) and catalytic amounts of copper chloride at 20°C . The reaction was accompanied by a distinct color change from the dark **8** to the bright orange stannoles in all cases. For the isolation of **10** and **12**, carried out by column chromatography, it was necessary to condition the silica with triethylamine to prevent decomposition of the stannoles. The need for this procedure already gave some indication of their lower stability compared to the phenyl-substituted stannole **11**, which did not show any decomposition on silica. Initially, stannoles without halides and with substituents of different steric hindrance at the tin atom were prepared ($R = \text{Me}, n\text{Bu}, \text{Ph}$, **10–12**) to investigate the stability of the different stannoles under cross-coupling conditions, which would be later used for polymerization.

The stabilities of these stannoles (**10–12**) were examined by performing reactions with a 2-iodo thiophene **13**, applying standard cross-coupling conditions (Scheme 6).^[21] In the case of $R = \text{Me}$ and $R = n\text{Bu}$ (**10** and **12**), a conversion of the starting material of over 99% was found, but the reaction mixture was highly complex and the stannoles had completely decomposed.^[22] The phenyl substituted stannole **11** however, showed a much higher stability under cross-coupling conditions, with a conversion of 40 to 50%. These results indicated that the use of phenyl-substituted stannoles should offer a much higher stability.



Scheme 6. Examination of the stability of stannoles **10**, **11**, and **12** under cross-coupling (polymerization) conditions.

Based on these results, an iodinated stannole **9**, bearing phenyl groups at the tin, was prepared in a yield of 81% (Scheme 5) and fully characterized. The determined $^nJ(^{119}\text{Sn}, ^{13}\text{C})$ values support the assignment of carbon signals, showing similar coupling constants to hexaphenylstannole (see the Supporting Information).^[23] The molecular structure of **9** was determined by X-ray crystallography (Figure 1): the

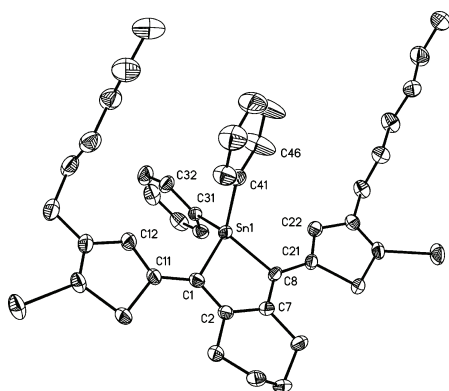
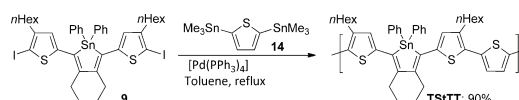


Figure 1. ORTEP drawing of **9**, thermal ellipsoids set at 50% probability. Hydrogen atoms and two disordered carbon atoms are omitted for clarity. Selected bond lengths [Å]: Sn1–C8 2.1328(3), Sn1–C1 2.1385(4), C1–C2 1.3724(5), C2–C7 1.4882(5), C7–C8 1.3675(5).

stannole ring is essentially planar, while the two phenyl rings are twisted from this plane, with torsion angles of 85.98° (C32–C31–Sn1–C1) and 83.11° (C46–C41–Sn1–C8). The smallest angle of the strongly distorted tetrahedral environment of the tin atom is 83.85° (C1–Sn1–C8), which is similar to other reported values.^[1e, 16c, 23] Compared to other Group 14 metallocenes, this endocyclic angle increases from stannoles to germales to siloles, showing the influence of the large atomic radius of tin and the long carbon–tin bonds.^[1e] The Sn1–C8 and Sn1–C1 bonds are, as expected, much longer than the C–C bonds of the stannole. The C–C bond alternation of the 1,3-dienyl moiety is comparable to the values of another thiophene-substituted stannole,^[1e] but less pronounced than in other reported structures without thiophenes attached to the stannole, possibly because of extended conjugation.^[16c, 23, 24] The two thiophene rings are arranged anti-coplanar to the central stannole ring, with dihedral angles of 178.04° (C7–C8–C21–C22) and 177.77° (C2–C1–C11–C12). This high planarity of the whole molecule should ensure an effective conjugation, an important factor for a semiconducting polymer. The bulky phenyl groups do not perturb this

planarity, making them good candidates as stabilizing substituents for stannoles.

Having solved the problems of synthesizing a halide-containing stannole and of finding an appropriate, stable-enough substituent for the tin, the polymerization was carried out by a Stille cross-coupling reaction between **9** and the double-stannylated thiophene **14** (Scheme 7). The reaction



Scheme 7. Cross-coupling of **9** and **14**, yielding 90% of the polymer TStTT ($M_w = 17.0$ kDa, PDI = 2.5).

was heated to reflux in toluene, using 5 mol% $[\text{Pd}(\text{PPh}_3)_4]$ as a catalyst, to afford a purple-black polymer in 90% yield after purification by precipitation. ^{119}Sn NMR spectroscopy and MALDI mass spectrometry indicated that the reaction was completely tin selective, without any noticeable decomposition of the stannole: the ^{119}Sn NMR of the monomer **9** showed one signal at $\delta = -79.9$ ppm which was slightly shifted to $\delta = -81.1$ ppm in the polymer TStTT, and no additional signal was observed. The MALDI-MS analysis showed a mass difference of 792.2 Da between corresponding peaks, which corresponds to the mass of the expected repeat unit.^[25]

The polymer showed good solubility in common solvents (CHCl_3 , CH_2Cl_2 , chlorobenzene, toluene, THF) at 20°C. Number- and weight-average molecular weights were determined by gel permeation chromatography (GPC) to be $M_n = 6.8$ kDa and $M_w = 17.0$ kDa (calibrated with polystyrene standards), giving a polydispersity index (PDI) of 2.5. As the chain length of polymers prepared by step-growth polymerizations is extremely sensitive to unwanted side reactions, this comparatively high molecular weight underlines the extremely high nucleophile-selectivity of the reaction. The polymer was thermally stable up to 300°C and, somewhat unusually for a phenyl-containing polymer, not completely X-ray amorphous.^[25]

UV/Vis spectra (for luminescence spectra, see the Supporting Information) from polymer TStTT were obtained in chloroform and compared to those of monomer **9** (Figure 2). The polymer TStTT shows a broad absorption in solution with a $\lambda_{\text{max}} = 536$ nm. This value displays a significant bathochro-

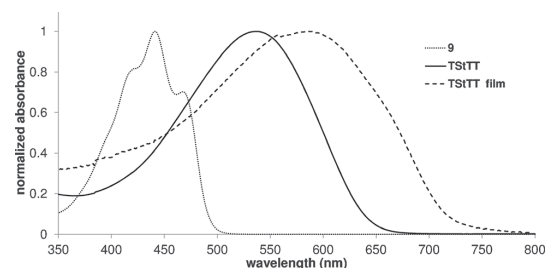



Figure 2. Absorption spectra of **9** and TStTT in chloroform and as a film.

- [16] a) B. Wrackmeyer, P. Thoma, S. Marx, T. Bauer, R. Kempe, *Eur. J. Inorg. Chem.* **2014**, 2103–2112; b) B. Wrackmeyer, P. Thoma, S. Marx, G. Glatz, R. Kempe, *Z. Anorg. Allg. Chem.* **2013**, 639, 1205–1213; c) B. Wrackmeyer, U. Klaus, W. Milius, E. Klaus, T. Schaller, *J. Organomet. Chem.* **1996**, 517, 235–242; d) B. Wrackmeyer, *J. Organomet. Chem.* **1989**, 364, 331–342; e) L. Killian, B. Wrackmeyer, *J. Organomet. Chem.* **1977**, 132, 213–221.
- [17] N. Miyaura, A. Suzuki, *Chem. Rev.* **1995**, 95, 2457–2483.
- [18] E. Negishi, S. J. Holmes, J. M. Tour, J. A. Miller, F. E. Cederbaum, D. R. Swanson, T. Takahashi, *J. Am. Chem. Soc.* **1989**, 111, 3336–3346.
- [19] C. F. Harris, D. Ravindranathan, S. Huo, *Tetrahedron Lett.* **2012**, 53, 5389–5392.
- [20] a) J. R. Nitschke, S. Zürcher, T. D. Tilley, *J. Am. Chem. Soc.* **2000**, 122, 10345–10352; b) U. Rosenthal, A. Ohff, W. Baumann, A. Tillack, H. Görls, V. V. Burlakov, V. B. Shur, *Z. Anorg. Allg. Chem.* **1995**, 621, 77–83.
- [21] C. Lin, T. Endo, M. Takase, M. Iyoda, T. Nishinaga, *J. Am. Chem. Soc.* **2011**, 133, 11339–11350.
- [22] It was not possible to identify the formed products.
- [23] J. Ferman, J. P. Kakareka, W. T. Klooster, J. L. Mullin, J. Quattrucci, J. S. Ricci, H. J. Tracy, W. J. Vining, S. Wallace, *Inorg. Chem.* **1999**, 38, 2464–2472.
- [24] T. Kuwabara, J.-D. Guo, S. Nagase, M. Minoura, R. H. Herber, M. Saito, *Organometallics* **2014**, 33, 2910–2913.
- [25] See the Supporting Information.
- [26] T.-A. Chen, X. Wu, R. D. Rieke, *J. Am. Chem. Soc.* **1995**, 117, 233–244.

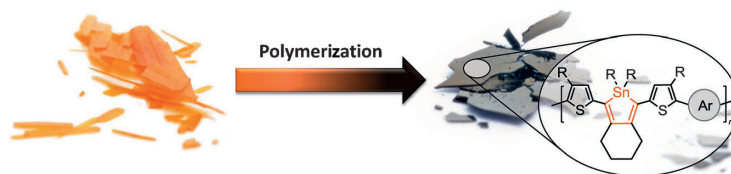
Communications



Nucleophile-Selective Cross-Coupling

J. Linshoef, E. J. Baum, A. Hussain,
P. J. Gates, C. Näther,
A. Staubitz* 

Highly Tin-Selective Stille Coupling:
Synthesis of a Polymer Containing
a Stannole in the Main Chain



The budding potential of stannoles: A stannole monomer is prepared and employed in a highly tin-selective Stille coupling, giving a well-defined and non-annulated stannole-containing polymer,

the first example from this class of π -conjugated polymers. Compared to polythiophenes, a strong bathochromic shift in the absorption spectrum was observed.

Nucleophil-selektive Kreuzkupplung

Hoch Zinn-selektive Stille-Kupplung: Polymersynthese mit einem Stannol in der Hauptkette**

Julian Linshoef, Evan J. Baum, Andreas Hussain, Paul J. Gates, Christian Näther und Anne Staubitz*

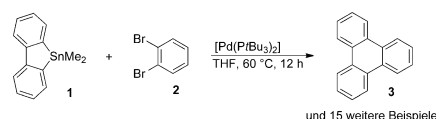
Abstract: Die Einbringung von Gruppe-14-Metallolen in halbleitende Polymere führt zu ungewöhnlichen optoelektronischen Eigenschaften. Polymere mit Stannol-Einheiten waren bisher jedoch nicht zugänglich. Wir berichten über eine Syntheseroute zu einem wohldefinierten stannolhaltigen Polymer, dem ersten Beispiel dieser Klasse von π -konjugierten Polymeren. Dies wurde erreicht durch die Entwicklung doppelt funktionalisierter Stannol-Monomere und durch eine hochselektive Stille Kupplungsreaktion, welche das Zinn im Stannol unberührt lässt. Im Vergleich mit Poly(3-*n*-hexylthiophen) zeigt die Absorption des erhaltenen Polymers eine bemerkenswerte bathochrome Verschiebung.

Das formale Ersetzen der Methylengruppe in Cyclopentadienen durch schwerere Gruppe-14-Elemente ändert ihre elektronischen Eigenschaften dramatisch.^[1] Durch die Einbringung von Si, Ge oder Sn wird die Energie der zwei σ^* -Orbitale der exocyclischen E-R-Bindungen (mit E = Si, Ge, Sn) im Vergleich zu C-R deutlich herabgesetzt, was eine effiziente Wechselwirkung mit den π^* -Orbitalen des Dien-systems ermöglicht. Dies führt zu einem deutlichen Absinken der LUMO-Niveaus im Vergleich zu Cyclopentadienen.^[1b,d,e] Daher sind diese Gruppe-14-Metallole interessante Heterocyclen für den Einbau in halbleitende Polymere: Es ist zu erwarten, dass sich diese Polymere durch niedrige Bandlücken und neuartige Ladungstransporteigenschaften auszeichnen.^[2] Sila- und Germafluorene^[3] wurden ebenso wie Silole und Germole^[4] bereits in Polymere eingebunden, was zu deutlichen Verbesserungen bei elektronischen Bauteilen führte.^[5] Außerdem wurden Gruppe-14-Heterole auch als 1,1-verknüpfte Metallole verwendet.^[1b,6] Betrachtet man Zinn, so gibt es einige Arbeiten zu Stannafluorenen,^[7] doch

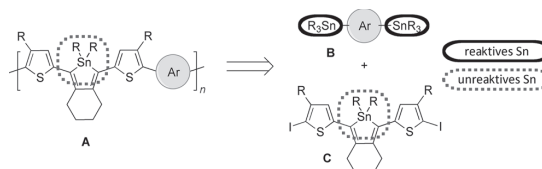
die Chemie der Stannole wurde bisher deutlich weniger untersucht.^[1e,8]

Bis heute wurde kein Stannol mit reaktiven Halogenfunktionalitäten veröffentlicht, die Kreuzkupplungen ermöglichen könnten – weder direkt am Dienyrling, noch an weiteren aromatischen Substituenten an diesem Ring. Das Problem ist hierbei, dass Zinn-Heterocyclen selbst äußerst vielseitige nucleophile Verbindungen für Stille-Kreuzkupplungen darstellen. Tatsächlich könnte man Stannole als cyclische Vinyl-Zinn-Verbindungen betrachten, welche regelmäßig in Kreuzkupplungen verwendet werden.^[10] Abhängig von den Reaktionsbedingungen können diese sogar reaktiver sein als Aryl-Zinn-Verbindungen.^[11] Die kürzlich beschriebene Reaktivität der verwandten Stannafluorene verdeutlicht das Problem, reaktive Organozinn-Verbindungen in Kreuzkupplungen zu verwenden, wenn man eine Reaktion am Zinn-Zentrum verhindern möchte: In diesen Arbeiten wurde gezeigt, dass Stannafluorene **1** glatt mit Dibrombenzolen **2** reagieren und Triphenylene **3** in hohen Ausbeuten liefern (Schema 1).^[9,12]

Im Folgenden stellen wir die erste Nucleophil-selektive Stille-Kreuzkupplung dar, welche zwischen einer endo- und zwei exocyclischen Zinn-Funktionalitäten unterscheidet (Schema 2). Dies ermöglicht die Synthese des ersten wohldefinierten nichtanellierten stannolhaltigen Polymers des Typs **A** (Schema 2), welches eine starke bathochrome Verschiebung im Vergleich zum verwandten Poly(3-*n*-hexylthiophen) (P3HT) zeigt. Um ein Monomer des Typs **C** zu synthetisieren, mussten zwei zentrale Herausforderungen



Schema 1. Die Reaktion zwischen Stannafluorenen **1** und Dielektrophilen **2** kann zu den Kreuzkupplungsprodukten **3** führen (in diesem Beispiel isoliert in 87% Ausbeute).^[9]



Schema 2. Zinn-selektive Kreuzkupplungen ermöglichen die Synthese von stannolhaltigen Polymeren.

[*] J. Linshoef, E. J. Baum, A. Hussain, Prof. Dr. A. Staubitz
Otto-Diels-Institut für Organische Chemie, Universität Kiel
24098 Kiel (Deutschland)
E-Mail: astaubitz@oc.uni-kiel.de

Prof. Dr. C. Näther
Institut für Anorganische Chemie, Universität Kiel
24098 Kiel (Deutschland)

Dr. P. J. Gates
School of Chemistry, University of Bristol
Bristol BS8 1TS (Großbritannien)

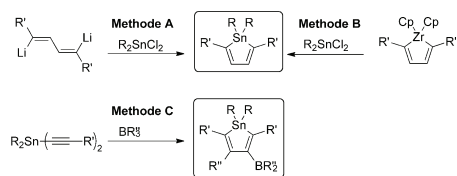
[**] J.L. dankt der Deutschen Bundesstiftung Umwelt (DBU) für ein Promotionsstipendium. E.J.B. dankt dem Deutschen Akademischen Austauschdienst (DAAD) für ein RISE-Stipendium. Wir danken Dr. Franz J. Mayer von Bruker Daltonik GmbH für die Messung des MALDI-TOF-Spektrums unseres Polymers **TSITT**.

Hintergrundinformationen zu diesem Beitrag sind im WWW unter <http://dx.doi.org/10.1002/ange.201407377> zu finden.

bewältigt werden: Zunächst musste eine Syntheseroute entwickelt werden, welche die Herstellung eines Stannol-Monomers mit elektrophilen funktionellen Gruppen (Bromide oder Iodide) am Kohlenstoffgerüst für eine spätere Polymerisation im Heterocyclus geschützt werden, sodass es unter Polymerisationsbedingungen stabil bleibt. Eine Realisierung stellten wir uns hierbei durch ein kinetisch deaktiviertes Zinn-Zentrum im Stannol-Monomer vor.

Die Reaktivitäten und Funktionalisierungsmöglichkeiten der Stannole sind nahezu komplett unerforscht. Insbesondere sind keine Arbeiten über mit Bromid/Iodid funktionalisierte Stannole bekannt. Dies bezieht sich nicht nur auf Bromid/Iodid-Substituenten direkt am Ring, sondern es wurden ebenfalls keine Stannole synthetisiert, welche bromierte/iodierte Arylsubstituenten aufweisen.

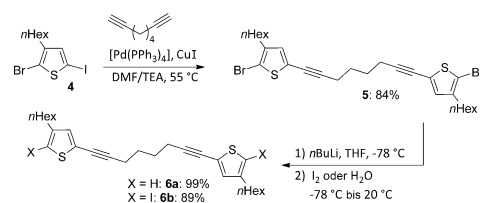
Es gibt drei etablierte Methoden für die Herstellung von Stannolen: Im Allgemeinen können sie durch die In-situ-Synthese eines dilithiierten Butadiens erhalten werden, welches man mit R_2SnCl_2 ^[8a,13] reagieren lässt (Methode A, Schema 3). Die zweite Route beinhaltet einen Zr-Sn-Aus-



Schema 3. Mögliche Synthesemethoden für Stannole.

tausch^[1e,14] von Zirconacyclopentadienen mit R_2SnCl_2 (Methode B). Eine andere Möglichkeit ist die 1,1-Carborborierung von aktivierten Zinn-Diacetylen – auch als Wrackmeyer-Reaktion bekannt –, welche im Allgemeinen die gewünschten Stannole in hohen Ausbeuten liefert (Methode C).^[15]

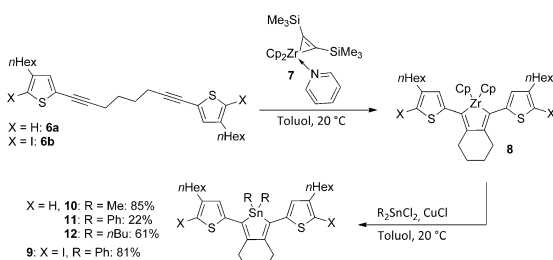
Da die Anwesenheit von Halogeniden ($R' = -Ar-X$; Schema 3) essenziell für das geplante Monomer ist, ist eine Route über ein dilithiiertes Butadien aufgrund der potentiell unselektiven Halogen-Lithium-Austauschreaktionen problematisch. Obwohl Methode C eine direkte Möglichkeit für die Synthese von Stannolen (und anderen Metallolen) darstellt,^[16] wurde sie zu diesem Zeitpunkt nicht verfolgt, da man hierbei ein Bor-Atom in 3- oder 4-Position erhalten würde. Solch unsymmetrische Monomere würden in der folgenden Polykondensation wahrscheinlich zu regioirregulären Polymeren führen. Daher wurde ein Zirconacyclopentadien als Stannol-Vorstufe ausgewählt, flankiert von zwei Halogenid-substituierten 3-*n*-Hexylthiophenen. Für diese Route wurde das Octadiin-verknüpfte Bis(thiophen) **5** in einer elektrophil selektiven Sonogashira-Kreuzkupplung hergestellt, ohne dass Produkte unselektiver Kreuzkupplungen mit dem Bromid festgestellt werden konnten (Schema 4). Bromid-Lithium-Austausch und anschließende Reaktion mit Wasser oder Iod bei $-78^\circ C$ führte zu der protonierten bzw. iodierten Spezies **6a** und **6b**. Der Bromid-Iodid-Austausch wurde aufgrund der höheren Reaktivität von Iodiden in



Schema 4. Synthese des Thiophen-flankierten Octadiins **6**.

Kreuzkupplungen durchgeführt,^[17] wodurch eine spätere Polymerisation erleichtert wird.

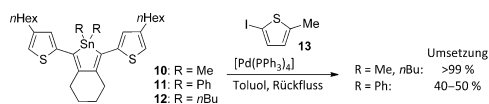
Das gebräuchliche Reagens für die Synthese von Zirconacyclopentadienen aus Diinen ist das in situ hergestellte Negishi-Reagens.^[18] Allerdings ist dieses hochreaktive Reagens problematisch bei Halogenid-funktionalisierten Verbindungen, da es auch C-X-Insertionen eingeht.^[19] Ein deutlich milderer Reagens ist Rosenthals Zirconocen,^[20] das für ein Bromid-funktionalisiertes Zirconacyclopentadien verwendet wurde.^[4a] Deshalb wurde Rosenthals Zirconocen **7** in einer Reaktion mit **6** in Toluol bei $20^\circ C$ für 18 h eingesetzt, wobei eine dunkelrote Lösung entstand (Schema 5). Kupferchlorid



Schema 5. Synthese diverser Stannole über eine Zirconacyclopentadien-Eintopfreaktion.

fördert den Zr-Sn-Austausch nicht nur in THF,^[14a-c] sondern auch in Toluol, wodurch es möglich wird, die Reaktion als Eintopfreaktion durchzuführen: Das luft- und feuchtigkeitsempfindliche Zirconacyclopentadien **8** wurde bei $20^\circ C$ innerhalb von 3 h direkt in das entsprechende Stannol, unter Verwendung von R_2SnCl_2 (mit $R = Me, nBu, Ph$) mit katalytischen Mengen an Kupferchlorid, überführt. Die Reaktion ging in allen Fällen mit einem deutlichen Farbwechsel vom dunklen **8** zu den hellorangenen Stannolen einher. Für die Isolierung von **10** und **12**, die mittels Säulenchromatographie durchgeführt wurden, war es notwendig, das Kieselgel mit Triethylamin zu behandeln, um eine Zersetzung der Stannole zu verhindern. Dies war ein erstes Anzeichen für die geringe Stabilität von **10** und **12** im Vergleich zu dem phenylsubstituierten Stannol **11**, das keinerlei Zersetzung auf Kieselgel zeigte. Zunächst wurden Stannole ohne Halogenide, aber mit verschiedenen großen Substituenten am Zinn-Atom hergestellt ($R = Me, nBu, Ph$, **10–12**). Damit wurde die Stabilität der Stannole unter Kreuzkupplungsbedingungen, wie sie später für eine Polymerisation verwendet würden, untersucht.

Die Stabilitäten der Stannole (**10–12**) wurden untersucht, indem Reaktionen mit 2-Iodthiophen **13** unter gewöhnlichen Kreuzkupplungsbedingungen^[21] durchgeführt wurden (Schema 6). Im Fall von R = Me und R = *n*Bu (**10** und **12**)



Schema 6. Untersuchung der Stabilitäten der Stannole **10**, **11** und **12** unter Kreuzkupplungs-/Polymerisationsbedingungen.

wurden > 99% der Ausgangsverbindung umgesetzt, aber das Reaktionsgemisch war sehr komplex und die Stannole wurden vollständig zersetzt.^[22] Das phenylsubstituierte Stannol **11** zeigte unter Kreuzkupplungsbedingungen jedoch eine deutlich höhere Stabilität mit einer Umsetzung von 40 bis 50%. Diese Ergebnisse deuteten darauf hin, dass die Verwendung von phenylsubstituierten Stannolen allgemein eine deutlich höhere Stabilität bieten sollte.

Basierend auf diesen Ergebnissen wurde ein iodiertes Stannol **9**, das Phenylgruppen am Zinn trägt, in einer Ausbeute von 81% hergestellt und vollständig charakterisiert (Schema 5). Die ermittelten ¹¹⁹J(¹¹⁹Sn, ¹³C)-Werte stützen die Zuordnung der Kohlenstoffsignale, und die Kopplungskonstanten sind denen von Hexaphenylstannol ähnlich (siehe die Hintergrundinformationen).^[23] Die Molekülgeometrie von **9** wurde mittels Röntgenkristallographie ermittelt (Abbildung 1): Der Stannolring ist nahezu planar, wobei die

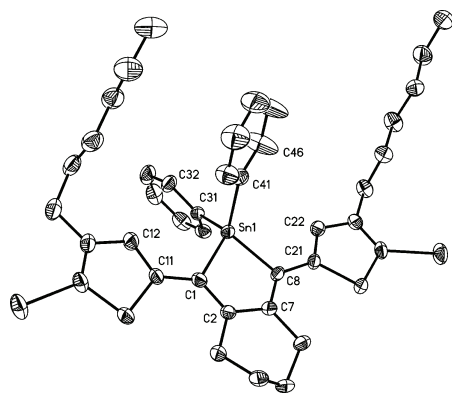
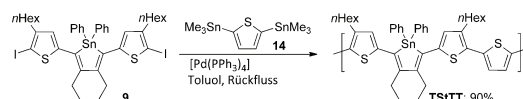


Abbildung 1. ORTEP-Zeichnung von **9** (Schwingungsellipsoide mit 50% Aufenthaltswahrscheinlichkeit). H-Atome und zwei ungeordnete C-Atome wurden zur besseren Übersicht weggelassen. Ausgewählte Bindungslängen [Å]: Sn1-C8 2.1328(3), Sn1-C1 2.1385(4), C1-C2 1.3724(5), C2-C7 1.4882(5), C7-C8 1.3675(5).

beiden Phenylringe mit Torsionswinkeln von 85.98° (C32-C31-Sn1-C1) und 83.11° (C46-C41-Sn1-C8) aus dieser Ebene herausgedreht sind. Der kleinste Winkel der stark verzerrten tetraedrischen Umgebung des Zinn-Atoms ist 83.85° (C1-Sn1-C8), vergleichbar mit anderen berichteten Wer-

ten.^[1e, 16c, 23] Vergleicht man diesen endocyclischen Winkel mit den Werten von anderen Gruppe-14-Metallolen, so wird er größer von Stannolen zu Germolen zu Silolen, was den Einfluss des großen Atomradius und der langen Kohlenstoff-Zinn-Bindung zeigt.^[1e] Die Sn1-C8- und Sn1-C1-Bindungen sind wie erwartet deutlich länger als die C-C-Bindungen des Stannols. Die C-C-Bindungsalternierung des 1,3-Dienylrestes ist vergleichbar mit den Werten eines anderen thiophensubstituierten Stannols,^[1e] aber sie ist weniger stark ausgeprägt als bei anderen berichteten Molekülstrukturen ohne an das Stannol gebundene Thiophene.^[16c, 23, 24] Dies ist möglicherweise auf eine verbesserte Konjugation zurückzuführen. Die beiden Thiophenringe sind antikoplanar zu dem zentralen Stannolring ausgerichtet, mit Diederwinkeln von 178.04° (C7-C8-C21-C22) und 177.77° (C2-C1-C11-C12). Diese hohe Planarität des Moleküls sollte eine effiziente Konjugation sicherstellen, was ein wichtiger Faktor für halbleitende Polymere ist. Die sperrigen Phenylgruppen stören diese Planarität nicht, wodurch sie zu guten Kandidaten als stabilisierende Substituenten für Stannole werden.

Nachdem das Problem, ein halogenidsubstituiertes Stannol zu synthetisieren und einen angemessenen Substituenten mit ausreichender Stabilität für das Zinn zu finden, gelöst werden konnte, wurde die Polymerisation mittels Stille-Kreuzkupplung zwischen **9** und dem doppelt stannylierten Thiophen **14** durchgeführt (Schema 7). Die Reaktionsmi-



Schema 7. Kreuzkupplung zwischen **9** und **14**, welche das Polymer **TSITT** ($M_w = 17.0$ kDa, PDI = 2.5) in 90% Ausbeute ergibt.

schung wurde unter Verwendung von 5 Mol-% [Pd(PPh₃)₄] als Katalysator in Toluol zum Rückfluss erhitzt. Dabei wurde ein dunkelviolett Polymer in 90% Ausbeute nach Aufreinigung per Fällung erhalten. ¹¹⁹Sn-NMR-Spektroskopie und MALDI-MS deuten darauf hin, dass die Reaktion komplett Zinn-selektiv war, ohne dass eine nennenswerte Zersetzung der Stannole beobachtet werden konnte: Das ¹¹⁹Sn-NMR-Spektrum des Monomers **9** zeigte ein Signal bei -79.9 ppm, welches geringfügig zu -81.1 ppm im Polymer **TSITT** verschoben wurde, und es wurde kein zusätzliches Signal beobachtet. MALDI-MS Analyse zeigte eine Massendifferenz von 792.2 Da zwischen den entsprechenden Peaks, was der Masse der erwarteten Wiederholungseinheit entspricht.^[25]


Das Polymer zeigte eine gute Löslichkeit in üblichen Lösungsmitteln (CHCl₃, CH₂Cl₂, Chlorbenzol, Toluol, THF) bei 20°C. Das Zahlen- und Massenmittel der Molmasse wurde per Gelpermeationschromatographie (GPC) zu $M_n = 6.8$ kDa und $M_w = 17.0$ kDa bestimmt (kalibriert mit Polystyrol-Standards), was einen PDI von 2.5 ergibt. Da die Kettenlänge bei über Stufenwachstumsreaktionen hergestellten Polymeren sehr empfindlich auf unerwünschte Nebenreaktionen reagiert, unterstreicht das relativ hohe Molekulargewicht die extrem ausgeprägte Nucleophil-Selektivität der Reaktion. Das Polymer war thermisch stabil bis 300°C und nicht

- Chem.* **2005**, *117*, 6711–6714; f) B. Wrackmeyer, G. Kehr, S. Willbold, S. Ali, *J. Organomet. Chem.* **2002**, *646*, 125–133; g) B. Wrackmeyer, K. H. von Locquenghien, S. Kundler, *J. Organomet. Chem.* **1995**, *503*, 289–295.
- [9] Siehe Lit. [7a].
- [10] a) A. F. Littke, G. C. Fu, *Angew. Chem. Int. Ed.* **1999**, *38*, 2411–2413; *Angew. Chem.* **1999**, *111*, 2568–2570; b) W. Su, S. Urgaonkar, J. G. Verkade, *Org. Lett.* **2004**, *6*, 1421–1424; c) D. R. McKean, G. Parrinello, A. F. Renaldo, J. K. Stille, *J. Org. Chem.* **1987**, *52*, 422–424.
- [11] a) A. M. Echavarren, J. K. Stille, *J. Am. Chem. Soc.* **1987**, *109*, 5478–5486; b) A. Kamimura, M. So, S. Ishikawa, H. Uno, *Org. Lett.* **2013**, *15*, 1402–1405.
- [12] B. Kumar, C. E. Strasser, B. T. King, *J. Org. Chem.* **2012**, *77*, 311–316.
- [13] a) A. J. Ashe III, S. Mahmoud, *Organometallics* **1988**, *7*, 1878–1880; b) M. Saito, M. Nakamura, T. Tajima, *Heterocycles* **2009**, *78*, 657–668; c) E. H. Bray, W. Huebel, I. Caplier, *J. Am. Chem. Soc.* **1961**, *83*, 4406–4413.
- [14] a) C. Fan, W. E. Piers, M. Parvez, *Angew. Chem. Int. Ed.* **2009**, *48*, 2955–2958; *Angew. Chem.* **2009**, *121*, 2999–3002; b) Y. Ura, Y. Li, F.-Y. Tsai, K. Nakajima, M. Kitora, T. Takahashi, *Heterocycles* **2000**, *52*, 1171–1189; c) Y. Ura, L. Yanzhong, X. Zhenfeng, T. Takahashi, *Tetrahedron Lett.* **1998**, *39*, 2787–2790; d) S. Kim, K. H. Kim, *Tetrahedron Lett.* **1995**, *36*, 3725–3728; e) P. J. Fagan, W. A. Nugent, *J. Am. Chem. Soc.* **1988**, *110*, 2310–2312.
- [15] Wichtige Übersichten zu diesem Thema: a) B. Wrackmeyer, *Coord. Chem. Rev.* **1995**, *145*, 125–156; b) B. Wrackmeyer, *Heteroat. Chem.* **2006**, *17*, 188–208; c) G. Kehr, G. Erker, *Chem. Commun.* **2012**, *48*, 1839–1850.
- [16] a) B. Wrackmeyer, P. Thoma, S. Marx, T. Bauer, R. Kempe, *Eur. J. Inorg. Chem.* **2014**, 2103–2112; b) B. Wrackmeyer, P. Thoma, S. Marx, G. Glatz, R. Kempe, *Z. Anorg. Allg. Chem.* **2013**, *639*, 1205–1213; c) B. Wrackmeyer, U. Klaus, W. Milius, E. Klaus, T. Schaller, *J. Organomet. Chem.* **1996**, *517*, 235–242; d) B. Wrackmeyer, *J. Organomet. Chem.* **1989**, *364*, 331–342; e) L. Killian, B. Wrackmeyer, *J. Organomet. Chem.* **1977**, *132*, 213–221.
- [17] N. Miyaura, A. Suzuki, *Chem. Rev.* **1995**, *95*, 2457–2483.
- [18] E. Negishi, S. J. Holmes, J. M. Tour, J. A. Miller, F. E. Cederbaum, D. R. Swanson, T. Takahashi, *J. Am. Chem. Soc.* **1989**, *111*, 3336–3346.
- [19] C. F. Harris, D. Ravindranathan, S. Huo, *Tetrahedron Lett.* **2012**, *53*, 5389–5392.
- [20] a) J. R. Nitschke, S. Zürcher, T. D. Tilley, *J. Am. Chem. Soc.* **2000**, *122*, 10345–10352; b) U. Rosenthal, A. Ohff, W. Baumann, A. Tillack, H. Görls, V. V. Burlakov, V. B. Shur, *Z. Anorg. Allg. Chem.* **1995**, *621*, 77–83.
- [21] C. Lin, T. Endo, M. Takase, M. Iyoda, T. Nishinaga, *J. Am. Chem. Soc.* **2011**, *133*, 11339–11350.
- [22] Es war nicht möglich, die gebildeten Produkte zu identifizieren.
- [23] J. Ferman, J. P. Kakareka, W. T. Klooster, J. L. Mullin, J. Quattrucci, J. S. Ricci, H. J. Tracy, W. J. Vining, S. Wallace, *Inorg. Chem.* **1999**, *38*, 2464–2472.
- [24] T. Kuwabara, J.-D. Guo, S. Nagase, M. Minoura, R. H. Herber, M. Saito, *Organometallics* **2014**, *33*, 2910–2913.
- [25] Siehe die Hintergrundinformationen.
- [26] T.-A. Chen, X. Wu, R. D. Rieke, *J. Am. Chem. Soc.* **1995**, *117*, 233–244.

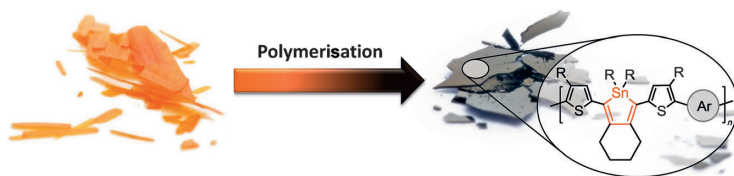
Zuschriften



Nucleophil-selektive Kreuzkupplung

J. Linshoef, E. J. Baum, A. Hussain,
P. J. Gates, C. Näther,
A. Staubitz* 

Hoch Zinn-selektive Stille-Kupplung:
Polymersynthese mit einem Stannol in
der Hauptkette

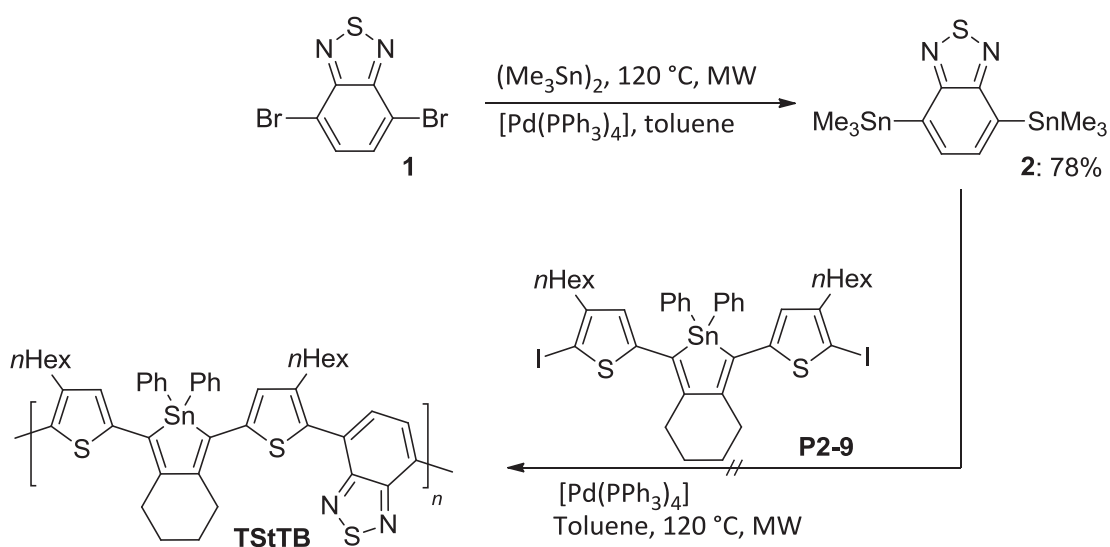


Das aufkeimende Potenzial der Stannole:
Eine Syntheseroute zu einem Stannol-
monomer ist beschrieben. Dieses Mono-
mer wurde in einer hoch Zinn-selektiven
Stille-Kupplung eingesetzt, was zu einem
wohldefinierten und nichtanellierten

stannolhaltigen Polymer führte – das
erste Beispiel aus dieser Klasse von π -
konjugierten Polymeren. Im Vergleich mit
Polythiophenen zeigt sich eine starke
bathochrome Verschiebung im Absorp-
tionsspektrum.

3.2.1.2 Stannole-Thiophene-Benzothiadiazole Copolymers

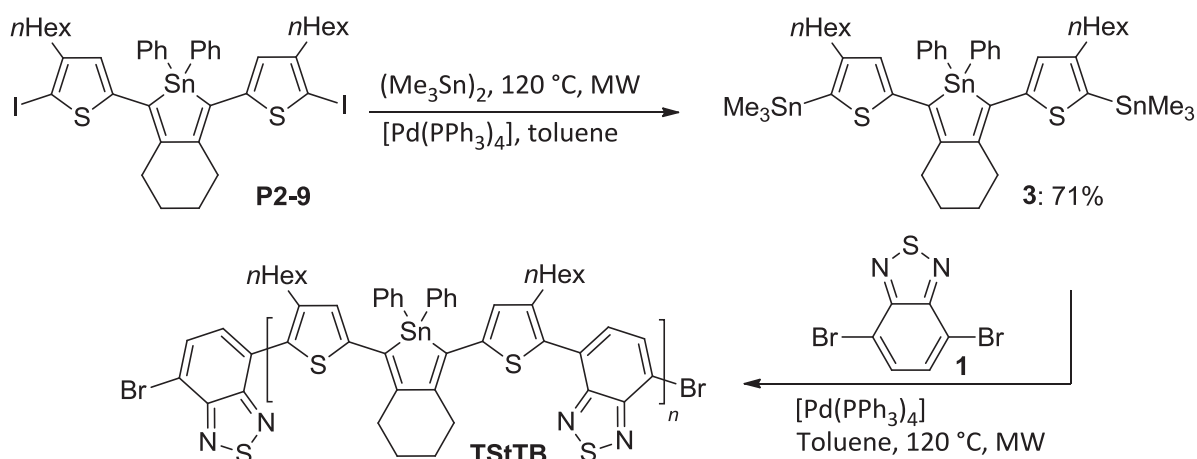
It is an established method in the preparation of semiconducting polymers to use the push-pull concept to reduce the band gap.^[47] Since thiophenes have a π -excessive nature^[48] and stannoles electron accepting abilities,^[49] the prepared polymer **TStTT** (see chapter 3.2.1.1) exhibits an electron rich-poor-rich-rich structure. It was therefore also envisaged to incorporate the well-established and commercially available 4,7-dibromo-2,1,3-benzothiadiazole **1**^[50] to obtain an alternating electron rich - electron poor structure. Following this concept, it was necessary to either transform **1** (Scheme 3) or the stannole monomer **P2-9** into a dinucleophile (see below, Scheme 4).



Scheme 3. Synthesis of nucleophilic **2**, and attempted polymerization with **P2-9**.

Dinucleophilic **2** could be prepared in a yield of 78% by reaction of **1** with hexamethylditin in a microwave for 6 h at 120 °C. Shorter reaction times or conventional heating led to no or only very low conversions. However, subsequent polymerization with the stannole **P2-9** was unsuccessful: even after 18 h under microwave irradiation at 120 °C, no distinct color change was observed, and TLC analysis showed that the starting materials were not converted. Higher reaction temperatures were not tested, because they led to an explosion of the microwave reaction vessel during the synthesis of **2**, presumably due to decomposition of the benzothiadiazole. Because of this low reactivity of the electron poor **2**, instead a derivative of **P2-9**, where both iodide functional groups had to be replaced by tin functional groups (Scheme 4, **3**), was used as the nucleophilic component for the polymerization. Monomer **3** could be synthesized by heating for 30 min to 120 °C in the microwave and purification by column chromatography,^[51] and could be isolated in a yield of 71 % (Scheme 4). This reaction is another

example of an entirely nucleophile selective cross-coupling, because only the hexamethyldistannane reacted whereas the stannole ring remained untouched. The cross-coupling reaction of **3** and **1** displayed a completely different reactivity compared to the polymerization of **P2-9** (see chapter 3.2.1.1).



Scheme 4. Transformation of electrophilic **P2-9** into nucleophilic **3**, and cross-coupling reaction with **1** to **TStTB** ($n = 1$; 6% yield).

Under the same reaction conditions which were successful for the polymerization of **P2-9** with 2,5-bis(trimethylstannyl)thiophene (see chapter 3.2.1.1), no polymer was obtained. In a microwave apparatus, a reaction time of 8 h was necessary to obtain a distinct color change from orange to deep red. Analysis of the reaction mixture showed a substantial amount of residual starting material, without any polymer formation. However, the bis-coupled product **TStTB** with $n = 1$ could be isolated in a yield of 6 % and was fully characterized. This sluggish reactivity further illustrates the dramatic influence of the stannole ring in this case on the flanking thiophenes: With less electron withdrawing substituents, stannylated thiophenes couple with **1** without difficulty.^[52]

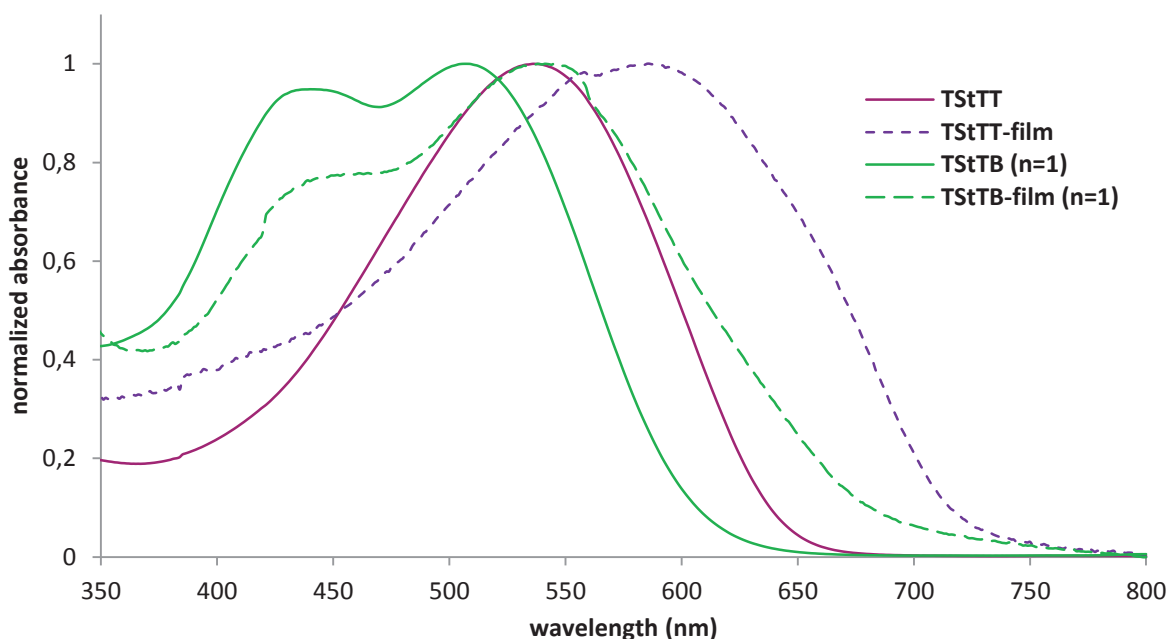


Figure 18. Absorption spectra of **TStTB** ($n = 1$) in solution (chloroform) and as film in comparison with **TStTT** (see chapter 3.2.1.1).

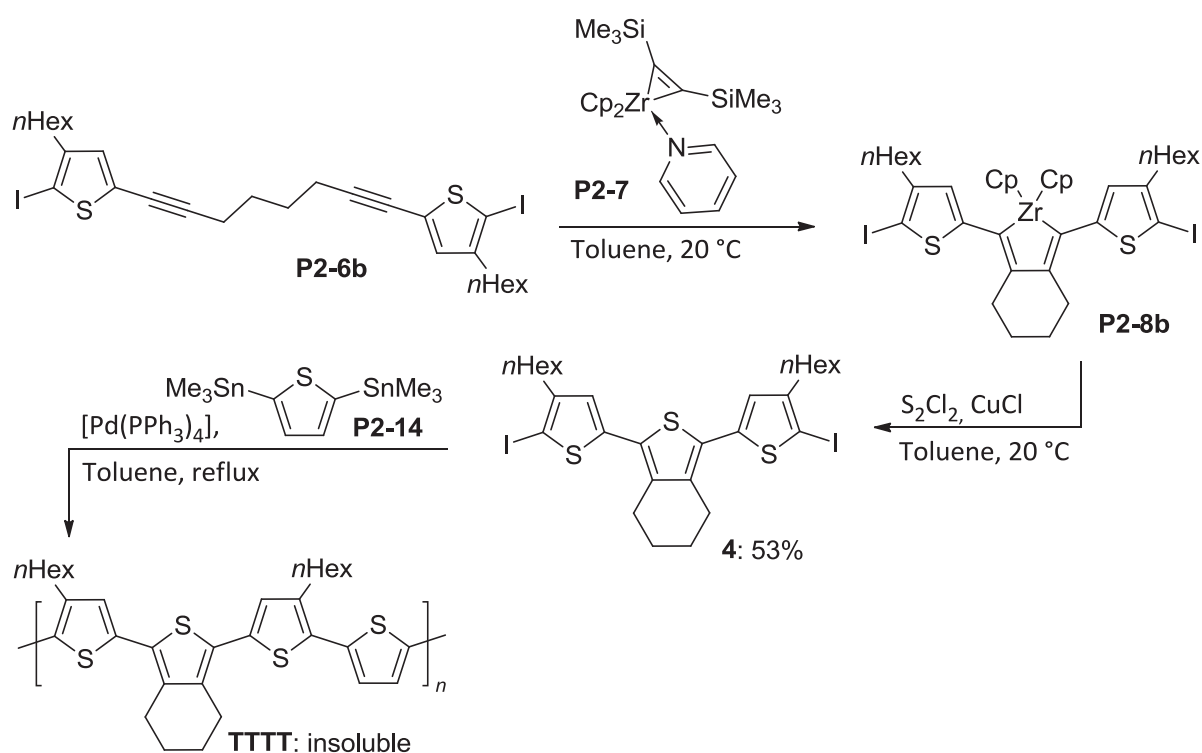
In the absorption spectrum, **TStTB** ($n = 1$) shows a broad absorption in solution with a $\lambda_{\text{max}} = 507$ nm (Figure 18). A film of **TStTB** ($n = 1$) was obtained by spin-coating the polymer onto a quartz substrate, leading to a red-shift of 34 nm ($\lambda_{\text{max}} = 541$ nm) compared to the spectrum in solution. This results in a band gap of E_g (film, **TStTB** ($n = 1$)) = 1.8 eV. **TStTB** ($n = 1$) showed in spite of the much shorter conjugation length an even broader absorption than **TStTT**, suggesting that the combination of stannoles and benzothiadiazoles will have a high potential as broad band absorption materials.

3.2.2 Further Comparison of Stannole Containing Polymers

A comparison between the stannole polymer **TStTT** and poly(3-hexylthiophene) was already made (see chapter 3.2.1.1) in order to investigate the influence of the tin atom on the light absorption of the polymer. To get an even better insight into the influence of tin on the electronic and film forming properties, it was also envisaged to perform a comparison with a polythiophene that has not only the same degree of polymerization, but also the same side chain pattern like polymer **TStTT**, as side chains are known to dramatically influence the electronic properties of organic semiconductors.

An appropriate monomer for this purpose was synthesized analogously to the synthesis of the stannole monomer **P2-9** (see chapter 3.2.1.1): Zirconacyclopentadiene **P2-8B** was prepared *in*

situ out of the octadiyne **P2-6b**, which was then reacted in a copper(I) chloride catalyzed Zr-S exchange with disulfur dichloride to give the thiophene monomer **4** in a yield of 53% (Scheme 5). The purification of **4** was complicated due to a byproduct that was difficult to remove; it was not possible to identify this side product, because it decomposed before a full characterization was possible. The polymerization of **4** was carried out under the same conditions as for **TSstTT**, with **P2-14** as a comonomer, giving a dark red suspension after 15 h. Surprisingly, the polymer **TTTT** which was obtained was of too low solubility for an analysis in any common solvent (chloroform, dichloromethane, THF, toluene, chlorobenzene), although these solvents solubilized the stannole polymer **TSstTT** without problems. Therefore, analysis of **TTTT** and a comparison between **TSstTT** and **TTTT** was impossible.



Scheme 5. Synthesis of thiophene monomer **4** and polymerization with **P2-14**, leading to the insoluble polymer **TTTT**.

However, the UV/Vis spectrum of thiophene monomer **4** was obtained in chloroform and compared to the one of **P2-9** (Figure 19). The stannole monomer **P2-9** has an absorption maximum of $\lambda_{\text{max}} = 441$ nm, while the absorption maximum of **4** is significantly blue-shifted by 65 nm with a $\lambda_{\text{max}} = 376$ nm. This shows that the exchange of a sulfur atom with a diphenyltin group dramatically decreases the HOMO-LUMO gap of the molecule.

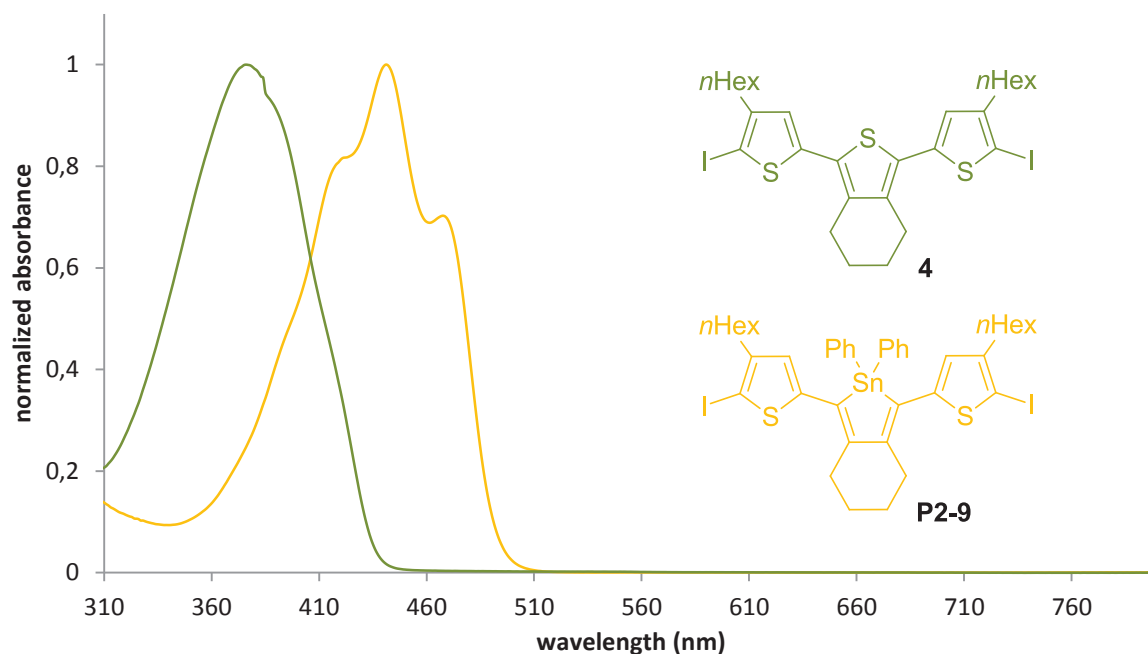


Figure 19. Absorption spectra of **4** and **P2-9** in chloroform.

In addition, it was possible to obtain single crystals of **4** and to perform an X-ray analysis. Contrary to the molecular structure of **P2-9**, two crystallographically independent molecules were found in the asymmetric unit. In both molecules, the two outer thiophene rings are arranged anti-coplanar to the central thiophene ring, as it was also observed for **P2-9** (see chapter 3.2.1.1).

The results of the X-ray analysis were published in *Acta Cryst.* **2014**, *E70*, o1133-o1134 (see following pages).

**“Crystal structure of 1,3-bis(4-hexyl-5-iodothiophen-2-yl)-4,5,6,7-tetrahydro-2-benzothio-
phene”**

J. Linshoef, C. Näther, A. Staubitz, *Acta Cryst.* **2014**, *E70*, o1133-o1134.

Reprinted with permission from International Union of Crystallography.

DOI: 10.1107/S1600536814019667

Scientific contribution to this paper:

In this publication, I carried out the synthetic work. A. Staubitz and I wrote the article together. C. Näther carried out the X-ray crystallography measurement and assisted in preparing the manuscript.



ISSN 1600-5368

OPEN ACCESS

Crystal structure of 1,3-bis(4-hexyl-5-iodothiophen-2-yl)-4,5,6,7-tetrahydro-2-benzothiophene

Julian Linshoef^a, Christian Näther^b and Anne Staubitz^{a*}

^aOtto-Diels-Institut für Organische Chemie, Christian-Albrechts-Universität Kiel, Otto-Hahn-Platz 4, 24118 Kiel, Germany, and ^bInstitut für Anorganische Chemie, Christian-Albrechts-Universität Kiel, Max-Eyth-Str. 2, 24118 Kiel, Germany. *Correspondence e-mail: astaubitz@oc.uni-kiel.de

Received 27 August 2014; accepted 31 August 2014

Edited by M. Bolte, Goethe-Universität Frankfurt, Germany

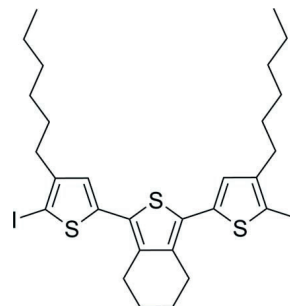
In the crystal structure of the title compound, C₂₈H₃₆I₂S₃, a terthiophene monomer, the central thiophene unit is arranged *anti*-coplanar to the two outer thiophene rings. There are two crystallographically independent molecules in the asymmetric unit, which show different conformations. In one molecule, the dihedral angles between the inner and the two outer thiophene rings are 15.7 (3) and 3.47 (3)°, whereas these values are 4.2 (3) and 11.3 (3)° for the second molecule. Differences are also found in the arrangement of the hexyl chains: in one of the two molecules, both chains are nearly in plane to the central moiety, whereas in the second molecule, only one chain is in plane and the other one is nearly perpendicular to the central moiety. Some of the C atoms are disordered and were refined using a split model with occupancy ratios of 0.65:0.35 and 0.70:0.30 in the two molecules.

Keywords: crystal structure; thiophene; 2-benzothiophene; monomer.

CCDC reference: 1021995

1. Related literature

For the synthesis of the starting materials, as well as the synthesis, crystal structure and polymerization of a similar thiophene-flanked stannole monomer, see: Linshoef *et al.* (2014). For typical bond lengths of other thiophene rings, see: Chaloner *et al.* (1997). For more information about thiophenes as important heterocycles for semiconducting materials, see: Thompson & Fréchet (2007); Mishra *et al.* (2009).



2. Experimental

2.1. Crystal data

C₂₈H₃₆I₂S₃
M_r = 722.55
Triclinic, *P*1̄
a = 13.4491 (4) Å
b = 14.9488 (5) Å
c = 16.1260 (5) Å
α = 73.387 (2)°
β = 71.208 (2)°
γ = 77.794 (3)°
V = 2915.60 (16) Å³
Z = 4
Mo Kα radiation
μ = 2.39 mm⁻¹
T = 200 K
0.16 × 0.10 × 0.08 mm

2.2. Data collection

Stoe IPDS-1 diffractometer
Absorption correction: numerical
(*X-SHAPE* and *X-RED32*; Stoe & Cie, 2008)
T_{min} = 0.748, T_{max} = 0.815
26585 measured reflections
12585 independent reflections
9932 reflections with I > 2σ(I)
R_{int} = 0.038

2.3. Refinement

R[F² > 2σ(F²)] = 0.034
wR(F²) = 0.085
S = 0.98
12585 reflections
640 parameters
3 restraints
H-atom parameters constrained
Δρ_{max} = 1.01 e Å⁻³
Δρ_{min} = -0.81 e Å⁻³

Data collection: *X-AREA* (Stoe & Cie, 2008); cell refinement: *X-AREA*; data reduction: *X-AREA*; program(s) used to solve structure: *SHELXS97* (Sheldrick, 2008); program(s) used to refine structure: *SHELXL97* (Sheldrick, 2008); molecular graphics: *XP* in *SHELXTL* (Sheldrick, 2008); software used to prepare material for publication: *PUBLICIF* (Westrip, 2010).

Acknowledgements

JL thanks the Deutsche Bundesstiftung Umwelt (DBU) for a PhD scholarship.

Supporting information for this paper is available from the IUCr electronic archives (Reference: BT6994).

data reports

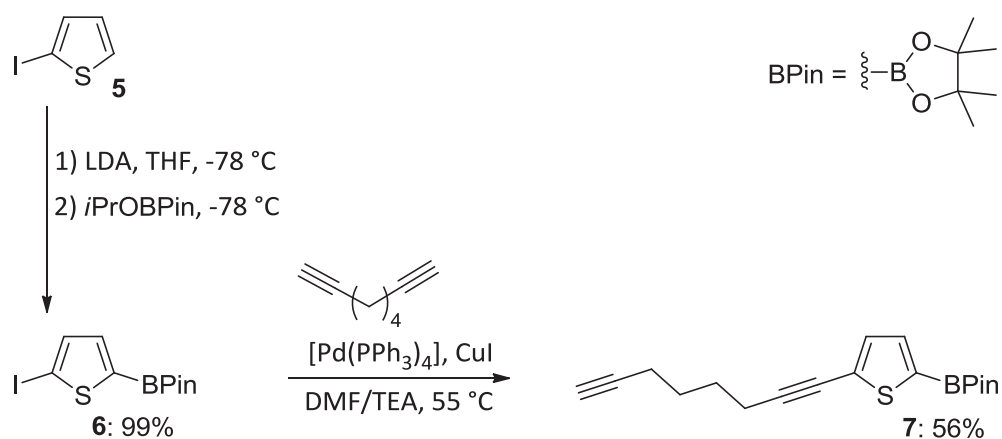
References

- Chaloner, P. A., Gunatunga, S. R. & Hitchcock, P. B. (1997). *J. Chem. Soc. Perkin Trans. 2*, pp. 1597–1604.
- Linshoeft, J., Baum, E. J., Hussain, A., Gates, P. J., Näther, C. & Staubitz, A. (2014). *Angew. Chem. Int. Ed.* **53**, doi:10.1002/anie.201407377.
- Mishra, A., Ma, C.-Q. & Bäuerle, P. (2009). *Chem. Rev.* **109**, 1141–1278.
- Sheldrick, G. M. (2008). *Acta Cryst. A* **64**, 112–122.
- Stoe & Cie (2008). *X-AREA*, *X-RED32* and *X-SHAPE*. Stoe & Cie, Darmstadt, Germany.
- Thompson, B. C. & Fréchet, J. M. J. (2007). *Angew. Chem. Int. Ed.* **47**, 58–77.
- Westrip, S. P. (2010). *J. Appl. Cryst.* **43**, 920–925.

3.3 Stannole Monomers for Chain Growth Polymerizations

The stannole containing polymer **TStTT** described in chapter 3.2.1.1 was prepared by using two different monomers, one bearing electrophilic groups, the other nucleophilic groups. Combining an electrophilic and nucleophilic group into only one monomer can have remarkable advantages for the polymerization process and the properties of the resulting polymer when it proceeds via a chain growth/living polymerization (see chapter 1.2).

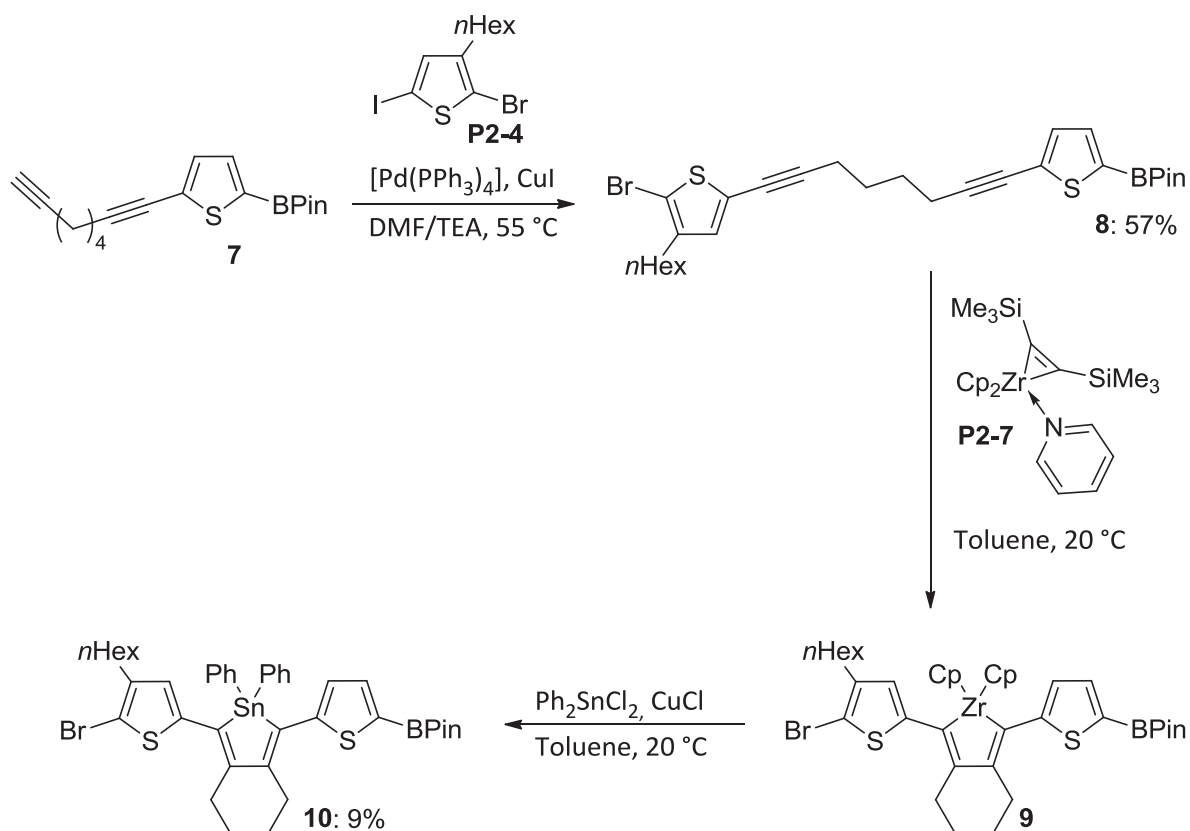
This approach required the synthesis of an asymmetric monomer, which was anticipated to be achieved by using nucleophile and/or electrophile selective cross-coupling reactions (compare chapter 3.1).



Scheme 6. Nucleophile selective cross-coupling leads to **7**.

2-Iodothiophene (**5**) was lithiated in the 5 position, using LDA at $-78\text{ }^{\circ}\text{C}$, and quenched with an isopropyl boronic ester to give **6** in nearly quantitative yield (Scheme 6). Subsequent Sonogashira cross-coupling with two equivalents of 1,7-octadiyne gave the respective mono-substituted species **7** in a yield of 56% (see below for a comment on the yield). This cross-coupling reaction is a very rare example of a nucleophile selective cross-coupling reaction, differentiating between a Sonogashira and a Suzuki reaction.^[53] Although both reactions need a base to proceed, mostly inorganic bases are used for Suzuki cross-coupling reactions, and organic bases give only very low conversions.^[54] In the case of **7**, some twofold Sonogashira coupled byproduct was observed, but no Suzuki coupled product. **7** was reacted with another thiophene **P2-4**, this time in a nucleophile and electrophile selective cross-coupling reaction (Scheme 7). Product **8** already contains the functional groups that are needed for a later polymerization, a bromide and a boronic ester. **8** was reacted in a one-pot reaction with zirconocene **P2-7**, forming the zirconacyclopentadiene **9**, which was transformed *in situ* to the

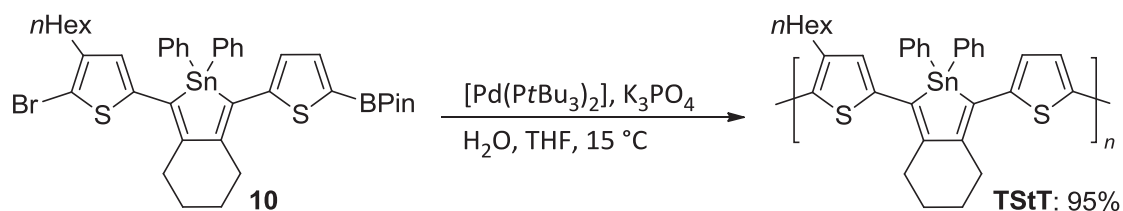
stannole **10**, using diphenyltin dichloride and copper(I) chloride. The formation of the intermediate **9** was controlled by ^1H NMR spectroscopy and was nearly quantitative, but the Zr-Sn exchange was problematic. A lower conversion was observed compared to the other prepared stannoles (see chapter 3.2), even if equimolar amounts of copper(I) chloride were used instead of catalytic amounts. In addition, purification by column chromatography was problematic: the compound was over-adsorbed by the silica gel, causing losses in yield, a phenomenon that was already observed during the purification of **7** and **8** and that is known for pinacol boronic esters.^[55] These factors contributed to a low isolated yield of 9% for **10**.



Scheme 7. A nucleophile and electrophile selective cross-coupling reaction leads to the thiophene flanked octadiyne **8**, which was transformed into the stannole monomer **10**.

The polymerization of **10** was carried out using $[\text{Pd}(\text{PtBu}_3)_2]$ as catalyst, tripotassium phosphate as a base and a mixture of water and THF as solvent. **TS_tT** was obtained as a dark blue-purple solid after precipitation into methanol (Scheme 8). Unfortunately, the polymer was barely soluble in common solvents (chloroform, dichloromethane, THF, toluene, chlorobenzene) at $20\text{ }^\circ\text{C}$, but ^1H and ^{119}Sn NMR spectra could be obtained (Figure 20). They indicated that the stannole ring stayed intact during polymerization and did not decompose. MALDI mass spectrometry of **TS_tT** confirmed these results, showing the expected mass difference of ca.

626 Da between corresponding peaks (Figure 21).^[56] Determination of the molecular weight of **TStT** by GPC using chloroform or THF at 20 °C was impossible due to the low solubility and a resulting poor signal to noise ratio.



Scheme 8. Polymerization of monomer **10**, yielding 95% of **TStT**.

However, it could be shown that a polymerization of stannole monomers is not only possible by Stille reaction (see chapter 3.2), but also via Suzuki cross-coupling. This degree of nucleophile selectivity in cross-coupling reactions has never been described so far.

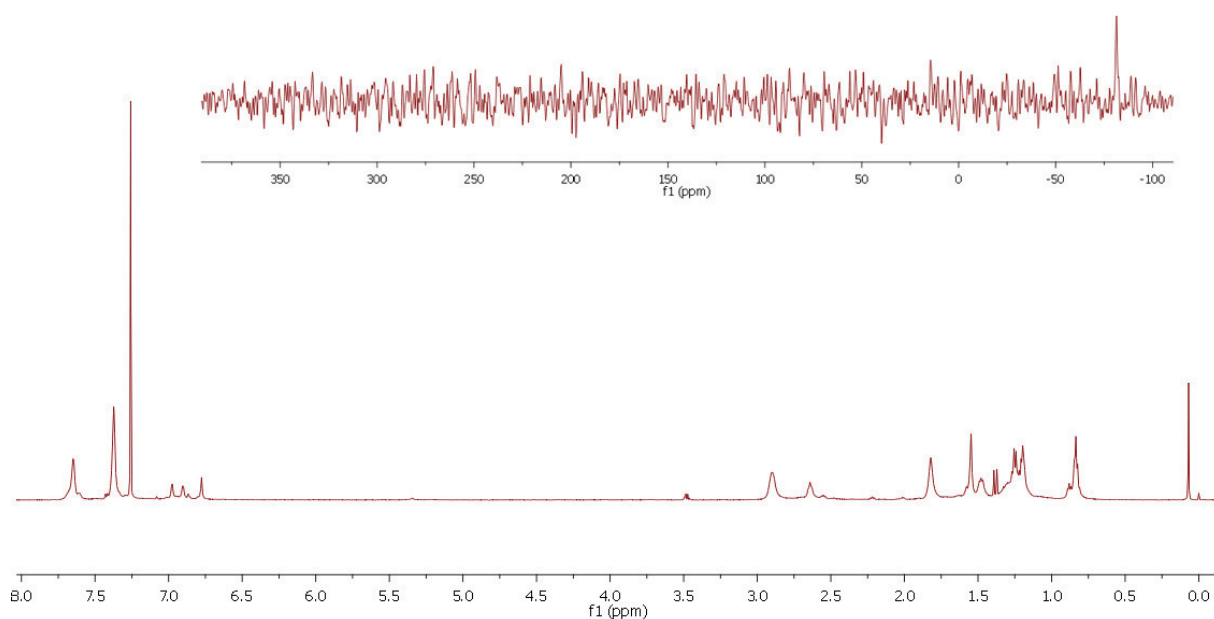


Figure 20. ^1H NMR (bottom) and ^{119}Sn NMR (top) spectra of polymer **TStT**.

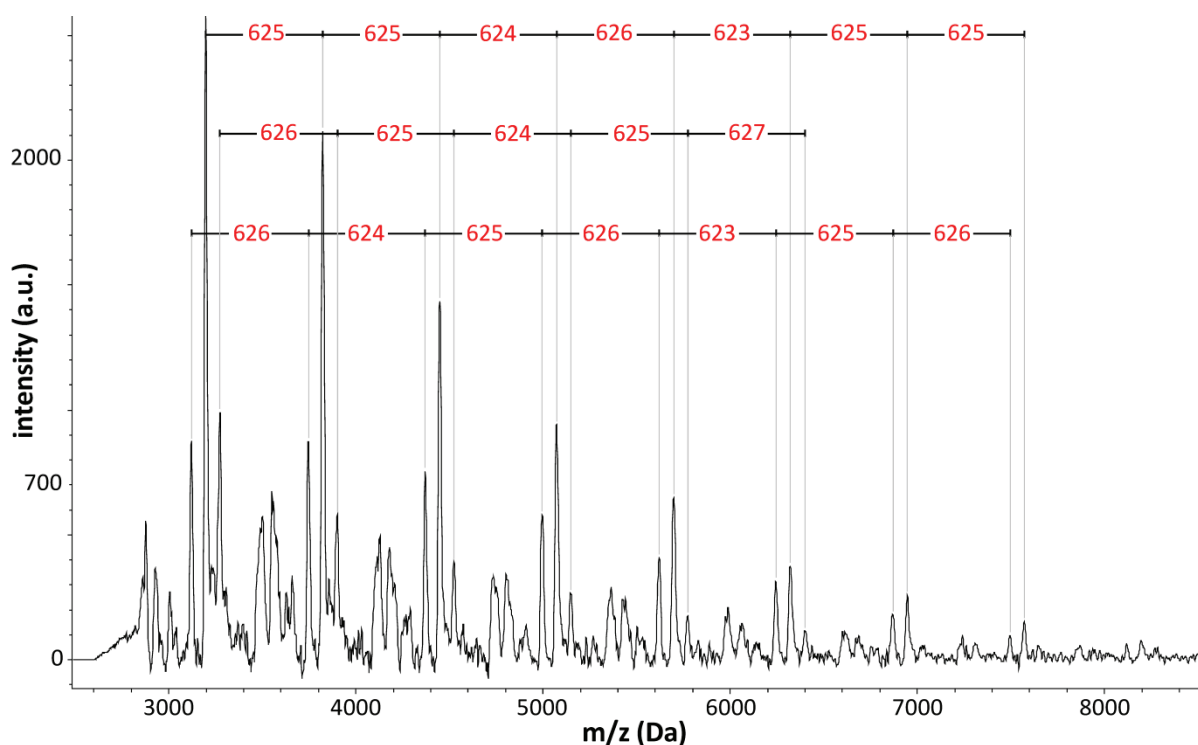


Figure 21. MALDI (dithranol) mass spectrum of **TSstT**, showing the repeat unit of the polymer.

The UV/Vis spectrum of **TSstT** in chloroform shows a λ_{\max} of 567 nm, while the absorption maximum of the spin-coated film is $\lambda_{\max} = 618$ nm (Figure 22). This red-shift of 51 nm is comparable to the 49 nm that were observed between the spectra of **TSstT** in solution and as film (compare chapter 3.2.1.1). However, a distinct difference between **TSstT** and **TSstTT** can be identified. The shift of ca. 30 nm between the two polymers shows their differences in structure: while the repeat unit of **TSstTT** contains three thiophene rings and one stannole, the ratio between the thiophene and stannole rings is only 2:1 for **TSstT**. Again, this points to the strong influence of the stannole ring onto the absorption properties of polymers. The influence of the hexyl chain, the boronic ester and the halogen atom seems negligible small, since the absorption spectra of monomers **10** and **P2-9** are essentially the same above 300 nm (see experimental section).

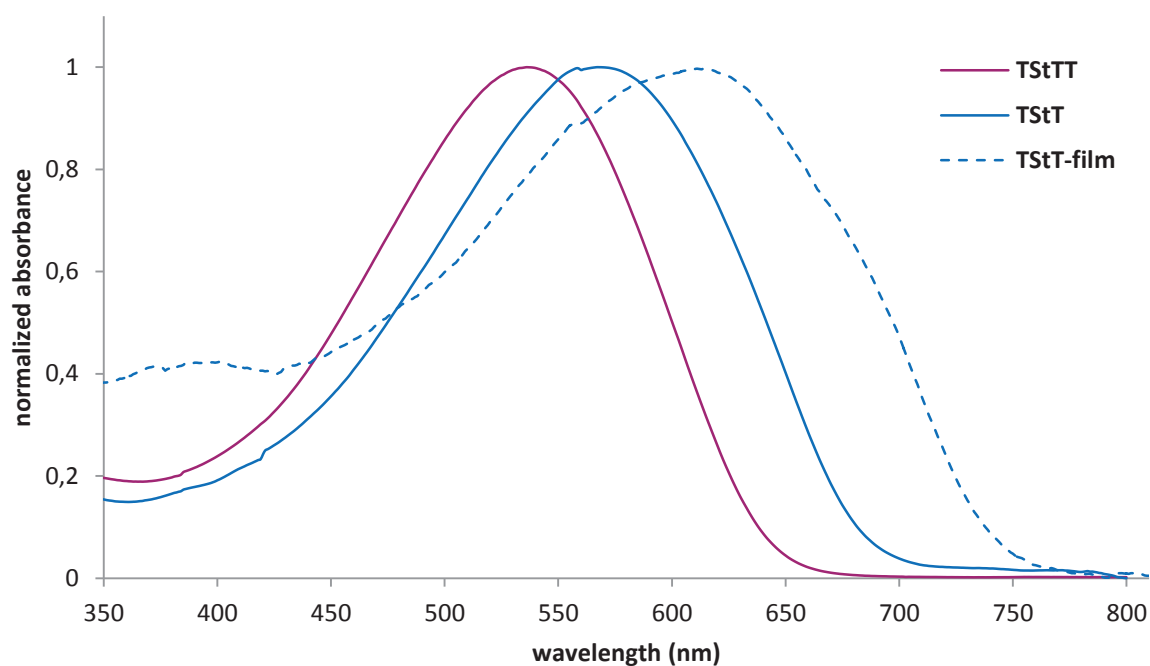
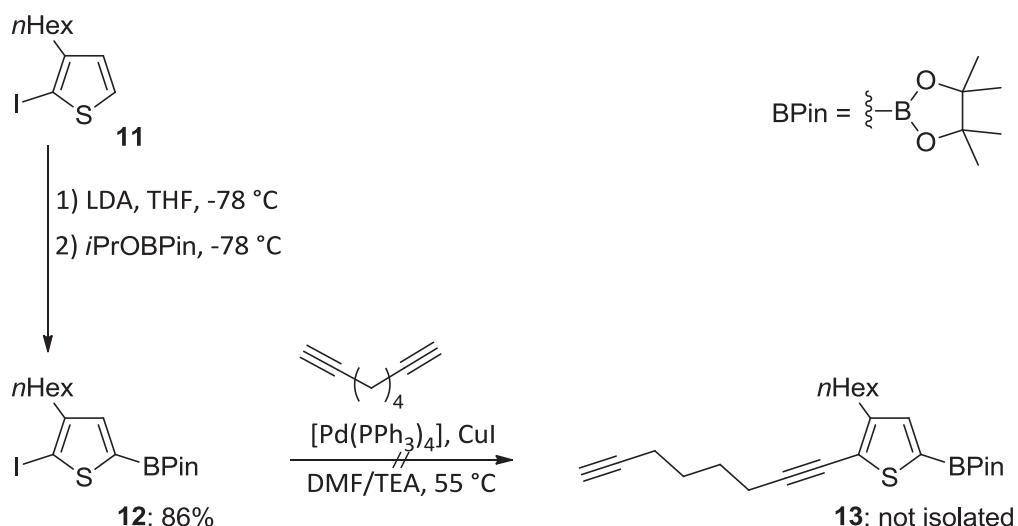


Figure 22. Absorption spectra of polymer **TSstT** in chloroform and as film.

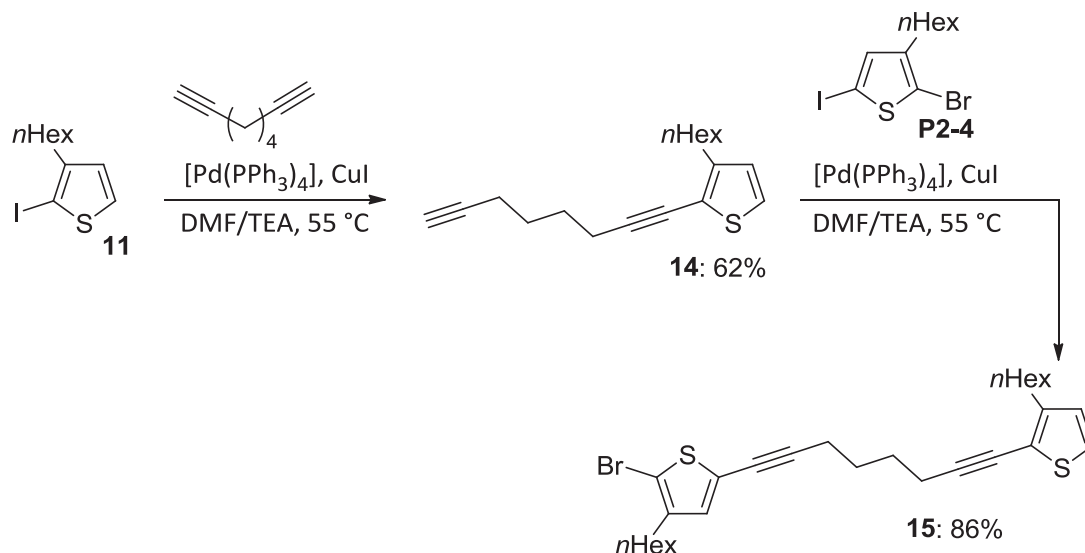
However, it has to be considered that the polymer length of **TSstT** is unknown and maybe not comparable to the length of **TSstTT**, which would also have an influence on the band gap. In order to obtain a polymer with a higher solubility that can be fully analyzed, the structure of the monomer has to be modified and more solubilizing alkyl chains are needed.^[57]

A reasonable solution would be another hexyl chain at the second thiophene that does not have any substituents in the 3/4 position in **10**. Though, a hexyl chain next to the boronic ester would cause head-to-head couplings in the polymer, as described for regioirregular P3AT (compare chapter 1.2).^[58] Thus, it was envisaged to incorporate a hexyl chain next to the stannole ring (which would give exclusively head-to-tail coupling), using a similar route like for **10**: the preparation of **12** worked in high yields, but the following purification of **13** was problematic (Scheme 9). ¹H NMR spectroscopy of the crude product showed slightly more byproducts than for **7**, for example the decomposition product without boronic ester. Purification by Kugelrohr and column chromatography was not possible, as it led to further decomposition of the product. Additionally, the previously described phenomenon of over-adsorption onto silica (see preparation of **10**) was even much stronger in this case.



Scheme 9. Attempted synthesis for **13**: the isolation was not possible.

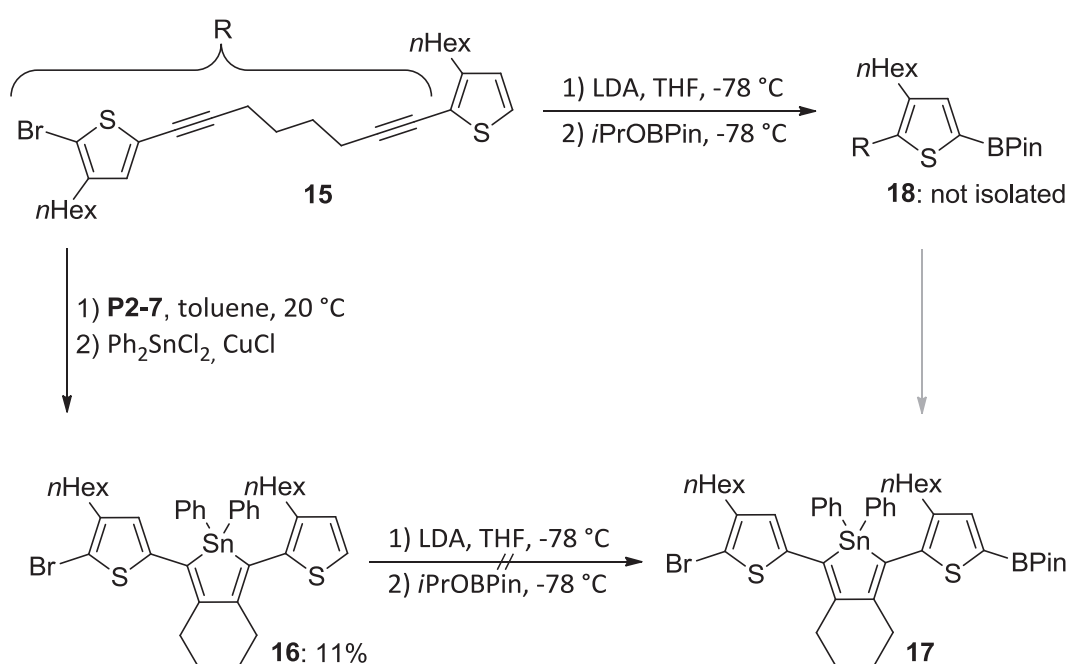
All substituents attached to the thiophene ring seem to have an extensive influence on the stability and affinity towards silica gel, since the purification by column chromatography of e. g. **12** was straightforward. Therefore, the boronic ester should not be introduced in the beginning of the synthetic route, but at a later stage, because subsequent structures might show a higher stability.



Scheme 10. Leaving out the boronic ester simplifies the synthesis of **15**.

Without the boronic ester, monosubstituted octadiyne **14** was obtained in good yields and without purification problems (Scheme 10). A second cross-coupling with **P2-4** afforded **15** in very good yields, again without observing any over-adsorption onto silica during column chromatography. The ring closure between the triple bonds with Rosenthal's zirconocene **P2-7** and Zr-Sn exchange was carried out in a one-pot reaction, yielding 11% of **16** (Scheme 11).

During this reaction, one unidentified side product was formed that decomposed during purification. Because lithiation of **16** with LDA did not lead to the lithiation of the thiophene ring, but to a decomposition of the stannole ring, **17** was not formed and the synthesis of **16** was not optimized. Instead, **15** was lithiated and the reaction was quenched with the isopropyl boronic ester. Mostly desired product was formed during the reaction, and **18** showed a good stability towards silica gel. However, the adverse properties concerning the over-adsorption onto silica were essentially the same like for **13**, leading to a substantial loss of material. It was not possible to isolate the pure product, and the following transformation to **17** was not carried out.



Scheme 11. Attempted synthesis of **17** via two different routes.

In order to find a way to purify **18**, alternative purification methods have to be developed and tested. Functionalization of the silica gel used for chromatographic purification with boronic acid could be an option,^[55] or purification by preparative GPC. Since the synthesis of **8** is now established, solubilizing groups could also be attached to the phenyl rings of Ph₂SnCl₂. Using not a pinacol, but another boronic ester or even another metal for the later polymerization would be two further options.

3.4 Rosenthal's Zirconocene – a Versatile Reagent

“Rosenthal's Zirconocene $\text{Cp}_2\text{Zr}(\text{pyr})(\text{Me}_3\text{SiC}\equiv\text{CSiMe}_3)$ ”

J. Linshoef, *Synlett* **2014**, *asap*.

Reprinted with permission from Georg Thieme Verlag. © Georg Thieme Verlag KG Stuttgart · New York.

DOI: 10.1055/s-0034-1379317.

One of the key steps in the synthesis of stannoles is the formation of the precursor, a zircona-cyclopentadiene. The considerable importance of the reagent used for these syntheses, Rosenthal's zirconocene $\text{Cp}_2\text{Zr}(\text{pyr})(\text{Me}_3\text{SiC}\equiv\text{CSiMe}_3)$ (**P2-7**), was already pointed out in chapter 3.2.1.1. In order to highlight also other important applications of Rosenthal's zirconocene, a short “Spotlight” was submitted and accepted for publication to the journal *Synlett*.



Figure 23. Crystals of Rosenthal's zirconocene $\text{Cp}_2\text{Zr}(\text{pyr})(\text{Me}_3\text{SiC}\equiv\text{CSiMe}_3)$, stored in a glovebox.

Rosenthal's Zirconocene

Compiled by Julian Linshoef

Julian Linshoef was born in Stade, Germany, and studied chemistry at Kiel University. He spent a few months in Nantes, France, as an ERASMUS student and obtained his diploma degree in 2010 at Kiel University. Currently, he is working towards his Ph.D. at the Otto-Diels-Institute for Organic Chemistry under guidance of Professor Dr. Anne Staubitz. His research focuses on main group heterocycles for semiconducting polymers.

Otto-Diels-Institut für Organische Chemie, Universität Kiel

Otto-Hahn-Platz 4

24098 Kiel (Germany)

E-mail: jlinshoef@oc.uni-kiel.de

Julian Linshoef gratefully acknowledges a Ph.D. scholarship from the Deutsche Bundesstiftung Umwelt (DBU).

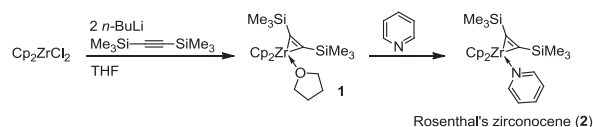


Introduction

The complex $\text{Cp}_2\text{Zr}(\text{pyr})(\text{Me}_3\text{SiC}\equiv\text{CSiMe}_3)$ is a dark purple to black solid and was first synthesized by Uwe Rosenthal and co-workers in 1995.¹ The applications are to some extent similar to those of the Negishi-reagent,² but Rosenthal's zirconocene provides some considerable advantages:³ it is stable in solutions of hydrocarbon solvents and as a solid, and it can be isolated and stored for several months in a glovebox without any noticeable decomposition. This lower reactivity of Rosenthal's zirconocene in comparison with the Negishi-reagent is accompanied by a higher selectivity, broadening the

scope of its applications. It plays an important role in organic and inorganic synthesis, as it forms for example zirconacyclopentadienes that can be transformed into a variety of different heterocycles.⁴

Rosenthal's zirconocene **2** can be prepared in a one-pot procedure, starting with Cp_2ZrCl_2 .^{3,5} The THF intermediate **1** is unstable and difficult to isolate.¹ Therefore, this complex is treated *in situ* with pyridine, giving high yields of **2** (up to 85%).

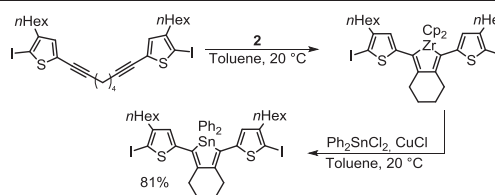


Scheme 1 Preparation of Rosenthal's reagent.

Abstracts

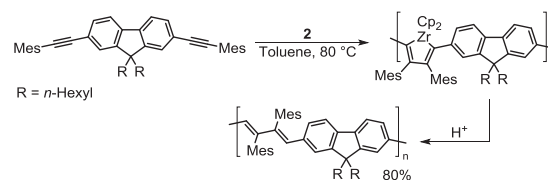
(A) Reductive Coupling of Halide Functionalized Alkynes

Rosenthal's zirconocene shows a much lower reactivity than the comparable Negishi-reagent.³ This mild reactivity not only allows the reductive coupling of bromide functionalized alkynes,⁶ but also of iodide substituted species.³ In the latter example, the zirconacyclopentadiene that was obtained was transformed *in situ* into a stannole by a Zr-Sn exchange, carried out in toluene, in an overall yield of 81%.



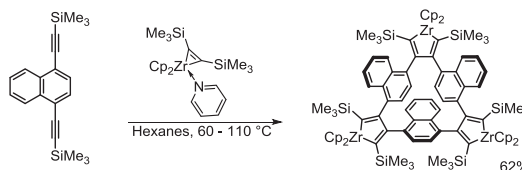
(B) Regioselective Polymerization

Regiochemistry has to be considered when a zirconacyclopentadiene is formed out of unsymmetrical alkynes. Tilley and co-workers reported the reductive coupling of, amongst others, mesityl substituted alkynes.⁷ The formation of fully regioselective products was observed, and the regioselectivity was attributed largely to steric effects. This led to the polymerization of a mesityl-terminated diyne, which was analyzed after demetalation. A bright yellow polymer with a high number-average molecular weight of $M_n = 24\,400$ Da was obtained.

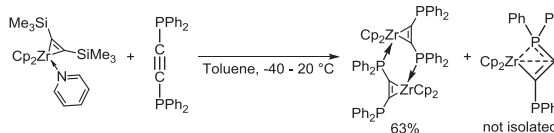


(C) *Stereoselective Macrocyclization*

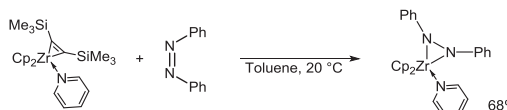
One option for the synthesis of macrocycles is to use high dilutions in order to avoid polymerizations.⁸ Another possibility is the synthesis under thermodynamic control. Because the formation of zirconacyclopentadienes is reversible, heating can give the thermodynamically more favored macrocycles in high yields. Using this strategy, a trimeric macrocycle was prepared by heating a solution of Rosenthal's zirconocene and a 1,4-bis(trimethylsilyl)(ethynyl)acene for 24 h at 60 °C and another 48 h at 110 °C.⁹ The '2 up, 1 down' diastereomer was isolated after purification in a yield of 62%.

(D) *Ligand Exchange with Phosphino-Acetylene*

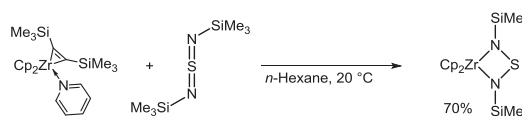
Bis(diphenylphosphino)acetylene was used in the reaction with $\text{Cp}_2\text{Zr}(\text{pyr})(\text{Me}_3\text{SiC}\equiv\text{CSiMe}_3)$ to form a dinuclear complex with an isolated yield of 63%.¹⁰ A four-membered heterometallacycle was observed in solution that is in equilibrium with the dinuclear complex. Interestingly, no zirconacyclopentadiene was formed when two equivalents of alkyne were used.

(E) *Ligand Exchange with Azobenzenes*

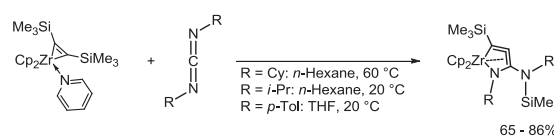
Kaleta et. al. showed that azobenzenes react in a ligand exchange process to yield diazazirconacyclopropanes.¹¹ The reaction was carried out in toluene, and after 18 h, orange crystals were isolated in a yield of 68%.

(F) *Ligand Exchange with Sulfurdiimides*

Four-membered zirconacycles containing nitrogen and sulfur were prepared by ligand exchange with sulfurdiimides.¹² The complex was analyzed by mass spectrometry, IR spectroscopy, elemental analysis and NMR spectroscopy, and NMR analysis showed the diamagnetic character.

(G) *Formation of Hetero-Zirconacycloallenes*

The synthesis of azazirconacycloallenes by reaction of the zirconocene $\text{Cp}_2\text{Zr}(\text{pyr})(\text{Me}_3\text{SiC}\equiv\text{CSiMe}_3)$ with carbodiimides was reported.¹³ Almost no byproducts were formed during the reaction, and the products could be isolated in yields of up to 86%. The mechanism was proposed to commence with a Si-C bond-cleavage, the carbodiimide is then inserted into the newly formed Zr-Si bond, followed by a C-C coupling. The structures of the isolated products were confirmed by X-ray analysis.

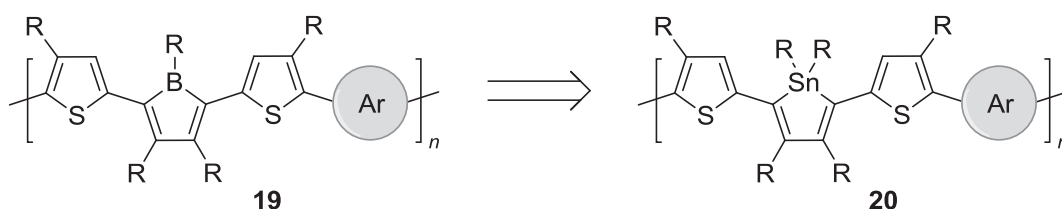


References

- Rosenthal, U.; Ohff, A.; Baumann, W.; Tillack, A.; Görls, H.; Burlakov, V. V.; Shur, V. B. *Z. Anorg. Allg. Chem.* **1995**, *621*, 77.
- Negishi, E.; Holmes, S. J.; Tour, J. M.; Miller, J. A.; Cederbaum, F. E.; Swanson, D. R.; Takahashi, T. *J. Am. Chem. Soc.* **1989**, *111*, 3336.
- Linshoef, J.; Baum, E. J.; Hussain, A.; Gates, P. J.; Näther, C.; Staubitz, A. *Angew. Chem. Int. Ed.* **2014**, *asap*, DOI: 10.1002/anie.201407377.
- a) Fagan, P. J.; Nugent, W. A. *J. Am. Chem. Soc.* **1988**, *110*, 2310; b) Fagan, P. J.; Nugent, W. A.; Calabrese, J. C. *J. Am. Chem. Soc.* **1994**, *116*, 1880.
- Nitschke, J. R.; Zürcher, S.; Tilley, T. D. *J. Am. Chem. Soc.* **2000**, *122*, 10345.
- Lucht, B. L.; Buretea, M. A.; Tilley, T. D. *Organometallics* **2000**, *19*, 3469.
- Miller, A. D.; Tannaci, J. F.; Johnson, S. A.; Lee, H.; McBee, J. L.; Tilley, T. D. *J. Am. Chem. Soc.* **2009**, *131*, 4917.
- Parker, D. *Macrocyclic Synthesis: A Practical Approach*; Oxford University Press: Oxford, 1996.
- Tannaci, J. F.; Kratter, I. H.; Rider, E. A.; McBee, J. L.; Miller, A. D.; Tilley, T. D. *Chem. Commun.* **2009**, 233.
- Haehnel, M.; Hansen, S.; Schubert, K.; Arndt, P.; Spannenberg, A.; Jiao, H.; Rosenthal, U. *J. Am. Chem. Soc.* **2013**, *135*, 17556.
- Kaleta, K.; Arndt, P.; Beweries, T.; Spannenberg, A.; Theilmann, O.; Rosenthal, U. *Organometallics* **2010**, *29*, 2604.
- Kaleta, K.; Ruhmann, M.; Theilmann, O.; Roy, S.; Beweries, T.; Arndt, P.; Villinger, A.; Jemmis, E. D.; Schulz, A.; Rosenthal, U. *Eur. J. Inorg. Chem.* **2012**, 2012, 611.
- Kaleta, K.; Ruhmann, M.; Theilmann, O.; Beweries, T.; Roy, S.; Arndt, P.; Villinger, A.; Jemmis, E. D.; Schulz, A.; Rosenthal, U. *J. Am. Chem. Soc.* **2011**, *133*, 5463.

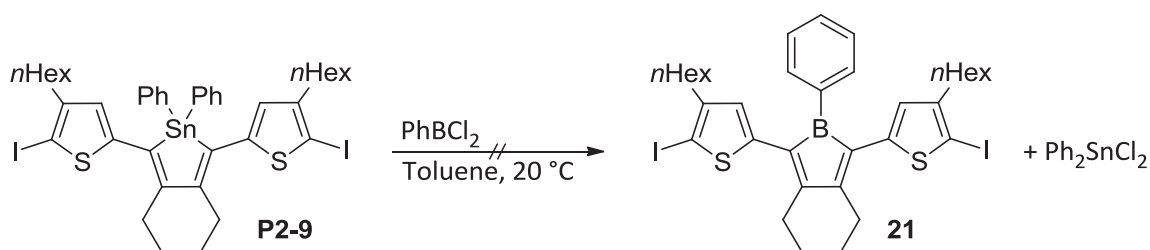
3.5 Boroles

The incorporation of boroles into semiconducting polymers might lead to new and unusual properties.^[46] This goal has never been achieved so far, especially because of the high reactivity of the antiaromatic heterocycle and not available precursors.^[59] Due to this high reactivity, the successful polymerization of a borole monomer seems unlikely, because the borole would probably react with the catalyst.^[41, 60] Instead, a transformation of a stannole containing polymer into a borole containing polymer seems to be an appropriate way, with stannoles as common precursors for boroles (Scheme 12).



Scheme 12. The preparation of a borole containing polymer should be possible by a polymer-analogous reaction.

For such a polymer-analogous reaction, it is advisable to ensure that the tin-boron exchange reaction proceeds without problems and that the resulting borole is stable at room temperature. To test this, stannole **P2-9** was reacted with phenylboron dichloride in toluene, resulting in an immediate color change from yellow-orange to blue-green (Scheme 13). Two or three seconds later, the blue-green color disappeared again and turned brownish.

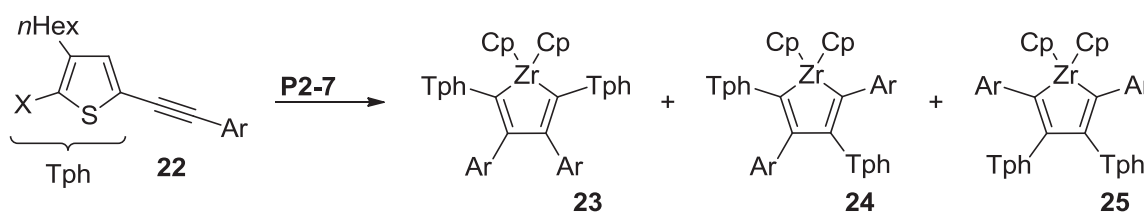


Scheme 13. Attempted synthesis of borole **21**.

Analysis of the crude product by ^1H NMR spectroscopy showed the formation of a complex reaction mixture, but the ^{119}Sn NMR spectrum showed only one signal, which was assigned to diphenyltin dichloride. The exclusive formation of this tin byproduct and the typical blue-green color indicate that the borole was formed during the reaction, but immediately reacted to further species.

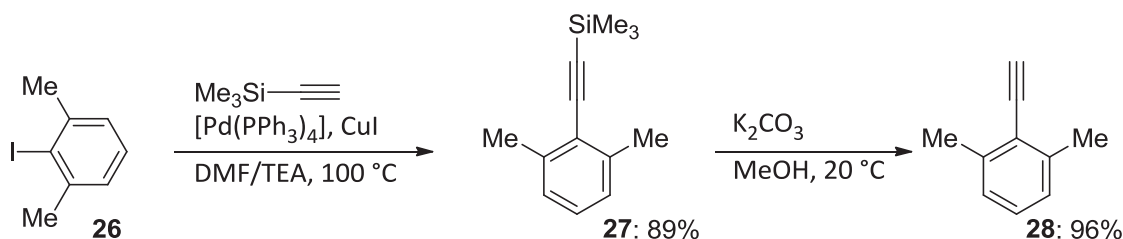
This high reactivity was to be expected, because the rare examples of isolated and investigated boroles are substituted in all positions with bulky groups.^[36] Thus, the alkyl ring attached to the 3/4 position is probably not bulky enough to protect the highly reactive borole ring. Instead, a stannole monomer like **P2-9**, but with two phenyl substituents in 3/4 position should offer a much higher stability.

In order to synthesize such a molecule, a new synthetic pathway had to be developed. Using only one diyne molecule as precursor for the formation of the respective zirconacyclopentadiene is not possible, but two alkyne molecules **22** have to be dimerized by Rosenthal's zirconocene **P2-7** (Scheme 14). This causes the problem of regioselectivity, because three different regioisomers **23** - **25** are possible and a separation of these was unlikely to be successful. However, Tilley and co-workers reported that only one regioisomer was formed during the reaction of **P2-7** with 1,3-dimethyl-2-(phenylethynyl)benzene (compare chapter 3.4).^[61] Thus, a 2,6-substituted phenyl ring that would potentially lead to the same regioselectivity was intended as aryl group attached to the triple bond.



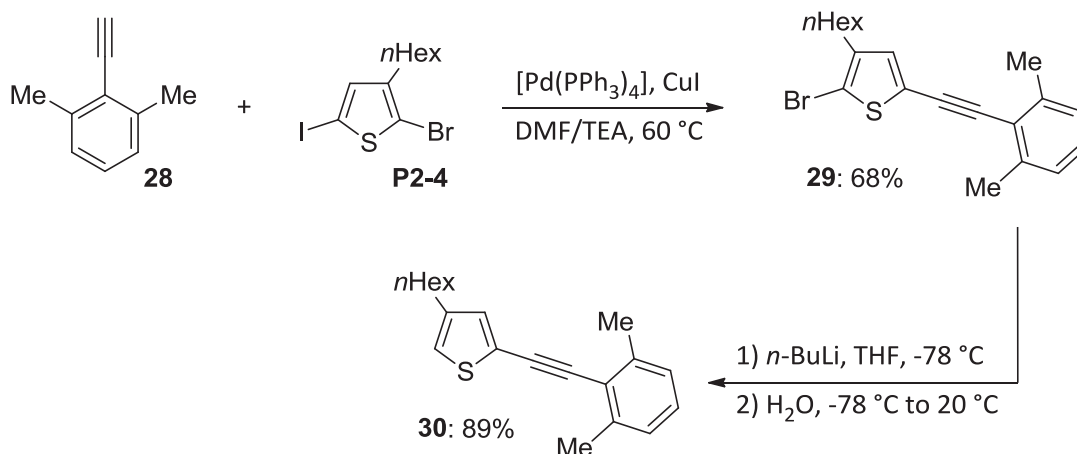
Scheme 14. Three different regioisomers are imaginable upon the formation of the stannole precursor, the zirconacyclopentadiene.

28 was synthesized starting with the iodinated benzene **26**, which was reacted in a Sonogashira cross-coupling reaction with trimethylsilylacetylene, giving 89% of **27** (Scheme 15). After removing the trimethylsilyl-group with potassium carbonate, the deprotected ethynylbenzene **28** was obtained.



Scheme 15. Synthesis of ethynyl dimethylbenzene **28**.

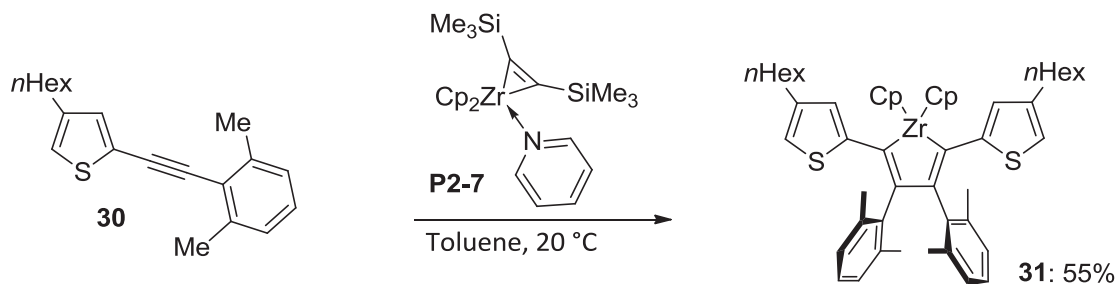
Electrophile selective cross-coupling of **28** with thiophene **P2-4** led to the brominated species **29** (Scheme 16). Treatment with *n*-butyllithium and quenching with water exchanged the bromide with a proton, giving **30** in 89% yield. This exchange was carried out to remove the reactive bromide, which could eventually thwart the formation of a borole out of the monomeric stannole. In a later polymer, these bromides would not be present anymore (apart from a possible end group) because they would have reacted during the polymerization process.



Scheme 16. Sonogashira cross-coupling of **28** and **P2-4**, followed by Br-Li-H exchange, leads to **30**.

Two equivalents of **30** were reacted with the zirconocene **P2-7**, using well-established reaction conditions (Scheme 17). All other prepared zirconacyclopentadienes that were mentioned in this thesis were used *in situ* and directly transformed to the desired heterocycles. In order to investigate the regioselectivity of the reaction, **31** was isolated as an air- and moisture sensitive compound in 55% yield. A fully regioselective cyclization was observed, as proven by NMR spectroscopy: only one set of signals was observed. A potential explanation for the observed regioselectivity could be the high steric hindrance between the methyl groups of the phenyl ring and the cyclopentadienyl-rings. The distinction between a product of type **23** and **25** (see Scheme 14) by standard NMR methods is difficult, but single crystals of **31** could be obtained. They were analyzed by X-ray crystallography (for a detailed report, see chapter 5.6.1), proving that the structure drawn in Scheme 17 is correct. There are two crystallographically independent molecules in the asymmetric unit, but their structures differ only slightly. In one of these two molecules, some carbon atoms of the hexyl chain are disordered (see Figure 24 for the first molecule; see chapter 5.6.1 for the second molecule with the disordered hexyl chain). The two phenyl rings are twisted from the zirconacyclopentadiene-plane with angles of 76.36°

(Figure 24) and 74.48° (see chapter 5.6.1), and the thiophene rings are twisted with angles of 45.52° (Figure 24) and 36.33° (see chapter 5.6.1).



Scheme 17. The formation of zirconacyclopentadiene **31** was fully regioselective.

The subsequent transformation of **31** into a stannole turned out to be less straightforward than for the other stannoles mentioned in this thesis. The standard reaction conditions of 3 h at 20°C , using diphenyltin dichloride, were unsuccessful, and no conversion was observed (Scheme 18). Increasing the reaction time to 18 h did not improve the conversion. The sluggish reactivity could be explained by the increased steric hindrance of the zirconacyclopentadiene, hindering the attack of the also bulky diphenyltin dichloride.

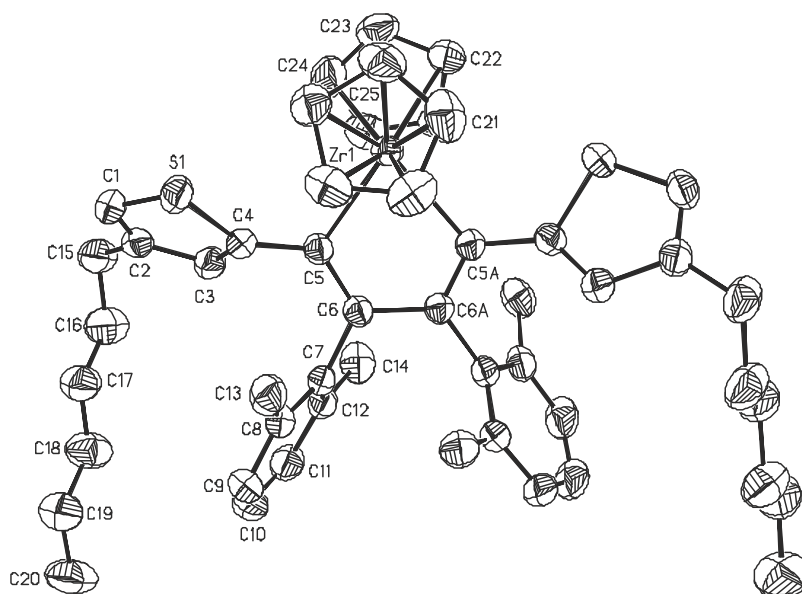
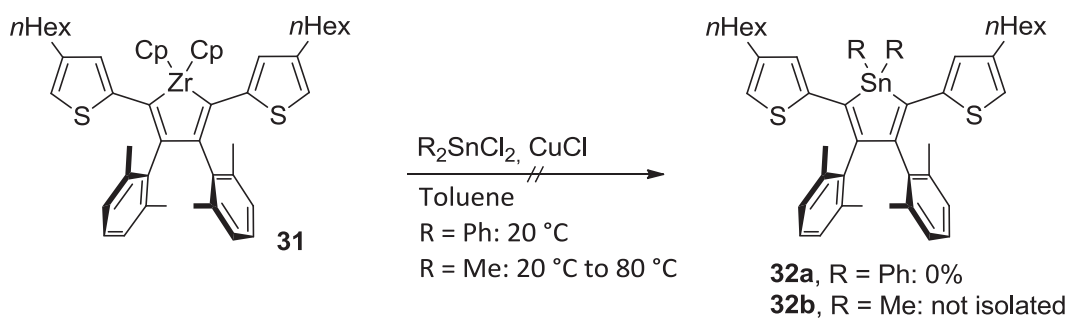


Figure 24. ORTEP drawing of **31**, showing a probability of 50% for thermal ellipsoids. Hydrogen atoms and a second crystallographically independent molecule are omitted for clarity.

However, this steric hindrance is needed for the formation of the zirconacyclopentadiene; thus, the sterically less demanding dimethyltin dichloride and higher reaction temperatures were tested. After 19 h at 20°C and another 16 h at 80°C , the partial formation of the stannole **32b** was observed by MALDI mass spectrometry. Because also quenched starting material was

found, the reaction was continued for another 8 h at 80 °C. After the subsequent aqueous work-up, only a complex reaction mixture and no stannole formation was observed.



Scheme 18. Attempted synthesis of stannole **32**.

Therefore, this reaction needs a systematical optimization of all possible reaction conditions. Other solvents, the amount of the catalyst copper(I) chloride, different reaction temperatures and times should be investigated. Using tin tetrachloride (and subsequent quenching of the stannole with e. g. methyl lithium) instead of dimethyltin dichloride could also be a possibility.

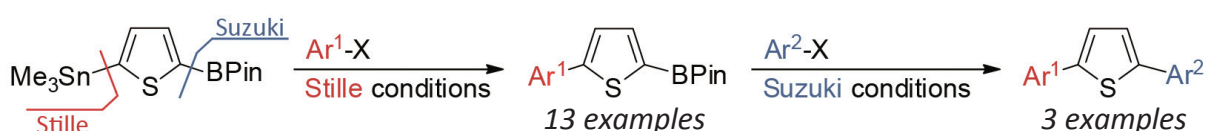
4 Summary and Outlook

The title of this work, “Main Group Heterocycles for Semiconducting Polymers”, aims in particular to the group 13 heterocycle borole, the group 14 heterocycle stannole and the group 16 heterocycle thiophene.

Nucleophile Selective Cross-Coupling Reactions

Thiophenes are probably *the* basic building blocks for semiconducting polymers, and one task of this work was to develop a new synthetic method that makes it easier to access a variety of different thiophene derivatives.

This was achieved by synthesizing a dinucleophilic thiophene, which contains a trimethyltin and a boronic ester functional group in chemically equivalent positions. With this “Sn-B-thiophene”, reaction conditions were systematically analyzed and optimized in over 40 reactions: different solvents, the reaction temperature and time, the type of catalyst and the catalyst loading were investigated. This led to a fully nucleophile selective cross-coupling reaction, where only the tin reacted in a high yielding Stille reaction and the boronic ester stayed intact. The scope of the Stille reaction was shown in 13 different examples, with electron rich, electron neutral and electron poor electrophiles. In addition, it was even possible to convert the boronic ester in one pot with the Stille reaction, simply by adding a second electrophile, a base and water to the reaction mixture.



Scheme 19. In over 40 optimization reactions, the conditions for a high yielding nucleophile selective cross-coupling reaction were identified and tested with different aromatic electrophiles.

This topic opened many new possibilities for subsequent research and was continued by other Ph.D. students. The work of A. Heinrich led to the development of nucleophile and electrophile selective cross-coupling reactions, yielding a molecule that contains a boronic ester and a bromide.^[45] These compounds can be used as monomers, and their polymerization may proceed with a chain growth (living) character. These investigations are already underway.

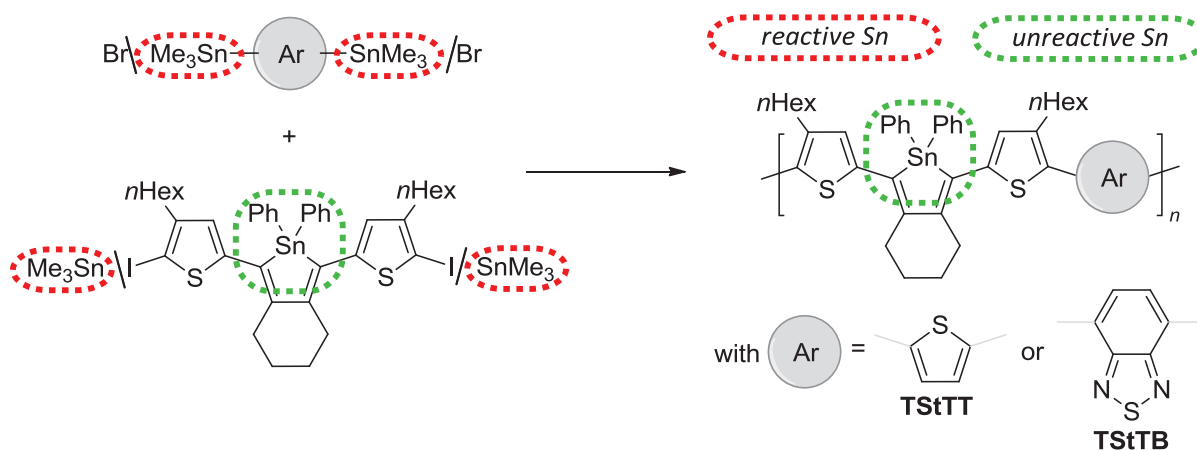
L. He extended the nucleophile selective cross-coupling reactions to vinyl and alkynyl bromides, giving an even wider scope of applications for the “Sn-B-thiophene”.^[62]

For further future work, the concept of nucleophile selective cross-coupling reactions could also be extended to other heterocycles, like e. g. furan or different azoles.

Group 14/16 Heterocycles for Polycondensation Polymers

In order to obtain a semiconducting polymer with a low band gap, an often used approach is the combination of thiophenes with an electron poor heterocycle. One example for such an electron poor heterocycle is a stannole, a compound that has never been incorporated into a polymer so far.

In this work, it is described how it was possible to obtain stannole monomers with two electrophilic or two nucleophilic groups. The electrophilic stannole monomer was polymerized with a thiophene comonomer in a nucleophile (tin) selective cross-coupling reaction, leaving the stannole intact. The resulting polymer showed that the stannole ring strongly influences the optoelectronic properties: compared to standard poly(3-hexylthiophene), a bathochromic shift of over 80 nm was observed. A comparison with a polythiophene with exactly the same side chains was not possible, as this polymer turned out to be insoluble.



Scheme 20. Electrophilic (with iodides) and nucleophilic (with Me_3Sn groups) stannole monomers were prepared and polymerized with thiophene and benzothiadiazole comonomers.

Using the nucleophilic stannole monomer, a transformation with a benzothiadiazole comonomer was possible. However, the conversion was very low, but the compound **TStTB** ($n = 1$) could be isolated. It turned out that the combination of stannoles, thiophenes and benzothiadiazoles dramatically lowers the band gap, as this small molecule semiconductors band gap of E_g (film) = 1.8 eV shows.

The next step would be to test the materials in devices like OFETs or OSCs. Depending on the results, an optimization of the material could be carried out: other comonomers could be

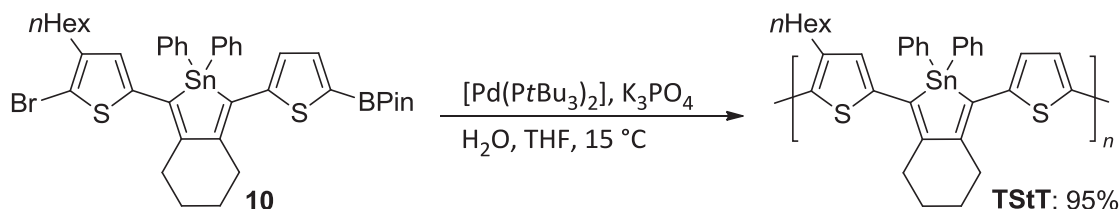
investigated, and the polymer length could be optimized. A variation in the ratio of stannole to thiophene units in the backbone could also lead to very different band gaps and to different morphologies. Other substituents at the thiophene rings, e. g. branched, shorter or longer alkyl chains will probably also have an influence on the device performances. Instead of using two phenyl substituents at the tin, other bulky groups could also be used and tested. **TS_ntB** ($n = 1$) is a very interesting material for small molecule solar cells. To test this, more amounts and higher yields are needed. Using not a dibromo, but a monobromo-benzothiadiazole in the reaction with **3** should give much higher yields.

Now that the way has been paved to the first stannole containing polymers, many new possibilities for high potential materials got opened.

Stannole Monomers for Chain Growth Polymerizations

The standard polymerization method for semiconducting polymers is to cross-couple two comonomers, one functionalized with two halides, and the other one with two metal groups. This method was used for the stannole polymers as described above. Another approach is to use a monomer that combines both functional groups in only one molecule, which could eventually lead to a chain growth (living) polymerization.

A synthetic route was developed that made it possible to obtain such a monomer **10**, using nucleophile –and electrophile selective cross-coupling reactions, differentiating between Sonogashira/Suzuki reaction and a bromide/iodide. Unfortunately, the resulting polymer **TS_nt** was hardly soluble, and a complete characterization as well as an investigation of the polymerization kinetics was not possible. However, the obtained UV/Vis spectra indicated that the reduction of thiophene rings from 3 to 2 from **TS_ntT** to **TS_nt** distinctly lowers the band gap even further.



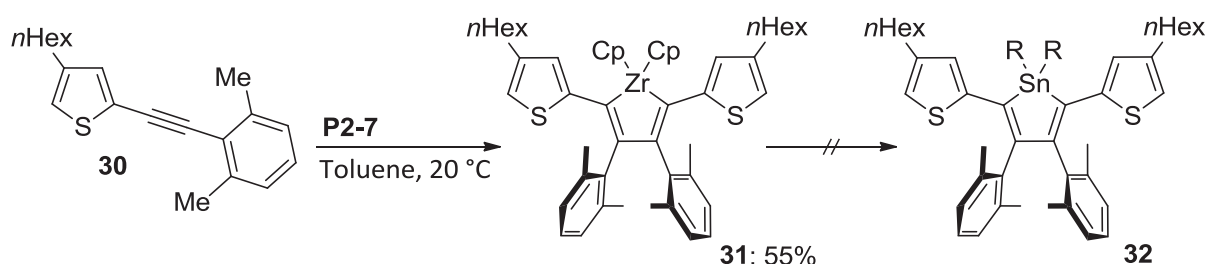
Scheme 21. Polymerization of monomer **10** yielded **TS_nt**, which was hardly soluble in common solvents.

To increase the solubility, more solubilizing alkyl chains must be incorporated into the monomer. Preliminary investigations showed that the purification of such a monomer is

substantially hindered, and further optimizations as described in detail in chapter 3.3 need to be pursued. As soon as such a monomer can be synthesized in high yields, the kinetics of the polymerizations is highly interesting. Will it proceed via a chain growth polymerization? Is it even living? Is it possible to prepare block copolymers? How does the polymerization method influence the performance of a device like an organic solar cell? This topic will provide a wide range of interesting investigations for future tasks.

Boroles

Another very interesting topic will be the incorporation of a borole into a semiconducting polymer. It turned out that the prepared stannole polymers do not offer a stability that is high enough to protect the forming antiaromatic ring from further reactions. Thus, a new route to stannole monomers with bulky phenyl rings in the backbone was developed. A central challenge was the formation of a fully regioselective zirconacyclopentadiene, which was achieved by using sterical hindering groups at the phenyl rings. The formation of the stannole needs further optimization as described in detail in chapter 3.5, but once this is achieved, the resulting stannole polymers should be transformable into the first borole containing polymer.



Scheme 22. The fully regioselective reaction to **31** was achieved, but the formation of stannole **32** needs further optimization.

It will then be highly interesting to investigate the morphology of the resulting polymers, and to find out the influence of the borole on the band gap. It would also be very interesting to see if it is possible to tune the band gap of the borole polymer just by adding a Lewis base: boroles react with a Lewis base with their free p_z -orbital, which increases their HOMO-LUMO gap.^[36] Simply by adding different amounts of a compound like pyridine to the borole polymer, it would potentially be possible to precisely adjust the band gap. This would make it extremely easy to prepare a polymer with the desired, specific electronic properties for a device.

5 Experimental Section

5.1 Supporting Information for *Org. Lett.* 2012, 14, 5644-5647.

Chemoselective Cross-Coupling Reactions with Differentiation Between Two Nucleophilic Sites on a Single Aromatic Substrate

Julian Linshoeft, Annika C. J. Heinrich, Stephan A. W. Segler, Paul J. Gates,[†] and Anne Staubitz*

Otto Diels-Institut für Organische Chemie, Universität Kiel, Otto-Hahn-Platz 4, 24118 Kiel (Germany)

* astaubitz@oc.uni-kiel.de

Supporting Information

Abbreviations	S1
General Methods and Materials	S2
GC Optimization Reactions	S4
Syntheses	S6
NMR spectra	S17
References	S36

Abbreviations

A	area
ATR	attenuated total reflectance
calcd.	calculated
CI	chemical ionization
COSY	correlated spectroscopy
d	doublet (NMR)
DMF	dimethylformamide
dppe	1,2-bis(diphenylphosphino)ethane
dppf	1,1'-bis(diphenylphosphino)ferrocene
EA	elemental analysis
EI	electron ionization
Fur	furan
GC	gas chromatography
GC/MS	gas chromatography-mass spectrometry
HMBC	heteronuclear multiple bond coherence
HSQC	heteronuclear single quantum coherence
IR	infrared
m	medium (concerning the intensity) (IR)
m	multiplet (NMR)
M.p.	melting point
MS	mass spectrometry
n	amount of substance
Naph	naphthalene
Pin	pinacol
RF	response factor
s	strong (concerning the intensity) (IR)
s	singlet (NMR)
SPhos	2-dicyclohexylphosphino-2',6'-dimethoxybiphenyl
t	triplet (NMR)
THF	tetrahydrofuran
TMEDA	tetramethylethylenediamine
Tph	thiophene
w	weak (concerning the intensity) (IR)

General Methods and Materials

All syntheses were carried out using standard Schlenk techniques under a dry and inert argon atmosphere. Glassware and NMR-tubes were dried in an oven at 200 °C for at least 2 h prior to use.

Analyses

¹H NMR, ¹³C NMR and ¹¹B NMR spectra were recorded at 300 K. ¹H NMR spectra were recorded on a Bruker AC 200 (200 MHz) spectrometer, a Bruker DRX 500 (500 MHz) spectrometer or a Bruker Avance 600 spectrometer. ¹³C NMR spectra were recorded on a Bruker AC 200 (200 MHz) spectrometer, a Bruker DRX 500 (125 MHz) spectrometer or a Bruker Avance 600 (151 MHz) spectrometer. ¹¹B NMR and ¹¹⁹Sn spectra were recorded on a Bruker DRX 500 (160 MHz) spectrometer. All ¹H NMR and ¹³C NMR spectra were referenced against the solvent residual proton signals (¹H) or the solvent itself (¹³C). ¹¹B NMR spectra were referenced externally against BF₃·OEt₂ in CDCl₃. ¹⁹F NMR spectra were referenced indirect by means of the ¹H NMR. ¹¹⁹Sn NMR spectra were calculated based on the ¹H NMR signal of TMS.

The exact assignment of the peaks was performed by two-dimensional NMR spectroscopy such as ¹H COSY, ¹H NOESY, ¹³C HSQC or ¹H/¹³C HMBC when possible.

EI and CI mass spectra were recorded on a Finnigan MAT 8200 or a Finnigan MAT 8230 apparatus.

Ultra High resolution ESI mass spectra were recorded on a Bruker Daltonics Apex IV Fourier transform Ion Cyclotron resonance mass spectrometer. The high resolution CI mass spectrum for compound **2c** was run on a VG Analytical Autospec apparatus.

IR spectra were recorded on a Perkin Elmer Paragon 1000 FT-IR spectrometer with a A531-G Golden-Gate-ATR-unit.

All melting points were recorded on an *Electrothermal melting point apparatus LG 1586* and are uncorrected.

The elementary analyses were performed on a Hekatech Euro EA Element Analyzer.

GC/MS analysis was performed on a Hewlett Packard 5890A gas chromatograph, equipped with a Hewlett Packard 5972A mass selective detector and an Agilent Technologies dimethylpolysiloxane column (19091S-931E, 15 m length, 0.25 mm diameter, 0.25 μm grain size).

GC analysis was performed on an Agilent Technologies 6890N gas chromatograph, equipped with an Agilent Technologies 7683 Series Injector, an Agilent Technologies (5 %-phenyl)-methylpolysiloxane column (19091J-413, 30 m length, 0.32 mm diameter, 0.25 μm grain size) and a flame ionization detector (FID).

Chemicals

All reagents were used without further purification unless otherwise noted.

1,3,5-Triisopropylbenzene	Alfa Aesar Inc.	96 %	distilled
1-Bromo-4-nitrobenzene	Acros Inc.	99 %	
1-Bromonaphthalene	Fluka	>95 %	
2-Bromo-1,4-dimethoxybenzene	Alfa Aesar Inc.	98 %	
3-Bromoanisole	Acros Inc.	98 %	
3-Bromopyridine	Alfa Aesar Inc.	99 %	
4-Bromoacetophenone	Alfa Aesar Inc.	98 %	
4-Bromobenzonitrile	Alfa Aesar Inc.	99 %	
4-Bromobenzotrifluoride	Alfa Aesar Inc.	99 %	
4-Bromo- <i>N,N</i> -dimethylaniline	Alfa Aesar Inc.	97 %	
5-Bromo-2-furoic acid	Alfa Aesar Inc.	99 %	
5-Bromofuran-2-carbaldehyde	Alfa Aesar Inc.	98 %	
Ammonium chloride	Grüssing Inc.	99.5 %	
Bromobenzene	ABCR	99.5 %	
H ₂ SO ₄	Grüssing	95 – 97 %	
K ₃ PO ₄	Sigma-Aldrich Inc.	>98 %	
Magnesium sulfate	Grüssing Inc.	99 %	
Methylithium	Acros Inc.	1.6 M in diethyl ether	
Molecular sieve, 3 Å	Alfa Aesar Inc.		
<i>n</i> -Butyllithium	Acros Inc.	2.5 M in hexanes	
Pd(dppe)Cl ₂	Strem Chemicals Inc.	98 %	
Pd(dppf)Cl ₂	Sigma-Aldrich Inc.	>98 %	
Pd(OAc) ₂	Strem Chemicals Inc.	>98 %	

Pd(PPh ₃) ₄	ABCR Inc.	99 %	
Pd(P ^t Bu ₃) ₂	Strem Chemicals Inc.	>98 %	
pinacol	ABCR Inc.	99 %	
Sodium	Merck Inc.	≥ 99 %	
Sodium chloride	Grüssing Inc.	99.5 %	
Sodium sulfate	Grüssing Inc.	99 %	
SPhos	Strem Chemicals Inc.	>98 %	
Thiophene	VWR Inc.	99 %	distilled
TMEDA	Acros Inc.	99.5 %	
Triisopropyl borate	Strem Chemicals Inc.	>98 %	
Trimethyltin chloride	Acros Inc.	99 %	

Solvents

All solvents were used freshly distilled after refluxing for several hours over the specified drying agent under nitrogen and were stored in a J. Young's-tube. If no drying agent is noted, the solvents were only distilled for purification. Water was degassed by bubbling argon through the water for 1 h.

Acetonitrile	HPLC-grade, dried and stored over 3 Å molecular sieve
Diethyl ether	-
Dioxane	Sodium with benzophenone as an indicator; stored over 3 Å molecular sieve
DMF	CaH ₂ ; stored over 3 Å molecular sieve
Ethyl acetate	-
Hexane	Sodium with benzophenone as an indicator; stored over 3 Å molecular sieve
Methanol	-
Pyridine	Distilled, then dried and stored over 3 Å molecular sieve
THF	Sodium with benzophenone as an indicator
Toluene	Sodium with benzophenone as an indicator; degassed by freeze-pump-thaw technique, stored over 3 Å molecular sieve

Chromatography

The silica gel used for chromatographic purification (Macherey-Nagel Inc.) had a grain size of 0.040 – 0.063 mm. Thin layer chromatography was performed using pre-coated plates from Macherey-Nagel Inc., ALUGRAM® Xtra SIL G/UV₂₅₄ and POLYGRAM® ALOX N/UV₂₅₄. Most of the chromatography purifications were carried out using a Biotage Isolera™ Flash Purification System.

GC Optimization Reactions

The yields for the optimization reactions were determined by GC by a multiple point internal standard method, using 1,3,5-triisopropylbenzene as a standard. The following equation was used for the calculation of the yields:

$$n(\text{analyte}) = \frac{A(\text{analyte})}{A(\text{standard})} \frac{n(\text{standard})}{RF}$$

where n is the amount of substance, A the integrated area and RF a system specific response factor.

Known amounts of **2a** and 1,3,5-triisopropylbenzene were used for the calibration curve. The response factor $RF=1.251$ was obtained from the slope of the following calibration curve (Figure SI 1).

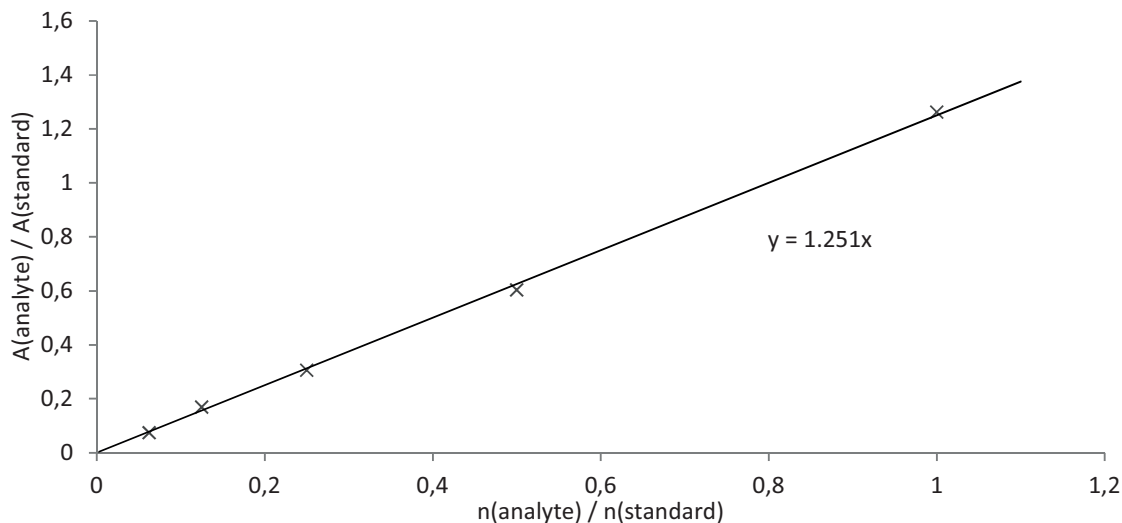


Figure SI 1. Calibration curve for **2a** using 1,3,5-triisopropylbenzene as an internal standard.

Typical procedure for the optimization reactions:

A solution of **1b** (205 mg, 0.55 mmol), 1-bromo-4-nitrobenzene (**5a**; 101 mg, 0.50 mmol), $\text{Pd}(\text{PPh}_3)_4$ (28.9 mg, 5 mol%) and the internal standard 1,3,5-triisopropylbenzene (102 mg, 0.50 mmol) in toluene (4 mL) was heated to 110 °C. After 16 h, a sample (0.1 mL) was taken from each reaction vessel, filtered through a short plug of silica (5 x 3 mm; eluent: ethyl acetate) and a syringe filter and was then used for GC analysis.

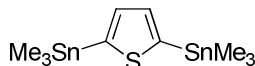
For all other reaction conditions, the parameters were varied as specified in Table SI 1.

Table SI 1. Optimization reactions.

Entry	Solvent	Catalyst	Loading	T [°C]	t [h]	Conversion [%]	Yield [%]
1	dioxane	[Pd(PPh ₃) ₄]	5 mol%	65	16	20	18
2	dioxane	[Pd(PPh ₃) ₄]	5 mol%	110	1.33	81	79
3	dioxane	[Pd(PPh ₃) ₄]	5 mol%	110	5	>99	>99
4	dioxane	[Pd(PPh ₃) ₄]	5 mol%	110	16	>99	80
5	dioxane	[Pd(dppe)Cl ₂]	5 mol%	110	24	>99	31
6	dioxane	[Pd(dppe)Cl ₂]	5 mol%	110	50	>99	3
7	dioxane	[Pd(dppe)Cl ₂]	5 mol%	110	72	>99	0
8	dioxane	Pd(OAc) ₂ /SPhos	5 mol% Pd(OAc) ₂ 10 mol% SPhos	110	1.33	>99	88
9	dioxane	Pd(OAc) ₂ /SPhos	5 mol% Pd(OAc) ₂ 10 mol% SPhos	110	5	>99	76
10	dioxane	[Pd(PrBu ₃) ₂]	5 mol%	110	1.33	>99	66
11	dioxane	[Pd(PrBu ₃) ₂]	5 mol%	110	5	>99	47
12	dioxane	[Pd(dppf)Cl ₂]	5 mol%	110	1.33	>99	96
13	dioxane	[Pd(dppf)Cl ₂]	5 mol%	110	5	>99	76
14	DMF	[Pd(PPh ₃) ₄]	5 mol%	65	16	95	75
15	DMF	[Pd(PPh ₃) ₄]	5 mol%	110	16	>99	23
16	DMF	[Pd(PPh ₃) ₄]	5 mol%	160	16	>99	0
17	toluene	[Pd(PPh ₃) ₄]	5 mol%	65	16	16	11
18	toluene	[Pd(PPh ₃) ₄]	5 mol%	110	1.33	95	81
19	toluene	[Pd(PPh ₃) ₄]	5 mol%	110	5	>99	>99
20	toluene	[Pd(PPh ₃) ₄]	5 mol%	110	16	>99	83
21	toluene	[Pd(dppe)Cl ₂]	5 mol%	110	16	41	41
22	toluene	[Pd(dppe)Cl ₂]	5 mol%	110	50	60	57
23	toluene	[Pd(dppe)Cl ₂]	5 mol%	110	72	95	61
24	toluene	Pd(OAc) ₂ /SPhos	5 mol% Pd(OAc) ₂ 10 mol% SPhos	110	1.33	>99	>99
25	toluene	Pd(OAc) ₂ /SPhos	5 mol% Pd(OAc) ₂ 10 mol% SPhos	110	5	>99	86
26	toluene	Pd(OAc) ₂ /SPhos	5 mol% Pd(OAc) ₂ 10 mol% SPhos	110	16	>99	25
27	toluene	Pd(OAc) ₂ /SPhos	5 mol% Pd(OAc) ₂ 10 mol% SPhos	65	0.17	22	21
28	toluene	Pd(OAc) ₂ /SPhos	5 mol% Pd(OAc) ₂ 10 mol% SPhos	65	1.33	67	66
29	toluene	Pd(OAc) ₂ /SPhos	5 mol% Pd(OAc) ₂ 10 mol% SPhos	65	3	88	87
30	toluene	Pd(OAc) ₂ /SPhos	5 mol% Pd(OAc) ₂ 10 mol% SPhos	65	4	>99	98
31	toluene	Pd(OAc) ₂ /SPhos	2.5 mol% Pd(OAc) ₂ 5 mol% SPhos	65	4	>99	98
32	toluene	Pd(OAc) ₂ /SPhos	1 mol% Pd(OAc) ₂ 2 mol% SPhos	65	18	>99	>99
33	toluene	Pd(OAc) ₂ /SPhos	1 mol% Pd(OAc) ₂ 2 mol% SPhos	65	22	>99	>99
34	toluene	[Pd(PrBu ₃) ₂]	5 mol%	110	1.33	>99	66
35	toluene	[Pd(PrBu ₃) ₂]	5 mol%	110	5	>99	50
36	toluene	[Pd(PrBu ₃) ₂]	5 mol%	110	16	>99	18
37	toluene	[Pd(dppf)Cl ₂]	5 mol%	110	1.33	>99	90
38	toluene	[Pd(dppf)Cl ₂]	5 mol%	110	5	>99	85
39	toluene	[Pd(dppf)Cl ₂]	5 mol%	110	16	>99	37
40	THF	[Pd(PPh ₃) ₄]	5 mol%	65	16	27	21
41	acetonitrile	[Pd(PPh ₃) ₄]	5 mol%	65	16	9	7
42	acetonitrile	[Pd(PPh ₃) ₄]	5 mol%	110	16	>99	69
43	pyridine	[Pd(PPh ₃) ₄]	5 mol%	65	16	>99	64
44	pyridine	[Pd(PPh ₃) ₄]	5 mol%	110	16	>99	36

Syntheses

2,5-bis(trimethylstannyl)thiophene (**4**)



2,5-Bis(trimethylstannyl)thiophene (**4**) was synthesized similar to a method described in the literature by Seitz et al.¹ and was modified as follows:

n-Butyllithium (16.0 mL, 40.0 mmol; 2.5 M in hexanes) was added within 10 min to a solution of thiophene (1.68 g, 20.0 mmol) and TMEDA (4.65 g, 40 mmol) in hexane (40 mL) at 0 °C. The reaction mixture was heated to reflux for 45 min and after cooling the suspension to 0 °C, a solution of trimethyltin chloride (7.97 g, 40.0 mmol), dissolved in THF (20 mL), was added within 10 min. After removal of the cooling bath, the reaction mixture was stirred for 15 h at 24 °C and was then quenched with a saturated solution of ammonium chloride (50 mL). The aqueous layer was extracted with diethyl ether (3 x 50 mL) and the combined organic layers were washed with brine (2 x 40 mL). The organic layer was dried over magnesium sulfate and the volatiles were removed *in vacuo* to afford 7.65 g (93 %, Lit.¹: 82 %) of a pale yellow solid.

¹H NMR (200 MHz, CDCl₃): δ = 7.40 (s, 2 H, Tph-*H*), 0.39 (s, 18 H, Sn(CH₃)₃) ppm.

¹³C NMR (50 MHz, CDCl₃): δ = 143.0 (Tph-*C*), 135.8 (Tph-*CH*), -8.2 (Sn(CH₃)₃) ppm.

¹¹⁹Sn NMR (187 MHz, CDCl₃): δ = -27.9 ppm.

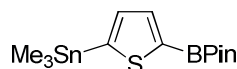
IR (ATR): $\tilde{\nu}$ = 3057 (w), 2982 (w), 2913 (w), 1751 (w), 1477 (w), 1390 (w), 1254 (w), 1188 (w), 953 (m), 921 (w), 797 (s), 764 (s), 734 (s), 531 (s), 515 (s) cm⁻¹.

MS (EI, 70 eV): *m/z* (%) = 412 (10) [M(¹²⁰Sn, ¹²⁰Sn)]⁺, 410 (12) [M(¹¹⁸Sn, ¹²⁰Sn)]⁺, 408 (10) [M(¹¹⁸Sn, ¹¹⁸Sn and ¹¹⁶Sn, ¹²⁰Sn)]⁺, 395 (100) [M - CH₃]⁺, 365 (9) [M - C₃H₉]⁺, 335 (5) [M - C₅H₁₅]⁺.

MS (CI, isobutane): *m/z* (%) = 411 (53) [M + H]⁺.

The NMR data are in agreement with the data found in the literature.¹

4,4,5,5-Tetramethyl-2-(5-(trimethylstannyl)thiophen-2-yl)-1,3,2-dioxaborolane (**1b**)



Methylolithium (625 μL, 1.00 mmol, 1.60 M in diethyl ether) was added within 10 min to a suspension of **4** (410 mg, 1.00 mmol) in THF (6 mL) at -100 °C. The slightly yellow solution was stirred for 2 h at -78 °C. 2-Isopropoxy-4,4,5,5-tetramethyl-1,3,2-dioxaborolane (186 mg, 1.00 mmol) was slowly added at this temperature and stirred for 1 h. Then the reaction mixture was warmed to 20 °C within 12 h without removing the cooling bath and was then quenched with water. The aqueous layer was washed with diethyl ether (3 x 20 mL). The combined organic layer were washed with brine (1 x 20 mL) and dried over sodium sulfate. The solvent was removed *in vacuo* and the crude product was purified by sublimation² (30 °C, 2 x 10⁻² mbar) to afford 205 mg (55 %) of a colorless solid.

Note: the compound was unstable to silica gel chromatography.

¹H NMR (500 MHz, CDCl₃): δ = 7.79 (d, 1 H, ³*J* = 3.2 Hz, Tph-*H*), 7.33 (d, 1 H, ³*J* = 3.2 Hz, Tph-*H*), 1.37 (s, 12 H, pin-CH₃), 0.40 (s, 9 H, Sn(CH₃)₃) ppm.

¹³C NMR (126 MHz, CDCl₃): δ = 146.5 (Tph-*C*), 137.8 (Tph-*CH*), 136.3 (Tph-*CH*), 84.1 (pin-C(CH₃)₄), 24.9 (BO₂C(CH₃)₄), -8.1 (Sn(CH₃)₃) ppm.³

¹¹⁹Sn NMR (187 MHz, CDCl₃): δ = -26.8 ppm.

¹¹B NMR (160 MHz, CDCl₃): δ = 28.8 ppm.

M.p.: 84 °C.

(1) D. E. Seitz, S. H. Lee, R. N. Hanson, J. C. Bottaro, *Synth. Commun.* **1983**, *13*, 121.

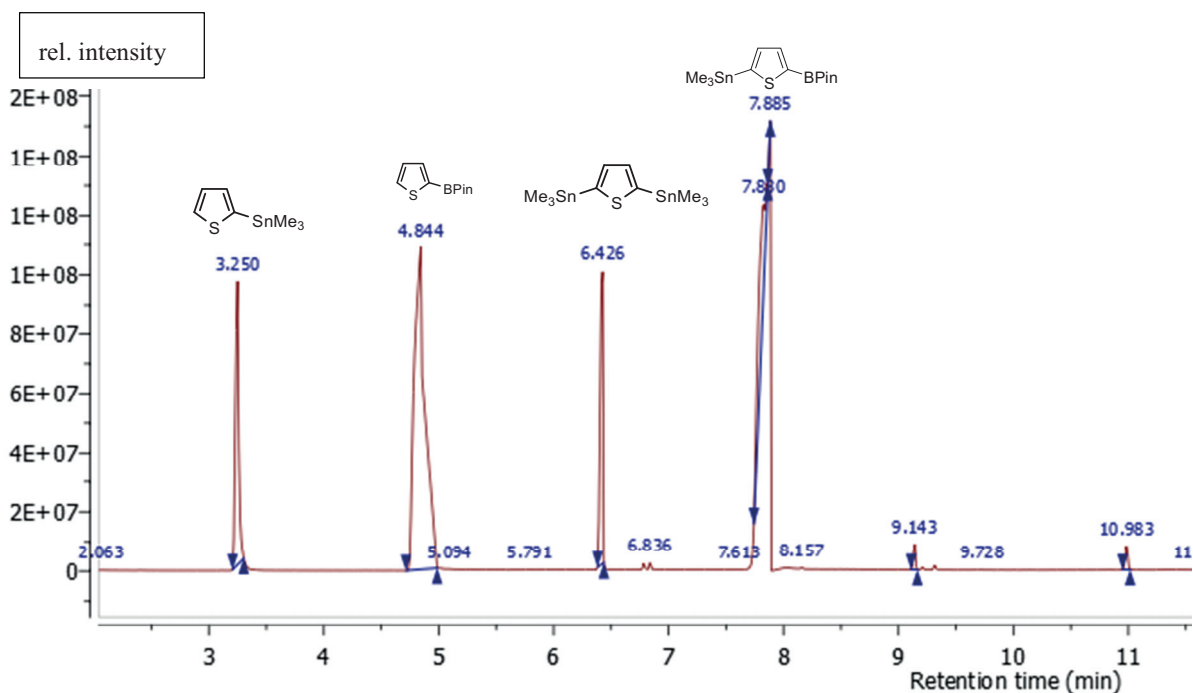
(2) The starting material, as well as the monostannylated and monoboronated species were sublimed first (25 °C, 2 x 10⁻² mbar) (see below).

(3) The carbon atom bound to boron was not visible due to the high quadrupole moment of the boron nucleus.

IR (ATR): = 2978 (m), 2920 (w), 1510 (s), 1418 (s), 1331 (s), 1254 (m), 1138 (s), 1064 (s), 1021 (m), 957 (m), 928 (m), 853 (m), 820 (m), 770 (s), 665 (s), 533 (s) cm^{-1} .

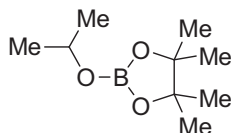
HRMS (ESI): Found 397.0432; calcd. for $\text{C}_{13}\text{H}_{23}\text{BNaO}_2\text{SSn}$ 397.0426.

EA (%): Found C (41.49), H (6.34), S (8.68); calcd. for $\text{C}_{13}\text{H}_{23}\text{BO}_2\text{SSn}$ C (41.87), H (6.22), S (8.60).



GS-MS of the crude product. The Intensity is not quantitative.

2-Isopropoxy-4,4,5,5-tetramethyl-1,3,2-dioxaborolane (*i*PrO-BPin)



2-Isopropoxy-4,4,5,5-tetramethyl-1,3,2-dioxaborolane was prepared similarly to a method described in the literature by Andersen et al.⁴ and was modified as follows:

Triisopropyl borate (22.8 g, 121 mmol) and pinacol (14.3 g, 121 mmol) in hexane (100 mL) were heated to 90 °C (external temperature) and a 2-propanol/hexane azeotrope was removed by distillation within 16 h. The residue was distilled (90 °C oil bath temperature, 7 mbar) to yield 20.6 g (92 %, Lit.⁴: 89 %) of a colorless oil.

¹H NMR (500 MHz, CDCl_3): δ = 4.29 (septet, 3J = 6.2 Hz, 1 H, $\text{CH}(\text{CH}_3)_2$), 1.20 (s, 12 H, pin- $\text{C}(\text{CH}_3)_2$), 1.15 (d, 3J = 6.2 Hz, 6 H, $\text{CH}(\text{CH}_3)_2$) ppm.

¹³C NMR (126 MHz, CDCl_3): δ = 82.5 (pin- $\text{C}(\text{CH}_3)_2$), 67.4 ($\text{CH}(\text{CH}_3)_2$), 24.6 (pin- $\text{C}(\text{CH}_3)_2$), 24.4 ($\text{CH}(\text{CH}_3)_2$) ppm.

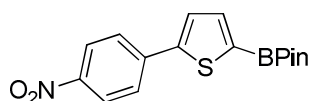
¹¹B NMR (160 MHz, CDCl_3): δ = 21.8 ppm.

IR (ATR): $\tilde{\nu}$ = 2979 (w), 1504 (w), 1473 (w), 1444 (m), 1373 (w), 1345 (w), 1319 (m), 1148 (m), 1121 (m), 958 (w), 905 (s), 852 (m), 727 (s), 672 (m), 648 (m) cm^{-1} .

(4) M. W. Andersen, B. Hildebrandt, G. Köster, R. W. Hoffmann, *Chem. Ber.* **1989**, *122*, 1777.

The NMR data are in agreement with the data found in the literature.⁴

4,4,5,5-Tetramethyl-2-(5-(4-nitrophenyl)thiophen-2-yl)-1,3,2-dioxaborolane (2a)



A solution **1b** (746 mg, 2.00 mmol), 1-bromo-4-nitrobenzene (**5a**; 404 mg, 2.00 mmol), Pd(OAc)₂ (4.5 mg, 1 mol%) and SPhos (16.4 mg, 2 mol%) in toluene (8 mL) was heated to 65 °C for 18 h. The reaction mixture was cooled to 20 °C and filtered through a short plug of silica gel (5 x 2 cm; eluent: ethyl acetate). After removal of the volatiles, the crude product was sublimed (120 °C, 8 x 10⁻³ mbar) to afford 649 mg (98 %) of a yellow solid.

¹H NMR (500 MHz, CDCl₃): δ = 8.24 (d, ³J = 8.8 Hz, 2 H, Ar-H), 7.78 (d, ³J = 8.8 Hz, 2 H, Ar-H), 7.64 (d, ³J = 3.7 Hz, 1 H, Tph-H), 7.52 (d, ³J = 3.7 Hz, 1 H, Tph-H), 1.37 (s, 12 H, pin-CH₃) ppm.

¹³C NMR (126 MHz, CDCl₃): δ = 148.1 (Tph-C), 147.2 (Ar-C), 140.5 (Ar-C), 138.5 (Tph-CH), 126.9 (Tph-CH), 126.6 (Ar-CH), 124.6 (Ar-CH), 84.6 (pin-C(CH₃)₂), 24.9 (pin-CH₃) ppm.³

¹¹B NMR (160 MHz, CDCl₃): δ = 28.4 ppm.

M.p.: 155 °C.

IR (ATR): $\tilde{\nu}$ = 2973 (m), 2929 (w), 1700 (s), 1593 (w), 1509 (m), 1454 (s), 1360 (s), 1215 (m), 1179 (s), 1145 (s), 1021 (w), 951 (m), 911 (m), 850 (m), 750 (m), 663 (m) cm⁻¹.

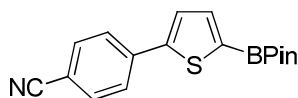
MS (EI, 70 eV): *m/z* (%) = 331 (100) [M]⁺.

MS (CI, isobutane): *m/z* (%) = 332 (100) [M + H]⁺.

HRMS (ESI): Found 354.0941; calcd. for C₁₆H₁₈BNNaO₄S 354.0942.

EA (%): Found C (58.66), H (5.42), N (4.25), S (9.69); calcd. for C₁₆H₁₈BNO₄S C (58.02), H (5.48), N (4.23), S (9.68).

4,4,5,5-Tetramethyl-2-(5-(4-benzonitrile)thiophen-2-yl)-1,3,2-dioxaborolane (2b)



A solution of **1b** (373 mg, 1.00 mmol), 4-bromobenzonitrile (**5b**; 182 mg, 1.00 mmol), Pd(OAc)₂ (2.3 mg, 1 mol%) and SPhos (8.2 mg, 2 mol%) in toluene (8 mL) was heated to 65 °C for 18 h. The reaction mixture was cooled to 20 °C and filtered through a short plug of silica gel (5 x 2 cm; eluent: ethyl acetate). After removal of the volatiles, the crude product was sublimed (70 °C, 1 x 10⁻² mbar) to afford 260 mg (84 %) of a pale yellow solid.

¹H NMR (500 MHz, CDCl₃): δ = 7.72 (d, ³J = 8.4 Hz, 2 H, Ar-H), 7.66 (d, ³J = 8.4 Hz, 2 H, Ar-H), 7.62 (d, ³J = 3.6 Hz, 1 H, Tph-H), 7.47 (d, ³J = 3.6 Hz, 1 H, Tph-H), 1.36 (s, 12 H, pin-CH₃) ppm.

¹³C NMR (126 MHz, CDCl₃): δ = 148.7 (Tph-C), 138.6 (Ar-C or CN), 138.4 (Tph-CH), 132.9 (Ar-CH), 126.5 (Ar-CH), 126.4 (Tph-CH), 118.9 (Ar-C or CN), 111.2 (Ar-C), 84.6 (pin-C(CH₃)₂), 24.9 (pin-CH₃) ppm.³

¹¹B NMR (160 MHz, CDCl₃): δ = 28.8 ppm.

M.p.: 180 °C.

IR (ATR): $\tilde{\nu}$ = 2975 (m), 2927 (w), 2216 (m), 1602 (m), 1532 (m), 1455 (s), 1357 (s), 1313 (m), 1143 (s), 1075 (m), 1022 (m), 956 (m), 806 (s), 661 (s), 548 (s) cm⁻¹.

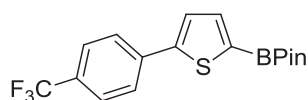
MS (EI, 70 eV): *m/z* (%) = 311 (100) [M]⁺, 296 (26) [M - CH₃]⁺.

MS (CI, isobutane): *m/z* (%) = 312 (100) [M + H]⁺.

HRMS (ESI): Found 334.1042; calcd. for C₁₇H₁₈BNNaO₂S 334.1044.

EA (%): Found C (65.55), H (5.92), N (4.53), S (9.99); calcd. for C₁₇H₁₈BNO₂S C (65.61), H (5.83), N (4.50), S (10.30).

4,4,5,5-Tetramethyl-2-(5-(4-(trifluoromethyl)phenyl)thiophen-2-yl)-1,3,2-dioxaborolane (2c)



A solution of **1b** (373 mg, 1.00 mmol), 4-bromobenzotrifluoride (**5c**; 225 mg, 1.00 mmol), Pd(OAc)₂ (2.3 mg, 1 mol%) and SPhos (8.2 mg, 2 mol%) in toluene (8 mL) was heated to 65 °C for 18 h. The reaction mixture was cooled to 20 °C and filtered through a short plug of silica gel (5 x 2 cm; eluent: ethyl acetate). After removal of the volatiles, the brown solid residue was purified by sublimation (70 °C, 2 x 10⁻² mbar) to obtain 287 mg (81 %) of a white solid.

¹H NMR (500 MHz, CDCl₃): δ = 7.74 (d, ³J = 8.1 Hz, 2 H, Ar-H), 7.65 – 7.62 (m, 3 H, Tph-H, Ar-H), 7.45 (d, ³J = 3.6 Hz, 1 H, Tph-H), 1.37 (s, 12 H, pin-CH₃) ppm.

¹³C NMR (126 MHz, CDCl₃): δ = 149.3 (Ar-C or Tph-C), 138.4 (Tph-CH), 137.7 (Ar-C or Tph-C), 129.8 (q, ²J = 32.6 Hz, CCF₃), 126.4 (Ar-CH), 126.2 – 125.95 (m, Ar-CH), 125.8 (Tph-CH), 124.9 (q, ¹J = 272.0 Hz, CF₃), 84.5 (pin-C(CH₃)₂), 24.9 (pin-CH₃) ppm.³

M.p.: 97 °C.

¹¹B NMR (160 MHz, CDCl₃): δ = 28.9 ppm.

¹⁹F NMR (471 MHz, CDCl₃): δ = -62.6 ppm.

IR (ATR): $\tilde{\nu}$ = 2989 (w), 1614 (w), 1537 (w), 1511 (w), 1459 (m), 1371 (m), 1358 (m), 1324 (s), 1305 (s), 1267 (m), 1210 (m), 1154 (m), 1140 (s), 1107 (s), 1063 (s), 1014 (m), 952 (m), 851 (m), 841 (m), 814 (s), 664 (s) cm⁻¹.

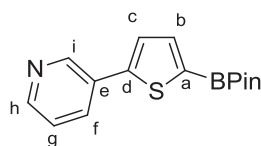
MS (EI, 70 eV): *m/z* (%) = 354 (100) [M]⁺, 339 (20) [M - CH₃]⁺.

MS (CI, isobutane): *m/z* (%) = 355 (100) [M + H]⁺.

HRMS (CI, methane): Found 355.1156; calcd. for C₁₇H₁₉BF₃O₂S 355.1151 [M + H]⁺.

EA (%): Found C (57.56), H (5.15), S (8.86); calcd. for C₁₇H₁₈BF₃O₂S C (57.65), H (5.12), S (9.05).

3-(5-(4,4,5,5-Tetramethyl-1,3,2-dioxaborolan-2-yl)thiophen-2-yl)pyridine (2e)



A solution of **1b** (746 mg, 2.00 mmol), 3-bromopyridine (**5e**; 316 mg, 2.00 mmol), Pd(OAc)₂ (4.5 mg, 1 mol%) and SPhos (16.4 mg, 2 mol%) in toluene (8 mL) was heated to reflux for 6 h. The reaction mixture was cooled to 20 °C, filtered through a short plug of silica (5 x 2 cm; eluent: ethyl acetate) and the volatiles were removed *in vacuo*. The yellow solid was sublimed (90 °C, 8 x 10⁻³ mbar) to afford 463 mg (81 %) of a colorless solid.

¹H NMR (500 MHz, CDCl₃): δ = 8.92 (dd, ⁴J = 1.8 Hz, ⁵J = 0.7 Hz, 1 H, H-i), 8.53 (dd, ³J = 4.8 Hz, ⁴J = 1.6 Hz, 1 H, H-f or H-h), 7.91 – 7.88 (m, 1 H, H-f or H-h), 7.63 (d, ³J = 3.6 Hz, 1 H, Tph-H), 7.43 (d, ³J = 3.6 Hz, 1 H, Tph-H), 7.31 (ddd, ³J = 7.9 Hz, ³J = 4.8 Hz, ⁵J = 0.7 Hz, 1 H, H-g), 1.36 (s, 12 H, pin-CH₃) ppm.

¹³C NMR (126 MHz, CDCl₃): δ = 149.0 (C-f or C-h), 147.4 (C-i), 147.3 (C-d), 138.4 (C-b or C-c), 133.3 (C-f or C-h), 130.4 (C-e), 125.6 (C-b or C-c), 123.8 (C-g), 84.5 (pin-C(CH₃)₂), 24.9 (pin-CH₃) ppm.³

¹¹B NMR (160 MHz, CDCl₃): δ = 28.8 ppm.

M.p.: 121 °C.

IR (ATR): $\tilde{\nu}$ = 2974 (w), 2927 (w), 1610 (w), 1577 (m), 1530 (m), 1481 (m), 1425 (m), 1381 (m), 1358 (m), 1253 (m), 1213 (m), 1181 (m), 1125 (s), 1063 (m), 1030 (s), 977 (s), 942 (s), 803 (s), 757 (s), 736 (s), 704 (s), 691 (s), 579 (m) cm⁻¹.

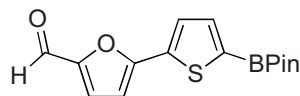
MS (EI, 70 eV): *m/z* (%) = 287 (100) [M]⁺, 272 (16) [M - CH₃]⁺.

MS (CI, isobutane): *m/z* (%) = 288 (100) [M + H]⁺.

HRMS (ESI): Found 310.1035; calcd. for C₁₅H₁₈BNNaO₂S 310.1044.

EA (%): Found C (61.58), H (6.31), N (4.63), S (10.96); calcd. for $C_{15}H_{18}BNO_2S$ C (62.73), H (6.32), N (4.88), S (11.17).

5-(5-(4,4,5,5-Tetramethyl-1,3,2-dioxaborolan-2-yl)thiophen-2-yl)furan-2-carbaldehyde (2f)



A solution of **1b** (373 mg, 1.00 mmol), 5-bromofuran-2-carbaldehyde (**5f**; 175 mg, 1.00 mmol), $Pd(OAc)_2$ (2.3 mg, 1 mol%) and SPhos (8.2 mg, 2 mol%) in toluene (8 mL) was heated to 65 °C for 18 h. The reaction mixture was cooled to 20 °C and filtered through a short plug of silica gel (5 x 2 cm; eluent: ethyl acetate). After removal of the volatiles, the red solid was purified by sublimation (120 °C, 1×10^{-2} mbar) to obtain 289 mg (95 %) of a brown-orange solid.

1H NMR (500 MHz, $CDCl_3$): δ = 9.63 (s, 1 H, CHO), 7.58 (d, $^3J = 3.7$ Hz, 1 H, Tph-H), 7.57 (d, $^3J = 3.7$ Hz, 1 H, Tph-H), 7.27 (d, $^3J = 3.7$ Hz, 1 H, Fur-H), 6.71 (d, $^3J = 3.7$ Hz, 1 H, Fur-H), 1.35 (s, 12 H, pin- CH_3) ppm.

^{13}C NMR (126 MHz, $CDCl_3$): δ = 177.2 (CHO), 154.7 (Fur-C), 151.9 (Fur-C), 138.0 (Tph-CH), 137.9 (Tph-C), 127.2 (Tph-CH), 123.3* (Fur-CH), 108.6 (Fur-CH), 84.6 (pin-C(CH_3)₂), 24.9 (pin- CH_3) ppm.³

* broad signal.

^{11}B NMR (160 MHz, $CDCl_3$): δ = 28.7 ppm.

M.p.: 124 °C.

IR (ATR): $\tilde{\nu}$ = 2976 (m), 2932 (w), 2810 (w), 1666 (s), 1581 (m), 1534 (s), 1435 (s), 1333(s), 1292 (m), 1244 (m), 1136 (s), 1021 (s), 958 (s), 853 (s), 761 (s), 658 (s) cm^{-1} .

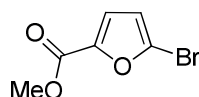
MS (EI, 70 eV): m/z (%) = 304 (100) $[M]^+$.

MS (CI, isobutane): m/z (%) = 305 (100) $[M + H]^+$.

HRMS (ESI): Found 327.0839; calcd. for $C_{15}H_{17}BNaO_4S$ 327.0833.

EA (%): Found C (59.40), H (5.69), S (10.33); calcd. for $C_{15}H_{17}BO_4S$ C (59.23), H (5.63), S (10.54).

5-Bromo-2-furoic acid methyl ester (5g)



A solution of 5-bromo-2-furoic acid (1.91 g, 10.0 mmol) and H_2SO_4 (2 mL) in methanol (60 mL) was heated to reflux for 26 h. After removal of the volatiles, the residue was poured into water (500 mL) and extracted with ethyl acetate (3 x 70 mL). The organic layer was washed with brine (50 mL) and dried over Na_2SO_4 . After removal of the solvent, a white solid was obtained without further purification necessary (2.00 g, 98 %).

1H NMR (500 MHz, $CDCl_3$): δ = 7.12 (d, $^3J = 3.5$ Hz, 1 H, Fur-H), 6.45 (d, $^3J = 3.5$ Hz, 1 H, Fur-H), 3.89 (s, 3 H, CH_3) ppm.

^{13}C NMR (126 MHz, $CDCl_3$): δ = 158.2 (COO), 146.4 (Fur-C), 127.7 (Fur-C), 120.2 (Fur-CH), 114.1 (Fur-CH), 52.2 (CH_3) ppm.

M.p.: 66 °C.

IR (ATR): $\tilde{\nu}$ = 3119 (w), 2957 (w), 2362 (w), 1705 (s), 1580 (s), 1463 (s), 1438 (s), 1353 (m), 1295 (s), 1209 (s), 1195 (s), 1155 (s), 1110 (s), 1019 (s), 979 (s), 921 (s), 799 (s), 753 (s), 599 (m) cm^{-1} .

MS (EI, 70 eV): m/z (%) = 206 (50) $[M(^{81}Br)]^+$, 204 (63) $[M(^{79}Br)]^+$, 175 (100) $[M(^{81}Br) - CH_3O]^+$, 173 (99) $[M(^{79}Br) - CH_3O]^+$.

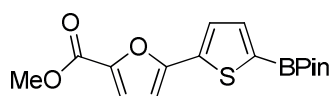
MS (CI, isobutane): m/z (%) = 207 (81) $[M(^{81}Br) + H]^+$, 205 (100) $[M(^{79}Br) + H]^+$.

HRMS (ESI): Found 226.9308; calcd. for $C_6H_5BrNaO_3$ 226.9314.

EA (%): Found C (35.10), H (2.43); calcd. for $C_6H_5BrO_3$ C (35.15), H (2.46).

The NMR data are in agreement with the data found in the literature.⁵

Methyl 5-(5-(4,4,5,5-tetramethyl-1,3,2-dioxaborolan-2-yl)thiophen-2-yl)furan-2-carboxylate (2g)



A solution of **1b** (373 mg, 1.00 mmol), 5-bromo-2-furoic acid methyl ester (**5g**; 205 mg, 1.00 mmol), Pd(OAc)₂ (2.3 mg, 1 mol%) and SPhos (8.2 mg, 2 mol%) in toluene (8 mL) was heated to 65 °C for 18 h. The reaction mixture was cooled to 20 °C, filtered through a short plug of silica (5 x 2 cm; eluent: ethyl acetate) and the volatiles were removed *in vacuo*. The brown solid was purified by sublimation (75 °C, 3 x 10⁻² mbar) to obtain 255 mg (76 %) of a pale yellow solid.

¹H NMR (500 MHz, CDCl₃): δ = 7.56 (d, ³J = 3.6 Hz, 1 H, Tph-*H*), 7.51 (d, ³J = 3.6 Hz, 1 H, Tph-*H*), 7.21 (d, ³J = 3.6 Hz, 1 H, Fur-*H*), 6.62 (d, ³J = 3.6 Hz, 1 H, Fur-*H*), 3.90 (s, 3 H, OCH₃), 1.35 (s, 12 H, pin-CH₃) ppm.

¹³C NMR (126 MHz, CDCl₃): δ = 159.1 (COO), 152.9 (Fur-*C*), 143.6 (Fur-*C*), 138.5 (Tph-*C*), 137.9 (Tph-CH), 126.3 (Tph-CH), 120.2 (Fur-CH), 107.8 (Fur-CH), 84.5 (pin-*C*(CH₃)₂), 52.0 (OCH₃), 24.9 (pin-CH₃) ppm.³

¹¹B NMR (160 MHz, CDCl₃): δ = 28.8 ppm.

M.p.: 110 °C.

IR (ATR): $\tilde{\nu}$ = 2979 (w), 1726 (s), 1536 (m), 1441 (s), 1371 (m), 1346 (s), 1329 (s), 1302 (s), 1273 (m), 1210 (m), 1136 (s), 1076 (m), 1020 (m), 982 (m), 851 (m), 811 (s), 761 (m), 662 (s) cm⁻¹.

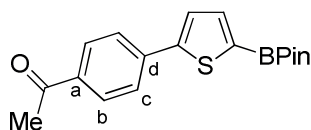
MS (EI, 70 eV): *m/z* (%) = 334 (100) [M]⁺.

MS (CI, isobutane): *m/z* (%) = 335 (100) [M + H]⁺.

HRMS (ESI): Found 357.0928; calcd. for C₁₆H₁₉BNaO₅S 357.0938.

EA (%): Found C (57.39), H (5.86), S (9.56); calcd. for C₁₆H₁₉BO₅S C (57.50), H (5.73), S (9.59).

1-(4-(5-(4,4,5,5-Tetramethyl-1,3,2-dioxaborolan-2-yl)thiophen-2-yl)phenyl)ethanone (2h)



A solution of **1b** (373 mg, 1.00 mmol), 4-bromoacetophenone (**5h**; 199 mg, 1.00 mmol), Pd(OAc)₂ (2.3 mg, 1 mol%) and SPhos (8.2 mg, 2 mol%) in toluene (8 mL) was heated to 65 °C for 18 h. The reaction mixture was cooled to 20 °C, filtered through a short plug of silica (5 x 2 cm; eluent: ethyl acetate) and the volatiles were removed *in vacuo*. The brown solid was purified by sublimation (75 °C, 4 x 10⁻² mbar) to obtain 291 mg (87 %) of a pale yellow solid.

¹H NMR (500 MHz, CDCl₃): δ = 7.97 (d, ³J = 8.7 Hz, 2 H, *H*-b), 7.72 (d, ³J = 8.7 Hz, 2 H, *H*-c), 7.62 (d, ³J = 3.6 Hz, 1 H, Tph-*H*), 7.48 (d, ³J = 3.6 Hz, 1 H, Tph-*H*), 2.61 (s, 3 H, COCH₃), 1.36 (s, 12 H, pin-CH₃) ppm.

¹³C NMR (126 MHz, CDCl₃): δ = 197.4 (CO), 149.7 (Tph-*C*), 138.7 (*C*-d), 138.4 (Tph-CH), 136.2 (*C*-a), 129.3 (CH-b), 126.1 (CH-c), 126.0 (Tph-CH), 84.5 (pin-*C*(CH₃)₂), 26.7 (COCH₃), 24.9 (pin-CH₃) ppm.³

¹¹B NMR (160 MHz, CDCl₃): δ = 28.7 ppm.

M.p.: 137 °C.

IR (ATR): $\tilde{\nu}$ = 2968 (w), 2926 (w), 1673 (s), 1602 (m), 1531 (m), 1505 (m), 1453 (m), 1355 (s), 1322 (s), 1305 (s), 1269 (s), 1145 (s), 1080 (m), 854 (m), 802 (s), 660 (s), 578 (m) cm⁻¹.

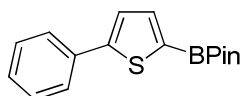
MS (EI, 70 eV): *m/z* (%) = 328 (100) [M]⁺, 313 (35) [M - CH₃]⁺.

MS (CI, isobutane): *m/z* (%) = 329 (100) [M + H]⁺.

HRMS (ESI): Found 351.1201; calcd. for C₁₈H₂₁BNaO₃S 351.1197.

EA (%): Found C (65.23), H (6.75), S (9.54); calcd. for C₁₈H₂₁BO₃S C (65.87), H (6.45), S (9.77).

(5) J.G. Montana, I. Fleming, R. Tacke, J. Daiss, Heterocyclic silicon compounds and their use in the treatment of diseases or conditions associated with GnRH (gonadotropin-releasing hormone), PCT Int. Pat. Appl. WO 2004/045625 A1 (03.06.2004).

4,4,5,5-Tetramethyl-2-(5-phenylthiophen-2-yl)-1,3,2-dioxaborolane (**2i**)

A solution of **1b** (746 mg, 2.00 mmol), bromobenzene (**5i**; 314 mg, 2.00 mmol), Pd(OAc)₂ (4.5 mg, 1 mol%) and SPhos (16.4 mg, 2 mol%) in toluene (8 mL) was heated to 65 °C for 18 h. The reaction mixture was cooled to 20 °C, filtered through a short plug of silica (5 x 2 cm; eluent: ethyl acetate) and the volatiles were removed *in vacuo*. The residue was purified by Kugelrohr distillation (130 °C, 0.1 mbar) and column chromatography (gradient from *n*-hexane to EtOAc) to afford 475 mg (83 %) of a white solid.

¹H NMR (500 MHz, CDCl₃): δ = 7.67 – 7.64 (m, 2 H, Ar-*H*), 7.60 (d, ³*J* = 3.6 Hz, 1 H, Tph-*H*), 7.41 – 7.36 (m, 3 H, Tph-*H*, Ar-*H*), 7.32 – 7.28 (m, 1 H, Ar-*H*), 1.36 (s, 12 H, pin-CH₃) ppm.

¹³C NMR (126 MHz, CDCl₃): δ = 151.5 (Tph-C), 138.3 (Tph-CH), 134.4 (Ar-C), 129.1 (Ar-CH), 128.1 (Ar-CH), 126.4 (Ar-CH), 124.6 (Tph-CH), 84.3 (pin-C(CH₃)₂), 24.9 (pin-CH₃) ppm.³

¹¹B NMR (160 MHz, CDCl₃): δ = 28.9 ppm.

M.p.: 59 °C.

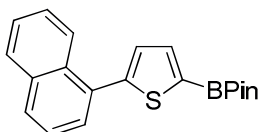
IR (ATR): $\tilde{\nu}$ = 2986 (m), 2932 (w), 1531 (s), 1499 (w), 1456 (s), 1443 (s), 1353 (s), 1331 (s), 1295 (s), 1137 (s), 1077 (m), 1020 (m), 854 (s), 813 (s), 758 (s), 662 (s) cm⁻¹.

MS (EI, 70 eV): *m/z* (%) = 286 (100) [M]⁺.

MS (CI, isobutane): *m/z* (%) = 287 (100) [M + H]⁺.

HRMS (ESI): Found 309.1098; calcd. for C₁₆H₁₉BNaO₂S 309.1091.

EA (%): Found C (66.94), H (6.86), S (11.34); calcd. for C₁₆H₁₉BO₂S C (67.15), H (6.69), S (11.20).

4,4,5,5-Tetramethyl-2-(5-(naphthalen-1-yl)thiophen-2-yl)-1,3,2-dioxaborolane (**2j**)

A solution of **1b** (373 mg, 1.00 mmol), 1-bromonaphthalene (**5j**; 207 mg, 1.00 mmol), Pd(OAc)₂ (2.3 mg, 1 mol%) and SPhos (8.2 mg, 2 mol%) in toluene (8 mL) was heated to 65 °C for 40 h. The reaction mixture was cooled to 20 °C, filtered through a short plug of silica (5 x 2 cm; eluent: ethyl acetate) and the volatiles were removed *in vacuo*. The black solid was purified by sublimation (90 °C, 2 x 10⁻² mbar) to obtain 307 mg (91 %) of a white solid.

¹H NMR (500 MHz, CDCl₃): δ = 8.25 – 8.22 (m, 1 H, Naph-*H*), 7.92 – 7.86 (m, 2 H, Naph-*H*), 7.73 (d, ³*J* = 3.5 Hz, 1 H, Tph-*H*), 7.59 (dd, ³*J* = 7.1 Hz, ⁴*J* = 1.1 Hz, 1 H, Naph-*H*), 7.54 – 7.47 (m, 3 H, Naph-*H*), 7.34 (d, ³*J* = 3.5 Hz, 1 H, Tph-*H*), 1.40 (s, 12 H, pin-CH₃) ppm.

¹³C NMR (126 MHz, CDCl₃): δ = 149.2 (Tph-C), 137.6 (Tph-CH), 134.0 (Naph-C), 132.6 (Naph-C), 131.8 (Naph-C), 129.1 (Tph-CH or Naph-CH), 128.7 (Tph-CH or Naph-CH), 128.4 (Tph-CH or Naph-CH), 128.2 (Tph-CH or Naph-CH), 126.6 (Naph-CH), 126.2 (Naph-CH), 125.9 (Naph-CH), 125.4 (Naph-CH), 84.3 (pin-C(CH₃)₂), 24.9 (pin-CH₃) ppm.³

¹¹B NMR (160 MHz, CDCl₃): δ = 29.0 ppm.

M.p.: 138 °C.

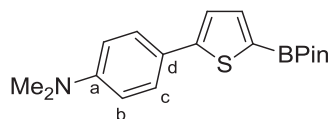
IR (ATR): $\tilde{\nu}$ = 2977 (w), 2926 (w), 1531 (m), 1475 (m), 1389 (m), 1371 (m), 1349 (s), 1331 (s), 1294 (m), 1262 (m), 1140 (s), 1063 (m), 1049 (m), 854 (m), 822 (m), 798 (s), 774 (s), 662 (s), 606 (m) cm⁻¹.

MS (EI, 70 eV): *m/z* (%) = 336 (100) [M]⁺.

MS (CI, isobutane): *m/z* (%) = 337 (100) [M + H]⁺.

HRMS (ESI): Found 359.1254; calcd. for C₂₀H₂₁BNaO₂S 359.1248.

EA (%): Found C (70.13), H (6.30), S (9.39); calcd. for C₂₀H₂₁BO₂S C (71.44), H (6.29), S (9.54).

***N,N*-Dimethyl-4-(5-(4,4,5,5-tetramethyl-1,3,2-dioxaborolan-2-yl)thiophen-2-yl)aniline (2k)**

A solution of **1b** (373 mg, 1.00 mmol), 4-bromo-*N,N*-dimethylaniline (**5k**; 200 mg, 1.00 mmol), Pd(OAc)₂ (2.3 mg, 1 mol%) and SPhos (8.2 mg, 2 mol%) in toluene (8 mL) was heated to 65 °C for 18 h. The reaction mixture was cooled to 20 °C, filtered through a short plug of silica (5 x 2 cm; eluent: ethyl acetate) and the volatiles were removed *in vacuo*. The raw-product was purified by sublimation (75 °C, 9 x 10⁻³ mbar) to obtain 123 mg (37 %) of a yellow solid.

¹H NMR (500 MHz, CDCl₃): δ = 7.56 (d, ³J = 3.6 Hz, 1 H, Tph-*H*), 7.54 (d, ³J = 8.9 Hz, 2 H, *H*-c), 7.23 (d, ³J = 3.6 Hz, 1 H, Tph-*H*), 6.73 (d, ³J = 8.9 Hz, 2 H, *H*-b), 2.99 (s, 6 H, N(CH₃)₂), 1.35 (s, 12 H, pin-CH₃) ppm.

¹³C NMR (126 MHz, CDCl₃): δ = 152.6 (*C*-d or Tph-*C*), 150.4 (*C*-a), 138.4 (Tph-CH), 127.3 (CH-c), 122.8 (*C*-d or Tph-*C*), 122.5 (Tph-CH), 112.6 (CH-b), 84.1 (pin-C(CH₃)₂), 40.6 (N(CH₃)₂), 24.9 (pin-CH₃) ppm.³

¹¹B NMR (160 MHz, CDCl₃): δ = 28.7 ppm.

M.p.: 110 °C.

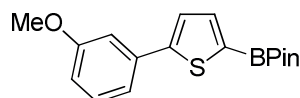
IR (ATR): $\tilde{\nu}$ = 2974 (m), 2928 (w), 1607 (m), 1535 (m), 1454 (s), 1443 (s), 1359 (s), 1299 (s), 1236 (m), 1208 (m), 1142 (s), 1071 (s), 1019 (m), 957 (m), 857 (m), 802 (s), 660 (s) cm⁻¹.

MS (EI, 70 eV): *m/z* (%) = 329 (100) [M]⁺.

MS (CI, isobutane): *m/z* (%) = 330 (96) [M + H]⁺, 329 (100) [M]⁺.

HRMS (ESI): Found 330.1693; calcd. for C₁₈H₂₅BNO₂S 330.1694.

EA (%): Found C (65.64), H (7.20), N (4.16), S (9.62); calcd. for C₁₈H₂₄BNO₂S C (65.66), H (7.35), N (4.25), S (9.74).

2-(5-(3-Methoxyphenyl)thiophen-2-yl)-4,4,5,5-tetramethyl-1,3,2-dioxaborolane (**2l**)

A solution of **1b** (746 mg, 2.00 mmol), 3-bromoanisole (**5l**; 374 mg, 2.00 mmol), Pd(OAc)₂ (4.5 mg, 1 mol%) and SPhos (16.4 mg, 2 mol%) in toluene (8 mL) was heated to 65 °C for 18 h. The reaction mixture was cooled to 20 °C, filtered through a short plug of silica (5 x 2 cm; eluent: ethyl acetate) and the volatiles were removed *in vacuo*. The brown oil was purified by column chromatography (gradient from *n*-pentane to EtOAc) to afford 560 mg (89 %) of a light blue oil.

¹H NMR (500 MHz, CDCl₃): δ = 7.58 (d, ³J = 3.6 Hz, 1 H, Tph-*H*), 7.36 (d, ³J = 3.6 Hz, 1 H, Tph-*H*), 7.28 (t, ³J = 6.9 Hz, 1 H, Ar-*H*), 7.24 (s, 1 H, Ar-*H*), 7.17 – 7.16 (m, 1 H, Ar-*H*), 6.85 – 6.82 (m, 1 H, Ar-*H*), 3.82 (s, 3 H, OCH₃), 1.34 (s, 12 H, pin-CH₃) ppm.

¹³C NMR (126 MHz, CDCl₃): δ = 160.1 (Ar-C-OCH₃), 151.3 (Tph-C), 138.2 (Tph-CH), 135.7 (Ar-C), 130.1 (Ar-CH), 124.8 (Tph-CH), 118.9 (Ar-CH), 113.8 (Ar-CH), 111.8 (Ar-CH), 84.3 (pin-C(CH₃)₂), 55.4 (OCH₃), 24.9 (pin-CH₃) ppm.³

¹¹B NMR (160 MHz, CDCl₃): δ = 29.0 ppm.

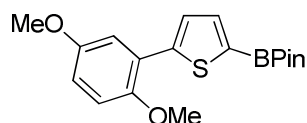
IR (ATR): $\tilde{\nu}$ = 2977 (w), 2935 (w), 1599 (w), 1578 (w), 1533 (m), 1460 (s), 1379 (m), 1351 (s), 1329 (s), 1298 (m), 1252 (m), 1211 (m), 1165 (m), 1139 (s), 1068 (m), 1022 (m), 957 (w), 852 (m), 812 (m), 774 (m), 685 (m), 663 (s) cm⁻¹.

MS (EI, 70 eV): *m/z* (%) = 316 (100) [M]⁺, 301 (7) [M – CH₃]⁺.

MS (CI, isobutane): *m/z* (%) = 317 (100) [M + H]⁺.

HRMS (ESI): Found 339.1206; calcd. for C₁₇H₂₁BNaO₃S 339.1197.

EA (%): Found C (64.49), H (6.51), S (10.19); calcd. for C₁₇H₂₁BO₃S C (64.57), H (6.69), S (10.14).

2-(5-(2,5-Dimethoxyphenyl)thiophen-2-yl)-4,4,5,5-tetramethyl-1,3,2-dioxaborolane (**2m**)

A solution of **1b** (373 mg, 1.00 mmol), 2-bromo-1,4-dimethoxybenzene (**5m**; 217 mg, 1.00 mmol), Pd(OAc)₂ (2.3 mg, 1 mol%) and SPhos (8.2 mg, 2 mol%) in toluene (8 mL) was heated to 65 °C for 18 h. The reaction mixture was cooled to 20 °C and filtered through a short plug of silica (5 x 2 cm; eluent: ethyl acetate). After removal of the volatiles, the blue oil was purified by column chromatography (gradient from *n*-hexane to EtOAc) to afford 230 mg (66 %) of a pale yellow oil that solidified upon standing.

¹H NMR (500 MHz, CDCl₃): δ = 7.62 (d, ³J = 3.7 Hz, 1 H, Tph-*H*), 7.58 (d, ³J = 3.7 Hz, 1 H, Tph-*H*), 7.24 (d, ⁴J = 3.0 Hz, 1 H, Ar-*H*), 6.92 (d, ³J = 8.9 Hz, 1 H, Ar-*H*), 6.83 (dd, ³J = 8.9, ⁴J = 3.0 Hz, 1 H, Ar-*H*), 3.88 (s, 3 H, OCH₃), 3.81 (s, 3 H, OCH₃), 1.37 (s, 12 H, pin-CH₃) ppm.

¹³C NMR (126 MHz, CDCl₃): δ = 153.8 (Ar-C), 150.5 (Ar-C), 146.5 (Tph-C), 137.2 (Tph-CH), 127.1 (Tph-CH), 124.1 (Ar-C), 114.2 (Ar-CH), 114.2 (Ar-CH), 113.3 (Ar-CH), 84.1 (pin-C(CH₃)₂), 56.4 (OCH₃), 55.9 (OCH₃), 24.9 (pin-CH₃) ppm.³

¹¹B NMR (160 MHz, CDCl₃): δ = 29.0 ppm.

M.p.: 92 °C.

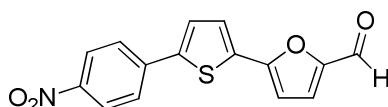
IR (ATR): $\tilde{\nu}$ = 3003 (w), 2973 2934 (w), 2834 (w), 1602 (w), 1526 (s), 1456 (s), 1435 (s), 1355 (s), 1331 (s), 1284 (s), 1272 (s), 1222 (s), 1139 (s), 1042 (s), 993 (m), 857 (m), 804 (s), 753 (m), 728 (m), 664 (s) cm⁻¹.

MS (EI, 70 eV): *m/z* (%) = 346 (100) [M]⁺.

MS (CI, isobutane): *m/z* (%) = 347 (100) [M + H]⁺.

HRMS (ESI): Found 369.1293; calcd. for C₁₈H₂₃BNaO₄S 369.1302.

EA (%): Found C (61.60), H (6.74), S (9.01); calcd. for C₁₈H₂₃BO₄S C (62.44), H (6.70), S (9.26).

5-(5-(4-Nitrophenyl)thiophen-2-yl)furan-2-carbaldehyde (3a)

A solution of **1b** (373 mg, 1.00 mmol), 1-bromo-4-nitrobenzene (**5a**; 202 mg, 1.00 mmol), Pd(OAc)₂ (2.3 mg, 1 mol%) and SPhos (8.2 mg, 2 mol%) in toluene (4 mL) was heated to 65 °C. After 18 h, a mixture of 5-bromo-2-furaldehyde (**5f**; 175 mg, 1.00 mmol) and K₃PO₄ (415 mg, 2.00 mmol) in degassed water (0.8 mL) and toluene (4 mL) was added. The reaction mixture was heated to 100 °C for 3 h, cooled to 20 °C and diluted with ethyl acetate (50 mL) before it was filtered through a short plug of silica (5 x 2 cm; eluent: ethyl acetate). After removal of the volatiles, the side-products were removed by sublimation (70 °C, 1 x 10⁻² mbar) to afford 250 mg (84 %) of a yellow-brown solid.

¹H NMR (600 MHz, CDCl₃): δ = 9.65 (s, 1 H, CHO), 8.27 (d, ³J = 8.9 Hz, 2 H, Ar-H), 7.76 (d, ³J = 8.9 Hz, 2 H, Ar-H), 7.54 (d, ³J = 3.9 Hz, 1 H, Tph-H), 7.47 (d, ³J = 3.9 Hz, 1 H, Tph-H), 7.32 (d, ³J = 3.7 Hz, 1 H, Fur-H), 6.76 (d, ³J = 3.7 Hz, 1 H, Fur-H) ppm.

¹³C NMR (151 MHz, CDCl₃): δ = 176.9 (CHO), 153.8 (Fur-C), 151.9 (Fur-C), 147.1 (Ar-C), 143.1 (Tph-C), 139.6 (Ar-C), 133.3 (Tph-C), 127.4 (Tph-CH), 126.7 (Tph-CH), 126.1 (Ar-CH), 124.6 (Ar-CH), 123.4* (Fur-CH), 108.5 (Fur-CH) ppm.

* broad signal.

M.p.: 191 °C.

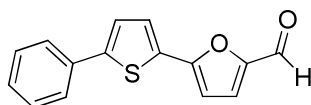
IR (ATR): $\tilde{\nu}$ = 3096 (w), 1668 (s), 1590 (s), 1538 (m), 1509 (s), 1480 (s), 1437 (m), 1394 (m), 1334 (s), 1274 (m), 1108 (m), 1024 (m), 955 (m), 851 (m), 803 (m), 778 (m), 747 (s), 686 (m), 658 (m) cm⁻¹.

MS (EI, 70 eV): *m/z* (%) = 299 (100) [M]⁺, 253 (12) [M-NO₂]⁺.

MS (CI, isobutane): *m/z* (%) = 300 (100) [M + H]⁺.

HRMS (ESI): Found 322.0158; calcd. for C₁₅H₉NNaO₄S 322.0144.

EA (%): Found C (59.04), H (3.04), N (4.64), S (10.87); calcd. for C₁₅H₉NO₄S C (60.19), H (3.03), N (4.68), S (10.71).

5-(5-Phenylthiophen-2-yl)furan-2-carbaldehyde (3b)

A solution of **1b** (373 mg, 1.00 mmol), bromobenzene (**5i**; 157 mg, 1.00 mmol), Pd(OAc)₂ (2.3 mg, 1 mol%) and SPhos (8.2 mg, 2 mol%) in toluene (4 mL) was heated to 65 °C. After 18 h, a mixture of 5-bromo-2-furaldehyde (**5f**; 175 mg, 1.00 mmol) and K₃PO₄ (415 mg, 2.00 mmol) in degassed water (0.8 mL) and toluene (4 mL) was added. The reaction mixture was heated to 100 °C for 3 h, cooled to 20 °C and diluted with ethyl acetate (50 mL) before it was filtered through a short plug of silica (5 x 2 cm; eluent: ethyl acetate). After removal of the volatiles, the crude product was purified by column chromatography (gradient from *n*-hexane to EtOAc) to obtain 192 mg (76 %) of a red solid.

¹H NMR (500 MHz, CDCl₃): δ = 9.61 (s, 1 H, CHO), 7.63 – 7.58 (m, 2 H, Ar-H), 7.47 (d, ³J = 3.9 Hz, 1 H, Tph-H), 7.43 – 7.37 (m, 2 H, Ar-H), 7.34 – 7.30 (m, 1 H, Ar-H), 7.29 (d, ³J = 3.9 Hz, 1 H, Tph-H), 7.28 (d, ³J = 3.7 Hz, 1 H, Fur-H), 6.67 (d, ³J = 3.7 Hz, 1 H, Fur-H) ppm.

¹³C NMR (126 MHz, CDCl₃): δ = 176.8 (CHO), 154.8 (Fur-C), 151.6 (Fur-C), 146.7 (Tph-C), 133.5 (Ar-C), 130.6 (Tph-C), 129.2 (Ar-CH), 128.4 (Ar-CH), 127.3 (Tph-CH), 125.9 (Ar-CH), 124.2 (Tph-CH), 123.9* (Fur-CH), 107.6 (Fur-CH) ppm.

* broad signal.

M.p.: 117 °C.

IR (ATR): $\tilde{\nu}$ = 2806 (w), 1663 (s), 1579 (m), 1538 (m), 1509 (m), 1478 (m), 1443 (m), 1389 (m), 1260 (m), 1236 (m), 1193 (m), 1019 (s), 952 (m), 791 (s), 754 (s), 687 (s), 584 (m) cm^{-1} .

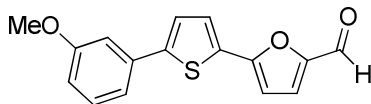
MS (EI, 70 eV): m/z (%) = 254 (100) $[\text{M}]^+$.

MS (CI, isobutane): m/z (%) = 255 (100) $[\text{M} + \text{H}]^+$.

HRMS (ESI): Found 277.0302; calcd. for $\text{C}_{15}\text{H}_{10}\text{NaO}_2\text{S}$ 277.0294.

EA (%): Found C (71.65), H (3.94), S (12.92); calcd. for $\text{C}_{15}\text{H}_{10}\text{O}_2\text{S}$ C (70.84), H (3.96), S (12.61).

5-(5-(3-Methoxyphenyl)thiophen-2-yl)furan-2-carbaldehyde (**3c**)



A solution of **1b** (373 mg, 1.00 mmol), 3-bromoanisole (**5i**; 187 mg, 1.00 mmol), $\text{Pd}(\text{OAc})_2$ (2.3 mg, 1 mol%) and SPhos (8.2 mg, 2 mol%) in toluene (4 mL) was heated to 65 °C. After 18 h, a mixture of 5-bromo-2-furaldehyde (**5f**; 175 mg, 1.00 mmol) and K_3PO_4 (415 mg, 2.00 mmol) in degassed water (0.8 mL) and toluene (4 mL) was added. The reaction mixture was heated to 100 °C for 3 h, cooled to 20 °C and diluted with ethyl acetate (50 mL) before it was filtered through a short plug of silica (5 x 2 cm; eluent: ethyl acetate). After removal of the volatiles, the crude product was purified by column chromatography (gradient from *n*-hexane to EtOAc) to afford 199 mg (70 %) of a yellow oil that solidified upon standing.

¹H NMR (500 MHz, CDCl_3): δ = 9.60 (s, 1 H, CHO), 7.46 (d, 3J = 3.9 Hz, 1 H, Tph-*H*), 7.33 – 7.29* (m, 1 H, Ar-*H*), 7.29* (d, 3J = 3.9 Hz, 1 H, Tph-*H*), 7.28* (d, 3J = 3.7 Hz, 1 H, Fur-*H*), 7.22 – 7.19 (m, 1 H, Ar-*H*), 7.15 – 7.12 (m, 1 H, Ar-*H*), 6.89 – 6.85 (m, 1 H, Ar-*H*), 6.67 (d, 3J = 3.7 Hz, 1 H, Fur-*H*), 3.85 (s, 3 H, OCH_3) ppm.

¹³C NMR (126 MHz, CDCl_3): δ = 176.8 (CHO), 160.2 (Ar-C- OCH_3), 154.8 (Fur-C), 151.6 (Fur-C), 146.6 (Ar-C or Tph-C or Fur-C), 134.8 (Ar-C or Tph-C or Fur-C), 130.7 (Ar-C or Tph-C or Fur-C), 130.2 (Ar-CH), 127.2 (Tph-CH), 124.4 (Tph-C or Fur-CH), 123.8* (Tph-C or Fur-CH), 118.5 (Ar-CH), 114.0 (Ar-CH), 111.6 (Ar-CH), 107.6 (Fur-CH), 55.5 (OCH_3) ppm.

* broad signal.

M.p.: 91 °C.

IR (ATR): $\tilde{\nu}$ = 2920 (w), 2837 (w), 1653 (s), 1576 (m), 1535 (m), 1507 (m), 1471 (m), 1431 (m), 1393 (m), 1288 (m), 1262 (m), 1218 (m), 1168 (m), 1050 (m), 1021 (s), 956 (m), 856 (m), 787 (m), 760 (s), 680 (s) cm^{-1} .

MS (EI, 70 eV): m/z (%) = 284 (100) $[\text{M}]^+$.

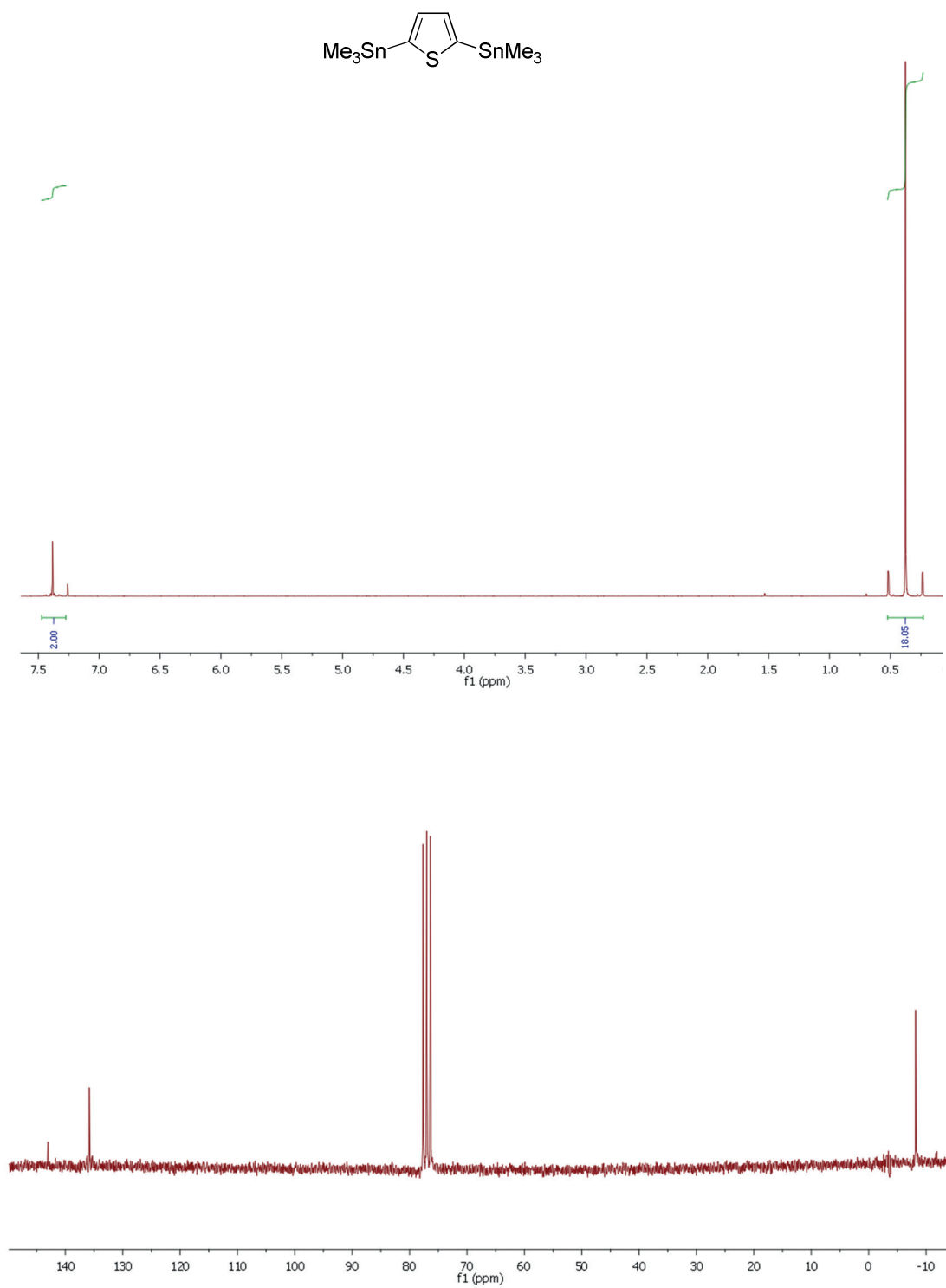
MS (CI, isobutane): m/z (%) = 285 (100) $[\text{M} + \text{H}]^+$.

HRMS (ESI): Found 307.0402; calcd. for $\text{C}_{16}\text{H}_{12}\text{NaO}_3\text{S}$ 307.0399.

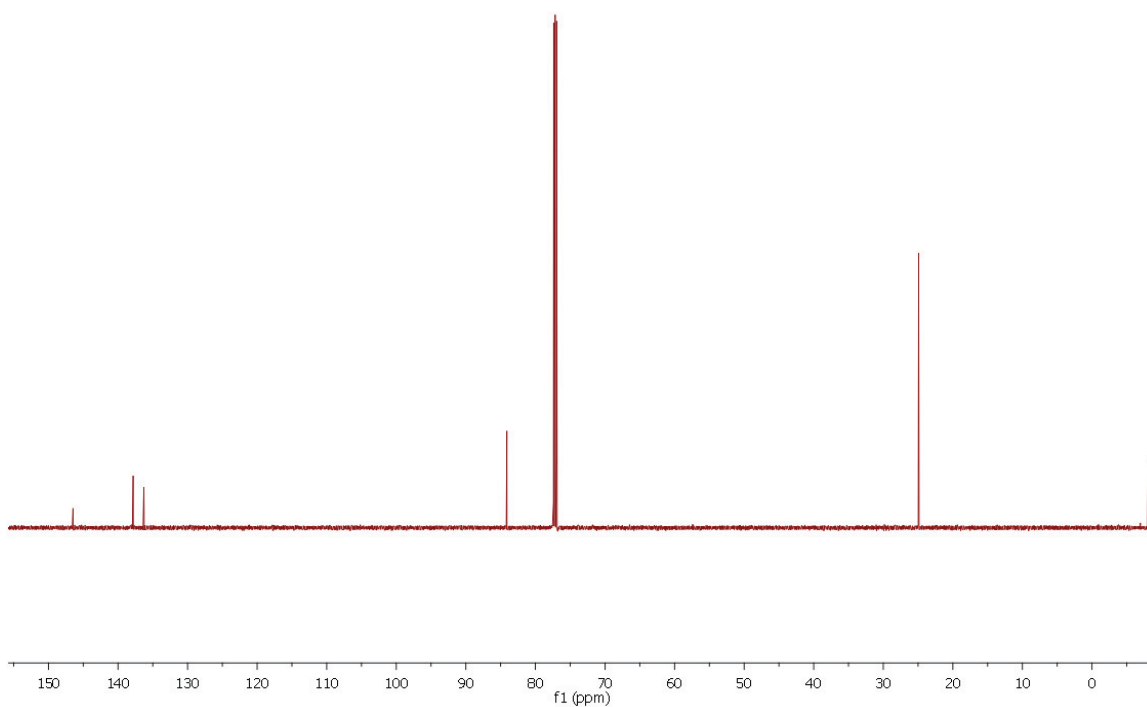
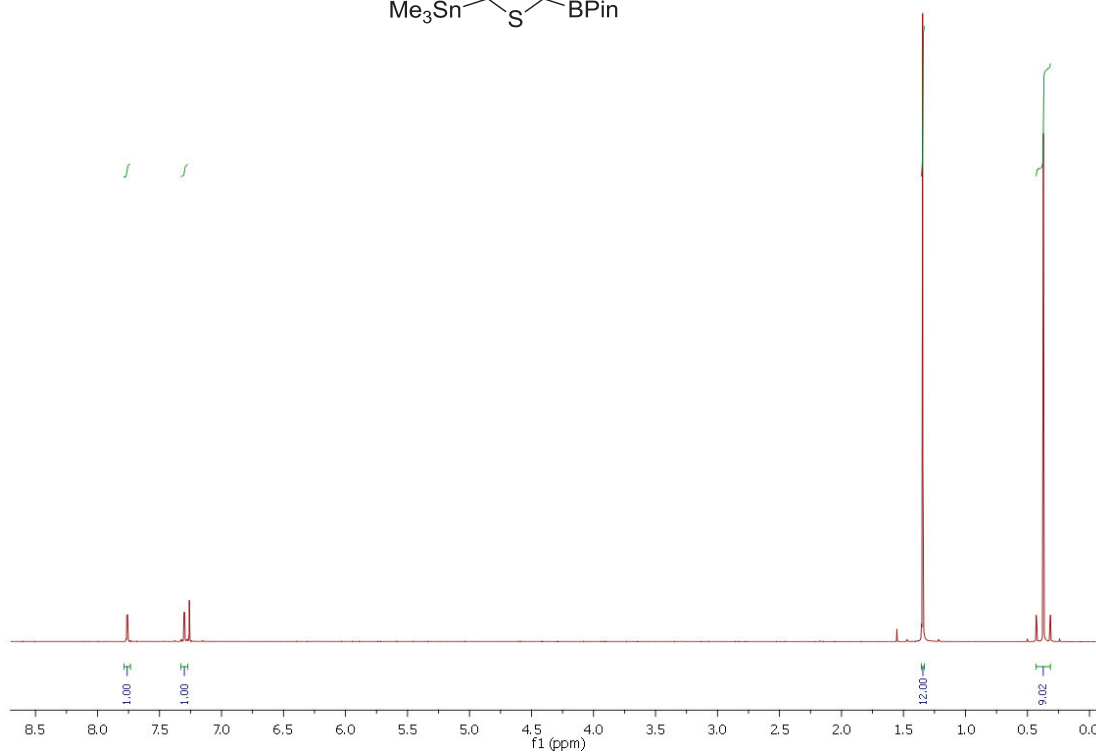
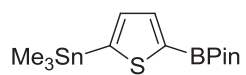
EA (%): Found C (67.07), H (4.25), S (11.26); calcd. for $\text{C}_{16}\text{H}_{12}\text{O}_3\text{S}$ C (67.59), H (4.25), S (11.28).

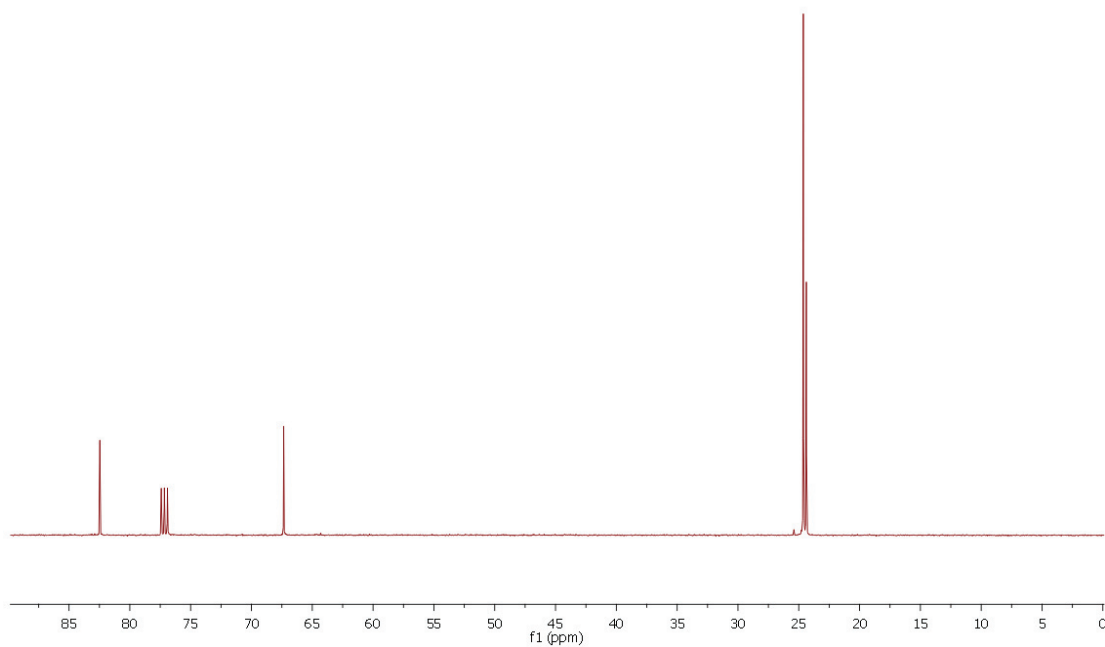
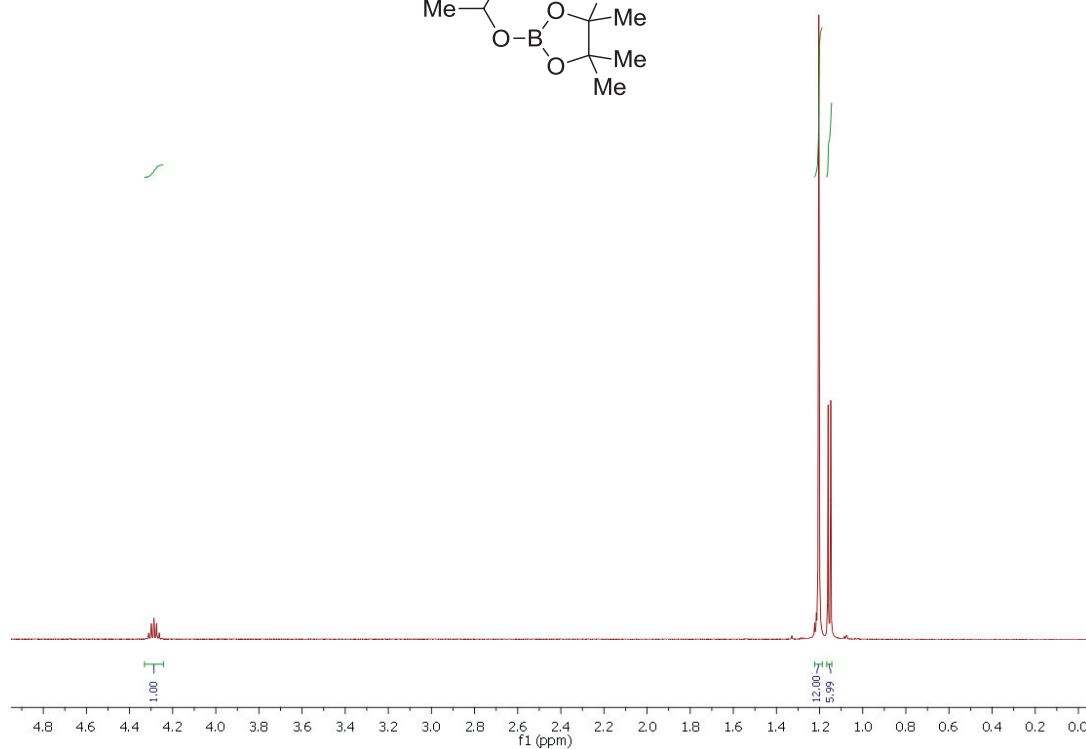
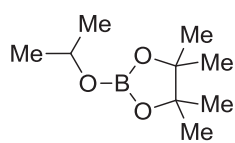
NMR Spectra

2,5-bis(trimethylstannyl)thiophene (4)

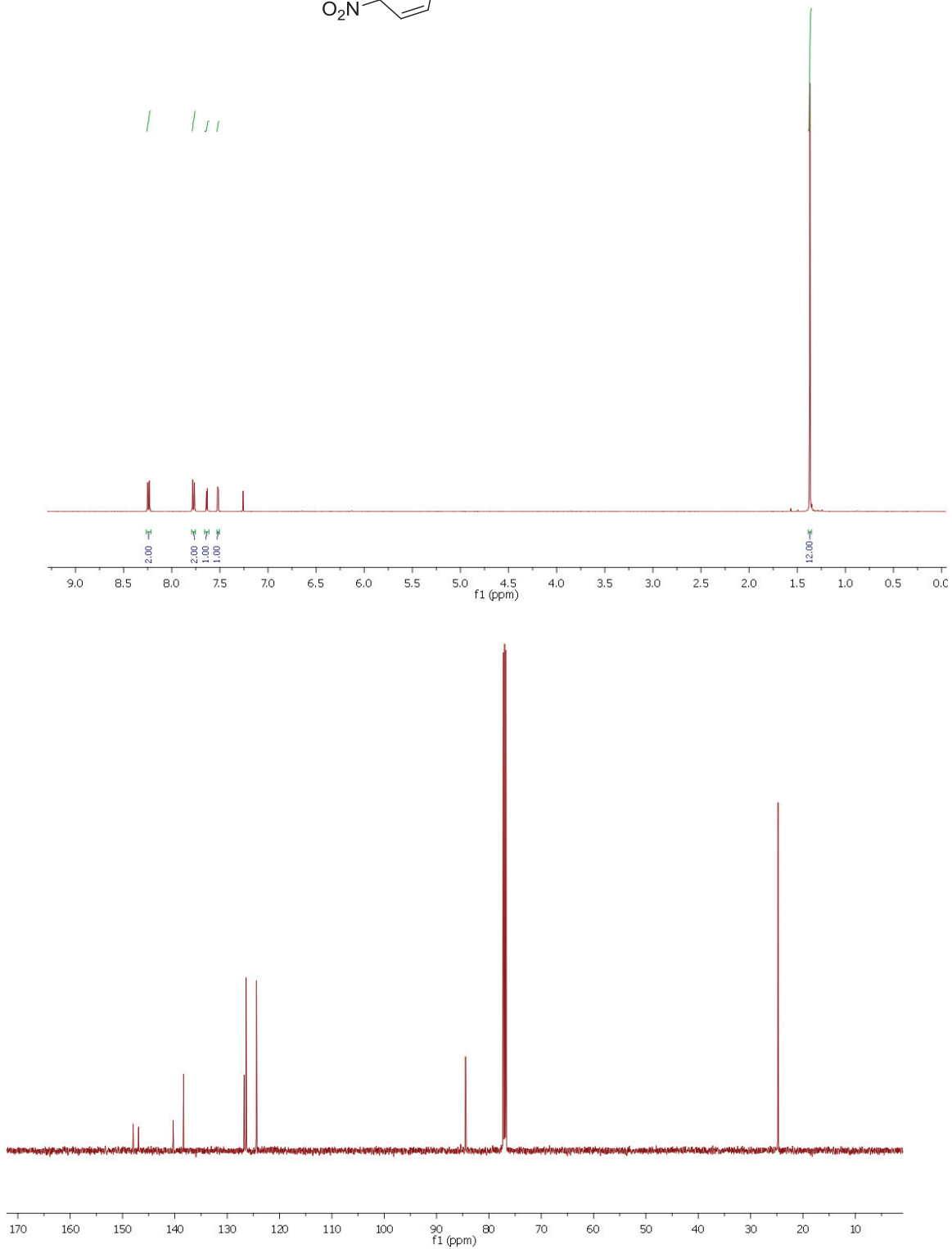
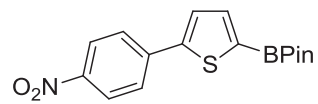


4,4,5,5-Tetramethyl-2-(5-(trimethylstannyl)thiophen-2-yl)-1,3,2-dioxaborolane (1b)

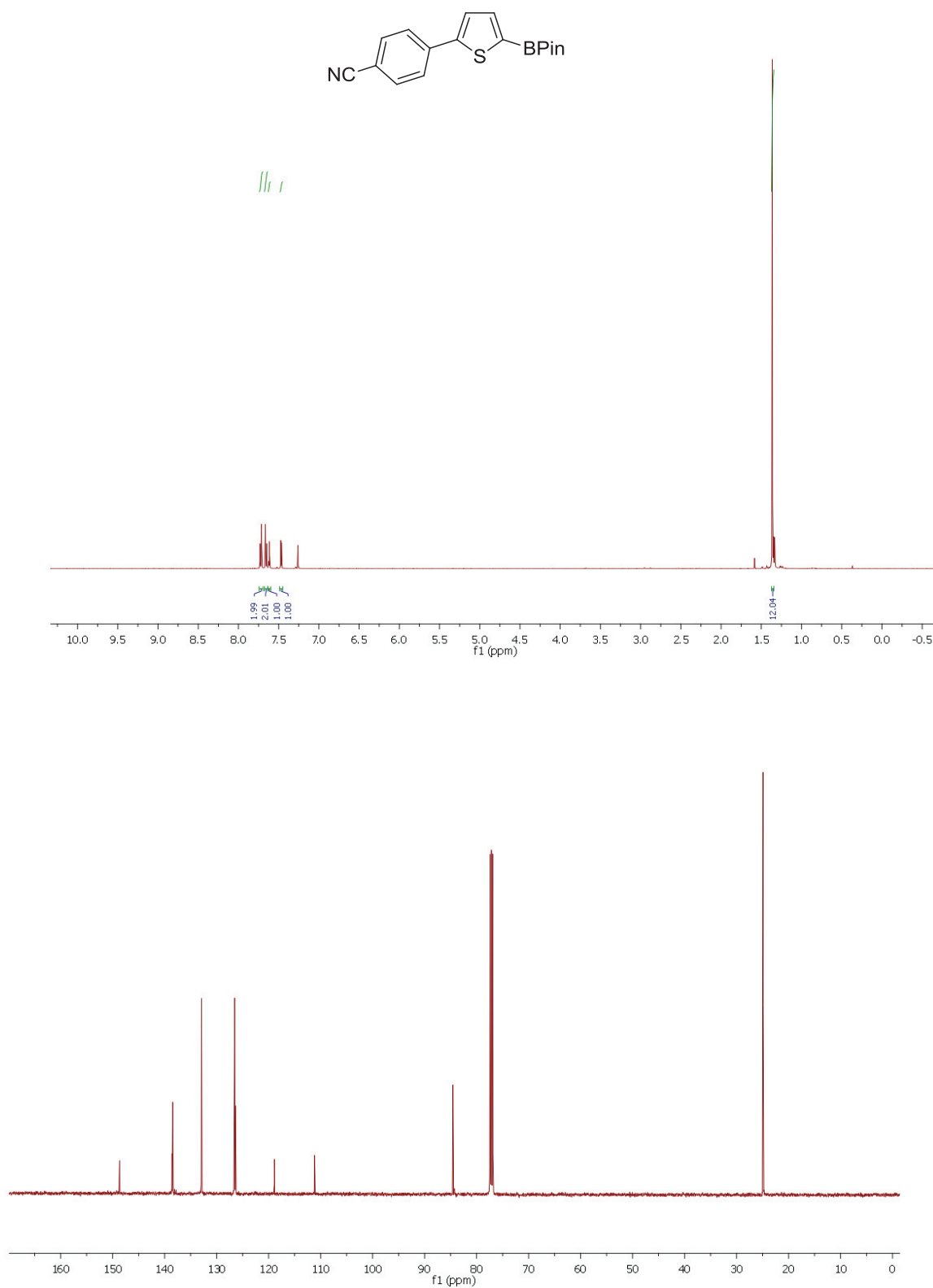


2-Isopropoxy-4,4,5,5-tetramethyl-1,3,2-dioxaborolane (*i*PrO-BPin)

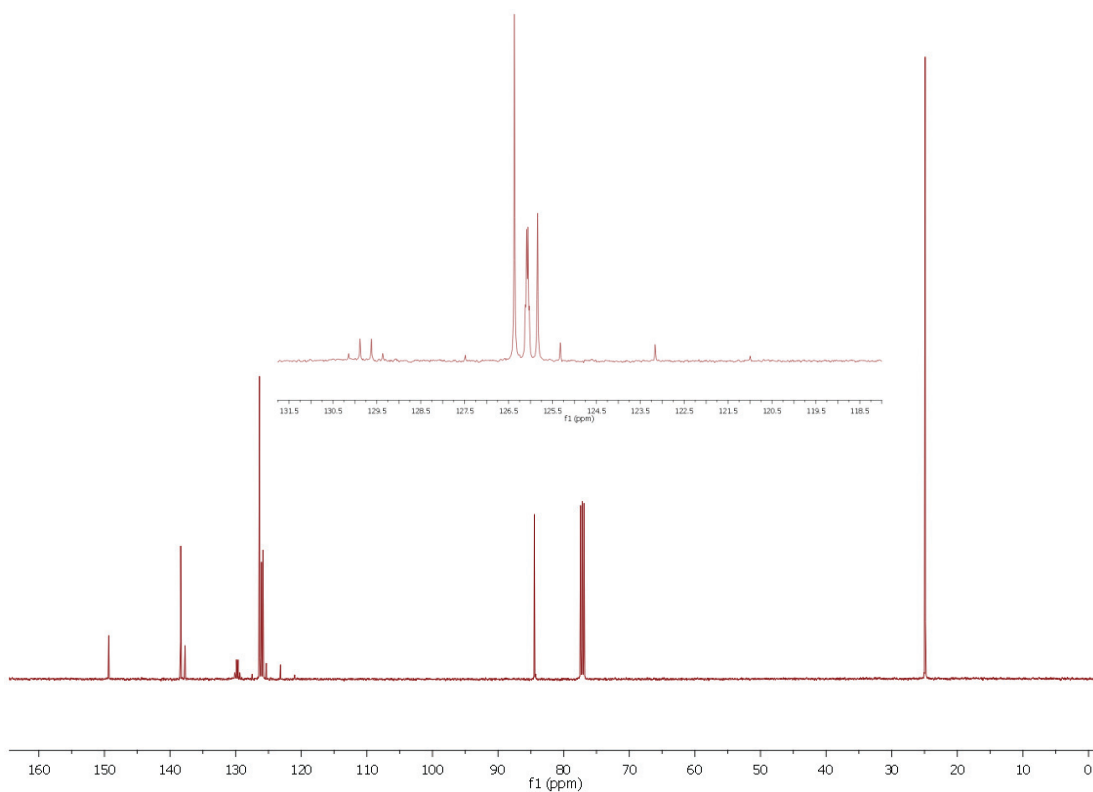
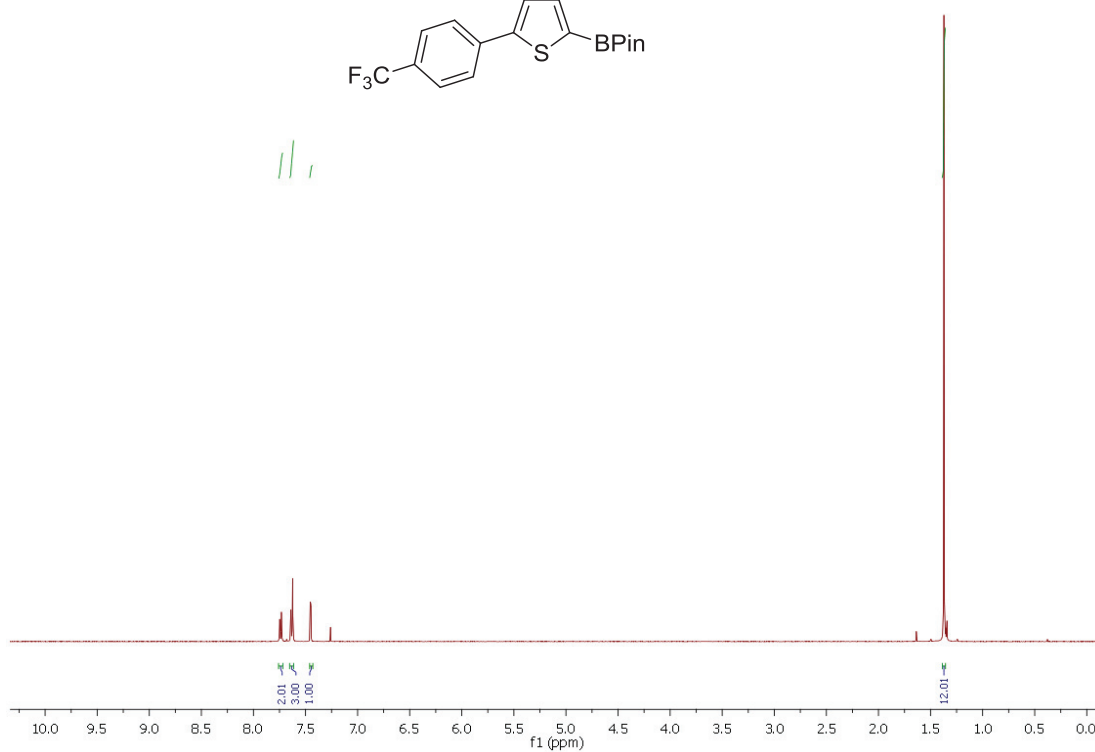
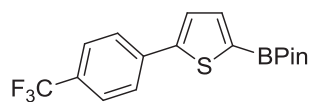
4,4,5,5-Tetramethyl-2-(5-(4-nitrophenyl)thiophen-2-yl)-1,3,2-dioxaborolane (2a)



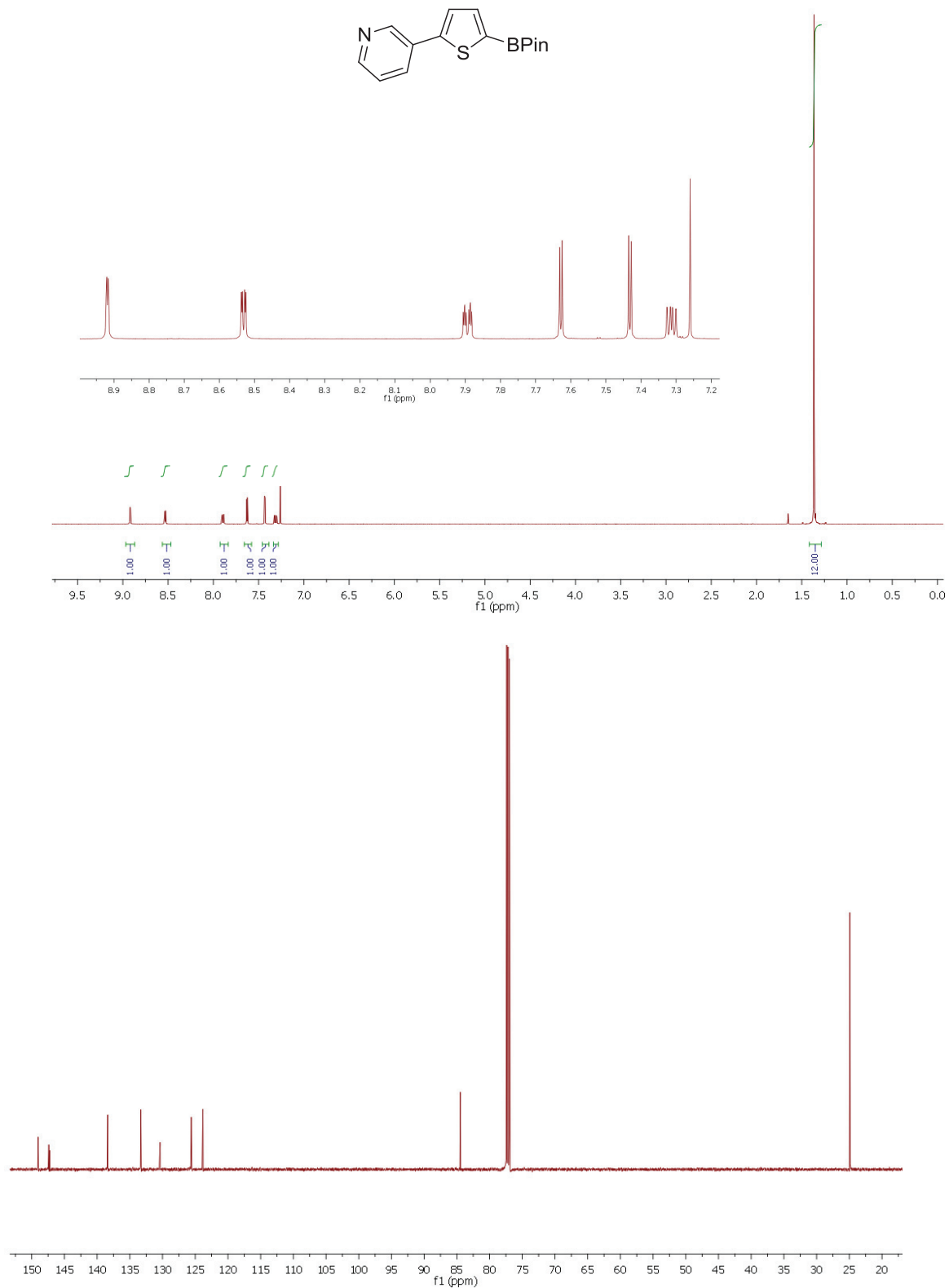
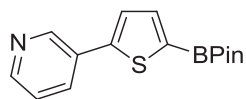
4,4,5,5-Tetramethyl-2-(5-(4-benzonitrile)thiophen-2-yl)-1,3,2-dioxaborolane (2b)



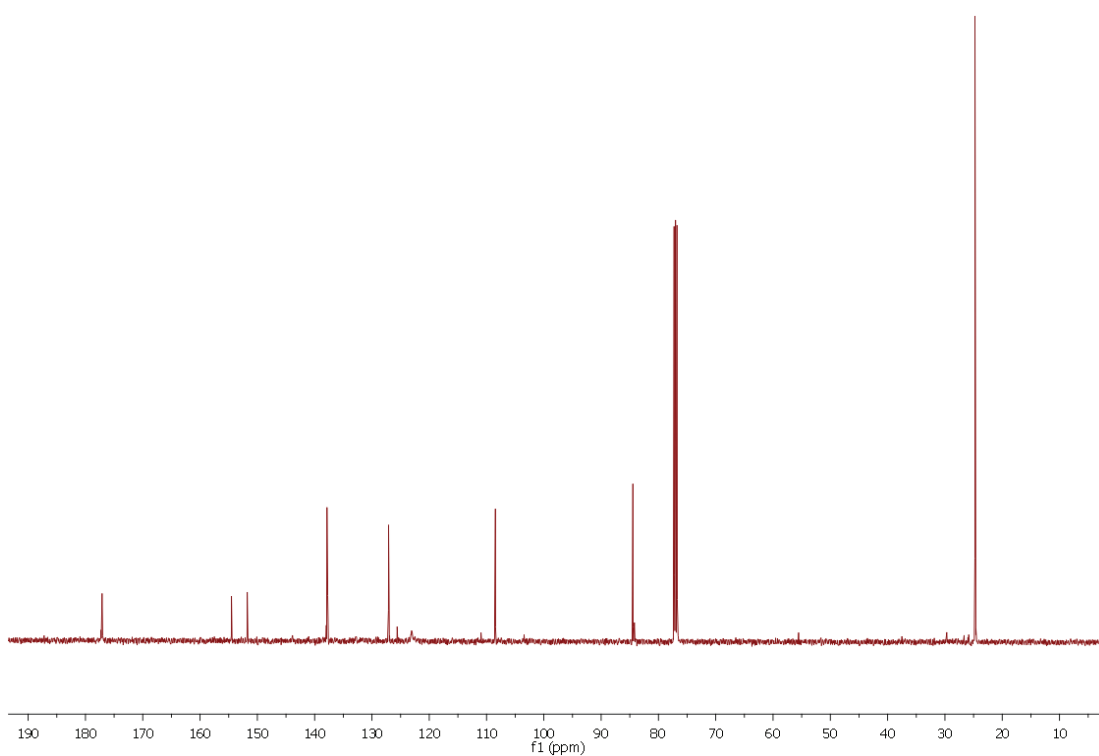
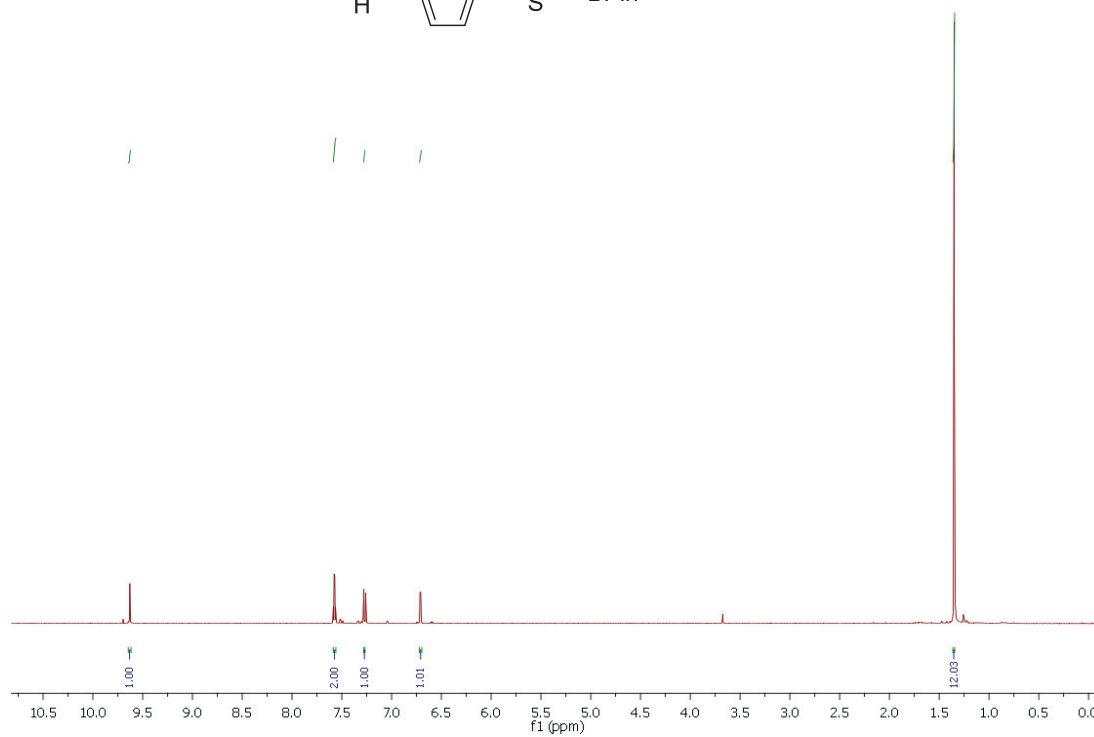
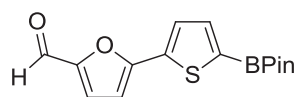
4,4,5,5-Tetramethyl-2-(5-(4-(trifluoromethyl)phenyl)thiophen-2-yl)-1,3,2-dioxaborolane (2c)

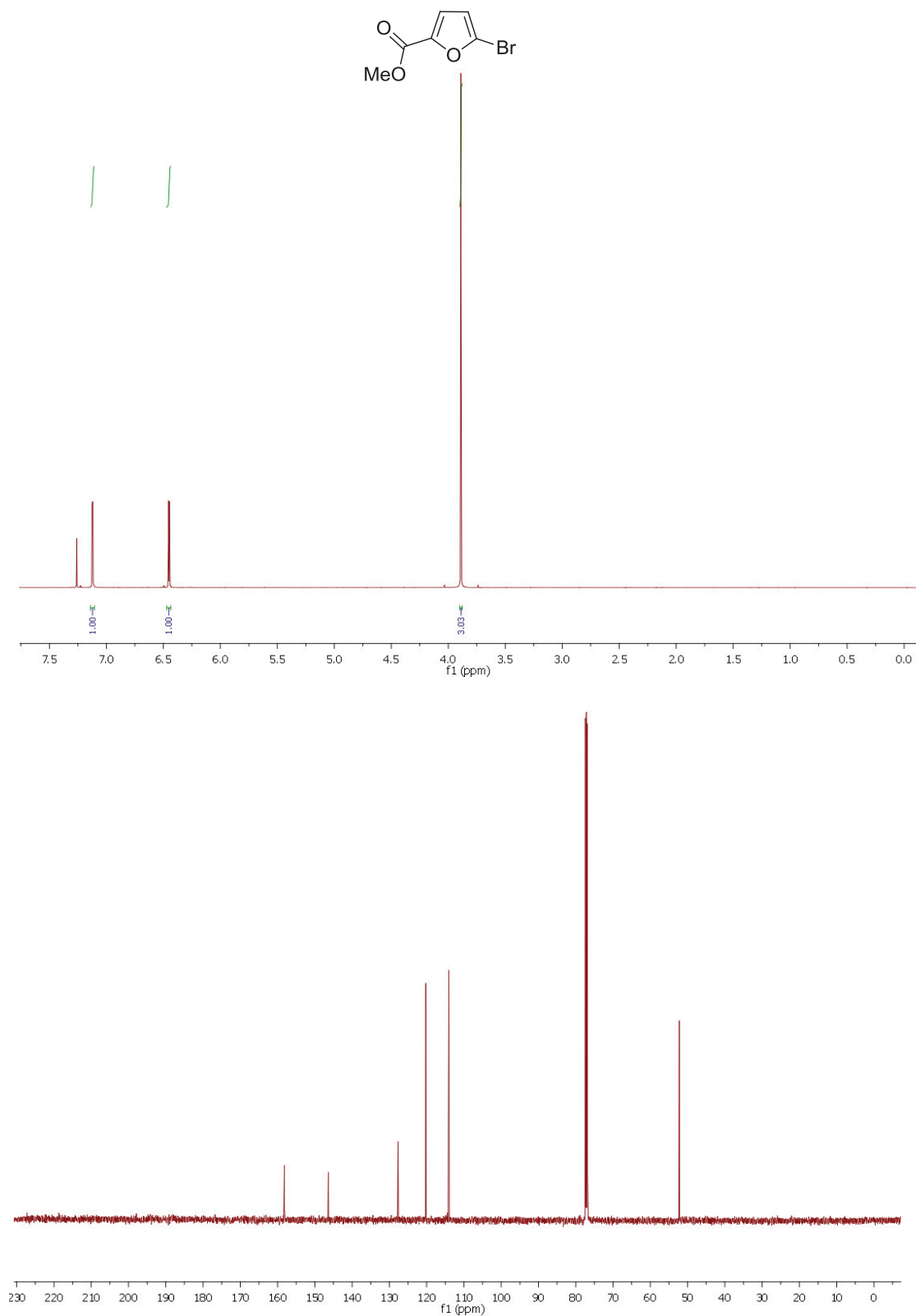


3-(5-(4,4,5,5-Tetramethyl-1,3,2-dioxaborolan-2-yl)thiophen-2-yl)pyridine (2e)

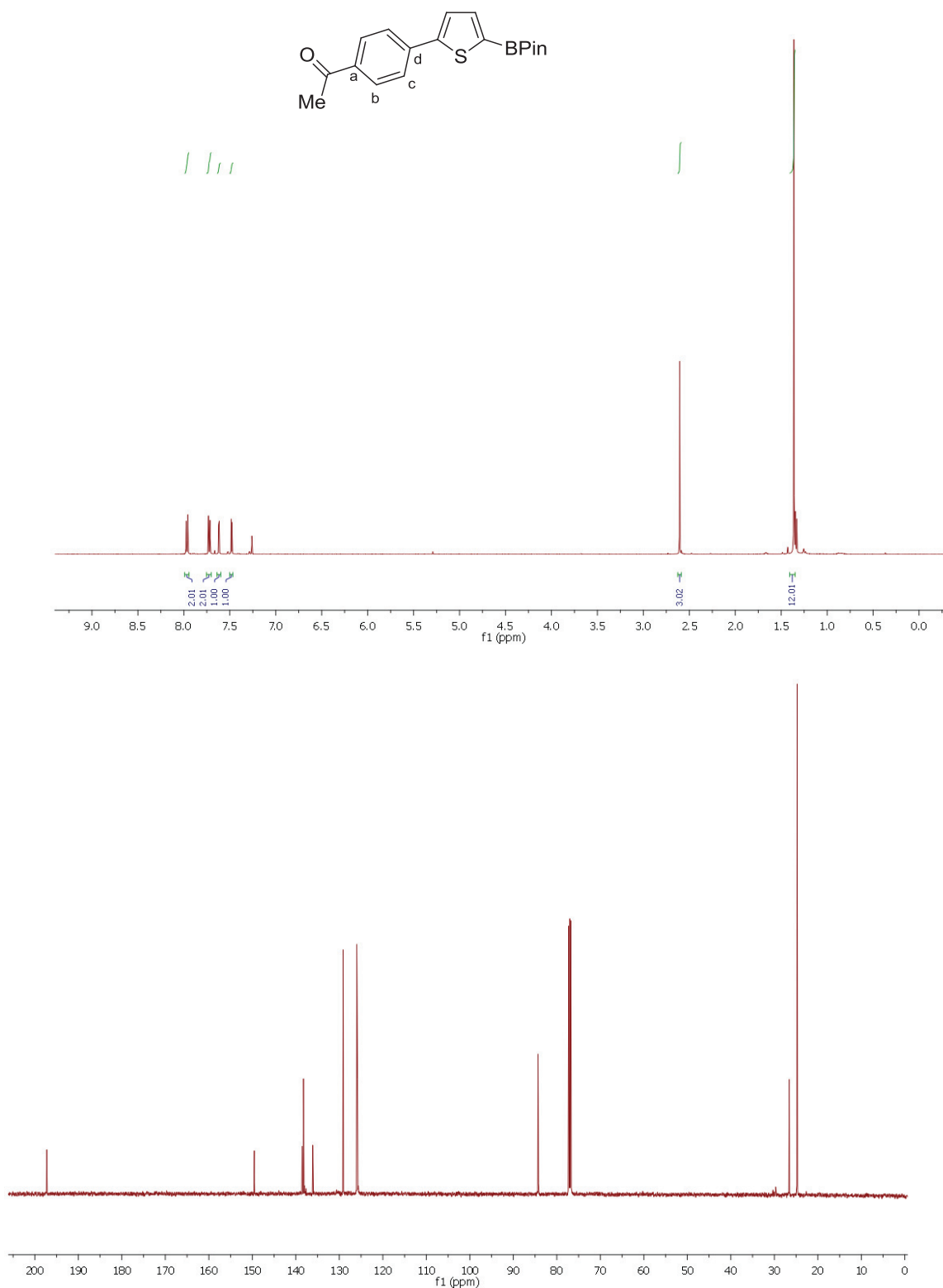


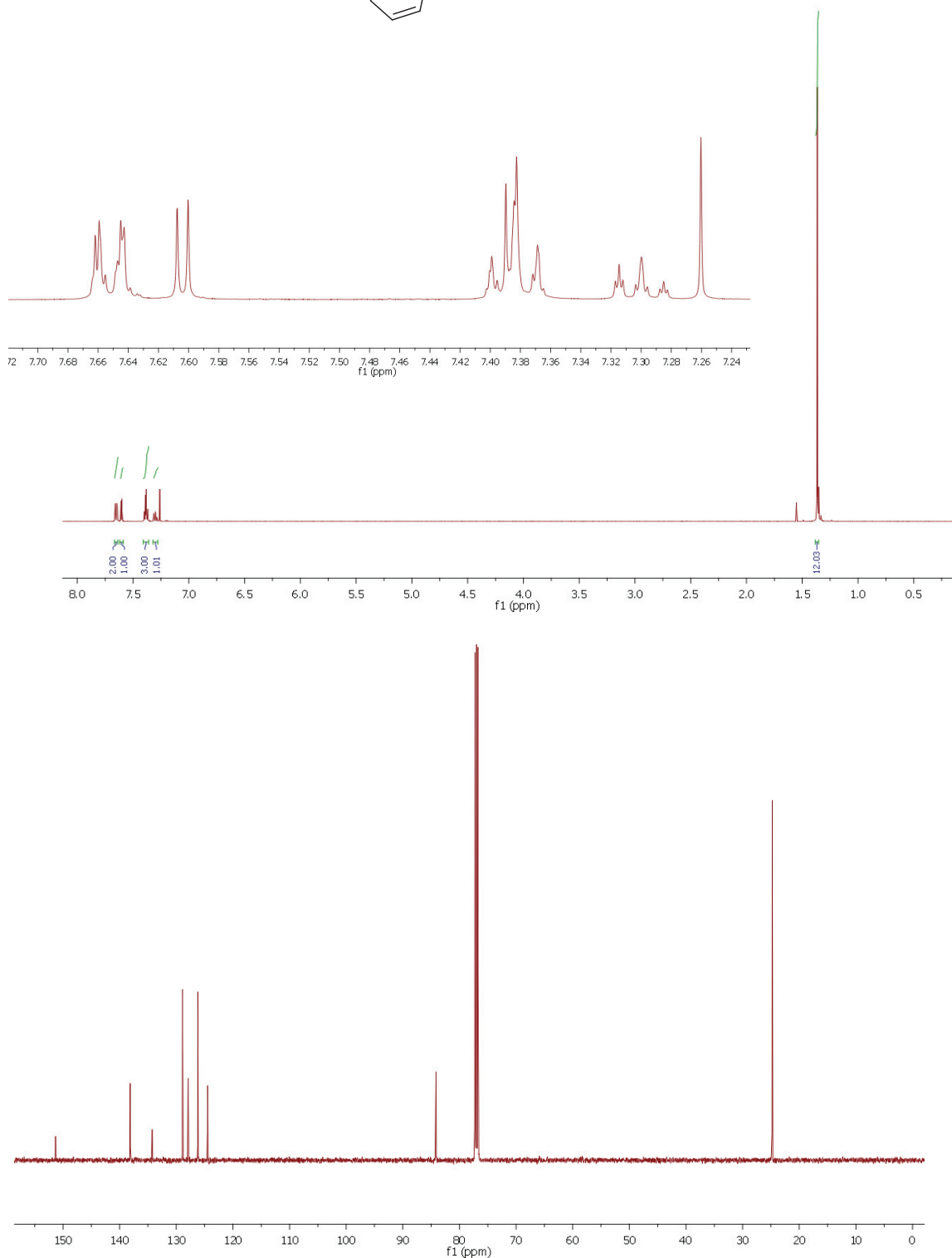
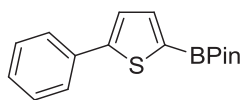
5-(5-(4,4,5,5-Tetramethyl-1,3,2-dioxaborolan-2-yl)thiophen-2-yl)furan-2-carbaldehyde (2f)



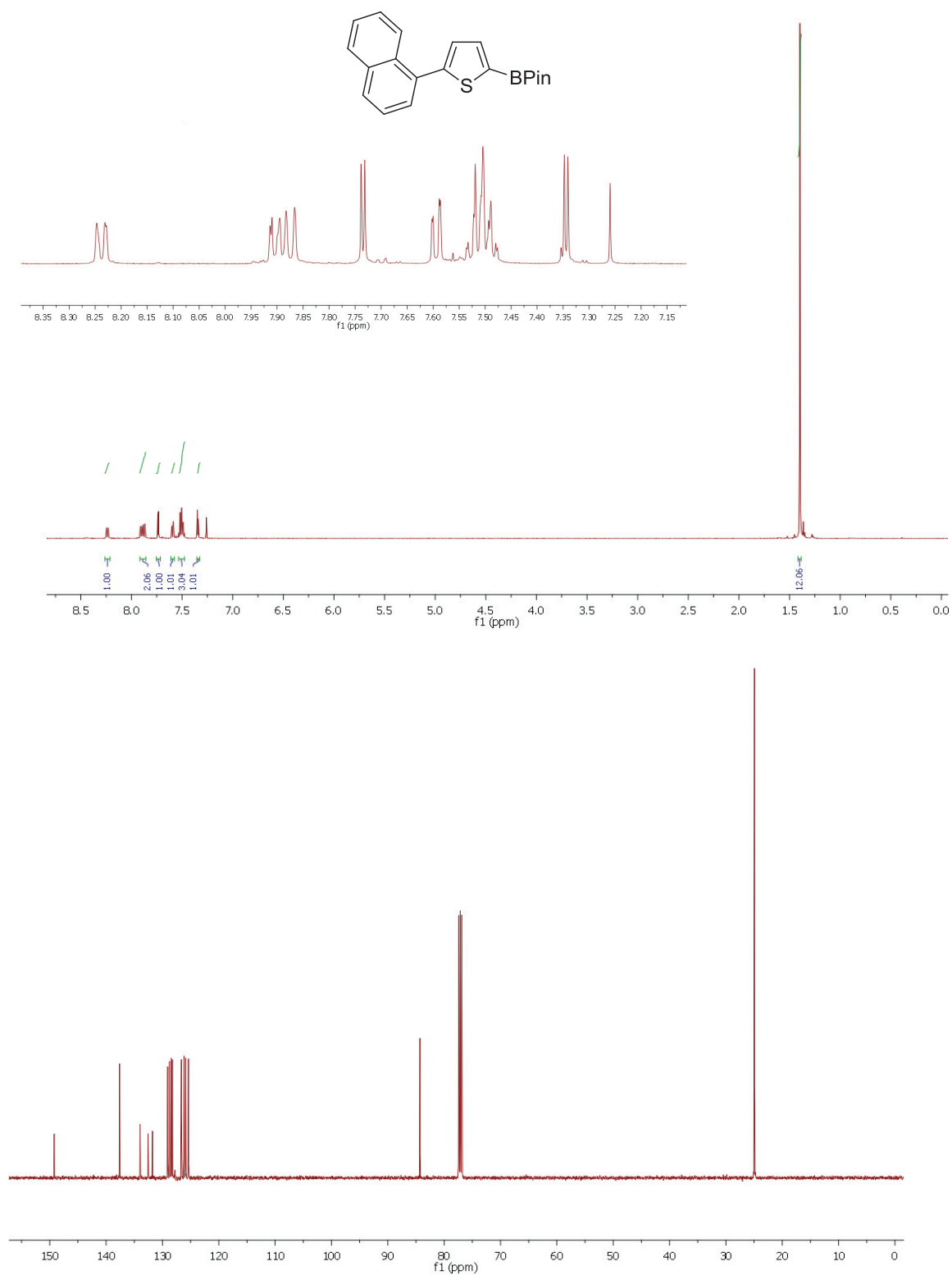
5-Bromo-2-furoic acid methyl ester (5g)

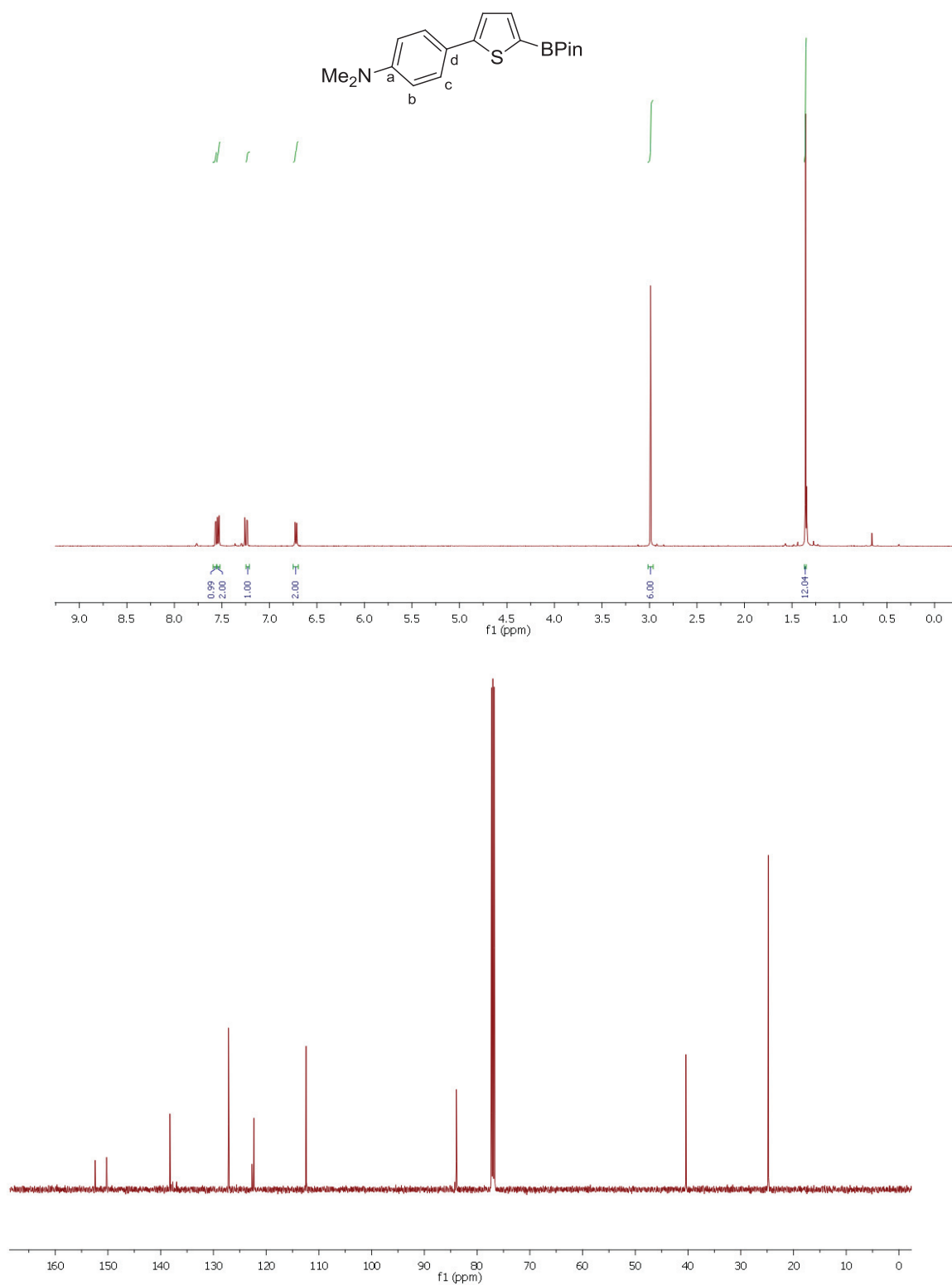
1-(4-(5-(4,4,5,5-Tetramethyl-1,3,2-dioxaborolan-2-yl)thiophen-2-yl)phenyl)ethanone (2h)



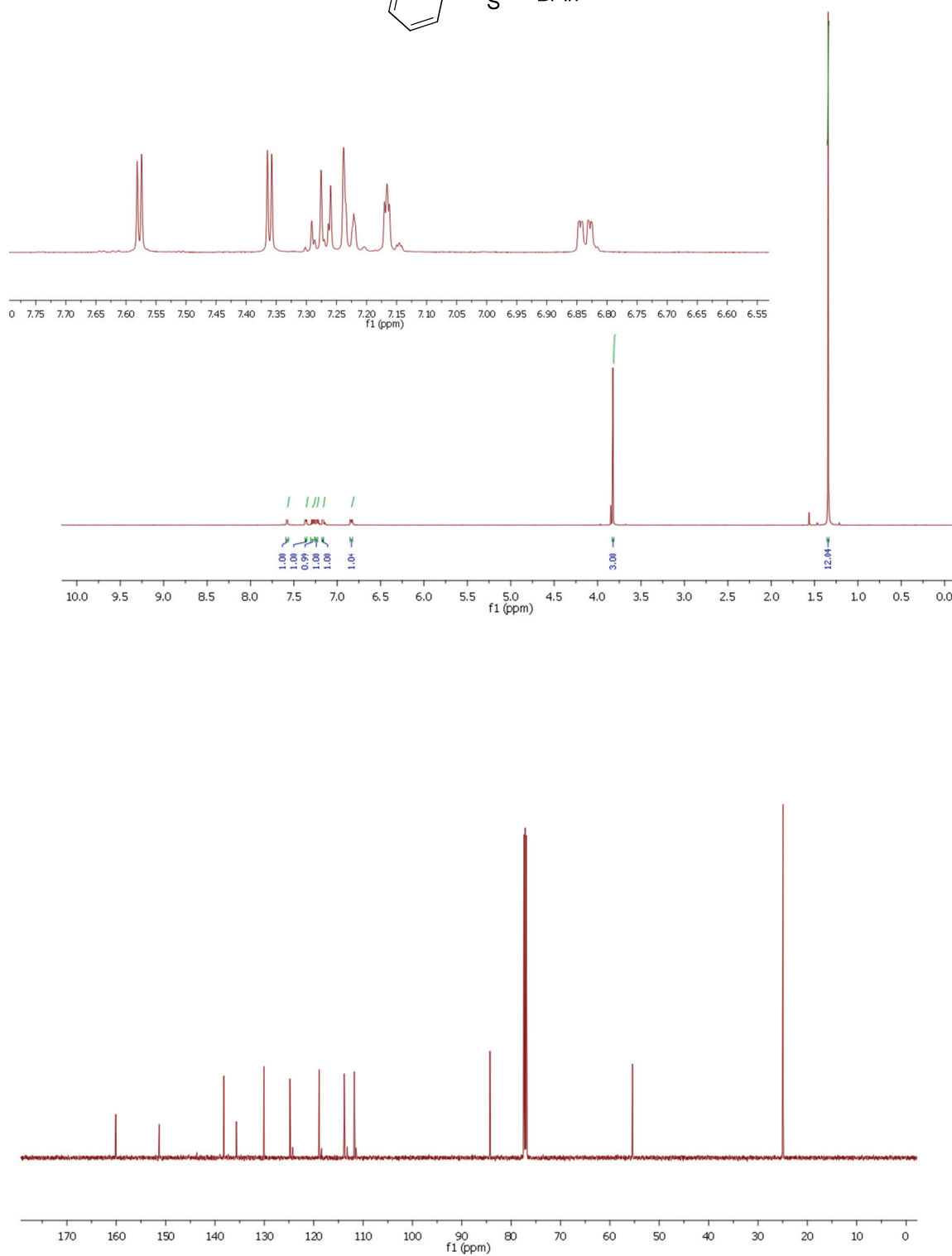
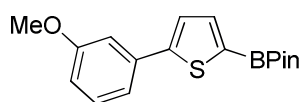
4,4,5,5-Tetramethyl-2-(5-phenylthiophen-2-yl)-1,3,2-dioxaborolane (2i)

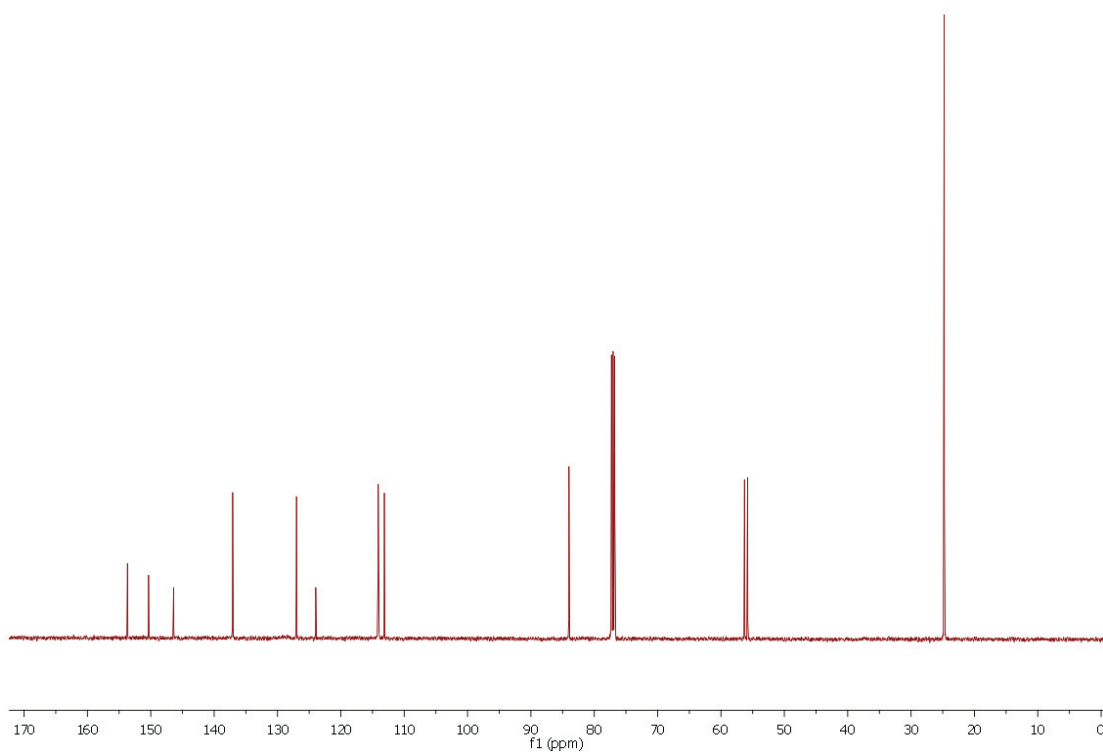
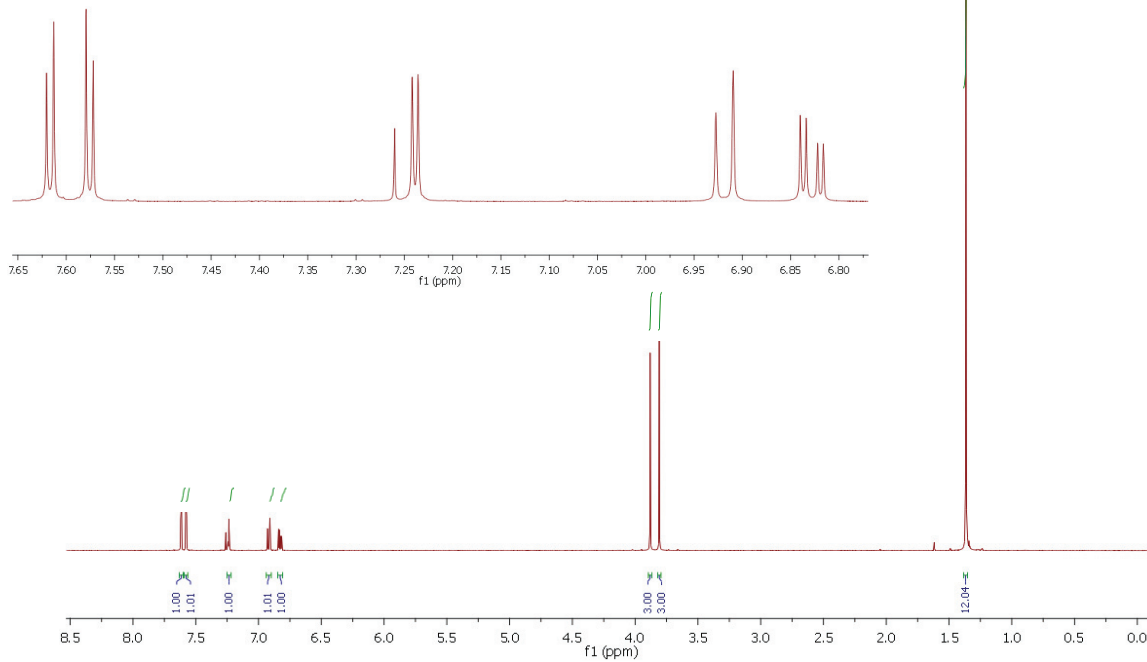
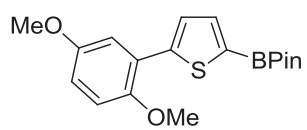
4,4,5,5-Tetramethyl-2-(5-(naphthalen-1-yl)thiophen-2-yl)-1,3,2-dioxaborolane (2j)



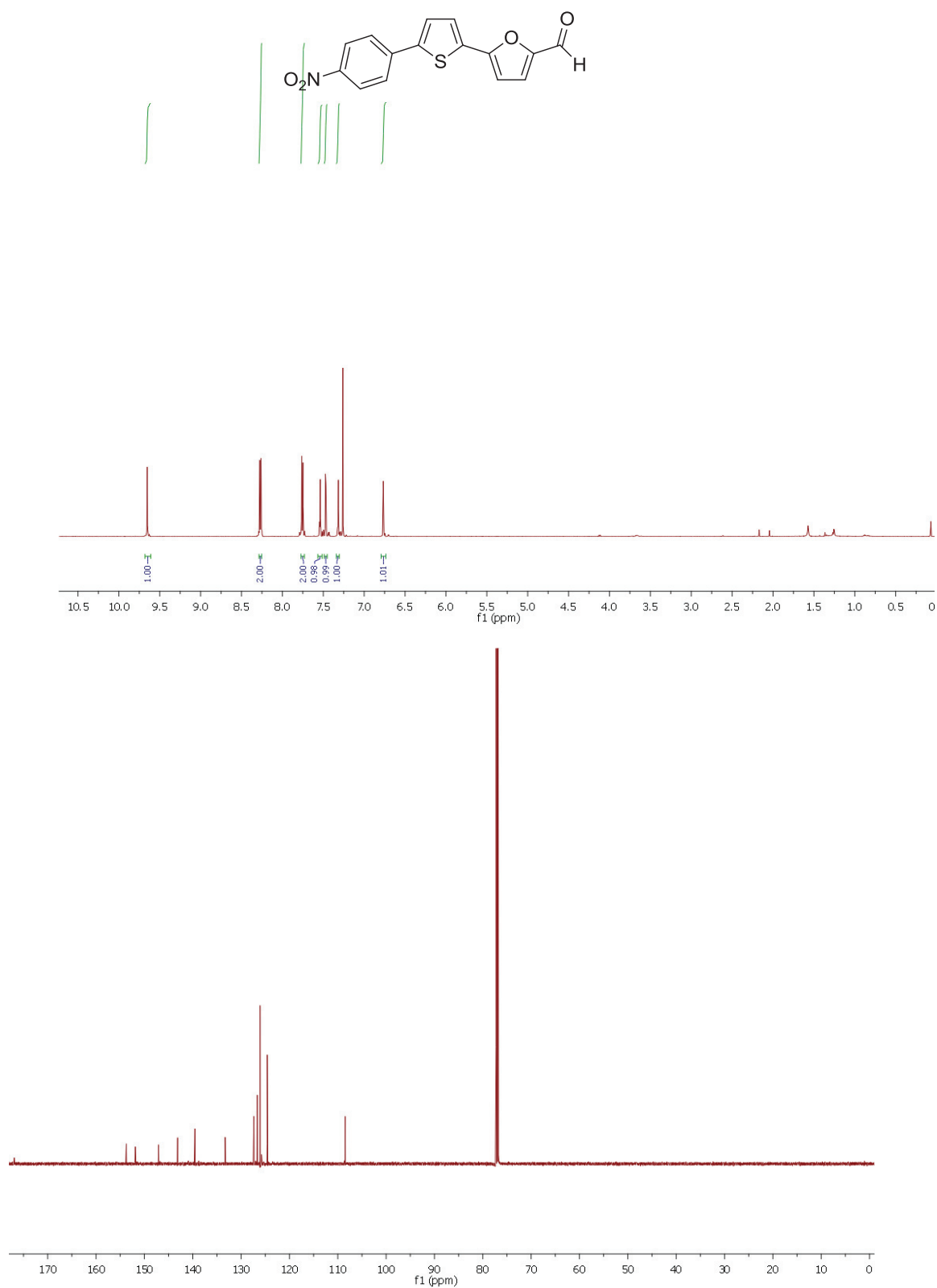
N,N-Dimethyl-4-(5-(4,4,5,5-tetramethyl-1,3,2-dioxaborolan-2-yl)thiophen-2-yl)aniline (2k)

2-(5-(3-Methoxyphenyl)thiophen-2-yl)-4,4,5,5-tetramethyl-1,3,2-dioxaborolane (21)

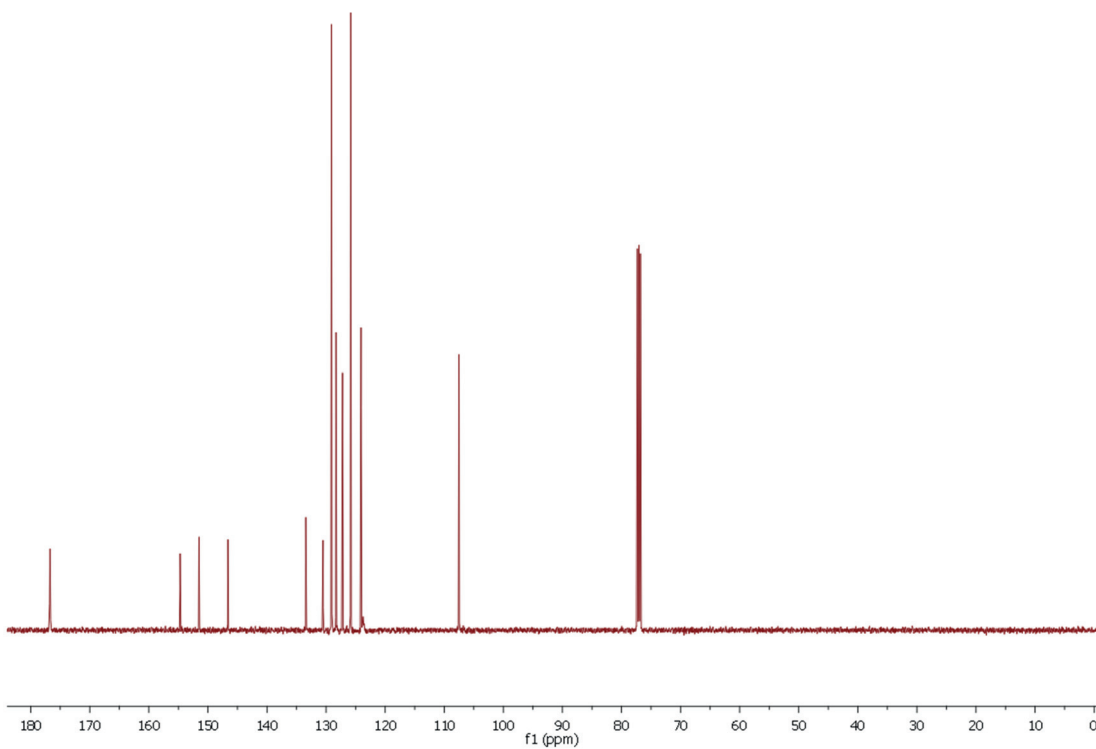
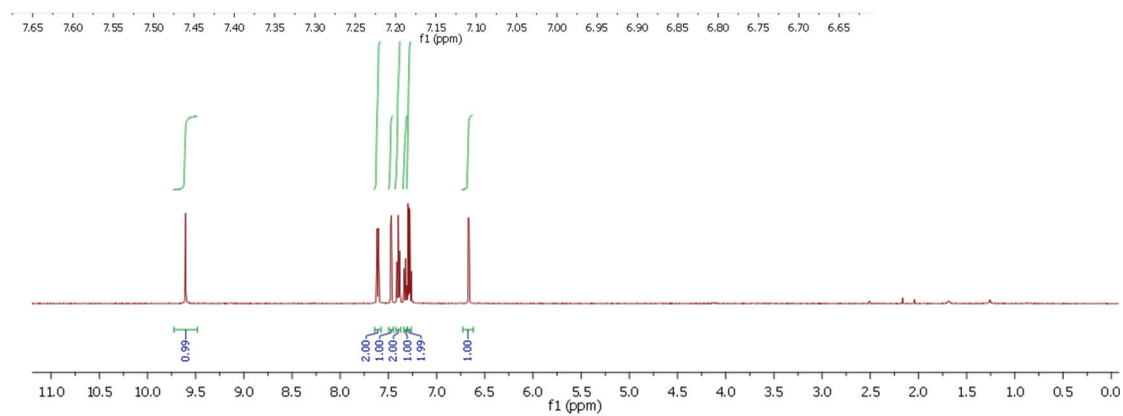
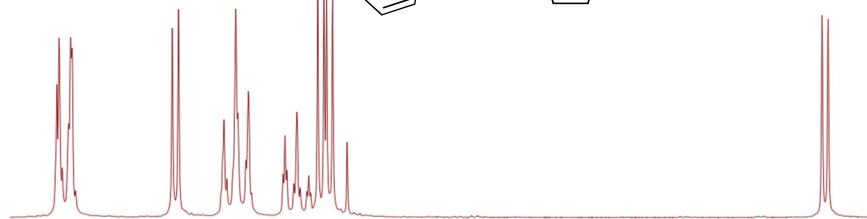
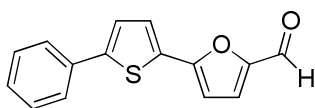


2-(5-(2,5-Dimethoxyphenyl)thiophen-2-yl)-4,4,5,5-tetramethyl-1,3,2-dioxaborolane (2m)

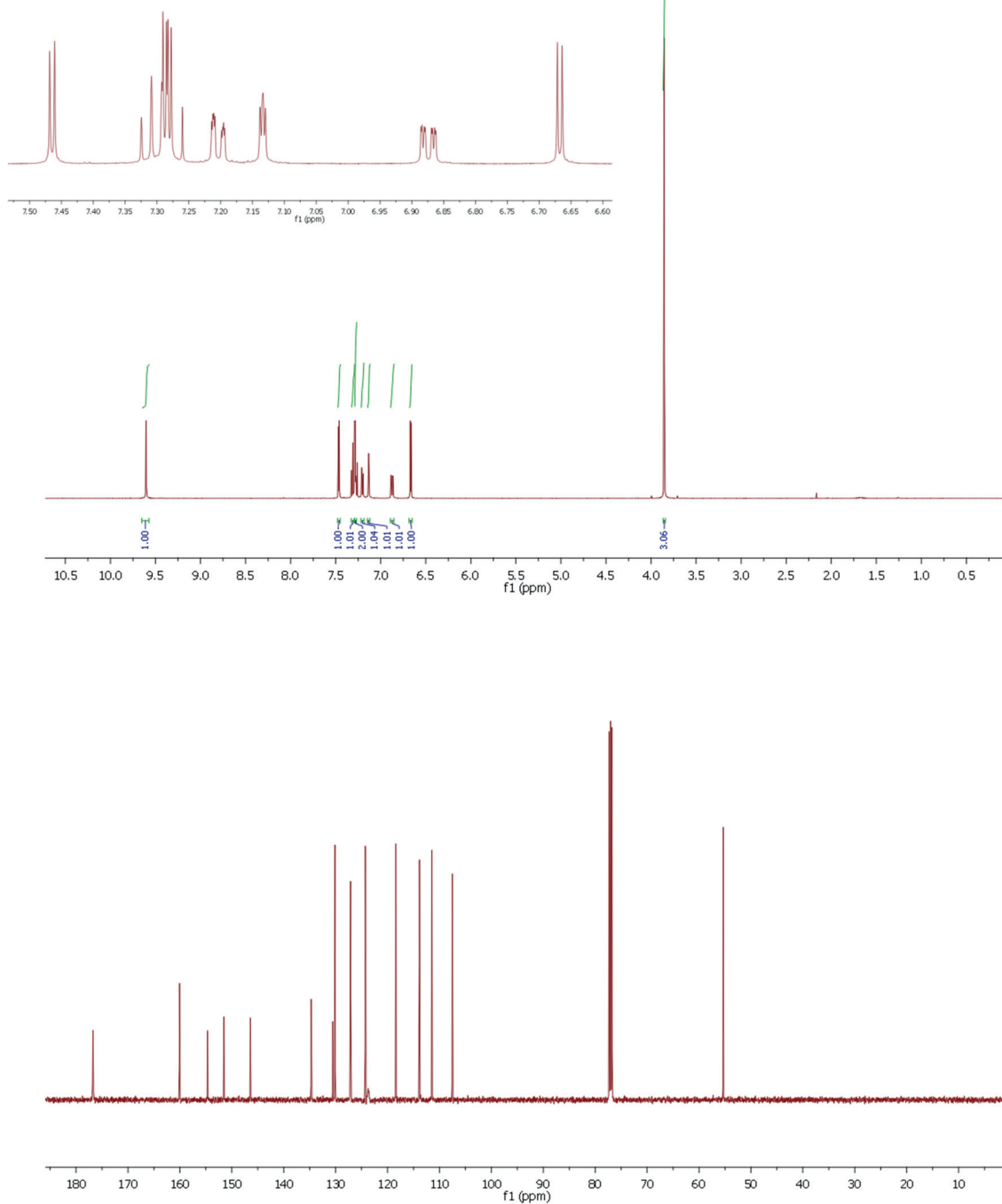
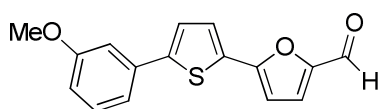
5-(5-(4-Nitrophenyl)thiophen-2-yl)furan-2-carbaldehyde (3a)



5-(5-Phenylthiophen-2-yl)furan-2-carbaldehyde (3b)



5-(5-(3-Methoxyphenyl)thiophen-2-yl)furan-2-carbaldehyde (3c)



References

- (1) D. E. Seitz, S. H. Lee, R. N. Hanson, J. C. Bottaro, *Synth. Commun.* **1983**, *13*, 121.
- (2) An impurity sublimed first (25 °C, 2×10^{-2} mbar).
- (3) The carbon atom bound to boron was not visible due to the high quadrupole moment of the boron nucleus.
- (4) M. W. Andersen, B. Hildebrandt, G. Köster, R. W. Hoffmann, *Chem. Ber.* **1989**, *122*, 1777.
- (5) J.G. Montana, I. Fleming, R. Tacke, J. Daiss, Heterocyclic silicon compounds and their use in the treatment of diseases or conditions associated with GnRH (gonadotropin-releasing hormone), PCT Int. Pat. Appl. WO 2004/045625 A1 (03.06.2004).

5.2 Supporting Information for *Angew. Chem.* 2014, *asap*.**Supporting Information**

for

Highly Tin-Selective Stille Coupling: Synthesis of a Polymer Containing a Stannole in the Main Chain*Julian Linshoef, Evan J. Baum, Andreas Hussain, Paul J. Gates, Christian Näther, and Anne Staubitz**

Abbreviations	2
General Methods and Materials	3
Syntheses.....	6
Luminescence Spectra.....	22
^1H NMR Spectra and $^{13}\text{C}\{^1\text{H}\}$ NMR Spectra	24
Single Crystal Data.....	34
References.....	41

Abbreviations

ATR	attenuated total reflectance
calcd.	calculated
COSY	correlated spectroscopy
Cp	cyclopentadienyl
d	doublet (NMR)
DCM	dichloromethane
DCTB	<i>trans</i> -2-[3-(4- <i>tert</i> -butylphenyl)-2-methyl-2-propenylidene]malononitrile
DMF	dimethylformamide
DTA	differential thermal analysis
DTG	derivative thermogravimetry
equiv	equivalents
ESI	electrospray ionization
GPC	gel permeation chromatography
HMBC	heteronuclear multiple bond coherence
HRMS	high resolution mass spectrometry
HSQC	heteronuclear single quantum coherence
HTph	hexylthiophene
IR	infrared
m	medium (concerning the intensity) (IR)
m	multiplet (NMR)
MALDI	Matrix-assisted laser desorption/ionisation
M.p.	melting point
NIS	<i>N</i> -iodosuccinimide
NMR	nuclear magnetic resonance
PDI	polydispersity index
PTFE	polytetrafluoroethylene
R _f	retardation factor
s	strong (concerning the intensity) (IR)
s	singlet (NMR)
t	triplet (NMR)
TEA	triethylamine
TG	thermogravimetry
THF	tetrahydrofuran
Tph	thiophene
UV/Vis	ultraviolet–visible spectroscopy
w	weak (concerning the intensity) (IR)

General Methods and Materials

All syntheses were carried out using standard Schlenk techniques under a dry and inert argon atmosphere. Glassware and NMR-tubes were dried in an oven at 200 °C for at least 2 h prior to use.

Analyses

^1H NMR, ^{13}C NMR and ^{119}Sn NMR spectra were recorded at 300 K. ^1H NMR spectra were recorded on a Bruker DRX 500 (500 MHz) spectrometer or a Bruker Avance 600 spectrometer. $^{13}\text{C}\{^1\text{H}\}$ NMR spectra were recorded on a Bruker DRX 500 (125 MHz) spectrometer or a Bruker Avance 600 (151 MHz) spectrometer. ^{119}Sn spectra were recorded on a Bruker DRX 500 (160 MHz, 187 MHz) spectrometer. All ^1H NMR and $^{13}\text{C}\{^1\text{H}\}$ NMR spectra were referenced against the solvent residual proton signals (^1H) or the solvent itself (^{13}C). The reference for the ^{119}Sn NMR spectra was calculated based on the ^1H NMR signal of TMS.

The exact assignment of the peaks was performed by two-dimensional NMR spectroscopy such as ^1H COSY, ^1H NOESY, ^{13}C HSQC or $^1\text{H}/^{13}\text{C}$ HMBC when possible.

High-resolution accurate-mass ESI mass spectra were recorded on a Bruker Daltonics micrOTOF II mass spectrometer. High-resolution accurate-mass MALDI mass spectra and MALDI MS analysis of polymer **TS_tTT** were recorded on a Bruker Daltonics ultrafleXtreme TOF/TOF mass spectrometer.

M_n and M_w were determined on a Viscotek GPCmax VE2001, equipped with a Viscotek VE3580 RI detector (columns: Viscotek LT5000L 300 x 7.8 mm and LT4000L 300 x 7.8 mm).

IR spectra were recorded on a Perkin Elmer Paragon 1000 FT-IR spectrometer with a A531-G Golden-Gate-ATR-unit.

UV/Vis spectra were recorded on a Perkin Elmer Lambda14 spectrometer.

Luminescence spectra were recorded on a Perkin Elmer LS55 spectrometer.

The DTA-TG measurements were performed in a nitrogen atmosphere in Al_2O_3 crucibles using a Netzsch STA-409CD instrument. All measurements were performed with a flow rate of $75 \text{ mL}\cdot\text{min}^{-1}$ (nitrogen) and were corrected for buoyancy and current effects. The instruments were calibrated using standard reference materials.

X-ray powder diffraction measurements were performed on a Stoe Transmission Powder Diffraction System (STADI P) with $\text{CuK}\alpha$ radiation ($\lambda = 154.0598$ pm), equipped with a MYTHEN detector.

All melting points were recorded on an Electrothermal melting point apparatus LG 1586 and are uncorrected.

Microwave Apparatus

All microwave syntheses were performed on a Biotage Initiator+ SP Wave (Organic Synthesis Mode). The temperature was measured with an external IR sensor during microwave heating.

Chemicals

All reagents were used without further purification unless noted otherwise. **4**^[1] and 2,5-bis(trimethylstannyl)thiophene^[2] were prepared following literature procedures.

Reagent	Supplier	Purity	Comments
1,3,5-Trimethoxybenzene	Acros Inc.	99 %	
1,7-Octadiyne	VWR Inc.	98 %	
2-Methylthiophene	VWR Inc.	98 %	
4,7-Dibromo-2,1,3-benzothiadiazole	Alfa Aesar Inc.	98 %	
Acetic acid	Grüssing Inc.	99.5 %	
Ammonium chloride	Grüssing Inc.	99.5 %	
Bu_2SnCl_2	VWR Inc.	96 %	distilled
Cp_2ZrCl_2	ABCR Inc.	98 %	
CuCl	Alfa Aesar Inc.	99.995+ %	
CuI	Aldrich Inc.	99.999 %	
Hexamethylditin	Aldrich Inc.	99 %	
Iodine	Acros Inc.	99.5 %	
Magnesium sulfate	Grüssing Inc.	99 %	
Me_2SnCl_2	VWR Inc.	97 %	sublimed
$\text{Me}_3\text{SiC}\equiv\text{CSiMe}_3$	VWR Inc.	99 %	
Molecular sieve, 3 Å	Alfa Aesar Inc.		
<i>n</i> -Butyllithium	Acros Inc.	2.5 M in hexanes	
NIS	Molekula Inc.	95 %	
$[\text{Pd}(\text{PPh}_3)_4]$	ABCR Inc.	99 %	
Ph_2SnCl_2	VWR Inc.	96 %	distilled
Sodium	Merck Inc.	≥ 99 %	

Solvents

All solvents were freshly distilled after refluxing for several hours over the specified drying agent under nitrogen and were stored in a J. Young's-tube. If no drying agent is noted, the solvents were merely distilled for purification purposes.

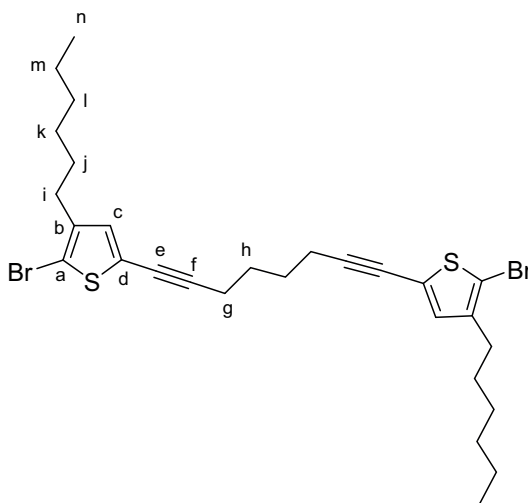
Solvent	Comments
CHCl ₃	VWR Inc.
Cyclohexane	BCD Inc.
DCM	BCD Inc.
Diethyl ether	BCD Inc.
DMF	Acros Inc., puriss. absolute over molecular sieve; stored in glovebox
<i>n</i> -Hexane	Walter CMP Inc.
Methanol	BCD Inc.
<i>n</i> -Pentane	Walter CMP Inc., LiAlH ₄ ; degassed by freeze-pump-thaw technique, stored over 3 Å molecular sieve in glovebox
Pyridine	Sigma Aldrich Inc.; CaH ₂ ; degassed by freeze-pump-thaw technique
TEA	Acros Inc., CaH ₂
THF	Sigma Aldrich Inc.; CaH ₂ with triphenylmethane as an indicator; degassed by freeze-pump-thaw technique, stored over 3 Å molecular sieve
Toluene	BCD Inc.; sodium with benzophenone as an indicator; degassed by freeze-pump-thaw technique, stored over 3 Å molecular sieve in glovebox

Chromatography

The silica gel used for chromatographic purification (Merck Inc. and Interchim Inc.) had a grain size of 0.015 – 0.050 mm. Thin layer chromatography was performed using pre-coated plates from Macherey-Nagel Inc., ALUGRAM® Xtra SIL G/UV₂₅₄ and POLYGRAM® ALOX N/UV₂₅₄. The chromatography purifications were carried out using an Interchim puriFlash® 430 purification system.

Syntheses

1,8-Bis(5-bromo-4-hexylthiophen-2-yl)octa-1,7-diyne (5)



A mixture of 2-bromo-3-(*n*-hexyl)-5-iodothiophene (6.52 g, 17.5 mmol), [Pd(PPh₃)₄] (404 mg, 350 μmol, 2 mol%) and copper(I) iodide (66.7 mg, 350 μmol, 2 mol%) in TEA (7 mL) and DMF (14 mL) was stirred at 20 °C. 1,7-Octadiyne (929 mg, 8.75 mmol) was added and the yellow-brown suspension was stirred at 55 °C for 21 h. The reaction mixture was quenched with a saturated solution of ammonium chloride (100 mL) and extracted with Et₂O (4 x 80 mL). The organic extracts were dried over magnesium sulfate and concentrated *in vacuo*. The crude product was purified via flash chromatography (cyclohexane; R_f = 0.37) to afford 4.36 g (84 %) of a yellow oil.

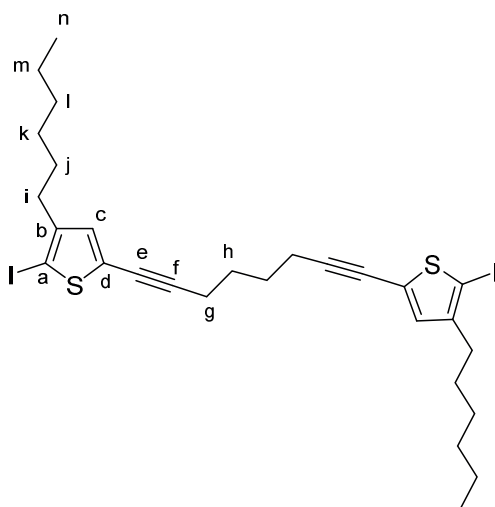
¹H NMR (500 MHz, CDCl₃): δ = 6.81 (s, 2 H, c), 2.51 – 2.42 (m, 8 H, g and i), 1.77 - 1.68 (m, 4 H, h), 1.58 – 1.49 (m, 4 H, j)*, 1.35 – 1.24 (m, 12 H, k, l and m), 0.88 (t, 6 H, ³J = 6.9 Hz, n) ppm.

* overlapping with the water signal.

¹³C NMR (126 MHz, CDCl₃): δ = 142.0 (b), 132.0 (c), 123.7 (d), 108.4 (a), 94.6 (f), 73.8 (e), 31.6 (l), 29.5 (i or j), 29.4 (i or j), 28.8 (k), 27.6 (h), 22.6 (m), 19.3 (g), 14.1 (n) ppm.

IR (ATR): $\tilde{\nu}$ = 2925 (s), 2856 (s), 1547 (w), 1441 (m), 1324 (m), 1196 (m), 1006 (w), 834 (s), 733 (w), 661 (w), 581 (w), 534 (m) cm⁻¹.

HRMS (ESI) *m/z*: Found 595.0694; calcd. for [M + H]⁺ C₂₈H₃₇Br₂S₂ 595.0698.

1,8-Bis(4-hexyl-5-iodothiophen-2-yl)octa-1,7-diyne (6b)

n-Butyllithium (6.12 mL, 15.3 mmol; 2.50 M in hexanes) was added dropwise within 15 min to a solution of **5** (4.16 g, 6.97 mmol) in THF (50 mL) at $-78\text{ }^{\circ}\text{C}$. The orange-brown solution was stirred for 60 min and iodine (5.30 g, 20.9 mmol) in THF (10 mL) was added within 5 min. The brown suspension was allowed to warm to $16\text{ }^{\circ}\text{C}$ over the course of 2 h after removal of the cooling bath. The reaction mixture was quenched with a saturated solution of sodium thiosulfate (100 mL). The aqueous layer was extracted with diethyl ether (3 x 100 mL) and the combined organic layers were dried over magnesium sulfate. The volatiles were removed *in vacuo* and the residue was purified by column chromatography (cyclohexane; $R_f = 0.25$) to obtain 4.26 g (89 %) of a pale yellow oil.

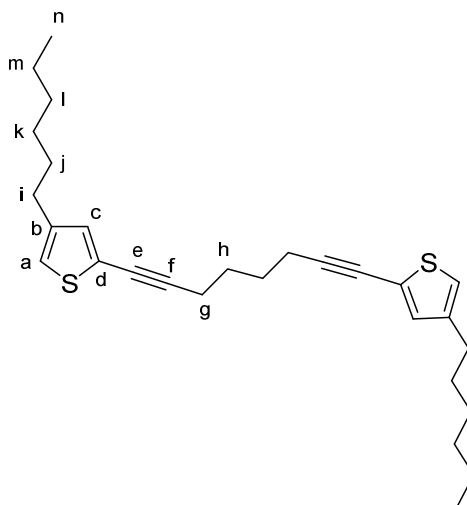
$^1\text{H NMR}$ (500 MHz, CDCl_3): $\delta = 6.75$ (s, 2 H, c), 2.50 – 2.43 (m, 8 H, g and i), 1.76 – 1.69 (m, 4 H, h), 1.57 – 1.49 (m, 4 H, j)*, 1.36 – 1.24 (m, 12 H, k, l and m), 0.92 – 0.85 (m, 6 H, n) ppm.

* overlapping with the water signal.

$^{13}\text{C NMR}$ (126 MHz, CDCl_3): $\delta = 147.1$ (b), 131.6 (c), 128.8 (d), 95.5 (f), 74.0 (a or e), 73.8 (a or e), 32.2 (i), 31.6 (l), 29.8 (j), 28.8 (k), 27.6 (h), 22.6 (m), 19.3 (g), 14.1 (n) ppm.

IR (ATR): $\tilde{\nu} = 2924$ (s), 2854 (s), 1704 (w), 1538 (w), 1457 (m), 1362 (m), 1324 (m), 1263 (w), 1194 (m), 835 (s), 738 (s), 658 (w), 560 (w), 533 (m) cm^{-1} .

HRMS (ESI) m/z : Found 691.0398; calcd. for $[\text{M} + \text{H}]^+ \text{C}_{28}\text{H}_{37}\text{I}_2\text{S}_2$ 691.0421.

1,8-Bis(4-hexylthiophen-2-yl)octa-1,7-diyne (6a)

n-Butyllithium (5.00 mL, 12.5 mmol; 2.50 M in hexanes) was added dropwise within 5 min to a solution of **5** (3.30 g, 5.53 mmol) in THF (50 mL) at -78 °C. The orange-brown solution was stirred for 60 min and water (1 mL) was added dropwise within 5 min. The suspension was allowed to warm to 16 °C after removal of the cooling bath and a saturated solution of ammonium chloride (50 mL) was added. The reaction mixture was then extracted with diethyl ether (3 x 80 mL) and the combined organic layers were dried over magnesium sulfate. The volatiles were removed *in vacuo* and the residue was filtered over a short plug of silica (2 x 4 cm; eluent: cyclohexane) to obtain 2.41 g (99 %) of a pale yellow oil.

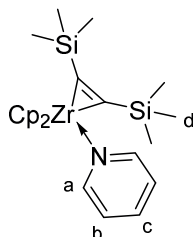
¹H NMR (600 MHz, CDCl₃): δ = 6.96 (d, ⁴J = 1.2 Hz, 2 H, c), 6.76 (d, ⁴J = 1.2 Hz, 2 H, a), 2.53 (t, ³J = 7.7 Hz, 4 H, i), 2.51 – 2.44 (m, 4 H, g), 1.80 – 1.71 (m, 4 H, h), 1.62 – 1.55 (m, 4 H, j), 1.36 – 1.24 (m, 12 H, k, l and m), 0.88 (t, ³J = 6.9 Hz, 6 H, n) ppm.

¹³C NMR (151 MHz, CDCl₃): δ = 142.9 (b), 132.4 (c), 123.5 (d), 120.7 (a), 93.3 (f), 74.5 (e), 31.6 (l), 30.3 (i and j)*, 28.9 (k), 27.7 (h), 22.6 (m), 19.3 (g), 14.1 (n) ppm.

* two signals.

IR (ATR): $\tilde{\nu}$ = 2925 (s), 2854 (s), 1543 (w), 1458 (m), 1377 (w), 1325 (w), 1196 (m), 838 (s), 735 (s), 647 (m), 586 (m) cm⁻¹.

HRMS (ESI) *m/z*: Found 439.2478; calcd. for [M + H]⁺ C₂₈H₃₉S₂ 439.2488.

Cp₂Zr(pyr)(Me₃SiC≡CSiMe₃) (7)

7 was prepared similarly to a method described in the literature by Tilley and co-workers.^[3] The work-up procedure was simplified by changing the solvent amounts and crystallization temperature from -80 °C to -30 °C. Although this reduced the yield by 20 % with respect to the yield reported by Tilley, it was higher than the yield we obtained by performing the work-up as reported.

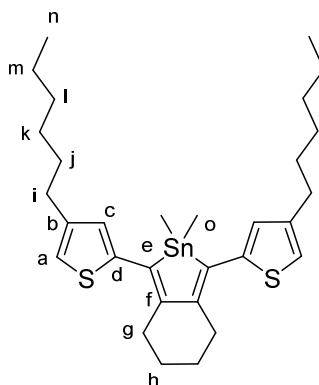
Cp₂ZrCl₂ (5.00 g, 17.1 mmol) and Me₃SiC≡CSiMe₃ (2.91 g, 17.1 mmol) were dissolved in THF (100 mL). *n*-Butyllithium (13.7 mL, 34.2 mmol; 2.50 M in hexanes) was added dropwise within 40 min to the colorless solution at -78 °C, resulting in a color change to pale yellow. The mixture was stirred for 10 min, then the cooling bath was removed and the reaction mixture was allowed to warm to 20 °C over 2 h. Pyridine (1.38 mL, 17.1 mmol) was added to the now dark red solution, which changed the color to dark purple. The solvent was removed *in vacuo* under inert conditions until only ca. 1 mL remained. Dry pentane (250 mL) was added in a glovebox, the solution was stirred for 20 h and was then filtered with a PTFE syringe filter (0.45 μm pore size). The solution was placed in a -30 °C freezer in a glovebox for 43 h, which resulted in the formation of black-purple crystals. The supernatant was removed by decantation and the crystals were dried *in vacuo* to yield 5.23 g (65 %).

¹H NMR (500 MHz, benzene-*d*₆): δ = 8.89 – 8.84 (m, 2 H, a), 6.81 (m, 1 H, c), 6.41 (m, 2 H, b), 5.47 (s, 10 H, Cp), 0.33 (s, 18 H, d) ppm.

¹³C NMR (126 MHz, benzene-*d*₆): δ = 154.0 (a), 136.5 (c), 123.1 (b), 106.4 (Cp), 2.5 (d) ppm.

The NMR data are in agreement with the data found in the literature.^[3]

1,3-Bis(4-hexylthiophen-2-yl)-2,2-dimethyl-4,5,6,7-tetrahydro-2H-benzo[c]stannole (10)



6a (101 mg, 230 μmol) and $\text{Cp}_2\text{Zr}(\text{pyr})(\text{Me}_3\text{SiC}\equiv\text{CSiMe}_3)$ (108 mg, 230 μmol) were dissolved in toluene (2 mL) and the dark red solution was stirred for 18 h at 20 $^\circ\text{C}$ under a nitrogen atmosphere. Me_2SnCl_2 (51.0 mg, 230 μmol), copper(I) chloride (2.3 mg, 23 μmol) and toluene (2 mL) were added in a glovebox and the dark mixture was stirred for 3 h at 20 $^\circ\text{C}$, over which time the solution turned bright orange. The suspension was quenched with water (25 mL) and the aqueous layer was extracted with cyclohexane (3 x 40 mL). The combined organic layers were dried over magnesium sulfate, the volatiles were removed *in vacuo* and the residue was purified by column chromatography (cyclohexane; $R_f = 0.75$). The column was conditioned by washing it with 3 CV TEA/cyclohexane 5:95, followed by 10 CV of pure cyclohexane). The product was obtained as a yellow oil (69 mg, 51 %).

$^1\text{H NMR}$ (500 MHz, CDCl_3): $\delta = 6.86$ (d, $^4J = 1.1$ Hz, 2 H, a), 6.68 (d, $^4J = 1.1$ Hz, 2 H, c), 2.82 – 2.73 (m, 4 H, g), 2.57 (d, $^3J = 7.6$ Hz, 4 H, i), 1.77 – 1.68 (m, 4 H, h), 1.66 – 1.56 (m, 4 H, j), 1.37 – 1.27 (m, 12 H, k, l and m), 0.92 – 0.76 (m, 6 H, n), 0.57 (s, 6 H, o; $^2J(^{119}\text{Sn}, ^1\text{H}) = 29.0$ Hz)* ppm.

* the signal shows satellites due to coupling with tin.

$^{13}\text{C NMR}$ (126 MHz, CDCl_3): $\delta = 148.4$ (f), 146.4 (d, $^2J = 33.2$ Hz)*, 143.2 (b), 132.0 (e), 129.0 (c, $^3J = 13.1$ Hz)*, 120.2 (a), 31.7 (g or k or l), 31.6 (g or k or l), 30.5 (i and j)**, 29.0 (k or l), 23.3 (h), 22.7 (m), 14.1 (n), -7.1 (o, $^1J = 168.0$ Hz)* ppm.

Signals that show satellites due to coupling with tin are marked with *. Coupling constants $^nJ(^{119}\text{Sn}, ^{13}\text{C})$ are given in parentheses when signal to noise ratio allowed the determination.

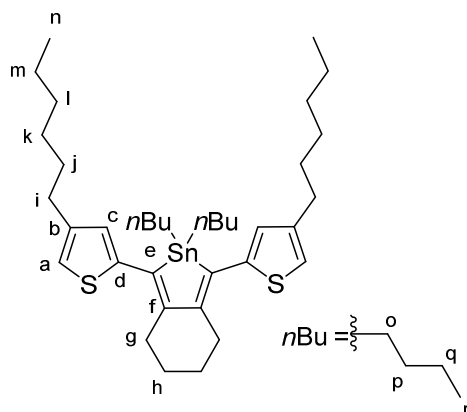
** two signals.

^{119}Sn NMR (187 MHz, CDCl_3): $\delta = -5.8$ ppm.

IR (ATR): $\tilde{\nu} = 2925$ (s), 2855 (s), 1634 (m), 1416 (m), 1282 (m), 1198 (m), 861 (m), 772 (s), 726 (s), 575 (s) cm^{-1} .

HRMS (ESI) m/z : Found 589.1973; calcd. for $[\text{M} + \text{H}]^+ \text{C}_{30}\text{H}_{45}\text{S}_2\text{Sn}$ 589.1982.

2,2-Dibutyl-1,3-bis(4-hexylthiophen-2-yl)-4,5,6,7-tetrahydro-2H-benzo[c]stannole (12)



6a (109 mg, 248 μmol) and $\text{Cp}_2\text{Zr}(\text{pyr})(\text{Me}_3\text{SiC}\equiv\text{CSiMe}_3)$ (122 mg, 260 μmol) were dissolved in toluene (2 mL) and the dark red solution was stirred for 18 h at 20 $^\circ\text{C}$ under an atmosphere of nitrogen. $n\text{Bu}_2\text{SnCl}_2$ (79 mg, 260 μmol), copper(I) chloride (2.5 mg, 25 μmol) and toluene (2 mL) were added in a glovebox and the dark mixture was stirred for 3 h at 20 $^\circ\text{C}$, over which time the solution turned yellow. The suspension was quenched with water (20 mL) and the aqueous layer was extracted with cyclohexane (3 x 40 mL). The combined organic layers were dried over magnesium sulfate. The volatiles were removed *in vacuo* and the residue was purified by column chromatography (cyclohexane; $R_f = 0.86$. The column was conditioned by washing it with 3 CV TEA/cyclohexane 5:95, followed by 10 CV of pure cyclohexane). The product was obtained as a yellow oil (101 mg, 61 %).

^1H NMR (500 MHz, CDCl_3): $\delta = 6.85$ (d, $^4J = 1.1$ Hz, 2 H, a), 6.65 (d, $^4J = 1.1$ Hz, 2 H, c), 2.81 – 2.74 (m, 4 H, g), 2.57 (t, $^3J = 7.6$ Hz, 4 H, i), 1.75 – 1.69 (m, 4 H, h), 1.65 – 1.56 (m, 8 H, j and o), 1.38 – 1.23 (m, 20 H, k, l, m, p and q), 0.92 – 0.86 (m, 6 H, n or r), 0.82 (t, $^3J = 7.3$ Hz, 6 H, n or r) ppm.

^{13}C NMR (126 MHz, CDCl_3): δ = 148.9 (f), 146.8 (d), 143.0 (b), 132.7 (e), 129.0 (c, $^3J = 12.0$ Hz)*, 120.0 (a), 31.7, 31.6, 30.5**, 29.1, 29.0, 27.0, 23.4 (h), 22.6, 14.1, 13.5 (n or r), 13.3 (n or r) ppm.

Signals that show satellites due to coupling with tin are marked with *. Coupling constants $^nJ(^{119}\text{Sn}, ^{13}\text{C})$ are given in parentheses when signal to noise ratio allowed the determination.

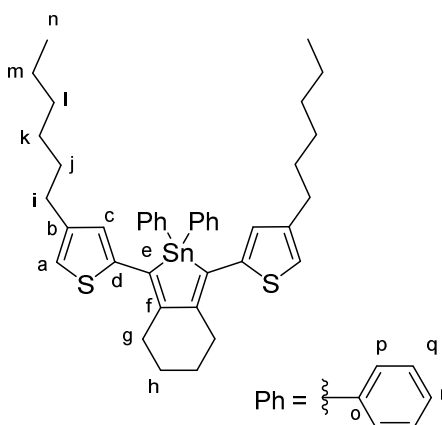
** two signals.

^{119}Sn NMR (187 MHz, CDCl_3): δ = -6.7 ppm.

IR (ATR): $\tilde{\nu}$ = 2954 (s), 2924 (s), 2855 (s), 1634 (m), 1417 (m), 1377 (m), 1283 (m), 864 (m), 774 (m), 726 (m), 546 (m), 455 (m) cm^{-1} .

HRMS (ESI) m/z : Found 673.2927; calcd. for $[\text{M} + \text{H}]^+$ $\text{C}_{36}\text{H}_{57}\text{S}_2\text{Sn}$ 673.2923.

1,3-Bis(4-hexylthiophen-2-yl)-2,2-diphenyl-4,5,6,7-tetrahydro-2H-benzo[c]stannole (11)



6a (112 mg, 255 μmol) and $\text{Cp}_2\text{Zr}(\text{pyr})(\text{Me}_3\text{SiC}\equiv\text{CSiMe}_3)$ (180 mg, 383 μmol) were dissolved in toluene (2 mL) and the dark red solution was stirred for 18 h at 20 $^\circ\text{C}$ under an atmosphere of nitrogen. Ph_2SnCl_2 (132 mg, 383 μmol), copper(I) chloride (2.6 mg, 26 μmol) and toluene (1 mL) were added in a glovebox. The reaction mixture was stirred at 20 $^\circ\text{C}$ for 4 h, and was then quenched with water (50 mL). The aqueous layer was extracted with diethyl ether (3 x 50 mL). The combined organic layers were dried over magnesium sulfate. The volatiles were removed *in vacuo* and the residue was purified by column chromatography (cyclohexane; $R_f = 0.20$). The column was conditioned by washing it with 3 CV TEA/cyclohexane 5:95,

followed by 10 CV of pure cyclohexane). The product was obtained as a yellow solid (40 mg, 22 %).

^1H NMR (500 MHz, CDCl_3): δ = 7.70 – 7.57 (m, 4 H, p)*, 7.38 – 7.33 (m, 6 H, q and r), 6.85 (s, 2 H, a), 6.80 (d, 4J = 1.0 Hz, 2 H, c), 2.91 – 2.81 (m, 4 H, g), 2.48 (t, 3J = 7.6 Hz, 4 H, i), 1.82 – 1.75 (m, 4 H, h), 1.53 – 1.46 (m, 4 H, j)**, 1.27 – 1.19 (m, 12 H, k, l and m), 0.88 – 0.82 (m, 6 H, n).

* the signal shows satellites due to coupling with tin.

** overlapping with the water signal.

^{13}C NMR (126 MHz, CDCl_3): δ = 149.4 (f), 145.6 (d), 143.0 (b), 138.5 (o), 137.3 (p, 2J = 20.4 Hz)*, 130.5 (c, 3J = 12.2 Hz)*, 130.1 (e), 129.3 (r, 4J = 6.1 Hz)*, 128.8 (q, 3J = 26.7 Hz)*, 120.8 (a), 31.8 (g or l), 31.7 (g or l), 30.3 (i and j)**, 28.9 (k), 23.3 (h), 22.6 (m), 14.1 (n) ppm.

Signals that show satellites due to coupling with tin are marked with *. Coupling constants $^nJ(^{119}\text{Sn}, ^{13}\text{C})$ are given in parentheses when signal to noise ratio allowed the determination.

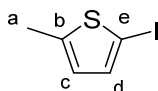
** two signals.

^{119}Sn NMR (187 MHz, CDCl_3): δ = -83.5 ppm.

M.p.: 97 °C.

IR (ATR): $\tilde{\nu}$ = 2922 (m), 2853 (m), 1428 (m), 1189 (w), 1135 (w), 1074 (w), 997 (w), 848 (m), 810 (m), 724 (s), 695 (s), 660 (w), 649 (w), 457 (w) cm^{-1} .

HRMS (ESI) m/z : Found 713.2318; calcd. for $[\text{M} + \text{H}]^+$ $\text{C}_{40}\text{H}_{49}\text{S}_2\text{Sn}$ 713.2298.

2-Iodo-5-methylthiophene (13)

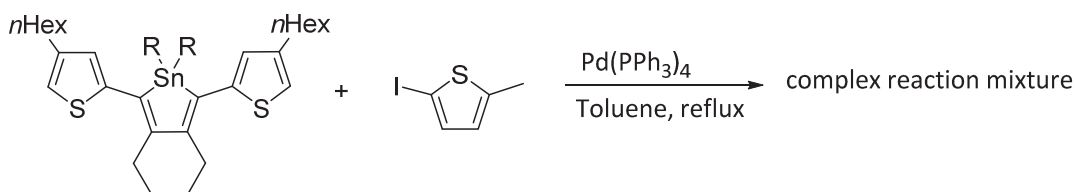
A suspension of 2-methylthiophene (1.96 g, 20.0 mmol) and NIS (4.61 g, 20.5 mmol) in a mixture of chloroform (25 mL) and acetic acid (10 mL) was shielded from light and was then stirred for 70 h under air. The red solution was concentrated *in vacuo* and a saturated solution of sodium hydrogen carbonate (50 mL) was added. Additional sodium hydrogen carbonate was added until the solution was neutralized before sodium thiosulfate was added until the red color disappeared. The aqueous layer was extracted with *n*-hexane (3 x 50 mL) and the combined organic layers were dried with sodium sulfate. The volatiles were removed *in vacuo* and the residue was distilled by Kugelrohr distillation (9 mbar, 100 °C) to obtain 3.92 g (87 %) of a yellow oil.

¹H NMR (500 MHz, CDCl₃): δ = 7.02 (d, 1 H, ³J = 3.5 Hz, d), 6.45 (dq, 1 H, ³J = 3.5, ⁴J = 1.1 Hz, c), 2.47 (d, 3 H, ⁴J = 1.1 Hz, a) ppm.

¹³C NMR (126 MHz, CDCl₃): δ = 146.1 (b), 137.0 (d), 127.1 (c), 69.5 (e), 15.5 (a) ppm.

The NMR data are in agreement with the data found in the literature.^[4]

Stability Test Reaction

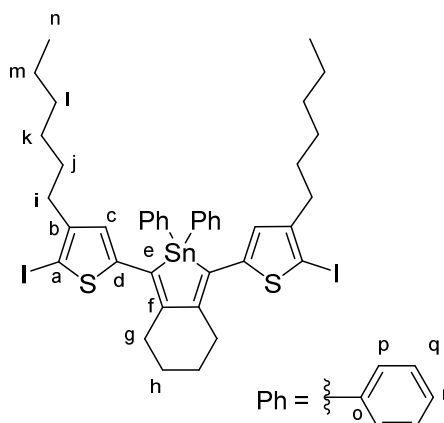


A yellow solution of the stannole (1 equiv), 2-iodo-5-methylthiophene (2 equiv), 1,3,5-trimethoxybenzene (ca. 1 equiv) as internal standard and [Pd(PPh₃)₄] (0.05 equiv) in toluene (5 mL) was prepared, and a sample of 0.5 mL was removed after stirring the mixture for 1 min. This sample was quenched with water (2 mL) and the aqueous layer was extracted with diethyl ether (4 mL). The organic layer was dried over magnesium sulfate, the volatiles were removed *in vacuo* and an NMR was obtained (used as *t*₀).

The reaction mixture was then heated to reflux for 15 h. The dark suspension was quenched with water (20 mL) and the aqueous layer was extracted with diethyl ether (2 x 40 mL). The combined organic layers were dried over magnesium sulfate. The volatiles were removed *in vacuo* and an NMR was taken.

The products that were formed are a complex mixture and not identifiable. The conversion was calculated from peak integrals.

	Stannole	2-Iodo-5-methylthiophene	1,3,5-Trimethoxybenzene	[Pd(PPh ₃) ₄]
R = Ph	11 (38 mg, 53 μmol)	24 mg, 106 μmol	11 mg, 67 μmol	3 mg, 2.7 μmol
R = Me	10 (32 mg, 54 μmol)	24 mg, 107 μmol	9 mg, 54 μmol	3 mg, 2.7 μmol
R = <i>n</i> Bu	12 (38 mg, 57 μmol)	26 mg, 114 μmol	8 mg, 48 μmol	3 mg, 2.7 μmol

1,3-Bis(4-hexyl-5-iodothiophen-2-yl)-2,2-diphenyl-4,5,6,7-tetrahydro-2H-benzo[c]stannole (9)

In a glovebox, **6b** (675 mg, 978 μmol) and $\text{Cp}_2\text{Zr}(\text{pyr})(\text{Me}_3\text{SiC}\equiv\text{CSiMe}_3)$ (461 mg, 978 μmol) were dissolved in toluene (10 mL) and the solution was stirred for 18 h at 20 $^\circ\text{C}$. Ph_2SnCl_2 (336 mg, 978 μmol), copper(I) chloride (9.7 mg, 98 μmol , 10 mol%) and toluene (2 mL) were added to the dark solution in a glovebox. The reaction mixture was stirred at 20 $^\circ\text{C}$ for 3 h over which time it turned bright orange. It was then quenched with water (50 mL) and the aqueous layer was extracted with diethyl ether (3 x 100 mL). The combined organic layers were dried over magnesium sulfate. The volatiles were removed *in vacuo*, the residue was filtered over a short plug of silica (2 x 5 cm, eluent DCM) and then recrystallized from cyclohexane to yield 764 mg (81 %) of an orange solid.

As an alternative purification method, the crude product can be purified by column chromatography (*n*-pentane; $R_f = 0.37$).

Single crystals could be obtained from a saturated solution (*n*-pentane) at 7 $^\circ\text{C}$ (crystallographic data see below).



^1H NMR (500 MHz, CDCl_3): δ = 7.62 – 7.56 (m, 4 H, p)*, 7.41 – 7.33 (m, 6 H, q and r), 6.59 (s, 2 H, c), 2.82 – 2.73 (m, 4 H, g), 2.44 – 2.37 (t, 3J = 7.5 Hz, 4 H, i), 1.82 – 1.74 (m, 4 H, h), 1.46 – 1.37 (m, 4 H, j), 1.25 – 1.17 (m, 12 H, k, l and m), 0.88 – 0.81 (m, 6 H, n) ppm.

* the signal shows satellites due to coupling with tin.

^{13}C NMR (126 MHz, CDCl_3): δ = 150.0 (d or f, 2J = 38.9 Hz)*, 149.6 (d or f, 2J = 36.1 Hz)*, 146.7 (b), 137.8 (o, 1J = 261.2 Hz)*, 137.1 (p, 2J = 20.6 Hz)*, 130.3 (e, 1J = 230.9 Hz)*, 129.8 (c, 3J = 12.0 Hz)*, 129.5 (r, 4J = 6.0 Hz)*, 129.0 (q, 3J = 26.7 Hz)*, 75.8 (a), 32.0 (i or l or g), 31.8 (i or l or g), 31.6 (i or l or g), 29.8 (j), 28.6 (k), 23.1 (h), 22.5 (m), 14.1 (n) ppm.

Signals that show satellites due to coupling with tin are marked with *. Coupling constants $^nJ(^{119}\text{Sn}, ^{13}\text{C})$ are given in parentheses when signal to noise ratio allowed the determination.

^{119}Sn NMR (187 MHz, CDCl_3): δ = -79.9 ppm.

λ_{max} (CHCl_3) = 441 nm (ϵ = $44.5 \times 10^3 \text{ L mol}^{-1} \text{ cm}^{-1}$).

M.p.: 92 °C.

IR (ATR): $\tilde{\nu}$ = 2925 (m), 2854 (m), 1519 (w), 1467 (w), 1429 (m), 1226 (w), 1181 (w), 1073 (w), 1022 (w), 997 (w), 809 (w), 726 (s), 697 (s), 659 (w), 465 (w) cm^{-1} .

HRMS (MALDI, colloidal graphite matrix) m/z : Found 964.0158; calcd. for $[\text{M}]^+$ $\text{C}_{40}\text{H}_{46}\text{I}_2\text{S}_2\text{Sn}$ 964.0147.

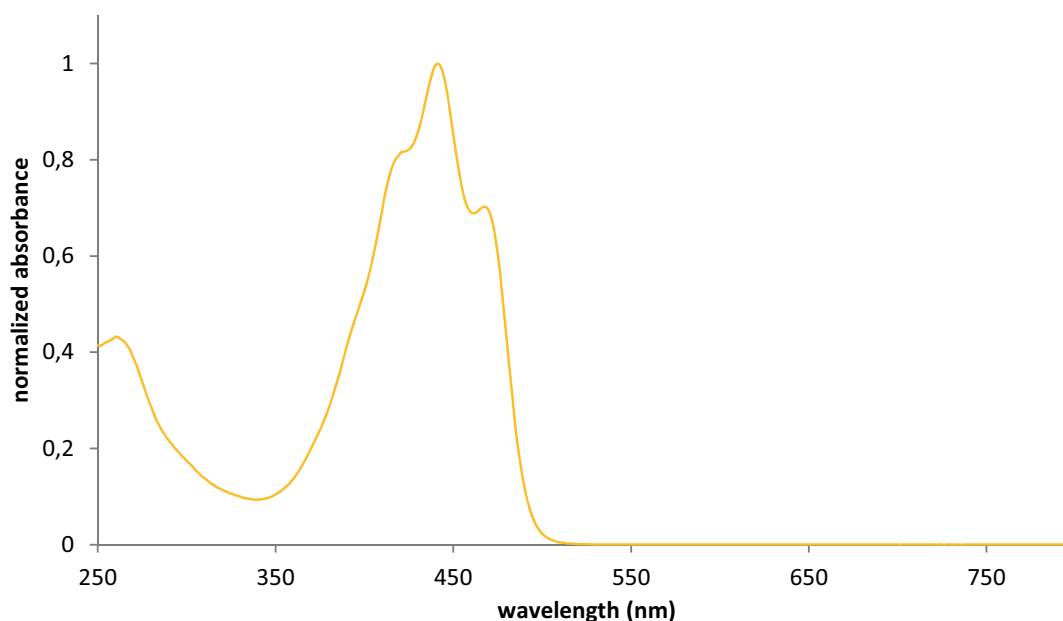
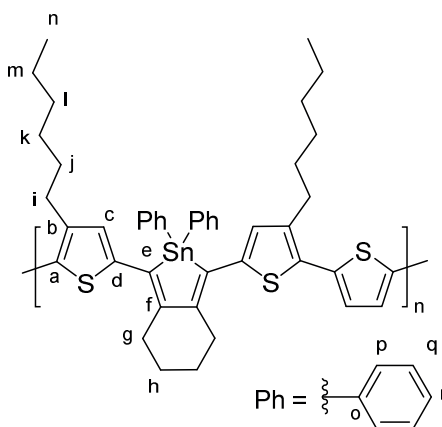


Figure SI 1. Full absorption spectrum of **9** in solution (chloroform).

Polymer TStTT

An orange-red solution of **9** (144.5 mg, 150 μmol), 2,5-bis(trimethylstannyl)thiophene (61.5 mg, 150 μmol) and $[\text{Pd}(\text{PPh}_3)_4]$ (8.7 mg, 7.5 μmol , 5 mol%) in toluene (5 mL), prepared in a glove box, was heated to reflux for 15 h. The deep purple solution was precipitated into methanol (150 mL). The polymer was collected by centrifugation, washed with methanol (150 mL) and dried *in vacuo* for 1 h to yield 107 mg (90 %) of a purple-black solid.

Samples for UV measurements of the polymer film were prepared by adding three drops of the polymer solution (5 mg/mL in CHCl_3) on a rotating quartz plate (100 rps).

λ_{max} (CHCl_3) = 536 nm ($\epsilon = 36.0 \times 10^3 \text{ L mol}^{-1} \text{ cm}^{-1}$; per monomer repeat unit).

M_n (GPC) = 6.8 kDa.

M_w (GPC) = 17.0 kDa.

PDI = 2.5.

$^1\text{H NMR}$ (500 MHz, CDCl_3): $\delta = 7.70 - 7.63$ (broad m, 4 H, p)*, 7.43 – 7.34 (broad m, 6 H, q and r), 7.07 – 7.02 (broad m, 2 H, Tph-H), 6.83 – 6.79 (broad m, 2 H, HTph-H), 2.97 – 2.83 (broad m, 4 H, g), 2.74 – 2.60 (broad m, 4 H, i), 1.87 – 1.77 (broad m, 4 H, h), 1.59 – 1.46 (broad m, 4 H, j), 1.34 – 1.14 (broad m, 12 H, k, l, m), 0.91 – 0.78 (broad m, 6 H, n) ppm.

* the signal shows satellites due to coupling with tin.

$^{13}\text{C NMR}$ (126 MHz, CDCl_3): $\delta = 149.8, 143.2, 139.1$ (b), 138.3 (Ph), 137.2 (p, $^2J = 20.5 \text{ Hz}$)*, 136.1 (Tph), 133.3 (HTph-CH), 131.6 (HTph), 130.3, 129.4 (Ph), 128.9 (q, $^3J = 26.9 \text{ Hz}$)*, 125.4 (Tph-CH), 31.8 (l or g), 31.7 (l or g), 30.2 (j), 29.2 (i), 29.0 (k), 23.2 (h), 22.5 (m), 14.1 (n) ppm.



Signals that show satellites due to coupling with tin are marked with *. Coupling constants ${}^nJ({}^{119}\text{Sn}, {}^{13}\text{C})$ are given in parentheses when signal to noise ratio allowed the determination.

${}^{119}\text{Sn}$ NMR (187 MHz, CDCl_3): $\delta = -81.1$ ppm.

IR (ATR): $\tilde{\nu} = 2923$ (m), 2855 (m), 1429 (m), 1074 (w), 997 (w), 817 (w), 724 (s), 695 (s), 619 (w) cm^{-1} .

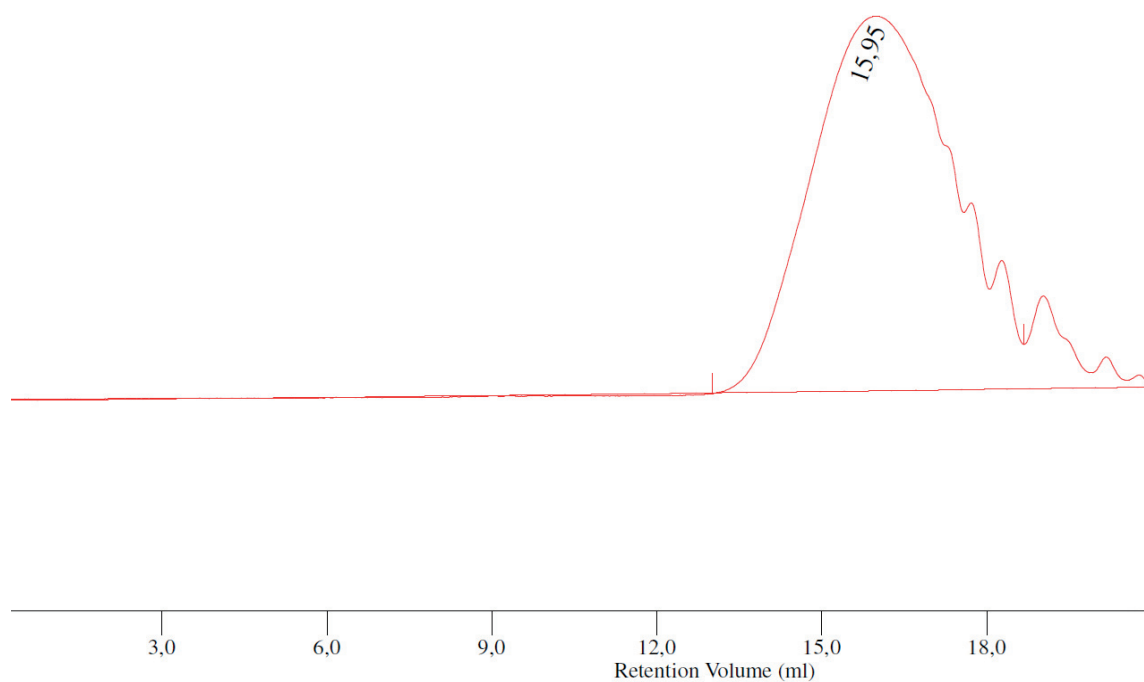


Figure SI 2. GPC trace of TStTT using chloroform as the eluent at a flow rate of 1 mL / min; calibrated against polystyrene standards.

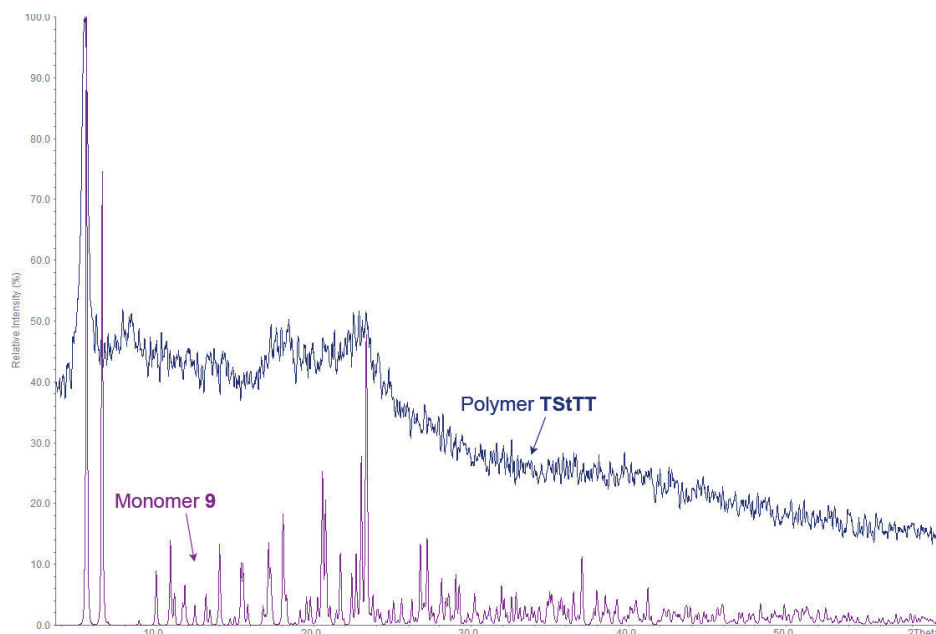


Figure SI 3. Experimental X-ray powder diffraction pattern of **TStTT** and calculated pattern of monomer **9**.

The experimental X-ray powder diffraction pattern of **TStTT** was compared to a pattern of monomer **9**, calculated from single crystal data. The polymer is in most instances X-ray amorphous, but a strong reflex was observed at 5.5 ° (Figure SI 3), which shows that **TStTT** is semicrystalline. Thermal analysis by TG/DTG between room temperature and 600 °C showed two mass losses of ca. 23 % at $T_1 = 300$ °C and $T_2 = 434$ °C.

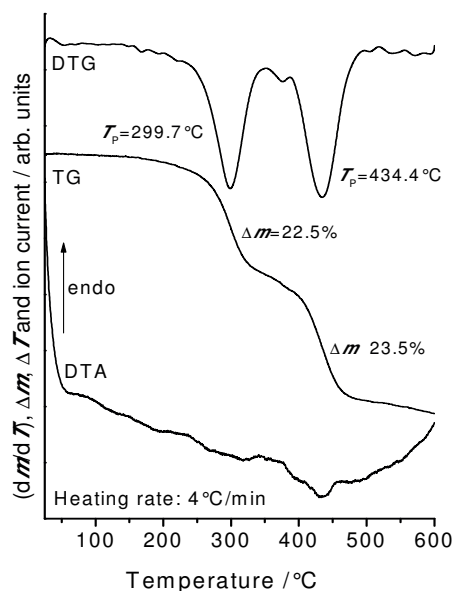


Figure SI 4. DTA, TG and DTG curve of **TStTT**.

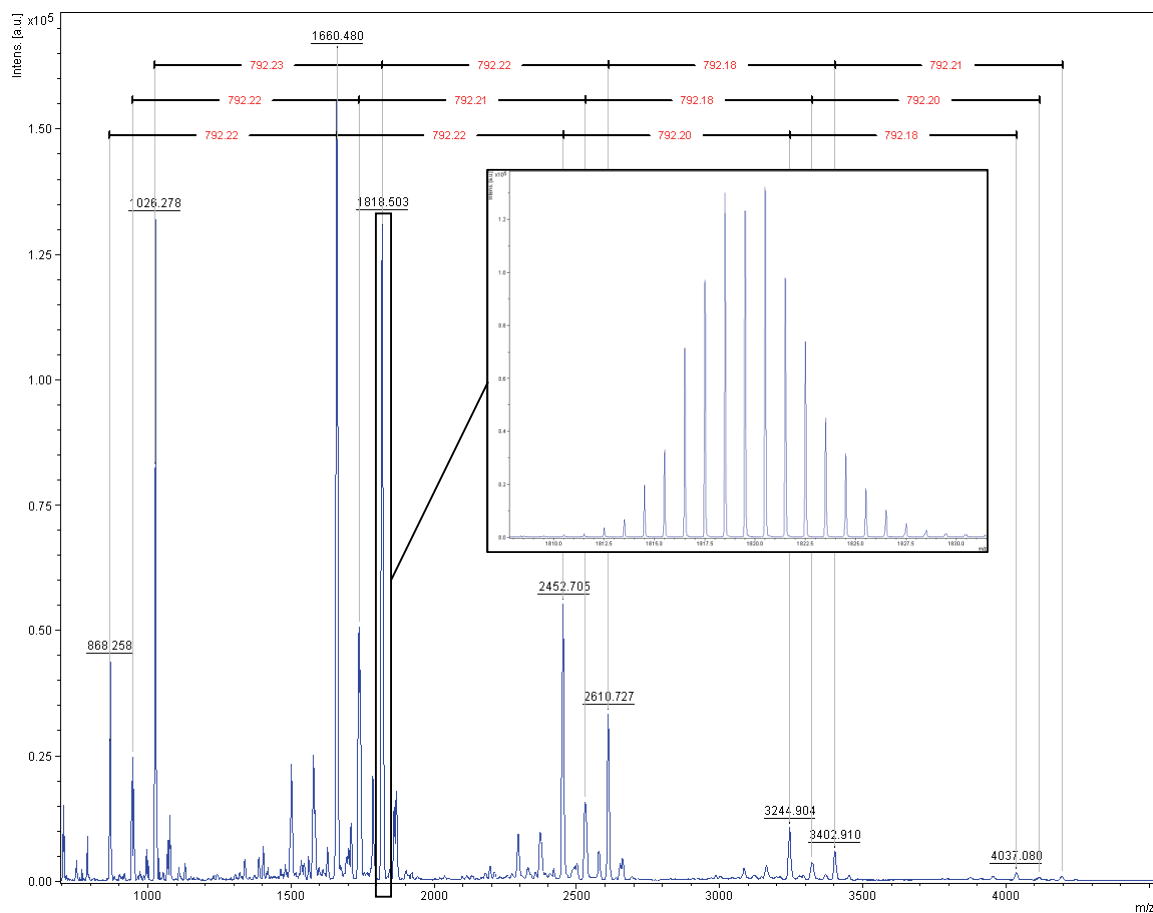


Figure SI 5. MALDI (DCTB) spectrum of TSstTT with the mass of the repeating unit indicated in the picture. The enlargement of a peak shows the characteristic isotopic distribution of tin compounds. Possible end groups could not be identified.

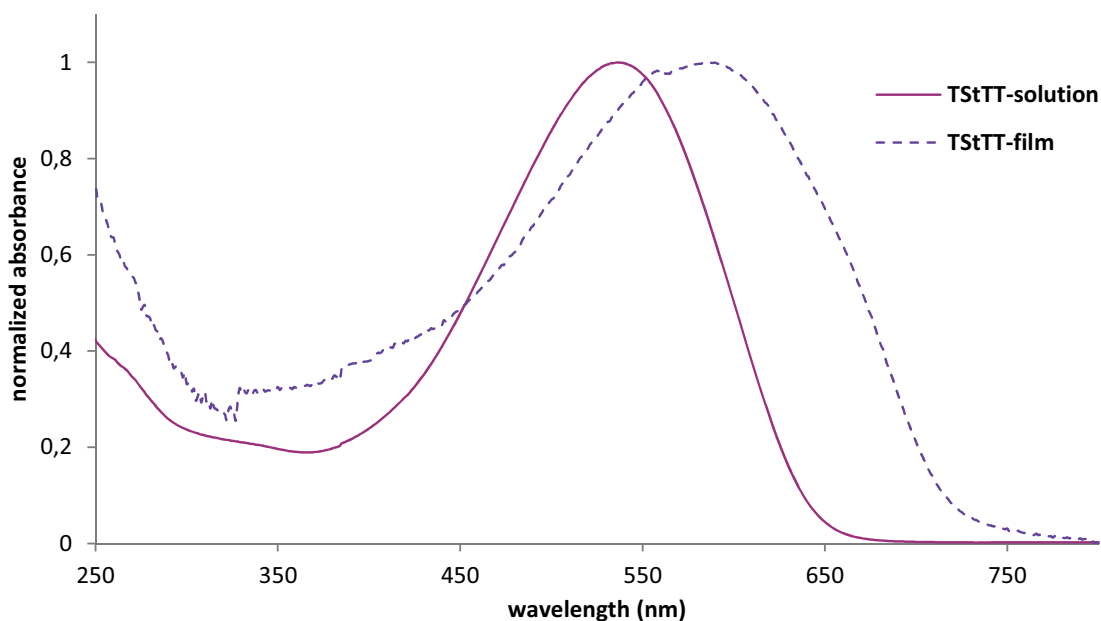


Figure SI 6. Full absorption spectra of TSstTT in solution (chloroform) and as film.

Luminescence Spectra

Luminescence spectra of polymer **TStTT** were recorded and compared to those of a rrP3HT with $n = 10$ repeat units (solvent: spectral grade chloroform, not degassed). The concentration of both polymers was identical in relation to the molecular masses of the repeat units: $c = 3.01 \times 10^{-6} \text{ mol L}^{-1}$ ($c = 2.38 \text{ mg L}^{-1}$ for **TStTT**; $c = 0.50 \text{ mg L}^{-1}$ for rrP3HT).

The luminescence was excited with the wavelengths of the absorption maxima, 536 nm for **TStTT** and 436 nm for rrP3HT ($n = 10$). Slit size was 10 nm, scan speed 120 nm min^{-1} .

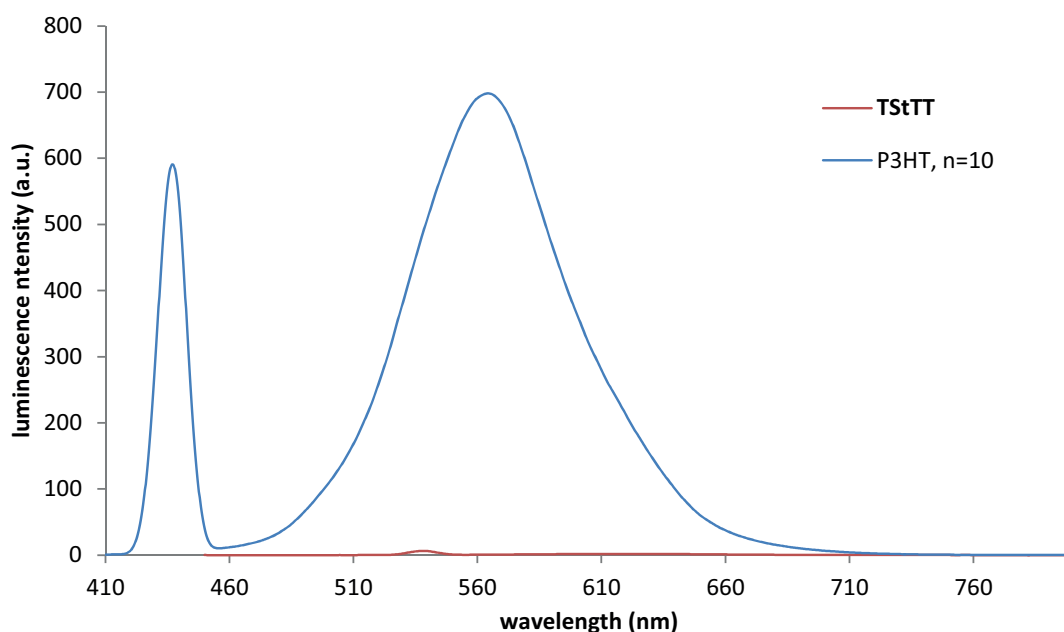


Figure SI 7. Luminescence spectra of **TStTT** and P3HT ($n = 10$) in solution (chloroform) at the same concentration (per repeat unit).

A strong luminescence was observed for P3HT (Figure SI 7, blue curve), while the stanole containing polymer **TStTT** showed only a very low intensity (red curve). The enlargement shows that the intensity is near the lower detection limit (Figure SI 8).

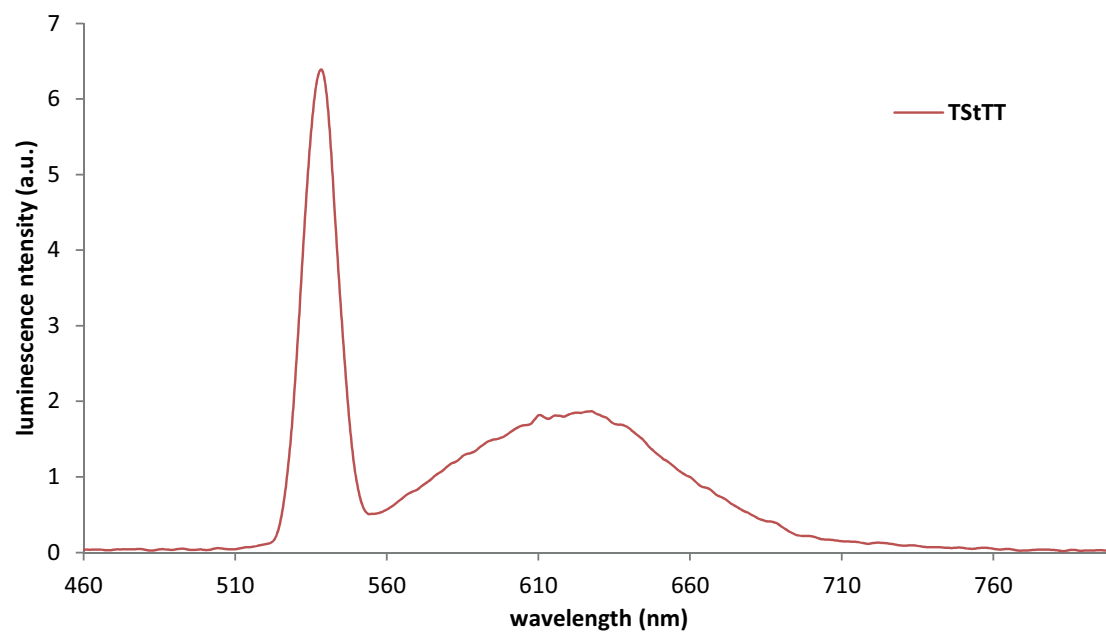
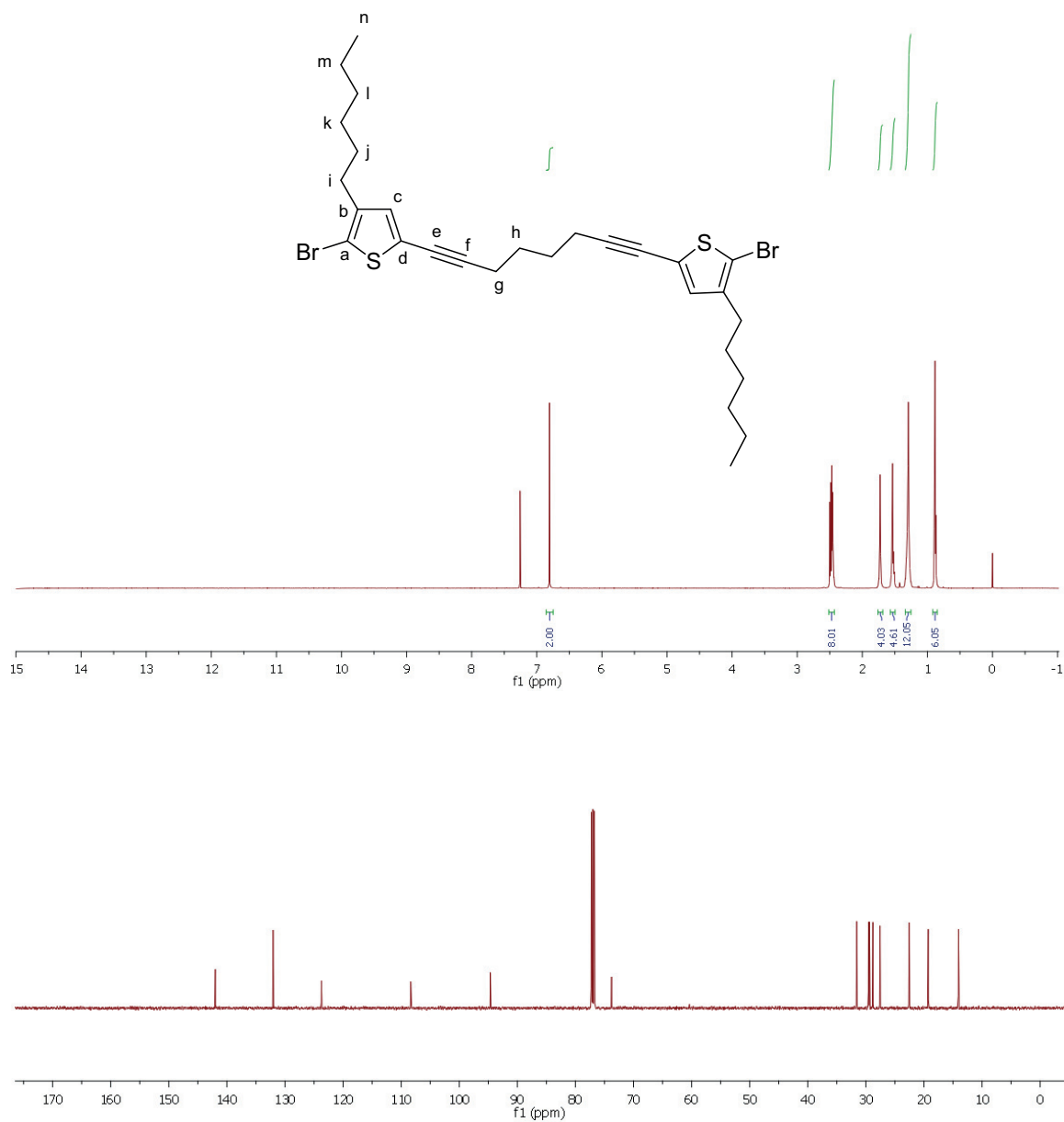
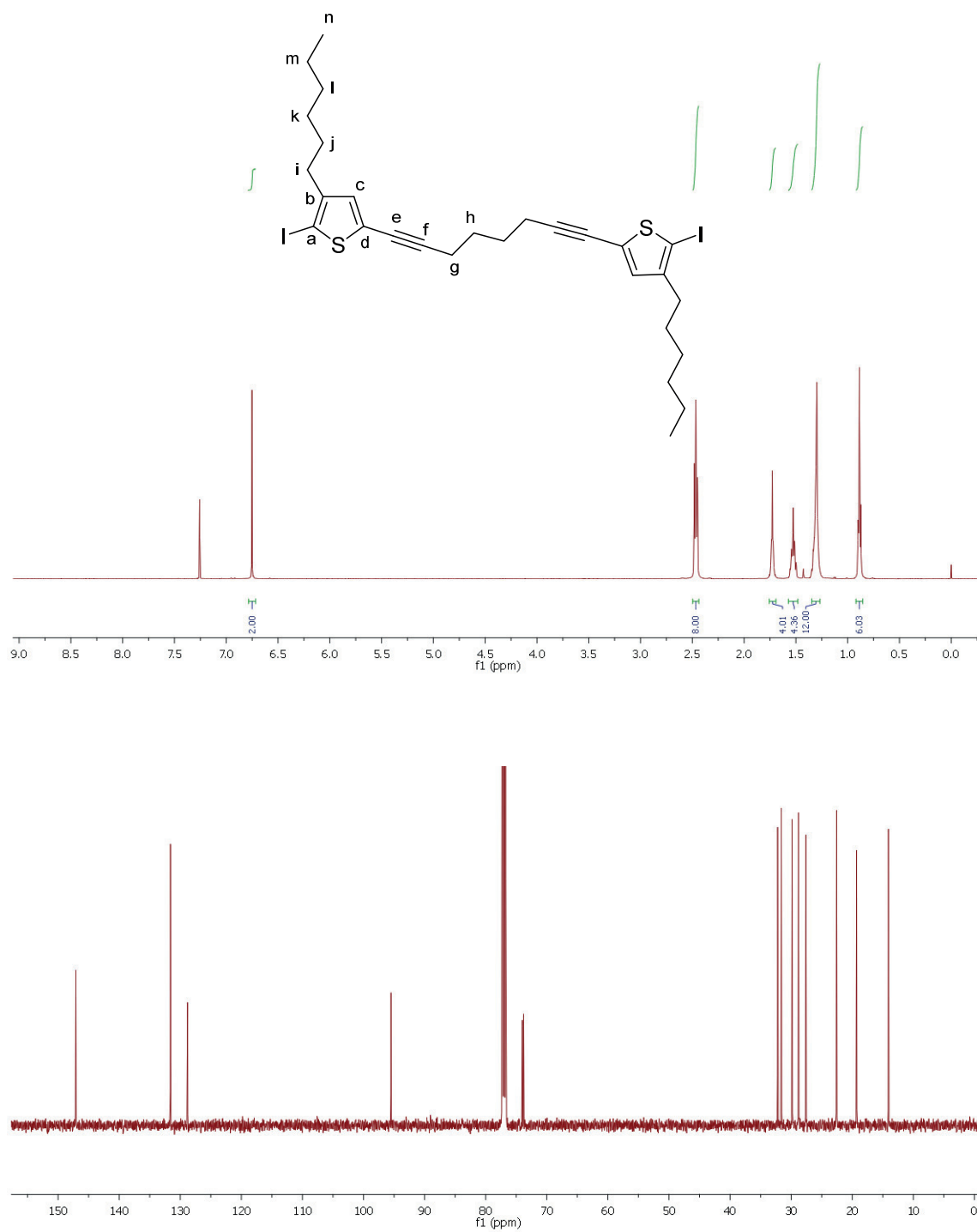
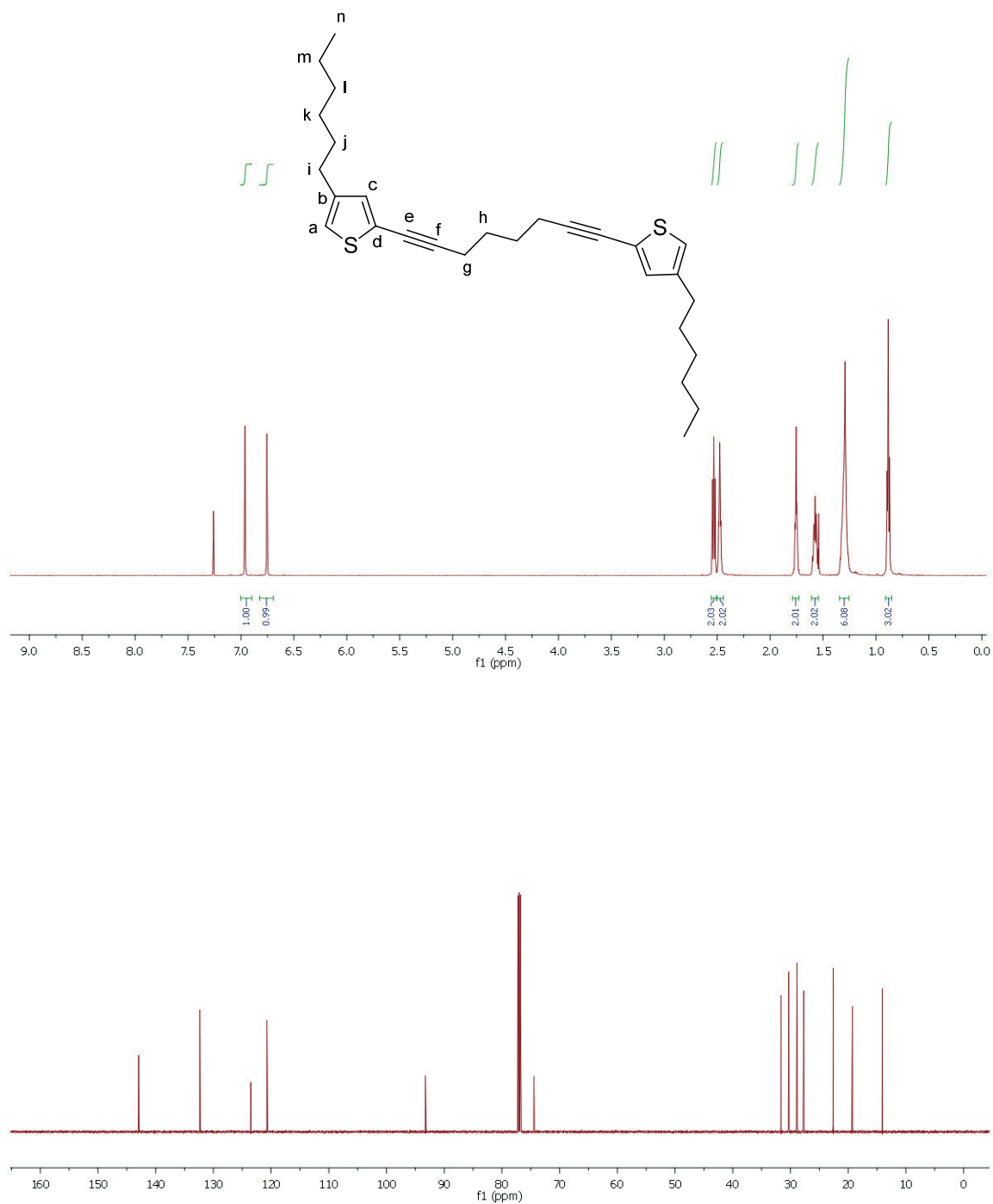
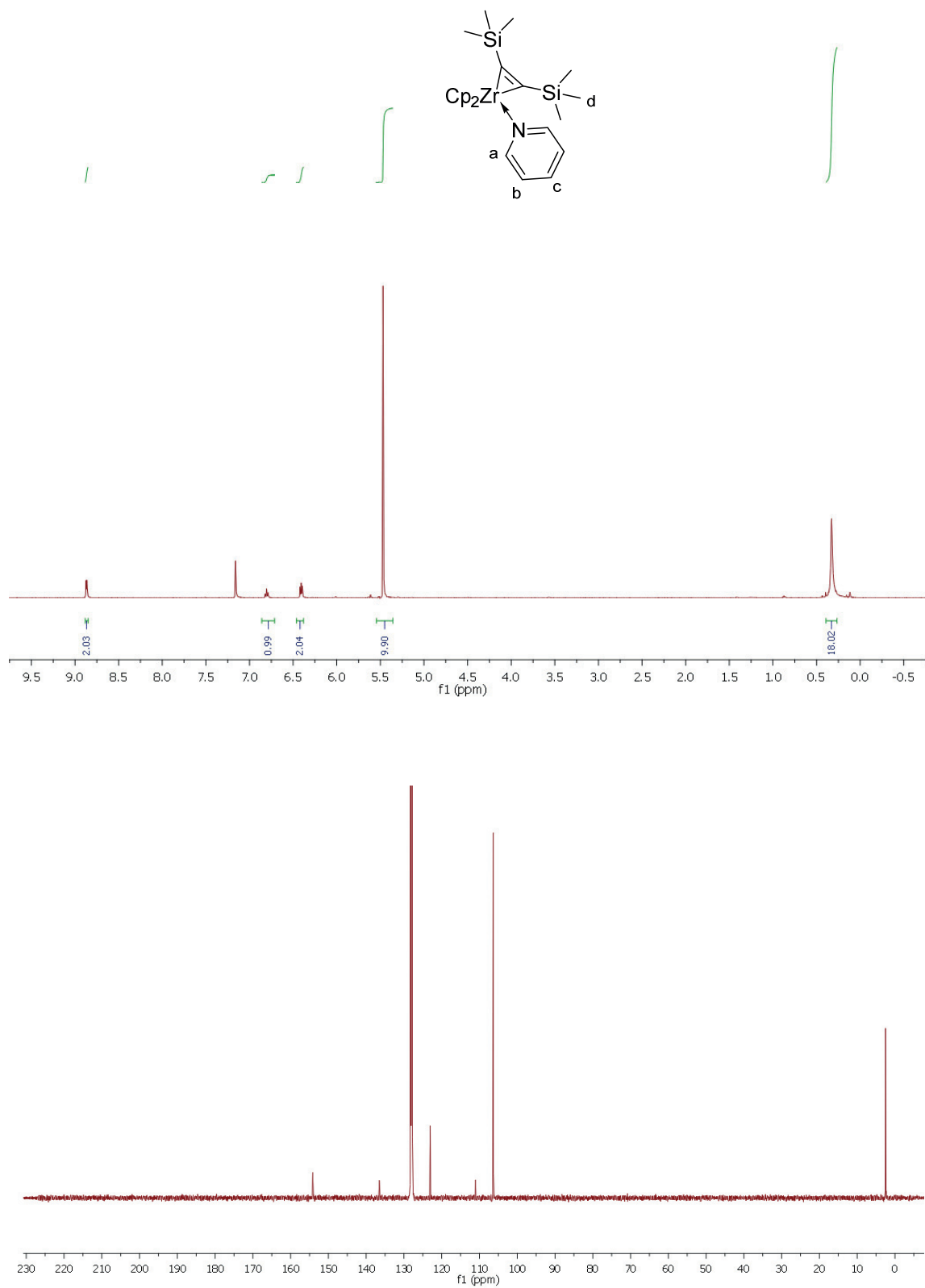


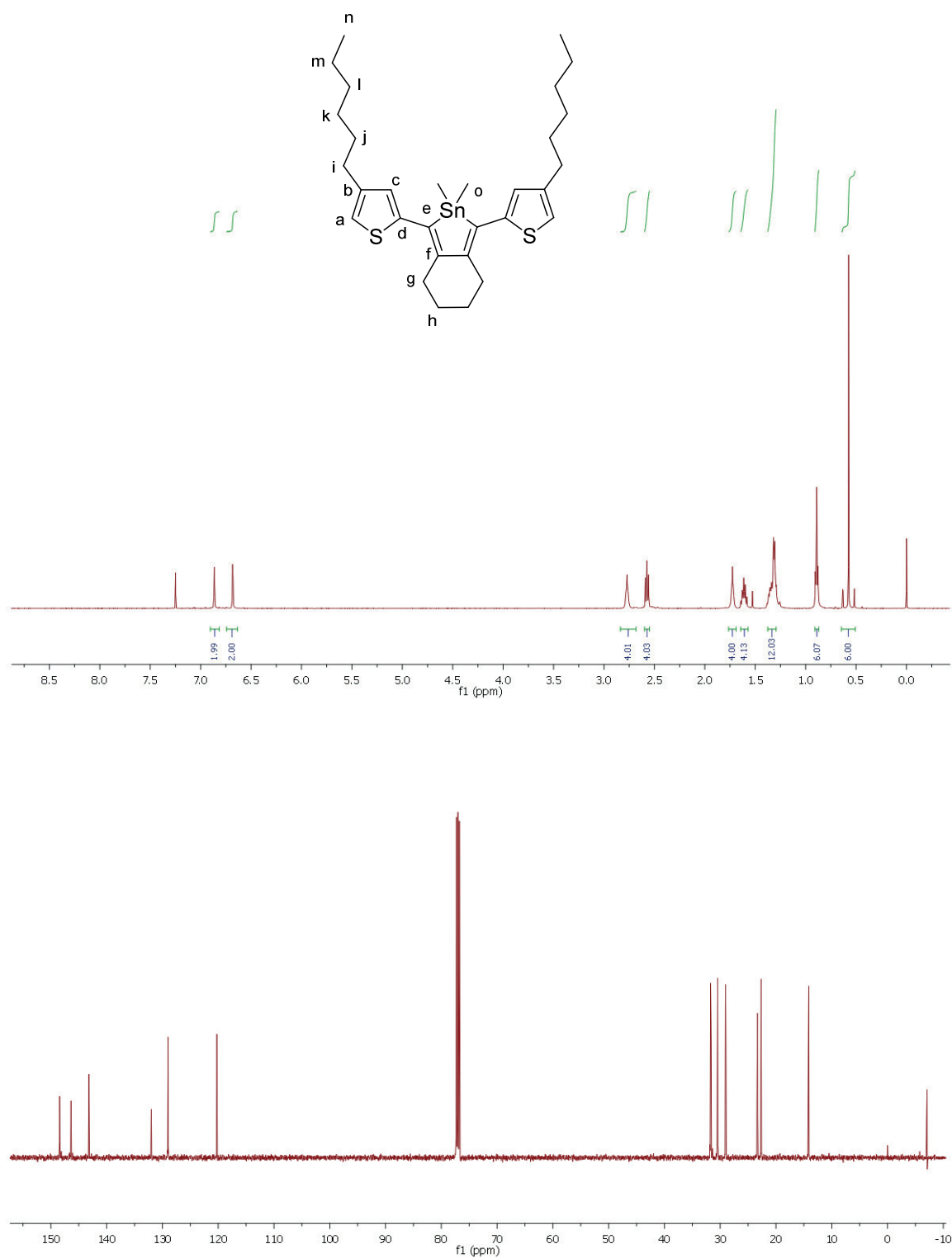
Figure SI 8. Enlargement of luminescence spectrum of **TStTT** (see figure SI 7).

^1H NMR Spectra and $^{13}\text{C}\{^1\text{H}\}$ NMR Spectra**1,8-Bis(5-bromo-4-hexylthiophen-2-yl)octa-1,7-diyne (5, CDCl_3)**

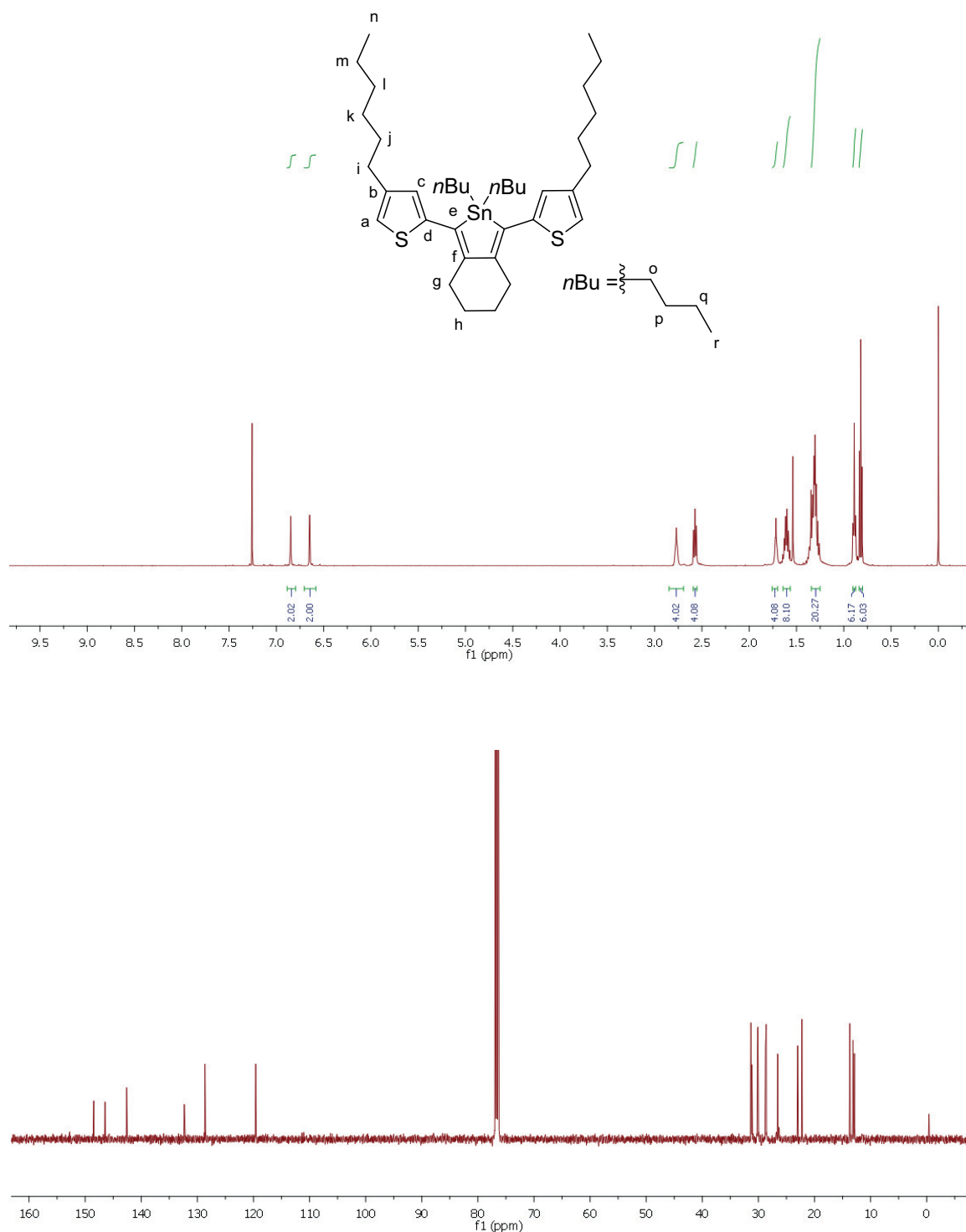
1,8-Bis(4-hexyl-5-iodothiophen-2-yl)octa-1,7-diyne (6b, CDCl₃)

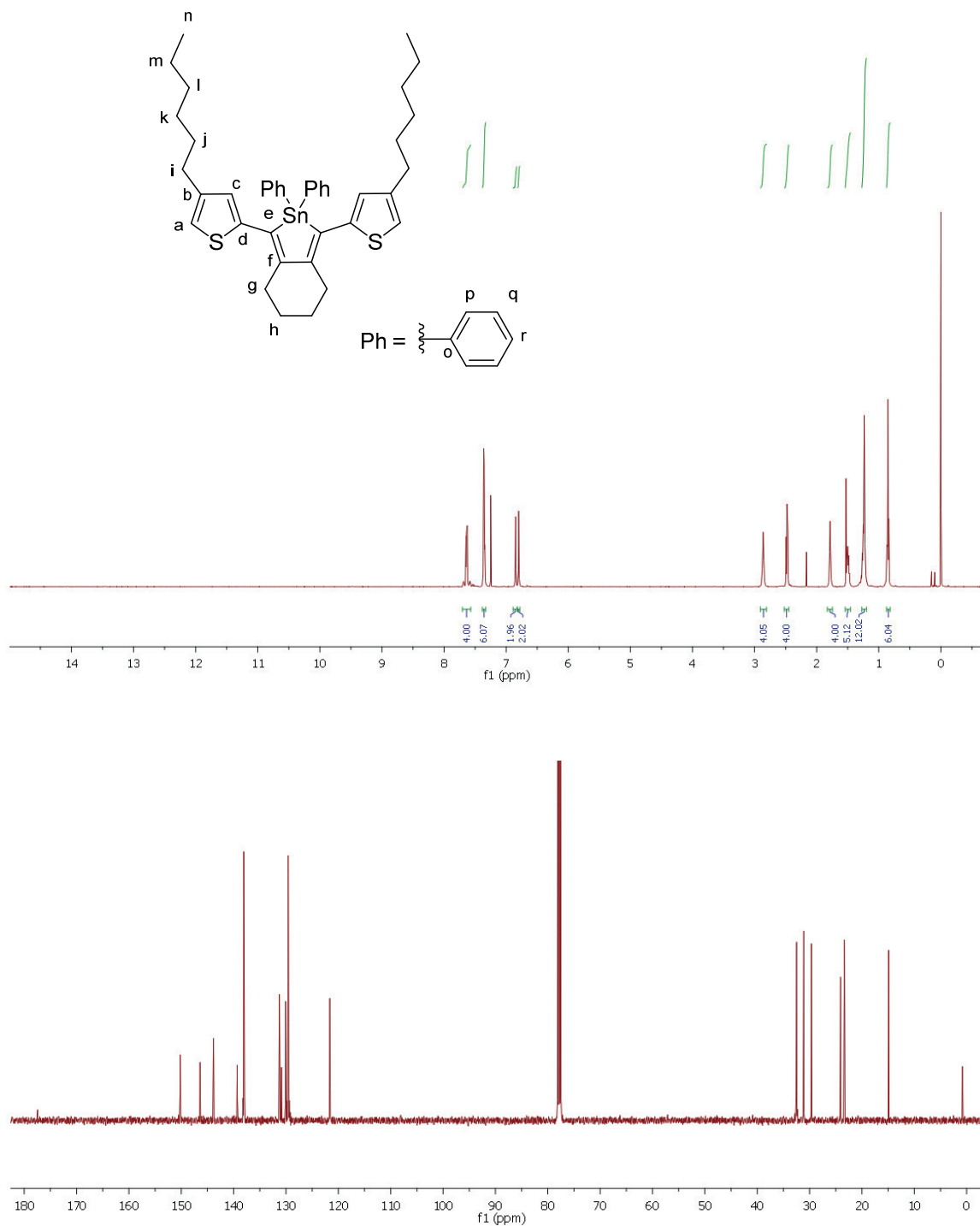
1,8-Bis(4-hexylthiophen-2-yl)octa-1,7-diyne (6a, CDCl₃)

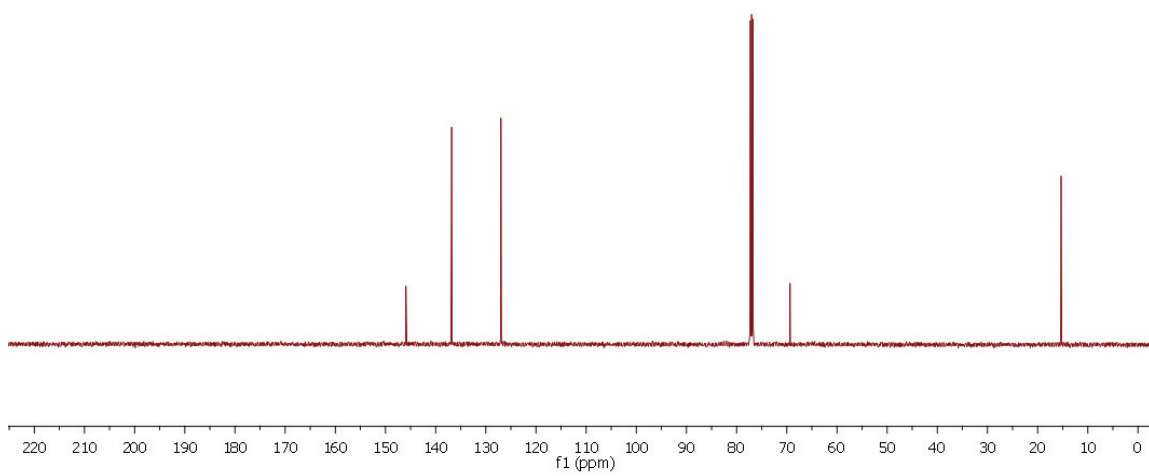
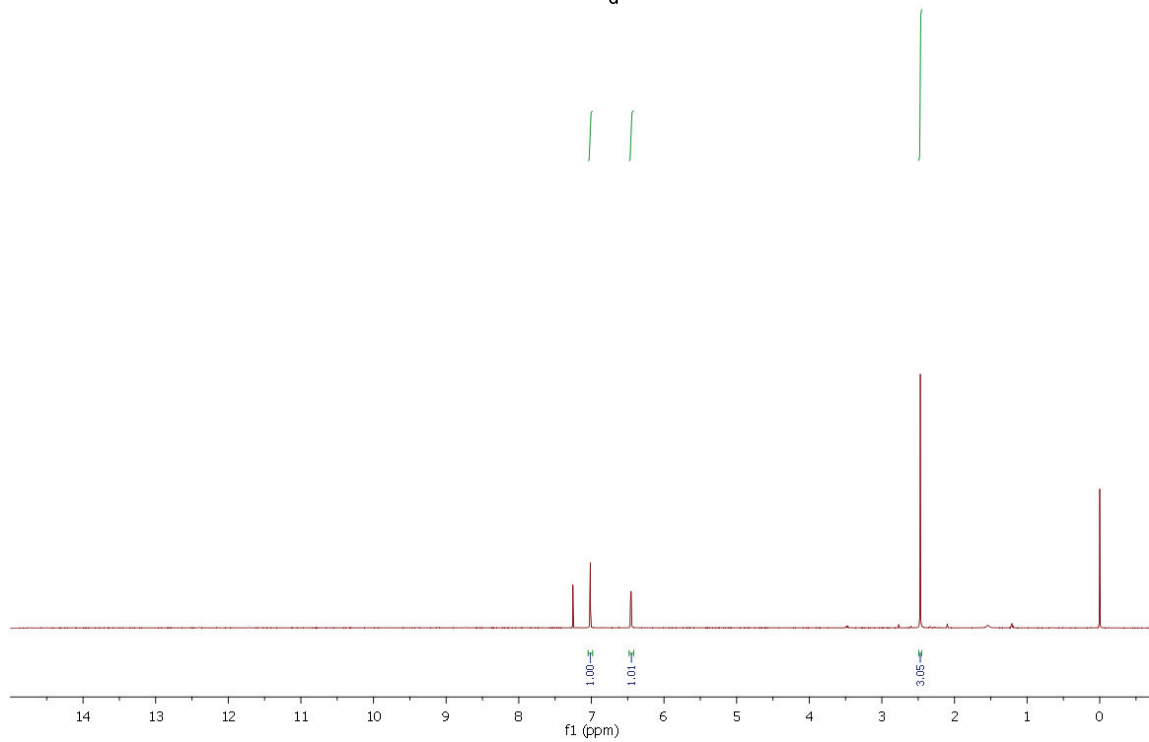
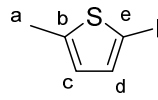
Cp₂Zr(pyr)(Me₃SiC≡CSiMe₃) (7, C₆D₆)

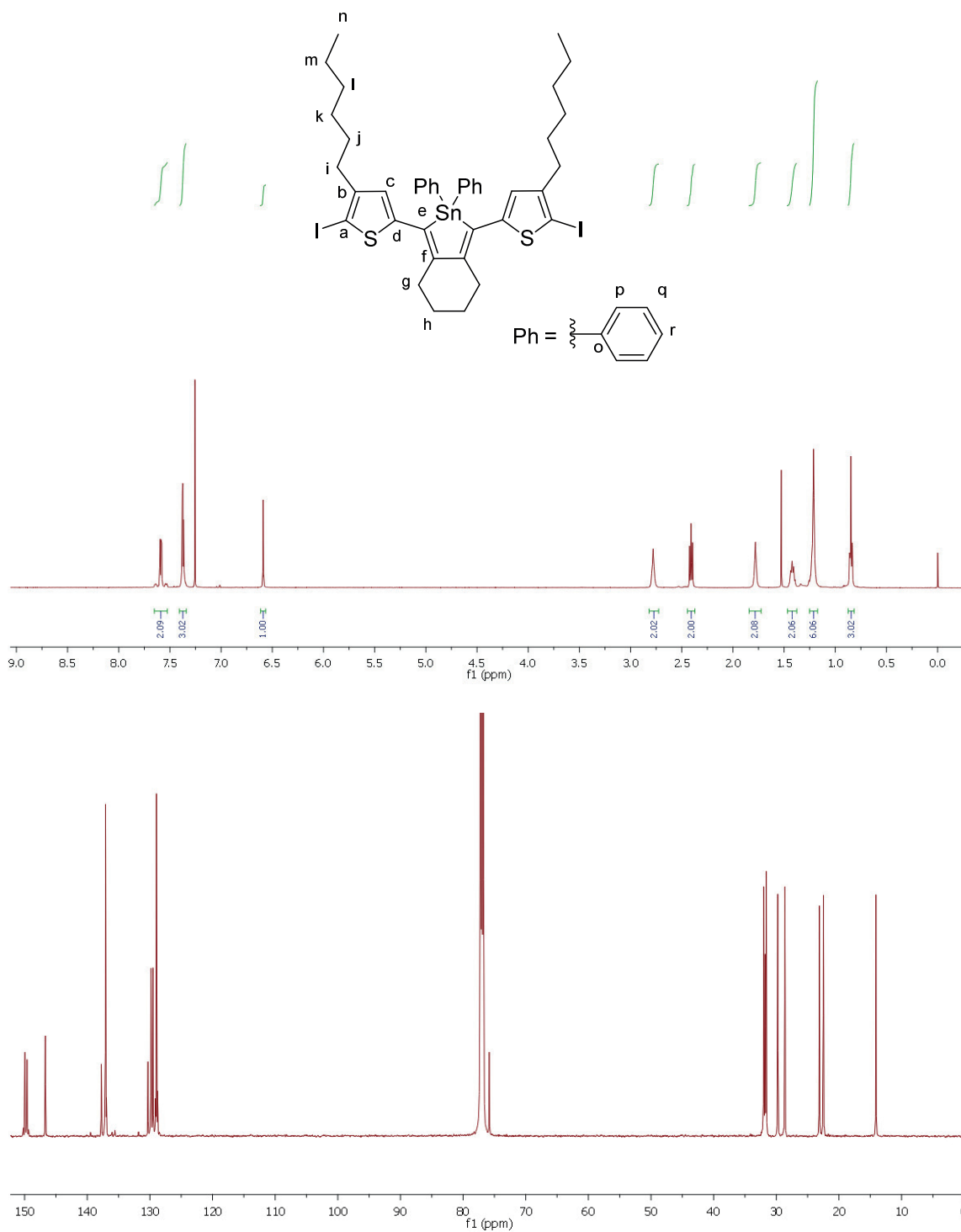
1,3-Bis(4-hexylthiophen-2-yl)-2,2-dimethyl-4,5,6,7-tetrahydro-2H-benzo[c]stannole (10, CDCl₃)

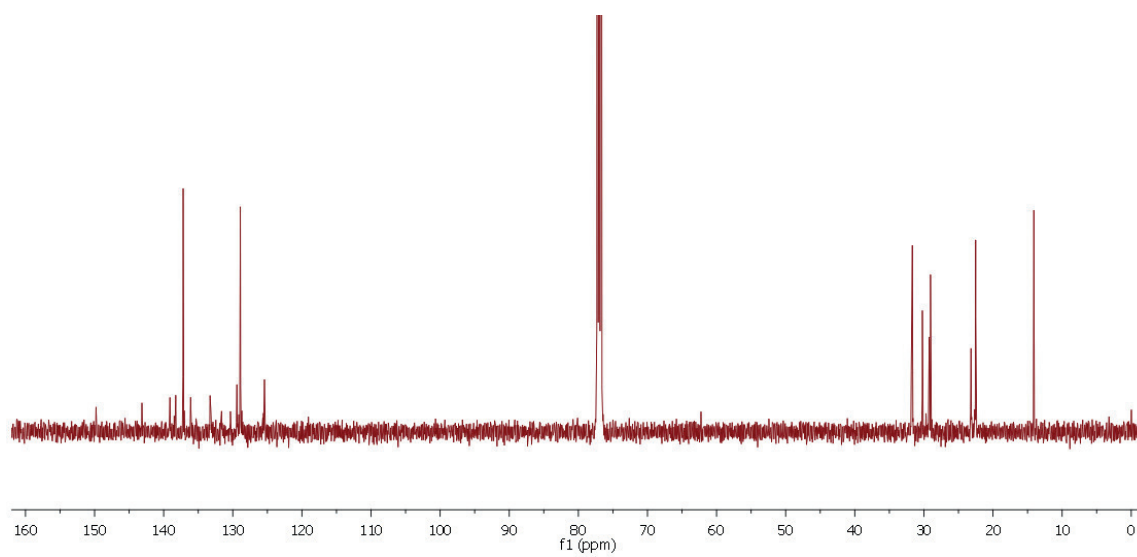
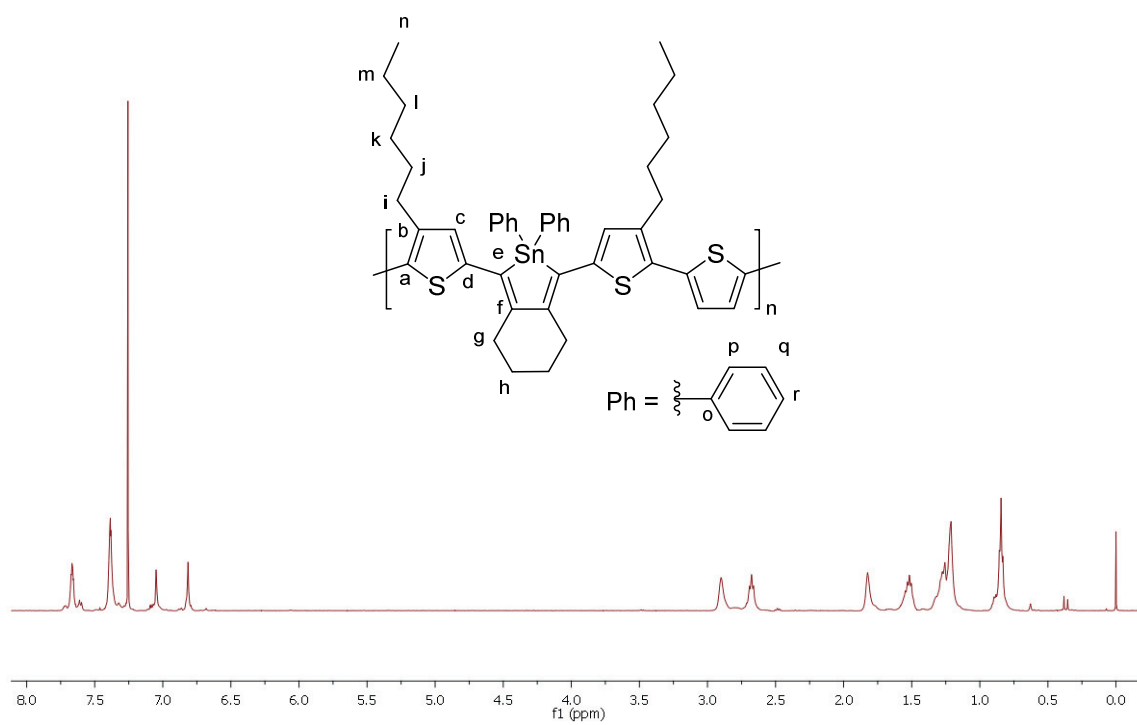
**2,2-Dibutyl-1,3-bis(4-hexylthiophen-2-yl)-4,5,6,7-tetrahydro-2H-benzo[c]stannole
(12, CDCl₃)**



1,3-Bis(4-hexylthiophen-2-yl)-2,2-diphenyl-4,5,6,7-tetrahydro-2H-benzo[*c*]stannole (11, CDCl₃)

2-Iodo-5-methylthiophene (13, CDCl₃)

1,3-Bis(4-hexyl-5-iodothiophen-2-yl)-2,2-diphenyl-4,5,6,7-tetrahydro-2H-benzo[c]stannole (9, CDCl₃)

Polymer TStTT (CDCl₃)

Single Crystal Data

1,3-Bis(4-hexyl-5-iodothiophen-2-yl)-2,2-diphenyl-4,5,6,7-tetrahydro-2H-benzo[c]stannole (9)

The data were measured using an Imaging Plate Diffraction System (IPDS-1) from STOE & CIE and were corrected for absorption using X-Red and X-Shape from STOE & CIE (Min/max. transmission: 0.4839/0.7604). The structure was solved with direct methods using SHELXS-97 and refinement was performed against F^2 using SHELXL-97. All non-hydrogen atoms except two disordered C atoms of lower occupancy (sof=0.25) were refined anisotropic. The C-H atoms were positioned with idealized geometry and refined *isotropic* with $U_{\text{iso}}(\text{H}) = 1.2 \cdot U_{\text{eq}}(\text{C})$ (1.5 for methyl H atoms). Two C atoms are disordered and were refined using a split model. Selected crystal data and details on the structure determination can be found in table 1-5 (see below).

CCDC 1009717 contains the supplementary crystallographic data for this paper. These data can be obtained free of charge from the Cambridge Crystallographic Data Centre via http://www.ccdc.cam.ac.uk/data_request/cif.

Table 1. Crystal data and structure refinement for $\text{C}_{40}\text{H}_{46}\text{I}_2\text{S}_2\text{Sn}$.

Empirical formula	$\text{C}_{40}\text{H}_{46}\text{I}_2\text{S}_2\text{Sn}$	
Formula weight	963.38	
Temperature	200(2) K	
Wavelength	0.71073 Å	
Crystal system	monoclinic	
Space group	$P2_1/c$	
Unit cell dimensions	$a = 15.9622(9)$ Å	$\alpha = 90^\circ$.
	$b = 25.4688(18)$ Å	$\beta = 96.753(7)^\circ$.
	$c = 9.4909(6)$ Å	$\gamma = 90^\circ$.
Volume	$3831.6(4)$ Å ³	
Z	4	
Density (calculated)	1.670 Mg/m ³	
Absorption coefficient	2.414 mm ⁻¹	
F(000)	1896	
Crystal size	0.15 x 0.1 x 0.06 mm ³	
Theta range for data collection	2.05 to 25.95°.	
Index ranges	-19 ≤ h ≤ 19, -31 ≤ k ≤ 31, -11 ≤ l ≤ 11	
Reflections collected	36970	

Independent reflections	7452 [R(int) = 0.0733]
Completeness to theta = 25.95°	99.3 %
Refinement method	Full-matrix least-squares on F ²
Data / restraints / parameters	7452 / 0 / 415
Goodness-of-fit on F ²	0.980
Final R indices [I > 2σ(I)]	R1 = 0.0359, wR2 = 0.0841
R indices (all data)	R1 = 0.0484, wR2 = 0.0894
Extinction coefficient	0.00253(17)
Largest diff. peak and hole	0.727 and -0.913 e.Å ⁻³

Table 2. Atomic coordinates ($\times 10^4$) and equivalent isotropic displacement parameters ($\text{\AA}^2 \times 10^3$).U(eq) is defined as one third of the trace of the orthogonalized U_{ij} tensor.

	x	y	z	U(eq)
Sn(1)	2937(1)	4431(1)	4971(1)	23(1)
C(1)	3889(2)	4747(1)	3806(4)	25(1)
C(2)	4399(2)	4342(1)	3483(4)	24(1)
C(3)	5115(3)	4429(1)	2593(4)	33(1)
C(4)	5372(4)	3939(2)	1829(7)	37(1)
C(5)	5599(4)	3524(2)	2957(8)	39(1)
C(4')	5705(14)	3933(8)	2600(30)	48(5)
C(5')	5258(15)	3437(8)	2330(20)	43(5)
C(6)	4793(2)	3349(2)	3587(4)	33(1)
C(7)	4251(2)	3803(1)	4010(4)	25(1)
C(8)	3608(2)	3714(1)	4813(4)	24(1)
C(11)	3915(2)	5295(1)	3441(4)	26(1)
C(12)	3344(3)	5665(1)	3794(4)	35(1)
C(13)	3482(3)	6188(1)	3343(4)	34(1)
C(14)	4173(3)	6204(1)	2639(4)	33(1)
C(15)	2961(3)	6662(2)	3677(5)	46(1)
C(16)	2075(3)	6529(2)	4009(5)	42(1)
C(17)	1492(3)	6341(2)	2734(5)	47(1)
C(18)	620(3)	6182(2)	3058(5)	50(1)
C(19)	6(4)	6077(2)	1733(6)	62(1)
C(20)	-844(4)	5889(3)	2016(7)	75(2)
S(1)	4658(1)	5609(1)	2518(1)	31(1)
I(1)	4703(1)	6866(1)	1794(1)	46(1)
C(21)	3282(2)	3227(1)	5322(4)	25(1)
C(22)	2642(2)	3181(1)	6164(4)	27(1)
C(23)	2389(2)	2664(1)	6469(4)	28(1)
C(24)	2855(2)	2314(1)	5797(4)	29(1)
C(25)	1681(3)	2529(2)	7322(4)	34(1)
C(26)	846(3)	2429(2)	6402(4)	35(1)
C(27)	124(3)	2285(2)	7246(5)	43(1)
C(28)	-689(3)	2152(2)	6318(5)	40(1)
C(29)	-1441(3)	2041(2)	7095(6)	53(1)
C(30)	-2252(3)	1928(2)	6121(7)	64(2)
S(2)	3592(1)	2595(1)	4872(1)	28(1)
I(2)	2723(1)	1500(1)	5783(1)	46(1)
C(31)	2791(2)	4772(1)	6989(4)	25(1)
C(32)	2273(3)	5213(1)	7026(4)	34(1)
C(33)	2225(3)	5479(2)	8295(5)	45(1)
C(34)	2689(3)	5312(2)	9527(5)	45(1)
C(35)	3184(3)	4868(2)	9510(4)	41(1)
C(36)	3237(2)	4602(2)	8249(4)	30(1)
C(41)	1733(3)	4459(1)	3694(4)	30(1)
C(42)	1672(3)	4684(2)	2370(5)	46(1)
C(43)	910(4)	4703(2)	1521(6)	61(1)
C(44)	197(4)	4509(2)	1985(6)	65(2)
C(45)	250(4)	4269(3)	3262(7)	90(2)
C(46)	1018(3)	4248(3)	4137(6)	77(2)

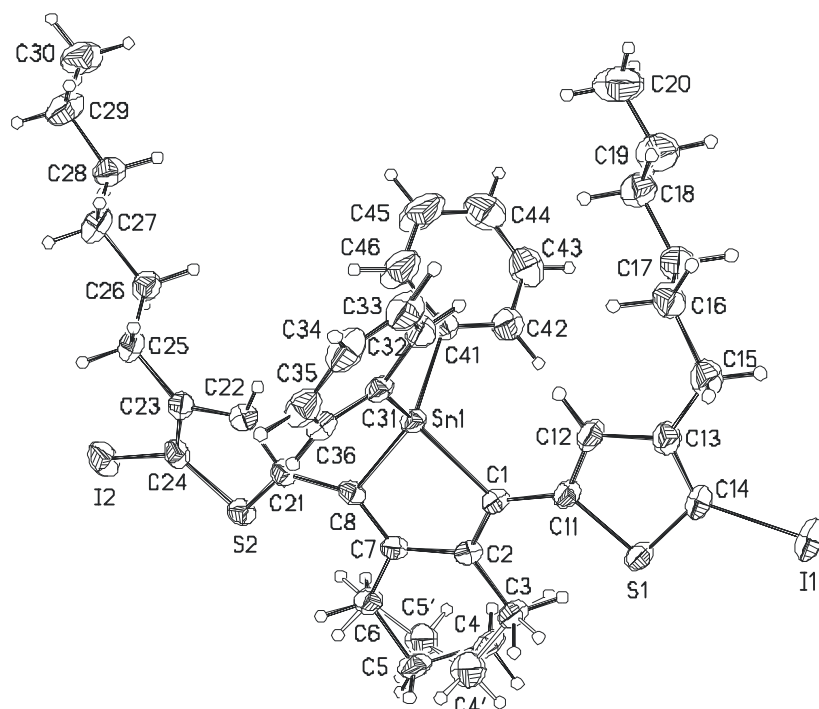


Table 3. Bond lengths [Å] and angles [°].

Sn(1)-C(8)	2.133(3)	Sn(1)-C(31)	2.140(3)
Sn(1)-C(1)	2.139(3)	Sn(1)-C(41)	2.150(4)
C(1)-C(2)	1.373(5)	C(21)-C(22)	1.373(5)
C(1)-C(11)	1.440(5)	C(21)-S(2)	1.751(3)
C(2)-C(7)	1.488(5)	C(22)-C(23)	1.417(5)
C(2)-C(3)	1.515(5)	C(23)-C(24)	1.366(5)
C(3)-C(4)	1.523(6)	C(23)-C(25)	1.505(5)
C(3)-C(4')	1.58(2)	C(24)-S(2)	1.706(4)
C(4)-C(5)	1.517(9)	C(24)-I(2)	2.083(3)
C(5)-C(6)	1.547(6)	C(25)-C(26)	1.528(6)
C(4')-C(5')	1.46(3)	C(26)-C(27)	1.523(6)
C(5')-C(6)	1.49(2)	C(27)-C(28)	1.518(6)
C(6)-C(7)	1.527(5)	C(28)-C(29)	1.508(6)
C(7)-C(8)	1.368(5)	C(29)-C(30)	1.527(8)
C(8)-C(21)	1.449(5)	C(31)-C(36)	1.387(5)
C(11)-C(12)	1.379(5)	C(31)-C(32)	1.399(5)
C(11)-S(1)	1.748(4)	C(32)-C(33)	1.392(6)
C(12)-C(13)	1.423(5)	C(33)-C(34)	1.376(7)
C(13)-C(14)	1.356(6)	C(34)-C(35)	1.380(7)
C(13)-C(15)	1.519(5)	C(35)-C(36)	1.386(6)
C(14)-S(1)	1.711(4)	C(41)-C(46)	1.372(6)
C(14)-I(1)	2.087(4)	C(41)-C(42)	1.373(6)
C(15)-C(16)	1.523(6)	C(42)-C(43)	1.379(7)
C(16)-C(17)	1.515(7)	C(43)-C(44)	1.360(8)
C(17)-C(18)	1.515(6)	C(44)-C(45)	1.351(8)
C(18)-C(19)	1.525(8)	C(45)-C(46)	1.398(8)
C(19)-C(20)	1.492(8)		

Table 3. Bond lengths [\AA] and angles [$^\circ$].

C(8)-Sn(1)-C(1)	83.85(14)	C(8)-Sn(1)-C(41)	114.30(14)
C(8)-Sn(1)-C(31)	121.25(13)	C(1)-Sn(1)-C(41)	109.77(14)
C(1)-Sn(1)-C(31)	118.01(13)	C(31)-Sn(1)-C(41)	107.88(14)
C(2)-C(1)-C(11)	129.9(3)	C(14)-S(1)-C(11)	91.86(18)
C(1)-C(2)-C(7)	119.8(3)	C(22)-C(21)-C(8)	126.0(3)
C(1)-C(2)-C(3)	121.3(3)	C(22)-C(21)-S(2)	108.4(2)
C(7)-C(2)-C(3)	118.8(3)	C(8)-C(21)-S(2)	125.5(3)
C(2)-C(3)-C(4)	114.1(3)	C(21)-C(22)-C(23)	116.6(3)
C(2)-C(3)-C(4')	111.7(8)	C(24)-C(23)-C(22)	109.0(3)
C(4)-C(3)-C(4')	31.9(8)	C(24)-C(23)-C(25)	125.9(3)
C(5)-C(4)-C(3)	106.9(5)	C(22)-C(23)-C(25)	125.0(3)
C(4)-C(5)-C(6)	109.4(5)	C(23)-C(24)-S(2)	114.4(3)
C(5')-C(4')-C(3)	114.4(17)	C(23)-C(24)-I(2)	126.3(3)
C(4')-C(5')-C(6)	105.6(16)	S(2)-C(24)-I(2)	119.3(2)
C(5')-C(6)-C(7)	116.5(8)	C(23)-C(25)-C(26)	113.0(3)
C(5')-C(6)-C(5)	30.0(8)	C(27)-C(26)-C(25)	113.7(3)
C(7)-C(6)-C(5)	114.0(3)	C(28)-C(27)-C(26)	113.3(4)
C(8)-C(7)-C(2)	120.0(3)	C(29)-C(28)-C(27)	115.6(4)
C(8)-C(7)-C(6)	120.4(3)	C(28)-C(29)-C(30)	114.0(5)
C(2)-C(7)-C(6)	119.5(3)	C(24)-S(2)-C(21)	91.59(17)
C(7)-C(8)-C(21)	130.6(3)	C(36)-C(31)-C(32)	118.3(3)
C(12)-C(11)-C(1)	124.4(3)	C(36)-C(31)-Sn(1)	123.1(3)
C(12)-C(11)-S(1)	108.4(3)	C(32)-C(31)-Sn(1)	118.3(3)
C(1)-C(11)-S(1)	127.2(3)	C(33)-C(32)-C(31)	120.4(4)
C(11)-C(12)-C(13)	115.9(3)	C(34)-C(33)-C(32)	120.3(4)
C(14)-C(13)-C(12)	109.9(3)	C(33)-C(34)-C(35)	119.8(4)
C(14)-C(13)-C(15)	125.1(3)	C(34)-C(35)-C(36)	120.2(4)
C(12)-C(13)-C(15)	124.9(4)	C(35)-C(36)-C(31)	121.0(4)
C(13)-C(14)-S(1)	114.0(3)	C(46)-C(41)-C(42)	118.2(4)
C(13)-C(14)-I(1)	127.1(3)	C(46)-C(41)-Sn(1)	122.3(3)
S(1)-C(14)-I(1)	118.8(2)	C(42)-C(41)-Sn(1)	119.5(3)
C(13)-C(15)-C(16)	114.3(3)	C(41)-C(42)-C(43)	120.8(5)
C(17)-C(16)-C(15)	113.8(4)	C(44)-C(43)-C(42)	120.9(5)
C(18)-C(17)-C(16)	114.5(4)	C(45)-C(44)-C(43)	119.1(5)
C(17)-C(18)-C(19)	113.4(4)	C(44)-C(45)-C(46)	120.6(5)
C(20)-C(19)-C(18)	114.7(5)	C(41)-C(46)-C(45)	120.3(5)

Table 4. Anisotropic displacement parameters ($\text{\AA}^2 \times 10^3$). The anisotropic displacement factor exponent takes the form: $-2\pi^2 [h^2 a^{*2} U^{11} + \dots + 2 h k a^* b^* U^{12}]$

	U ¹¹	U ²²	U ³³	U ²³	U ¹³	U ¹²
Sn(1)	22(1)	21(1)	27(1)	-1(1)	9(1)	1(1)
C(1)	22(2)	27(2)	28(2)	-1(1)	6(1)	-3(1)
C(2)	20(2)	27(2)	26(2)	-4(1)	4(1)	-1(1)
C(3)	29(2)	27(2)	45(2)	-4(2)	15(2)	-4(2)
C(4)	34(3)	40(3)	41(3)	-7(2)	25(3)	-5(2)
C(5)	25(3)	36(3)	60(4)	-3(3)	20(3)	3(2)
C(6)	29(2)	29(2)	41(2)	0(2)	12(2)	6(2)
C(7)	20(2)	26(2)	29(2)	-1(1)	2(1)	1(1)
C(8)	24(2)	20(2)	28(2)	-3(1)	1(1)	5(1)
C(11)	26(2)	23(2)	31(2)	-2(1)	9(2)	-5(1)
C(12)	36(2)	25(2)	47(2)	4(2)	19(2)	-3(2)
C(13)	38(2)	23(2)	42(2)	2(2)	9(2)	-1(2)
C(14)	38(2)	26(2)	37(2)	4(2)	8(2)	-9(2)
C(15)	51(3)	25(2)	64(3)	4(2)	17(2)	4(2)
C(16)	51(3)	29(2)	50(3)	1(2)	19(2)	11(2)
C(17)	47(3)	44(2)	52(3)	3(2)	19(2)	10(2)
C(18)	47(3)	48(3)	58(3)	6(2)	21(2)	5(2)
C(19)	53(3)	76(4)	58(3)	1(3)	11(3)	3(3)
C(20)	43(3)	103(5)	78(4)	0(4)	7(3)	9(3)
S(1)	28(1)	30(1)	38(1)	1(1)	12(1)	-6(1)
I(1)	57(1)	33(1)	50(1)	6(1)	14(1)	-17(1)
C(21)	28(2)	18(2)	28(2)	-1(1)	3(1)	0(1)
C(22)	28(2)	28(2)	25(2)	-4(1)	4(2)	-1(1)
C(23)	28(2)	29(2)	26(2)	0(1)	0(2)	-4(1)
C(24)	33(2)	19(2)	34(2)	2(1)	-5(2)	-4(1)
C(25)	39(2)	36(2)	26(2)	4(2)	6(2)	-8(2)
C(26)	35(2)	41(2)	31(2)	1(2)	5(2)	-2(2)
C(27)	47(3)	49(2)	34(2)	1(2)	14(2)	-12(2)
C(28)	35(2)	41(2)	46(2)	-3(2)	10(2)	2(2)
C(29)	46(3)	51(3)	67(3)	-6(2)	25(2)	-12(2)
C(30)	41(3)	49(3)	104(5)	-3(3)	18(3)	-9(2)
S(2)	28(1)	22(1)	36(1)	-4(1)	3(1)	2(1)
I(2)	51(1)	22(1)	61(1)	4(1)	-8(1)	-2(1)
C(31)	23(2)	23(2)	30(2)	-3(1)	11(1)	-1(1)
C(32)	39(2)	26(2)	41(2)	-1(2)	15(2)	5(2)
C(33)	54(3)	30(2)	55(3)	-8(2)	29(2)	1(2)
C(34)	59(3)	41(2)	38(2)	-12(2)	23(2)	-13(2)
C(35)	41(3)	52(2)	29(2)	-1(2)	6(2)	-13(2)
C(36)	26(2)	34(2)	32(2)	3(2)	9(2)	-2(2)
C(41)	30(2)	32(2)	30(2)	0(1)	6(2)	2(2)
C(42)	39(3)	54(3)	44(3)	11(2)	3(2)	-1(2)
C(43)	60(4)	75(4)	44(3)	18(2)	-5(2)	6(3)
C(44)	43(3)	83(4)	63(3)	5(3)	-15(3)	3(3)
C(45)	35(3)	166(7)	66(4)	37(4)	-3(3)	-30(4)
C(46)	39(3)	142(6)	48(3)	37(3)	-5(2)	-25(3)

Table 5. Hydrogen coordinates ($\times 10^4$) and isotropic displacement parameters ($\text{\AA}^2 \times 10^{-3}$).

	x	y	z	U(eq)
H(3A)	5611	4561	3214	39
H(3B)	4944	4703	1878	39
H(3C)	5453	4735	2966	39
H(3D)	4878	4508	1604	39
H(4A)	4900	3816	1137	44
H(4B)	5863	4015	1313	44
H(5A)	6013	3668	3717	47
H(5B)	5860	3218	2533	47
H(4C)	6094	3981	1872	58
H(4D)	6052	3911	3535	58
H(5C)	5660	3147	2233	51
H(5D)	4859	3458	1451	51
H(6A)	4449	3128	2880	39
H(6B)	4959	3129	4434	39
H(6C)	5211	3262	4410	39
H(6D)	4425	3038	3394	39
H(12)	2888	5577	4307	42
H(15A)	2918	6904	2857	55
H(15B)	3263	6849	4500	55
H(16A)	2114	6253	4748	50
H(16B)	1826	6845	4404	50
H(17A)	1432	6625	2016	56
H(17B)	1757	6037	2310	56
H(18A)	389	6464	3616	60
H(18B)	669	5861	3652	60
H(19A)	-65	6404	1170	75
H(19B)	257	5811	1148	75
H(20A)	-1197	5830	1113	112
H(20B)	-1108	6154	2568	112
H(20C)	-784	5560	2552	112
H(22)	2383	3480	6524	32
H(25A)	1606	2820	7986	40
H(25B)	1838	2211	7895	40
H(26A)	688	2748	5836	43
H(26B)	925	2140	5731	43
H(27A)	295	1980	7861	51
H(27B)	18	2584	7870	51
H(28A)	-832	2448	5657	48
H(28B)	-586	1840	5739	48
H(29A)	-1536	2347	7700	64
H(29B)	-1310	1735	7728	64
H(30A)	-2711	1860	6696	96
H(30B)	-2169	1619	5535	96
H(30C)	-2395	2232	5507	96
H(32)	1952	5332	6180	41
H(33)	1869	5777	8312	53
H(34)	2670	5501	10385	54
H(35)	3489	4744	10365	49
H(36)	3584	4299	8248	36
H(42)	2161	4827	2034	55
H(43)	882	4854	601	73
H(44)	-332	4542	1417	78
H(45)	-238	4114	3568	108
H(46)	1044	4086	5043	92

References

- [1] A. C. J. Heinrich, B. Thiedemann, P. J. Gates, A. Staubitz, *Org. Lett.* **2013**, *15*, 4666-4669.
- [2] J. Linshoef, A. C. J. Heinrich, S. A. W. Segler, P. J. Gates, A. Staubitz, *Org. Lett.* **2012**, *14*, 5644-5647.
- [3] J. R. Nitschke, S. Zürcher, T. D. Tilley, *J. Am. Chem. Soc.* **2000**, *122*, 10345-10352.
- [4] H. J. Reich, W. L. Whipple, *Can. J. Chem.* **2005**, *83*, 1577-1587.

5.3 Supporting Information for *Acta Cryst.* 2014, E70, o1133-o1134.

supporting information

supporting information

Acta Cryst. (2014). E70, o1133–o1134 [doi:10.1107/S1600536814019667]

Crystal structure of 1,3-bis(4-hexyl-5-iodothiophen-2-yl)-4,5,6,7-tetrahydro-2-benzothiophene

Julian Linshoef, Christian Näther and Anne Staubitz

S1. Experimental

S1.1. Synthesis and crystallization

1,8-Bis(4-hexyl-5-iodothiophen-2-yl)octa-1,7-diyne and $\text{Cp}_2\text{Zr}(\text{pyr})(\text{Me}_3\text{SiCCSiMe}_3)$ were prepared as previously described by Linshoef *et al.* (2014). CuCl (99.995+ %) was bought from Alfa Aesar, S_2Cl_2 (98 %) from VWR. Toluene was dried over sodium with benzophenone as an indicator, degassed by freeze-pump-thaw technique and stored over 3 Å molecular sieve in a glovebox.

1,8-Bis(4-hexyl-5-iodothiophen-2-yl)octa-1,7-diyne (716 mg, 1.04 mmol) and $\text{Cp}_2\text{Zr}(\text{pyr})(\text{Me}_3\text{SiCCSiMe}_3)$ (513 mg, 1.09 mmol) were dissolved in toluene (10 mL) and the dark red solution was stirred for 18 h at 20 °C under nitrogen. CuCl (10.3 mg, 104 μmol) and toluene (2 mL) were added in a glovebox under an atmosphere of nitrogen and the reaction mixture was cooled to 0 °C. S_2Cl_2 (147 mg, 1.09 mmol) was added dropwise within 1 min, resulting in an immediate color change from dark red to orange. The reaction mixture was stirred for 1 h at 0 °C, then for another 2 h at 20 °C, before it was quenched with water (50 mL). The aqueous layer was extracted with cyclohexane (3 x 80 mL). The combined organic layers were dried over magnesium sulfate. The volatiles were removed *in vacuo* and the crude product was filtered over a short plug of silica (cyclohexane; 3 x 4 cm). After removal of the volatiles, the orange oil was purified by column chromatography (*n*-hexane; $R_f = 0.62$) to obtain 395 mg (53 %) of a yellow oil that crystallized after 14 h at 7 °C.

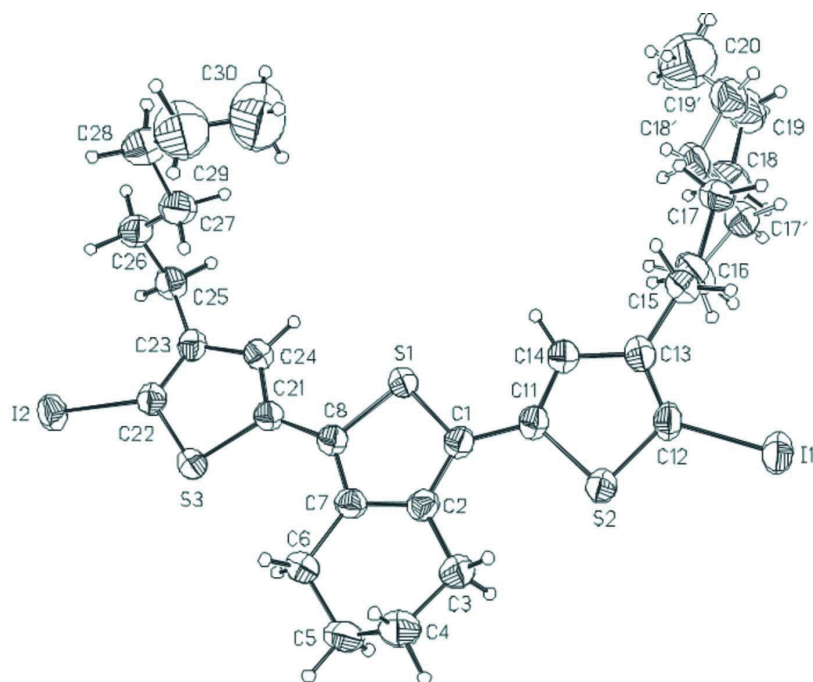
Single crystals could be obtained from a saturated solution (*n*-pentane) at 7 °C.

$^1\text{H NMR}$ (500 MHz, CDCl_3): $\delta = 6.79$ (s, 2 H, Tph-H), 2.72 – 2.81 (m, 4 H, $-\text{CH}_2\text{CH}_2\text{CH}_2\text{CH}_2-$), 2.52 (t, $^3J = 7.7$ Hz, 4 H, $-\text{CH}_2(\text{CH}_2)_4\text{CH}_3$), 1.81 – 1.76 (m, 4 H, $-\text{CH}_2\text{CH}_2\text{CH}_2\text{CH}_2-$), 1.62 – 1.55 (m, 4 H, $-\text{CH}_2\text{CH}_2(\text{CH}_2)_3\text{CH}_3$), 1.38 – 1.30 (m, 12 H, $-(\text{CH}_2)_2\text{CH}_2\text{CH}_2\text{CH}_2\text{CH}_3$), 0.87 – 0.80 (m, 6 H, $-(\text{CH}_2)_5\text{CH}_3$) ppm. **$^{13}\text{C NMR}$** (126 MHz, CDCl_3): $\delta = 147.6$ (Tph-C), 141.0 (Tph-C), 136.2 (Tph-C), 128.5 (Tph-C), 125.3 (Tph-CH), 73.7 (Tph-C), 32.3 ($-\text{CH}_2(\text{CH}_2)_4\text{CH}_3$), 31.6 (*n*Hex-C), 30.0 ($-\text{CH}_2\text{CH}_2(\text{CH}_2)_3\text{CH}_3$), 28.9 (*n*Hex-C), 27.1 ($-\text{CH}_2\text{CH}_2\text{CH}_2\text{CH}_2-$), 22.9 ($-\text{CH}_2\text{CH}_2\text{CH}_2\text{CH}_2-$), 22.6 ($-(\text{CH}_2)_4\text{CH}_2\text{CH}_3$), 14.1 ($-(\text{CH}_2)_5\text{CH}_3$) ppm.

S1.2. Refinement

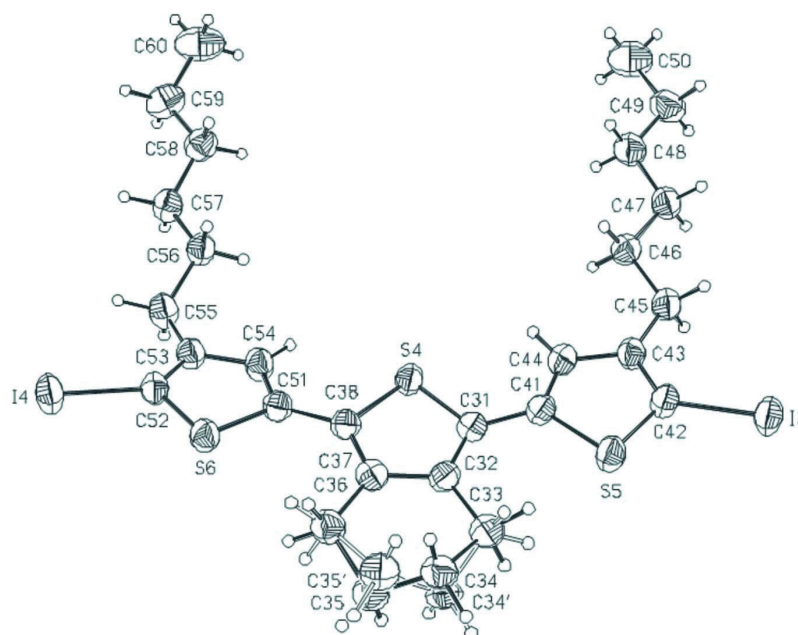
H atoms were positioned with idealized geometry and refined using a riding model with $U_{\text{iso}}(\text{H}) = 1.2 \cdot U_{\text{eq}}(\text{C})$ (1.5 for methyl H atoms). In one of the two crystallographically independent molecules the C atoms of one alkyl chain (C17—C19) and in the second molecule the ring C atoms C34—C35 are disordered over two positions and were refined using a split model. The site occupation factors were set to 0.65:0.35 for C17—C19 and C17'-C19', respectively, and to 0.70:0.30 for C34, C35 and C34', C35', respectively. The bonds C17—C18 and C18—C19 as well as the bond angles at C18 and C18' were restrained to the same value using the SAME instruction in SHELXL.

supporting information

**Figure 1**

Molecular structure of the first of the two crystallographically independent molecules with labelling and displacement ellipsoids drawn at the 50% probability level. The minor occupied atoms of the disordered sites are drawn with open bonds.

supporting information

**Figure 2**

Molecular structure of the second of the two crystallographically independent molecules with labeling and displacement ellipsoids drawn at the 50% probability level. The minor occupied atoms of the disordered sites are drawn with open bonds.

1,3-Bis(4-hexyl-5-iodothiophen-2-yl)-4,5,6,7-tetrahydro-2-benzothiophene*Crystal data* $C_{28}H_{36}I_2S_3$ $M_r = 722.55$ Triclinic, $P\bar{1}$ Hall symbol: $-P\ 1$ $a = 13.4491$ (4) Å $b = 14.9488$ (5) Å $c = 16.1260$ (5) Å $\alpha = 73.387$ (2)° $\beta = 71.208$ (2)° $\gamma = 77.794$ (3)° $V = 2915.60$ (16) Å³ $Z = 4$ $F(000) = 1432$ $D_x = 1.646$ Mg m⁻³Mo $K\alpha$ radiation, $\lambda = 0.71073$ Å $\theta = 1.4$ – 27.0 ° $\mu = 2.39$ mm⁻¹ $T = 200$ K

Block, yellow

 $0.16 \times 0.10 \times 0.08$ mm*Data collection*

Stoe IPDS-1

diffractometer

Radiation source: fine-focus sealed tube

Graphite monochromator

 ω scans

Absorption correction: numerical

(X-SHAPE and X-RED32; Stoe & Cie, 2008) $T_{\min} = 0.748$, $T_{\max} = 0.815$

26585 measured reflections

12585 independent reflections

9932 reflections with $I > 2\sigma(I)$ $R_{\text{int}} = 0.038$ $\theta_{\text{max}} = 27.0$ °, $\theta_{\text{min}} = 1.4$ ° $h = -17$ → 13 $k = -17$ → 19 $l = -20$ → 20

supporting information

Refinement

Refinement on F^2
 Least-squares matrix: full
 $R[F^2 > 2\sigma(F^2)] = 0.034$
 $wR(F^2) = 0.085$
 $S = 0.98$
 12585 reflections
 640 parameters
 3 restraints
 Primary atom site location: structure-invariant
 direct methods

Secondary atom site location: difference Fourier
 map
 Hydrogen site location: inferred from
 neighbouring sites
 H-atom parameters constrained
 $w = 1/[\sigma^2(F_o^2) + (0.0524P)^2]$
 where $P = (F_o^2 + 2F_c^2)/3$
 $(\Delta/\sigma)_{\max} = 0.002$
 $\Delta\rho_{\max} = 1.01 \text{ e } \text{\AA}^{-3}$
 $\Delta\rho_{\min} = -0.81 \text{ e } \text{\AA}^{-3}$

Special details

Geometry. All e.s.d.'s (except the e.s.d. in the dihedral angle between two l.s. planes) are estimated using the full covariance matrix. The cell e.s.d.'s are taken into account individually in the estimation of e.s.d.'s in distances, angles and torsion angles; correlations between e.s.d.'s in cell parameters are only used when they are defined by crystal symmetry. An approximate (isotropic) treatment of cell e.s.d.'s is used for estimating e.s.d.'s involving l.s. planes.

Refinement. Refinement of F^2 against ALL reflections. The weighted R -factor wR and goodness of fit S are based on F^2 , conventional R -factors R are based on F , with F set to zero for negative F^2 . The threshold expression of $F^2 > \sigma(F^2)$ is used only for calculating R -factors(gt) etc. and is not relevant to the choice of reflections for refinement. R -factors based on F^2 are statistically about twice as large as those based on F , and R -factors based on ALL data will be even larger.

Fractional atomic coordinates and isotropic or equivalent isotropic displacement parameters (\AA^2)

	<i>x</i>	<i>y</i>	<i>z</i>	$U_{\text{iso}}^*/U_{\text{eq}}$	Occ. (<1)
S1	0.45567 (6)	0.37865 (6)	0.67496 (5)	0.03750 (16)	
C1	0.4026 (2)	0.4189 (2)	0.77285 (19)	0.0365 (6)	
C2	0.4555 (3)	0.4893 (2)	0.7707 (2)	0.0369 (6)	
C3	0.4291 (3)	0.5402 (3)	0.8449 (2)	0.0460 (8)	
H3A	0.4175	0.4937	0.9038	0.055*	
H3B	0.3624	0.5836	0.8447	0.055*	
C4	0.5162 (4)	0.5958 (3)	0.8346 (3)	0.0611 (10)	
H4A	0.4889	0.6400	0.8748	0.073*	
H4B	0.5758	0.5521	0.8532	0.073*	
C5	0.5555 (4)	0.6499 (3)	0.7399 (3)	0.0579 (10)	
H5A	0.6088	0.6884	0.7368	0.069*	
H5B	0.4957	0.6934	0.7215	0.069*	
C6	0.6050 (3)	0.5866 (2)	0.6743 (2)	0.0439 (7)	
H6A	0.6142	0.6253	0.6119	0.053*	
H6B	0.6761	0.5568	0.6809	0.053*	
C7	0.5385 (3)	0.5110 (2)	0.6899 (2)	0.0363 (6)	
C8	0.5497 (3)	0.4561 (2)	0.6313 (2)	0.0366 (6)	
C11	0.3116 (2)	0.3797 (2)	0.83951 (19)	0.0373 (7)	
S2	0.23062 (7)	0.43471 (7)	0.92356 (6)	0.0461 (2)	
C12	0.1472 (3)	0.3502 (3)	0.9634 (2)	0.0434 (7)	
I1	0.02175 (2)	0.35889 (2)	1.077875 (16)	0.05806 (8)	
C13	0.1778 (3)	0.2817 (2)	0.9163 (2)	0.0415 (7)	
C14	0.2721 (3)	0.3003 (2)	0.8453 (2)	0.0405 (7)	
H14	0.3052	0.2604	0.8048	0.049*	
C15	0.1216 (3)	0.1987 (3)	0.9326 (2)	0.0500 (8)	

supporting information

H15A	0.1750	0.1441	0.9197	0.060*	
H15B	0.0815	0.1823	0.9971	0.060*	
C16	0.0469 (4)	0.2163 (3)	0.8766 (3)	0.0669 (12)	
H16A	0.0798	0.2494	0.8139	0.080*	0.65
H16B	-0.0191	0.2556	0.9015	0.080*	0.65
H16C	0.0920	0.2255	0.8134	0.080*	0.35
H16D	0.0052	0.2783	0.8825	0.080*	0.35
C17	0.0222 (6)	0.1174 (5)	0.8787 (4)	0.0491 (14)	0.65
H17A	0.0888	0.0783	0.8545	0.059*	0.65
H17B	-0.0102	0.0847	0.9416	0.059*	0.65
C18	-0.0533 (7)	0.1300 (6)	0.8222 (5)	0.0706 (19)	0.65
H18A	-0.1205	0.1667	0.8491	0.085*	0.65
H18B	-0.0222	0.1676	0.7611	0.085*	0.65
C19	-0.0785 (11)	0.0394 (9)	0.8134 (13)	0.086 (4)	0.65
H19A	-0.0944	-0.0035	0.8741	0.103*	0.65
H19B	-0.1440	0.0546	0.7939	0.103*	0.65
C17'	-0.0328 (12)	0.1541 (10)	0.8842 (8)	0.057 (3)	0.35
H17C	-0.0524	0.1129	0.9455	0.069*	0.35
H17D	-0.0978	0.1928	0.8709	0.069*	0.35
C18'	0.0222 (10)	0.0962 (9)	0.8153 (8)	0.055 (3)	0.35
H18C	0.0930	0.0684	0.8234	0.066*	0.35
H18D	0.0331	0.1391	0.7545	0.066*	0.35
C19'	-0.0350 (16)	0.0173 (14)	0.8183 (19)	0.068 (5)	0.35
H19C	-0.0310	-0.0341	0.8722	0.082*	0.35
H19D	-0.1107	0.0413	0.8234	0.082*	0.35
C20	0.0046 (8)	-0.0140 (7)	0.7498 (5)	0.137 (3)	
H20A	-0.0228	-0.0692	0.7486	0.206*	0.65
H20B	0.0686	-0.0345	0.7705	0.206*	0.65
H20C	0.0220	0.0271	0.6891	0.206*	0.65
H20D	-0.0285	-0.0689	0.7562	0.206*	0.35
H20E	0.0809	-0.0325	0.7416	0.206*	0.35
H20F	-0.0073	0.0348	0.6973	0.206*	0.35
C21	0.6228 (3)	0.4527 (2)	0.5433 (2)	0.0369 (6)	
S3	0.72642 (7)	0.52062 (6)	0.49196 (5)	0.04087 (17)	
C22	0.7682 (3)	0.4704 (2)	0.4008 (2)	0.0403 (7)	
I2	0.898985 (19)	0.513595 (18)	0.295482 (14)	0.04890 (7)	
C23	0.7078 (2)	0.4054 (2)	0.4071 (2)	0.0373 (7)	
C24	0.6247 (3)	0.3963 (2)	0.4889 (2)	0.0389 (7)	
H24	0.5740	0.3542	0.5048	0.047*	
C25	0.7271 (3)	0.3473 (3)	0.3395 (2)	0.0431 (7)	
H25A	0.7538	0.3863	0.2781	0.052*	
H25B	0.6590	0.3286	0.3434	0.052*	
C26	0.8066 (3)	0.2587 (3)	0.3544 (2)	0.0486 (8)	
H26A	0.8123	0.2219	0.3105	0.058*	
H26B	0.8771	0.2777	0.3421	0.058*	
C27	0.7771 (3)	0.1957 (3)	0.4494 (3)	0.0531 (9)	
H27A	0.7782	0.2307	0.4928	0.064*	
H27B	0.7038	0.1819	0.4638	0.064*	

supporting information

C28	0.8498 (4)	0.1031 (3)	0.4625 (3)	0.0736 (13)	
H28A	0.9243	0.1160	0.4369	0.088*	
H28B	0.8381	0.0627	0.4284	0.088*	
C29	0.8330 (6)	0.0489 (5)	0.5621 (5)	0.123 (3)	
H29A	0.8822	-0.0106	0.5642	0.147*	
H29B	0.8531	0.0868	0.5940	0.147*	
C30	0.7303 (7)	0.0271 (6)	0.6098 (5)	0.143 (3)	
H30A	0.7275	-0.0028	0.6729	0.215*	
H30B	0.7118	-0.0162	0.5831	0.215*	
H30C	0.6799	0.0850	0.6065	0.215*	
S4	0.47208 (7)	0.86002 (6)	0.18105 (5)	0.03916 (17)	
C31	0.4655 (3)	0.7968 (2)	0.1083 (2)	0.0383 (7)	
C32	0.5396 (3)	0.8201 (2)	0.0258 (2)	0.0393 (7)	
C33	0.5569 (3)	0.7771 (3)	-0.0525 (2)	0.0505 (9)	
H33A	0.4875	0.7744	-0.0602	0.061*	0.70
H33B	0.5933	0.7119	-0.0398	0.061*	0.70
H33C	0.5440	0.7105	-0.0298	0.061*	0.30
H33D	0.5064	0.8111	-0.0877	0.061*	0.30
C34	0.6264 (4)	0.8375 (5)	-0.1429 (3)	0.0486 (12)	0.70
H34A	0.6490	0.8022	-0.1907	0.058*	0.70
H34B	0.5835	0.8974	-0.1635	0.058*	0.70
C35	0.7216 (6)	0.8577 (5)	-0.1263 (4)	0.0481 (15)	0.70
H35A	0.7694	0.8879	-0.1840	0.058*	0.70
H35B	0.7608	0.7981	-0.1001	0.058*	0.70
C34'	0.6651 (10)	0.7826 (9)	-0.1100 (8)	0.043 (2)	0.30
H34C	0.6772	0.7555	-0.1622	0.052*	0.30
H34D	0.7165	0.7477	-0.0758	0.052*	0.30
C35'	0.6773 (15)	0.8860 (12)	-0.1410 (8)	0.048 (4)	0.30
H35C	0.6153	0.9220	-0.1613	0.058*	0.30
H35D	0.7415	0.8958	-0.1926	0.058*	0.30
C36	0.6868 (3)	0.9229 (3)	-0.0616 (2)	0.0454 (8)	
H36A	0.7487	0.9282	-0.0435	0.054*	0.70
H36B	0.6612	0.9866	-0.0932	0.054*	0.70
H36C	0.7571	0.8989	-0.0508	0.054*	0.30
H36D	0.6788	0.9926	-0.0774	0.054*	0.30
C37	0.6008 (3)	0.8884 (2)	0.0213 (2)	0.0383 (7)	
C38	0.5744 (3)	0.9171 (2)	0.1006 (2)	0.0378 (7)	
C41	0.3850 (3)	0.7341 (2)	0.1398 (2)	0.0388 (7)	
S5	0.37041 (8)	0.66872 (7)	0.07245 (5)	0.0473 (2)	
C42	0.2639 (3)	0.6232 (2)	0.1546 (2)	0.0426 (7)	
I3	0.18641 (2)	0.532520 (19)	0.128836 (16)	0.05364 (7)	
C43	0.2389 (3)	0.6558 (2)	0.2308 (2)	0.0409 (7)	
C44	0.3098 (3)	0.7179 (2)	0.2210 (2)	0.0433 (7)	
H44	0.3055	0.7465	0.2678	0.052*	
C45	0.1470 (3)	0.6270 (3)	0.3120 (2)	0.0509 (9)	
H45A	0.1654	0.5605	0.3417	0.061*	
H45B	0.0849	0.6301	0.2905	0.061*	
C46	0.1148 (3)	0.6850 (3)	0.3818 (2)	0.0460 (8)	

supporting information

H46A	0.1012	0.7524	0.3522	0.055*
H46B	0.1736	0.6771	0.4087	0.055*
C47	0.0160 (3)	0.6556 (3)	0.4559 (2)	0.0503 (8)
H47A	-0.0417	0.6616	0.4282	0.060*
H47B	0.0307	0.5883	0.4856	0.060*
C48	-0.0217 (3)	0.7121 (3)	0.5265 (3)	0.0561 (9)
H48A	0.0366	0.7071	0.5532	0.067*
H48B	-0.0375	0.7791	0.4968	0.067*
C49	-0.1183 (3)	0.6826 (3)	0.6012 (3)	0.0612 (10)
H49A	-0.1048	0.6144	0.6279	0.073*
H49B	-0.1785	0.6929	0.5754	0.073*
C50	-0.1489 (5)	0.7351 (5)	0.6747 (4)	0.0949 (18)
H50A	-0.2117	0.7124	0.7213	0.142*
H50B	-0.1646	0.8026	0.6492	0.142*
H50C	-0.0902	0.7244	0.7014	0.142*
C51	0.6176 (3)	0.9826 (2)	0.1260 (2)	0.0375 (7)
S6	0.70220 (7)	1.06090 (6)	0.04923 (5)	0.04254 (18)
C52	0.7062 (3)	1.1091 (2)	0.1330 (2)	0.0402 (7)
I4	0.79965 (2)	1.214701 (18)	0.100870 (15)	0.05306 (7)
C53	0.6466 (3)	1.0684 (2)	0.2165 (2)	0.0401 (7)
C54	0.5969 (3)	0.9964 (2)	0.2108 (2)	0.0427 (7)
H54	0.5523	0.9602	0.2622	0.051*
C55	0.6328 (3)	1.0955 (3)	0.3029 (2)	0.0470 (8)
H55A	0.6564	1.1579	0.2883	0.056*
H55B	0.6787	1.0493	0.3369	0.056*
C56	0.5186 (3)	1.0994 (3)	0.3625 (2)	0.0439 (7)
H56A	0.4711	1.1379	0.3259	0.053*
H56B	0.4985	1.0349	0.3850	0.053*
C57	0.5026 (3)	1.1411 (3)	0.4426 (2)	0.0461 (8)
H57A	0.5473	1.1005	0.4808	0.055*
H57B	0.5269	1.2040	0.4199	0.055*
C58	0.3886 (3)	1.1508 (3)	0.4999 (2)	0.0515 (9)
H58A	0.3666	1.0872	0.5274	0.062*
H58B	0.3429	1.1860	0.4605	0.062*
C59	0.3710 (4)	1.2009 (3)	0.5741 (2)	0.0610 (11)
H59A	0.4191	1.1674	0.6117	0.073*
H59B	0.3896	1.2656	0.5464	0.073*
C60	0.2579 (5)	1.2063 (4)	0.6339 (3)	0.0900 (17)
H60A	0.2514	1.2390	0.6805	0.135*
H60B	0.2393	1.1425	0.6625	0.135*
H60C	0.2099	1.2409	0.5974	0.135*

Atomic displacement parameters (\AA^2)

	U^{11}	U^{22}	U^{33}	U^{12}	U^{13}	U^{23}
S1	0.0356 (4)	0.0392 (4)	0.0378 (3)	-0.0099 (3)	-0.0046 (3)	-0.0120 (3)
C1	0.0327 (15)	0.0405 (17)	0.0362 (14)	-0.0038 (13)	-0.0078 (12)	-0.0115 (12)
C2	0.0337 (16)	0.0366 (17)	0.0408 (15)	-0.0012 (13)	-0.0110 (13)	-0.0118 (12)

supporting information

C3	0.0455 (19)	0.051 (2)	0.0446 (16)	-0.0092 (16)	-0.0082 (14)	-0.0196 (15)
C4	0.064 (3)	0.068 (3)	0.062 (2)	-0.020 (2)	-0.0126 (19)	-0.0288 (19)
C5	0.072 (3)	0.049 (2)	0.059 (2)	-0.024 (2)	-0.0078 (19)	-0.0210 (17)
C6	0.0444 (19)	0.0410 (18)	0.0492 (17)	-0.0127 (15)	-0.0097 (15)	-0.0136 (14)
C7	0.0356 (16)	0.0310 (15)	0.0423 (15)	-0.0043 (12)	-0.0117 (13)	-0.0080 (12)
C8	0.0345 (16)	0.0345 (16)	0.0390 (14)	-0.0045 (13)	-0.0082 (12)	-0.0083 (12)
C11	0.0311 (15)	0.0435 (18)	0.0362 (14)	-0.0038 (13)	-0.0074 (12)	-0.0109 (12)
S2	0.0412 (4)	0.0539 (5)	0.0443 (4)	-0.0139 (4)	0.0001 (3)	-0.0215 (4)
C12	0.0317 (16)	0.055 (2)	0.0403 (15)	-0.0106 (15)	-0.0010 (13)	-0.0137 (14)
I1	0.04650 (14)	0.07347 (18)	0.04928 (13)	-0.01999 (12)	0.00718 (10)	-0.02162 (11)
C13	0.0359 (17)	0.0438 (18)	0.0408 (15)	-0.0079 (14)	-0.0075 (13)	-0.0055 (13)
C14	0.0373 (17)	0.0398 (18)	0.0419 (15)	-0.0058 (14)	-0.0069 (13)	-0.0099 (13)
C15	0.049 (2)	0.0397 (19)	0.0555 (19)	-0.0131 (16)	-0.0043 (16)	-0.0091 (15)
C16	0.085 (3)	0.074 (3)	0.0485 (19)	-0.047 (3)	-0.012 (2)	-0.0058 (18)
C17	0.058 (4)	0.041 (4)	0.049 (3)	-0.013 (3)	-0.010 (3)	-0.012 (3)
C18	0.076 (5)	0.076 (5)	0.074 (4)	-0.025 (4)	-0.033 (4)	-0.014 (4)
C19	0.081 (9)	0.102 (9)	0.088 (7)	-0.046 (7)	-0.012 (7)	-0.033 (7)
C17'	0.056 (8)	0.059 (9)	0.057 (6)	-0.020 (6)	-0.002 (6)	-0.020 (6)
C18'	0.048 (7)	0.061 (7)	0.058 (6)	-0.026 (6)	-0.006 (5)	-0.013 (5)
C19'	0.069 (14)	0.078 (11)	0.065 (9)	-0.031 (10)	-0.010 (11)	-0.021 (8)
C20	0.153 (8)	0.152 (8)	0.123 (6)	-0.028 (6)	-0.032 (5)	-0.059 (5)
C21	0.0330 (16)	0.0351 (16)	0.0412 (15)	-0.0048 (13)	-0.0083 (13)	-0.0089 (12)
S3	0.0392 (4)	0.0409 (4)	0.0423 (4)	-0.0131 (3)	-0.0045 (3)	-0.0116 (3)
C22	0.0355 (16)	0.0444 (18)	0.0383 (14)	-0.0072 (14)	-0.0049 (13)	-0.0105 (13)
I2	0.04303 (13)	0.05674 (15)	0.04192 (11)	-0.01741 (10)	-0.00180 (9)	-0.00759 (9)
C23	0.0314 (15)	0.0404 (17)	0.0378 (14)	-0.0035 (13)	-0.0093 (12)	-0.0072 (12)
C24	0.0354 (16)	0.0386 (17)	0.0433 (15)	-0.0091 (13)	-0.0094 (13)	-0.0093 (13)
C25	0.0442 (18)	0.050 (2)	0.0390 (15)	-0.0101 (15)	-0.0124 (14)	-0.0122 (13)
C26	0.046 (2)	0.056 (2)	0.0514 (18)	-0.0076 (16)	-0.0116 (15)	-0.0254 (16)
C27	0.051 (2)	0.045 (2)	0.066 (2)	-0.0058 (17)	-0.0192 (18)	-0.0142 (16)
C28	0.071 (3)	0.050 (3)	0.093 (3)	0.002 (2)	-0.018 (3)	-0.019 (2)
C29	0.095 (5)	0.077 (4)	0.156 (6)	0.006 (4)	-0.037 (5)	0.023 (4)
C30	0.120 (7)	0.122 (6)	0.127 (6)	0.003 (5)	-0.015 (5)	0.027 (5)
S4	0.0433 (4)	0.0374 (4)	0.0381 (3)	-0.0120 (3)	-0.0072 (3)	-0.0108 (3)
C31	0.0379 (17)	0.0375 (17)	0.0411 (15)	-0.0051 (13)	-0.0108 (13)	-0.0120 (12)
C32	0.0401 (17)	0.0372 (17)	0.0431 (15)	-0.0022 (14)	-0.0129 (13)	-0.0142 (13)
C33	0.047 (2)	0.061 (2)	0.0483 (18)	-0.0110 (17)	-0.0076 (15)	-0.0240 (16)
C34	0.043 (3)	0.059 (4)	0.045 (3)	-0.008 (3)	-0.005 (2)	-0.020 (3)
C35	0.047 (4)	0.054 (4)	0.042 (3)	-0.008 (3)	-0.007 (3)	-0.013 (3)
C34'	0.042 (6)	0.045 (7)	0.039 (5)	0.000 (5)	-0.002 (5)	-0.018 (5)
C35'	0.060 (10)	0.060 (10)	0.023 (5)	-0.014 (8)	-0.007 (6)	-0.008 (5)
C36	0.0458 (19)	0.050 (2)	0.0383 (15)	-0.0099 (16)	-0.0077 (14)	-0.0099 (14)
C37	0.0379 (17)	0.0366 (17)	0.0390 (14)	-0.0036 (13)	-0.0124 (13)	-0.0061 (12)
C38	0.0380 (17)	0.0331 (16)	0.0381 (14)	-0.0053 (13)	-0.0065 (12)	-0.0062 (12)
C41	0.0401 (17)	0.0370 (17)	0.0419 (15)	-0.0043 (14)	-0.0124 (13)	-0.0128 (12)
S5	0.0564 (5)	0.0510 (5)	0.0397 (4)	-0.0211 (4)	-0.0071 (4)	-0.0155 (3)
C42	0.0479 (19)	0.0400 (18)	0.0457 (16)	-0.0119 (15)	-0.0141 (14)	-0.0132 (13)
I3	0.05975 (16)	0.06070 (16)	0.05085 (12)	-0.02589 (12)	-0.01073 (11)	-0.02133 (10)

supporting information

C43	0.0407 (18)	0.0458 (19)	0.0411 (15)	-0.0101 (14)	-0.0120 (13)	-0.0138 (13)
C44	0.0449 (19)	0.0458 (19)	0.0453 (16)	-0.0091 (15)	-0.0120 (14)	-0.0186 (14)
C45	0.046 (2)	0.057 (2)	0.0526 (19)	-0.0167 (17)	-0.0035 (16)	-0.0226 (16)
C46	0.046 (2)	0.049 (2)	0.0450 (16)	-0.0104 (16)	-0.0076 (15)	-0.0159 (14)
C47	0.047 (2)	0.059 (2)	0.0487 (18)	-0.0158 (17)	-0.0071 (15)	-0.0182 (16)
C48	0.051 (2)	0.065 (3)	0.0522 (19)	-0.0120 (19)	-0.0051 (17)	-0.0212 (17)
C49	0.047 (2)	0.076 (3)	0.056 (2)	-0.009 (2)	-0.0033 (17)	-0.0207 (19)
C50	0.077 (4)	0.123 (5)	0.078 (3)	-0.014 (3)	0.016 (3)	-0.055 (3)
C51	0.0388 (17)	0.0336 (16)	0.0377 (14)	-0.0060 (13)	-0.0094 (13)	-0.0053 (12)
S6	0.0466 (5)	0.0427 (4)	0.0374 (4)	-0.0157 (4)	-0.0043 (3)	-0.0095 (3)
C52	0.0400 (17)	0.0389 (17)	0.0439 (15)	-0.0120 (14)	-0.0100 (13)	-0.0101 (13)
I4	0.05746 (15)	0.05634 (15)	0.04892 (12)	-0.03000 (12)	-0.00790 (10)	-0.00943 (10)
C53	0.0409 (17)	0.0409 (18)	0.0384 (14)	-0.0110 (14)	-0.0087 (13)	-0.0079 (12)
C54	0.0454 (19)	0.0417 (18)	0.0397 (15)	-0.0152 (15)	-0.0076 (14)	-0.0056 (13)
C55	0.051 (2)	0.052 (2)	0.0406 (16)	-0.0184 (17)	-0.0108 (15)	-0.0089 (14)
C56	0.049 (2)	0.0407 (18)	0.0425 (16)	-0.0128 (15)	-0.0097 (14)	-0.0094 (13)
C57	0.054 (2)	0.045 (2)	0.0395 (15)	-0.0126 (16)	-0.0128 (15)	-0.0071 (13)
C58	0.060 (2)	0.047 (2)	0.0462 (17)	-0.0076 (17)	-0.0114 (16)	-0.0127 (15)
C59	0.076 (3)	0.061 (3)	0.0448 (18)	0.000 (2)	-0.0180 (18)	-0.0164 (17)
C60	0.086 (4)	0.105 (4)	0.064 (3)	0.012 (3)	-0.004 (3)	-0.036 (3)

Geometric parameters (Å, °)

S1—C1	1.732 (3)	C30—H30B	0.9800
S1—C8	1.737 (3)	C30—H30C	0.9800
C1—C2	1.377 (5)	S4—C31	1.736 (3)
C1—C11	1.446 (4)	S4—C38	1.737 (3)
C2—C7	1.422 (4)	C31—C32	1.383 (4)
C2—C3	1.506 (4)	C31—C41	1.452 (5)
C3—C4	1.516 (5)	C32—C37	1.414 (5)
C3—H3A	0.9900	C32—C33	1.507 (4)
C3—H3B	0.9900	C33—C34'	1.457 (12)
C4—C5	1.491 (5)	C33—C34	1.594 (6)
C4—H4A	0.9900	C33—H33A	0.9900
C4—H4B	0.9900	C33—H33B	0.9900
C5—C6	1.520 (5)	C33—H33C	0.9900
C5—H5A	0.9900	C33—H33D	0.9900
C5—H5B	0.9900	C34—C35	1.494 (9)
C6—C7	1.504 (5)	C34—H34A	0.9900
C6—H6A	0.9900	C34—H34B	0.9900
C6—H6B	0.9900	C35—C36	1.527 (8)
C7—C8	1.374 (4)	C35—H35A	0.9900
C8—C21	1.451 (4)	C35—H35B	0.9900
C11—C14	1.368 (5)	C34'—C35'	1.51 (2)
C11—S2	1.735 (3)	C34'—H34C	0.9900
S2—C12	1.715 (4)	C34'—H34D	0.9900
C12—C13	1.364 (5)	C35'—C36	1.581 (15)
C12—I1	2.076 (3)	C35'—H35C	0.9900

supporting information

C13—C14	1.424 (4)	C35'—H35D	0.9900
C13—C15	1.503 (5)	C36—C37	1.502 (4)
C14—H14	0.9500	C36—H36A	0.9900
C15—C16	1.494 (6)	C36—H36B	0.9900
C15—H15A	0.9900	C36—H36C	0.9900
C15—H15B	0.9900	C36—H36D	0.9900
C16—C17'	1.517 (13)	C37—C38	1.380 (4)
C16—C17	1.571 (8)	C38—C51	1.446 (5)
C16—H16A	0.9900	C41—C44	1.366 (5)
C16—H16B	0.9900	C41—S5	1.732 (3)
C16—H16C	0.9901	S5—C42	1.716 (4)
C16—H16D	0.9900	C42—C43	1.367 (4)
C17—C18	1.520 (8)	C42—I3	2.072 (3)
C17—H17A	0.9900	C43—C44	1.411 (5)
C17—H17B	0.9900	C43—C45	1.511 (5)
C18—C19	1.518 (11)	C44—H44	0.9500
C18—H18A	0.9900	C45—C46	1.514 (5)
C18—H18B	0.9900	C45—H45A	0.9900
C19—C20	1.513 (17)	C45—H45B	0.9900
C19—H19A	0.9900	C46—C47	1.520 (5)
C19—H19B	0.9900	C46—H46A	0.9900
C17'—C18'	1.510 (13)	C46—H46B	0.9900
C17'—H17C	0.9900	C47—C48	1.505 (5)
C17'—H17D	0.9900	C47—H47A	0.9900
C18'—C19'	1.521 (14)	C47—H47B	0.9900
C18'—H18C	0.9900	C48—C49	1.504 (5)
C18'—H18D	0.9900	C48—H48A	0.9900
C19'—C20	1.24 (3)	C48—H48B	0.9900
C19'—H19C	0.9900	C49—C50	1.507 (6)
C19'—H19D	0.9900	C49—H49A	0.9900
C20—H20A	0.9800	C49—H49B	0.9900
C20—H20B	0.9800	C50—H50A	0.9800
C20—H20C	0.9800	C50—H50B	0.9800
C20—H20D	0.9800	C50—H50C	0.9800
C20—H20E	0.9801	C51—C54	1.371 (4)
C20—H20F	0.9801	C51—S6	1.739 (3)
C21—C24	1.370 (4)	S6—C52	1.722 (3)
C21—S3	1.742 (3)	C52—C53	1.368 (4)
S3—C22	1.721 (3)	C52—I4	2.072 (3)
C22—C23	1.356 (5)	C53—C54	1.418 (5)
C22—I2	2.079 (3)	C53—C55	1.505 (4)
C23—C24	1.422 (4)	C54—H54	0.9500
C23—C25	1.508 (4)	C55—C56	1.527 (5)
C24—H24	0.9500	C55—H55A	0.9900
C25—C26	1.529 (5)	C55—H55B	0.9900
C25—H25A	0.9900	C56—C57	1.525 (5)
C25—H25B	0.9900	C56—H56A	0.9900
C26—C27	1.528 (5)	C56—H56B	0.9900

supporting information

C26—H26A	0.9900	C57—C58	1.516 (5)
C26—H26B	0.9900	C57—H57A	0.9900
C27—C28	1.520 (6)	C57—H57B	0.9900
C27—H27A	0.9900	C58—C59	1.519 (5)
C27—H27B	0.9900	C58—H58A	0.9900
C28—C29	1.546 (8)	C58—H58B	0.9900
C28—H28A	0.9900	C59—C60	1.516 (7)
C28—H28B	0.9900	C59—H59A	0.9900
C29—C30	1.403 (10)	C59—H59B	0.9900
C29—H29A	0.9900	C60—H60A	0.9800
C29—H29B	0.9900	C60—H60B	0.9800
C30—H30A	0.9800	C60—H60C	0.9800
C1—S1—C8	92.38 (15)	C29—C30—H30A	109.5
C2—C1—C11	130.6 (3)	C29—C30—H30B	109.5
C2—C1—S1	110.7 (2)	H30A—C30—H30B	109.5
C11—C1—S1	118.6 (2)	C29—C30—H30C	109.5
C1—C2—C7	113.1 (3)	H30A—C30—H30C	109.5
C1—C2—C3	124.4 (3)	H30B—C30—H30C	109.5
C7—C2—C3	122.4 (3)	C31—S4—C38	92.22 (16)
C2—C3—C4	112.2 (3)	C32—C31—C41	131.2 (3)
C2—C3—H3A	109.2	C32—C31—S4	110.5 (2)
C4—C3—H3A	109.2	C41—C31—S4	118.2 (2)
C2—C3—H3B	109.2	C31—C32—C37	113.4 (3)
C4—C3—H3B	109.2	C31—C32—C33	124.6 (3)
H3A—C3—H3B	107.9	C37—C32—C33	122.1 (3)
C5—C4—C3	111.6 (3)	C34'—C33—C32	109.7 (5)
C5—C4—H4A	109.3	C32—C33—C34	110.6 (3)
C3—C4—H4A	109.3	C34'—C33—H33A	136.5
C5—C4—H4B	109.3	C32—C33—H33A	109.5
C3—C4—H4B	109.3	C34—C33—H33A	109.5
H4A—C4—H4B	108.0	C34'—C33—H33B	75.3
C4—C5—C6	112.6 (3)	C32—C33—H33B	109.5
C4—C5—H5A	109.1	C34—C33—H33B	109.5
C6—C5—H5A	109.1	H33A—C33—H33B	108.1
C4—C5—H5B	109.1	C34'—C33—H33C	109.7
C6—C5—H5B	109.1	C32—C33—H33C	109.7
H5A—C5—H5B	107.8	C34—C33—H33C	135.4
C7—C6—C5	112.1 (3)	H33A—C33—H33C	73.3
C7—C6—H6A	109.2	C34'—C33—H33D	109.7
C5—C6—H6A	109.2	C32—C33—H33D	109.7
C7—C6—H6B	109.2	C34—C33—H33D	74.8
C5—C6—H6B	109.2	H33B—C33—H33D	135.5
H6A—C6—H6B	107.9	H33C—C33—H33D	108.2
C8—C7—C2	113.1 (3)	C35—C34—C33	109.8 (5)
C8—C7—C6	125.7 (3)	C35—C34—H34A	109.7
C2—C7—C6	121.2 (3)	C33—C34—H34A	109.7
C7—C8—C21	132.2 (3)	C35—C34—H34B	109.7

supporting information

C7—C8—S1	110.7 (2)	C33—C34—H34B	109.7
C21—C8—S1	117.2 (2)	H34A—C34—H34B	108.2
C14—C11—C1	128.0 (3)	C34—C35—C36	109.6 (5)
C14—C11—S2	109.5 (2)	C34—C35—H35A	109.8
C1—C11—S2	122.4 (2)	C36—C35—H35A	109.8
C12—S2—C11	91.84 (16)	C34—C35—H35B	109.8
C13—C12—S2	113.2 (2)	C36—C35—H35B	109.8
C13—C12—H1	128.6 (3)	H35A—C35—H35B	108.2
S2—C12—H1	118.06 (19)	C33—C34'—C35'	105.9 (11)
C12—C13—C14	110.2 (3)	C33—C34'—H34C	110.6
C12—C13—C15	126.7 (3)	C35'—C34'—H34C	110.6
C14—C13—C15	123.1 (3)	C33—C34'—H34D	110.6
C11—C14—C13	115.2 (3)	C35'—C34'—H34D	110.6
C11—C14—H14	122.4	H34C—C34'—H34D	108.7
C13—C14—H14	122.4	C34'—C35'—C36	110.4 (10)
C16—C15—C13	113.4 (3)	C34'—C35'—H35C	109.6
C16—C15—H15A	108.9	C36—C35'—H35C	109.6
C13—C15—H15A	108.9	C34'—C35'—H35D	109.6
C16—C15—H15B	108.9	C36—C35'—H35D	109.6
C13—C15—H15B	108.9	H35C—C35'—H35D	108.1
H15A—C15—H15B	107.7	C37—C36—C35	112.4 (4)
C15—C16—C17'	127.6 (7)	C37—C36—C35'	107.9 (6)
C15—C16—C17	106.9 (4)	C37—C36—H36A	109.1
C15—C16—H16A	110.3	C35—C36—H36A	109.1
C17'—C16—H16A	113.7	C35'—C36—H36A	132.2
C17—C16—H16A	110.3	C37—C36—H36B	109.1
C15—C16—H16B	110.3	C35—C36—H36B	109.1
C17'—C16—H16B	81.0	C35'—C36—H36B	87.1
C17—C16—H16B	110.3	H36A—C36—H36B	107.9
H16A—C16—H16B	108.6	C37—C36—H36C	110.1
C15—C16—H16C	105.5	C35—C36—H36C	84.4
C17'—C16—H16C	105.5	C35'—C36—H36C	110.1
C17—C16—H16C	93.3	H36B—C36—H36C	128.9
H16B—C16—H16C	127.9	C37—C36—H36D	110.1
C15—C16—H16D	105.4	C35—C36—H36D	127.4
C17'—C16—H16D	105.3	C35'—C36—H36D	110.1
C17—C16—H16D	136.0	H36C—C36—H36D	108.4
H16A—C16—H16D	85.1	C38—C37—C32	113.1 (3)
H16C—C16—H16D	106.0	C38—C37—C36	124.7 (3)
C18—C17—C16	109.7 (5)	C32—C37—C36	122.3 (3)
C18—C17—H17A	109.7	C37—C38—C51	131.4 (3)
C16—C17—H17A	109.7	C37—C38—S4	110.8 (3)
C18—C17—H17B	109.7	C51—C38—S4	117.8 (2)
C16—C17—H17B	109.7	C44—C41—C31	128.5 (3)
H17A—C17—H17B	108.2	C44—C41—S5	109.4 (2)
C19—C18—C17	115.3 (8)	C31—C41—S5	122.1 (2)
C19—C18—H18A	108.4	C42—S5—C41	91.75 (16)
C17—C18—H18A	108.4	C43—C42—S5	113.0 (3)

supporting information

C19—C18—H18B	108.4	C43—C42—I3	127.7 (3)
C17—C18—H18B	108.4	S5—C42—I3	119.30 (17)
H18A—C18—H18B	107.5	C42—C43—C44	110.3 (3)
C20—C19—C18	117.9 (11)	C42—C43—C45	122.8 (3)
C20—C19—H19A	107.8	C44—C43—C45	126.9 (3)
C18—C19—H19A	107.8	C41—C44—C43	115.6 (3)
C20—C19—H19B	107.8	C41—C44—H44	122.2
C18—C19—H19B	107.8	C43—C44—H44	122.2
H19A—C19—H19B	107.2	C43—C45—C46	116.0 (3)
C18'—C17'—C16	105.3 (9)	C43—C45—H45A	108.3
C18'—C17'—H17C	110.7	C46—C45—H45A	108.3
C16—C17'—H17C	110.7	C43—C45—H45B	108.3
C18'—C17'—H17D	110.7	C46—C45—H45B	108.3
C16—C17'—H17D	110.7	H45A—C45—H45B	107.4
H17C—C17'—H17D	108.8	C45—C46—C47	111.5 (3)
C17'—C18'—C19'	115.9 (12)	C45—C46—H46A	109.3
C17'—C18'—H18C	108.3	C47—C46—H46A	109.3
C19'—C18'—H18C	108.3	C45—C46—H46B	109.3
C17'—C18'—H18D	108.3	C47—C46—H46B	109.3
C19'—C18'—H18D	108.3	H46A—C46—H46B	108.0
H18C—C18'—H18D	107.4	C48—C47—C46	114.1 (3)
C20—C19'—C18'	111.1 (17)	C48—C47—H47A	108.7
C20—C19'—H19C	109.4	C46—C47—H47A	108.7
C18'—C19'—H19C	109.4	C48—C47—H47B	108.7
C20—C19'—H19D	109.4	C46—C47—H47B	108.7
C18'—C19'—H19D	109.4	H47A—C47—H47B	107.6
H19C—C19'—H19D	108.0	C49—C48—C47	114.7 (4)
C19'—C20—H20A	116.7	C49—C48—H48A	108.6
C19—C20—H20A	109.5	C47—C48—H48A	108.6
C19'—C20—H20B	86.0	C49—C48—H48B	108.6
C19—C20—H20B	109.5	C47—C48—H48B	108.6
H20A—C20—H20B	109.5	H48A—C48—H48B	107.6
C19'—C20—H20C	122.4	C48—C49—C50	113.5 (4)
C19—C20—H20C	109.5	C48—C49—H49A	108.9
H20A—C20—H20C	109.5	C50—C49—H49A	108.9
H20B—C20—H20C	109.5	C48—C49—H49B	108.9
C19'—C20—H20D	109.5	C50—C49—H49B	108.9
C19—C20—H20D	103.0	H49A—C49—H49B	107.7
H20B—C20—H20D	109.8	C49—C50—H50A	109.5
H20C—C20—H20D	115.4	C49—C50—H50B	109.5
C19'—C20—H20E	109.6	H50A—C50—H50B	109.5
C19—C20—H20E	131.8	C49—C50—H50C	109.5
H20A—C20—H20E	105.9	H50A—C50—H50C	109.5
H20C—C20—H20E	87.7	H50B—C50—H50C	109.5
H20D—C20—H20E	109.5	C54—C51—C38	127.0 (3)
C19'—C20—H20F	109.3	C54—C51—S6	109.4 (2)
C19—C20—H20F	91.3	C38—C51—S6	123.5 (2)
H20A—C20—H20F	105.6	C52—S6—C51	91.69 (15)

supporting information

H20B—C20—H20F	129.4	C53—C52—S6	113.1 (2)
H20D—C20—H20F	109.5	C53—C52—I4	127.3 (2)
H20E—C20—H20F	109.5	S6—C52—I4	119.49 (17)
C24—C21—C8	127.2 (3)	C52—C53—C54	110.2 (3)
C24—C21—S3	109.4 (2)	C52—C53—C55	125.9 (3)
C8—C21—S3	123.4 (2)	C54—C53—C55	123.9 (3)
C22—S3—C21	91.49 (16)	C51—C54—C53	115.6 (3)
C23—C22—S3	113.4 (2)	C51—C54—H54	122.2
C23—C22—I2	127.3 (2)	C53—C54—H54	122.2
S3—C22—I2	119.31 (18)	C53—C55—C56	113.1 (3)
C22—C23—C24	110.5 (3)	C53—C55—H55A	109.0
C22—C23—C25	125.6 (3)	C56—C55—H55A	109.0
C24—C23—C25	123.9 (3)	C53—C55—H55B	109.0
C21—C24—C23	115.2 (3)	C56—C55—H55B	109.0
C21—C24—H24	122.4	H55A—C55—H55B	107.8
C23—C24—H24	122.4	C57—C56—C55	112.4 (3)
C23—C25—C26	112.8 (3)	C57—C56—H56A	109.1
C23—C25—H25A	109.0	C55—C56—H56A	109.1
C26—C25—H25A	109.0	C57—C56—H56B	109.1
C23—C25—H25B	109.0	C55—C56—H56B	109.1
C26—C25—H25B	109.0	H56A—C56—H56B	107.8
H25A—C25—H25B	107.8	C58—C57—C56	113.4 (3)
C27—C26—C25	113.8 (3)	C58—C57—H57A	108.9
C27—C26—H26A	108.8	C56—C57—H57A	108.9
C25—C26—H26A	108.8	C58—C57—H57B	108.9
C27—C26—H26B	108.8	C56—C57—H57B	108.9
C25—C26—H26B	108.8	H57A—C57—H57B	107.7
H26A—C26—H26B	107.7	C57—C58—C59	113.4 (3)
C28—C27—C26	114.2 (3)	C57—C58—H58A	108.9
C28—C27—H27A	108.7	C59—C58—H58A	108.9
C26—C27—H27A	108.7	C57—C58—H58B	108.9
C28—C27—H27B	108.7	C59—C58—H58B	108.9
C26—C27—H27B	108.7	H58A—C58—H58B	107.7
H27A—C27—H27B	107.6	C60—C59—C58	113.1 (4)
C27—C28—C29	113.7 (4)	C60—C59—H59A	109.0
C27—C28—H28A	108.8	C58—C59—H59A	109.0
C29—C28—H28A	108.8	C60—C59—H59B	109.0
C27—C28—H28B	108.8	C58—C59—H59B	109.0
C29—C28—H28B	108.8	H59A—C59—H59B	107.8
H28A—C28—H28B	107.7	C59—C60—H60A	109.5
C30—C29—C28	116.4 (7)	C59—C60—H60B	109.5
C30—C29—H29A	108.2	H60A—C60—H60B	109.5
C28—C29—H29A	108.2	C59—C60—H60C	109.5
C30—C29—H29B	108.2	H60A—C60—H60C	109.5
C28—C29—H29B	108.2	H60B—C60—H60C	109.5
H29A—C29—H29B	107.3		

5.4 General Methods and Materials for Unpublished Syntheses

All syntheses were carried out using standard Schlenk techniques under a dry and inert argon atmosphere. Glassware and NMR-tubes were dried in an oven at 200 °C for at least 2 h prior to use. All microwave syntheses were performed on a Biotage Initiator+ SP Wave (Organic Synthesis Mode). The temperature was measured with an external IR sensor during microwave heating.

5.4.1 Analyses

^1H NMR, ^{13}C NMR, ^{11}B NMR and ^{119}Sn NMR spectra were recorded at 300 K. ^1H NMR spectra were recorded on a Bruker DRX 500 (500 MHz) spectrometer or a Bruker Avance 600 (600 MHz) spectrometer. $^{13}\text{C}\{^1\text{H}\}$ NMR spectra were recorded on a Bruker DRX 500 (126 MHz) spectrometer or a Bruker Avance 600 (151 MHz) spectrometer. ^{11}B NMR, ^{29}Si NMR and ^{119}Sn NMR spectra were recorded on a Bruker DRX 500 (160 MHz, 99 MHz and 187 MHz) spectrometer. All ^1H NMR, $^{13}\text{C}\{^1\text{H}\}$ NMR and ^{29}Si NMR spectra were referenced against TMS, or against the solvent residual proton signals (^1H) or the solvent itself (^{13}C). ^{11}B NMR spectra were referenced against $\text{BF}_3\cdot\text{OEt}_2$ in CDCl_3 , the reference of the ^{119}Sn NMR spectra was calculated based on the ^1H NMR of TMS.

The exact assignment of the peaks was proved by two-dimensional NMR spectroscopy such as ^1H COSY, ^{13}C HSQC or $^1\text{H}/^{13}\text{C}$ HMBC when possible.

High-resolution accurate-mass ESI mass spectra were recorded on a Bruker Daltonics micrOTOF II mass spectrometer. High-resolution accurate-mass EI mass spectra were recorded on a Jeol AccuTOF JMS-T100GCV mass spectrometer. High-resolution accurate-mass MALDI mass spectra were recorded on a Bruker Daltonics ultrafleXtreme TOF/TOF mass spectrometer.

IR spectra were recorded on a Perkin Elmer Paragon 1000 FT-IR spectrometer with a A531-G Golden-Gate-ATR-unit.

UV/Vis spectra were recorded on a Perkin Elmer Lambda 14 spectrometer.

X-ray powder diffraction measurements were performed on a Stoe Transmission Powder Diffraction System (STADI P) with CuK_α radiation ($\lambda = 154.0598$ pm), equipped with a MYTHEN detector.

All melting points were recorded on an Electrothermal melting point apparatus LG 1586 and are uncorrected.

5.4.2 Chemicals

All reagents were used without further purification unless otherwise noted.

The preparation of *i*PrO-BPin (2-isopropoxy-4,4,5,5-tetramethyl-1,3,2-dioxaborolane) and 2,5-bis(trimethylstannyl)thiophene is described in the supporting information of *Org. Lett.* **2012** (see chapter 5.1). The preparation of **4** is described in the supporting information of *Acta Cryst.* **2014** (see chapter 5.3). The preparation of **P2-9** and Cp₂Zr(pyr)(Me₃SiC≡CSiMe₃) is described in the supporting information of *Angew. Chem.* **2014** (see chapter 5.2). **P2-4** (2-bromo-3-hexyl-5-iodothiophene) was prepared following a literature procedure.^[45] 3-Hexylthiophene was either bought (see following table) or prepared, starting with thiophene, following a literature procedure.^[63]

Reagent	Supplier	Purity	Comments
[Pd(PPh ₃) ₄]	ABCR Inc.	99 %	
[Pd(<i>t</i> -Bu ₃ P) ₂]	Strem Inc.	98 %	
1,7-Octadiyne	VWR Inc.	98 %	
2-Iodo-1,3-dimethylbenzene	Alfa Aesar Inc.	98 %	
2-Iodothiophene	Acros Inc.	98 %	
3-Hexylthiophene	Aldrich Inc.	>99 %	
4,7-Dibromo-2,1,3-benzothiadiazole	Alfa Aesar Inc.	98 %	
Ammonium chloride	Grüssing Inc.	99.5 %	
Calcium hydride	Acros Inc.	93 %	
Copper(I) chloride	Alfa Aesar Inc.	99.995+ %	
Copper(I) iodide	Aldrich Inc.	99.999 %	
Diisopropylamine	Honeywell Inc.	99 %	CaH ₂ , distilled
Dithranol	Aldrich Inc.	>98.0 %	
Ethynyltrimethylsilane	Aldrich Inc.	98 %	
Hexamethylditin	Aldrich Inc.	99 %	
Lithium aluminum hydride	Merck Inc.	95 %	
Magnesium sulfate	Grüssing Inc.	99 %	
Molecular sieves 3 Å	Merck Inc.		
<i>n</i> -Butyllithium	Acros Inc.	2.5 m in hexanes	
NIS	Molekula Inc.	95 %	
Ph ₂ SnCl ₂	VWR Inc.	96 %	distilled
Potassium carbonate	AppliChem Inc.	99 %	
Sodium	Merck Inc.	≥ 99 %	
Sodium chloride	Grüssing Inc.	99.5 %	
Sodium hydroxide	Grüssing Inc.	98 %	
Thiophene	VWR Inc.	99 %	distilled
Tripotassium phosphate	Aldrich Inc.	>98 %	

5.4.3 Solvents

All solvents were freshly distilled after refluxing for several hours over the specified drying agent under nitrogen or argon and were stored in a J. Young's-tube. If no drying agent is noted, the solvents were merely distilled for purification purposes.

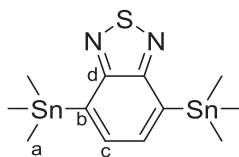
Solvent	Comments
Acetic acid	Grüssing Inc.
Benzene- d_6	Deutero Inc., sodium
$CDCl_3$	Deutero Inc., CaH_2
Chlorobenzene	TCI Inc.
Chloroform	VWR Inc., HPLC grade
Cyclohexane	BCD Inc.
DCM	BCD Inc.
Diethyl ether	BCD Inc.
DMF	Acros Inc., puriss. absolute over molecular sieve
DMSO	Acros Inc., 99.7+% extra dry over molecular sieve
Ethyl acetate	BCD Inc.
Methanol	Baker Inc.
<i>n</i> -Hexane	Walter CMP Inc.
<i>n</i> -Pentane	Walter CMP Inc., lithium aluminum hydride; degassed by freeze-pump-thaw technique
TEA	Acros Inc., CaH_2
THF	Sigma Aldrich Inc.; CaH_2 with triphenylmethane as an indicator; degassed by freeze-pump-thaw technique
Toluene	BCD Inc.; sodium with benzophenone as an indicator; degassed by freeze-pump-thaw technique

5.4.4 Chromatography

The silica gel used for chromatographic purification (Merck Inc. and Interchim Inc.) had a grain size of 0.015 - 0.050 mm. Thin layer chromatography was performed using pre-coated plates from Macherey-Nagel Inc., ALUGRAM[®] Xtra SIL G/UV₂₅₄ and POLYGRAM[®] ALOX N/UV₂₅₄. The chromatography purifications were carried out using an Interchim puriFlash[®] 430 purification system.

5.5 Unpublished Syntheses

5.5.1 4,7-Bis(trimethylstannyl)benzo[*c*][1,2,5]thiadiazole (2)



4,7-Dibromo-2,1,3-benzothiadiazole (294 mg, 1.00 mmol), [Pd(PPh₃)₄] (46.2 mg, 40.0 μmol, 4 mol%) and hexamethylditin (721 mg, 2.20 mmol) were suspended in toluene (4 mL). The orange suspension was heated to 120 °C in a microwave apparatus for 6 h. The reaction mixture was quenched by opening the reaction vessel and adding water (50 mL). The aqueous layer was extracted with diethyl ether (3 x 50 mL) and the combined organic layers were dried with magnesium sulfate. The volatiles were removed *in vacuo* and the resulting brown oil was purified by column chromatography (cyclohexane; R_f = 0.77. The column was conditioned by washing it with 3 CV TEA/cyclohexane 5:95; followed by 10 CV of pure cyclohexane). The product (361 mg, 78 %) was obtained as a yellow oil that crystallized after 2 d at 6 °C to give a pale yellow solid.

¹H NMR (500 MHz, CDCl₃): δ = 7.63 (s, 2 H, c), 0.42 (s, 18 H, a; ²J(¹¹⁹Sn, ¹H) = 28.5 Hz)* ppm.

* the signal shows satellites due to coupling with tin.

¹³C NMR (126 MHz, CDCl₃): δ = 159.4 (d), 137.3 (b), 136.9 (c), -8.8 (a, ¹J = 181.5 Hz) ppm.

Signals that show satellites due to coupling with tin are marked with *. Coupling constants ⁿJ(¹¹⁹Sn, ¹³C) are given in parentheses when signal to noise ratio allowed the determination.

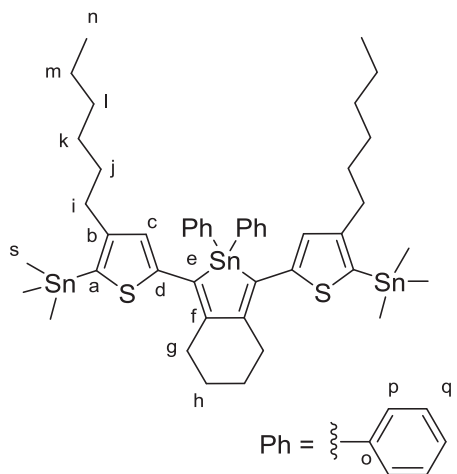
¹¹⁹Sn-NMR (187 MHz, CDCl₃): δ = -29.8 ppm.

M.p.: 50 °C.

IR (ATR): $\tilde{\nu}$ = 2980 (w), 2912 (w), 1698 (w), 1495 (w), 1458 (w), 1309 (w), 1186 (w), 872 (m), 846 (m), 832 (m), 765 (s), 719 (s), 615 (m), 577 (s), 527 (s), 512 (s), 465 (s) cm⁻¹.

HRMS (ESI) *m/z*: Found 448.9138; calcd. for C₁₁H₁₇N₂SSn₂ [M - CH₃]⁺ 448.9155.

5.5.2 1,3-Bis(4-hexyl-5-(trimethylstannyl)thiophen-2-yl)-2,2-diphenyl-4,5,6,7-tetrahydro-2H-benzo[c]stannole (3)



P2-9 (250 mg, 26.0 μmol), $[\text{Pd}(\text{PPh}_3)_4]$ (3.0 mg, 2.6 μmol , 10 mol%) and hexamethylditin (203 mg, 62 μmol) were dissolved in toluene (10 mL). The yellow solution was heated to 120 $^\circ\text{C}$ in a microwave apparatus for 30 min.^[64] Then, the volatiles were removed *in vacuo* and the crude product was purified by column chromatography (*n*-hexane/TEA 95:5; $R_f = 0.17$; the TEA was added to prevent decomposition) to obtain 190 mg (71 %) of a yellow solid.

^1H NMR (500 MHz, CDCl_3): $\delta = 7.72 - 7.57$ (m, 4 H, p)*, 7.37 – 7.31 (m, 6 H, q and r), 6.93 (s, 2 H, c), 2.93 – 2.84 (m, 4 H, g), 2.49 – 2.43 (t, $^3J = 7.6$ Hz, 4 H, i), 1.83 – 1.76 (m, 4 H, h), 1.48 – 1.38 (m, 4 H, j), 1.27 – 1.18 (m, 12 H, k, l and m), 0.85 (t, $^3J = 6.9$ Hz, 6 H, n), 0.35 (s, 18 H, s; $^2J(^{119}\text{Sn}, ^1\text{H}) = 28.5$ Hz)* ppm.

* the signal shows satellites due to coupling with tin.

^{13}C NMR (126 MHz, CDCl_3): $\delta = 151.0$ (d or f), 150.4 (b), 149.3 (d or f), 138.8 (o), 137.3 (p, $^2J = 20.5$ Hz)*, 133.7 (a), 132.4 (c), 129.4 (e), 129.1 (r), 128.7 (q, $^3J = 26.6$ Hz)*, 32.5 (i), 31.8 (g, j and k or l)**, 29.1 (k or l), 23.3 (h), 22.5 (m), 14.1 (n), -7.9 (s) ppm.

Signals that show satellites due to coupling with tin are marked with *. Coupling constants $^nJ(^{119}\text{Sn}, ^{13}\text{C})$ are given in parentheses when signal to noise ratio allowed the determination.

** this peak consists of three overlapping signals.

^{119}Sn NMR (187 MHz, CDCl_3): $\delta = -38.0, -84.0$ ppm.

$\lambda_{\text{max}} = 439$ nm ($\epsilon = 47.6 \times 10^3$ L mol $^{-1}$ cm $^{-1}$).

M.p.: 155 $^\circ\text{C}$.

IR (ATR): $\tilde{\nu} = 2925$ (m), 2853 (w), 1430 (w), 1184 (w), 1075 (w), 998 (w), 925 (w), 908 (w), 813 (m), 763 (m), 725 (s), 695 (s), 526 (m), 512 (m), 466 (m) cm $^{-1}$.

HRMS (MALDI, dithranol) m/z : Found 1040.1530; calcd. for $C_{46}H_{64}S_2Sn_3$ 1040.1510.

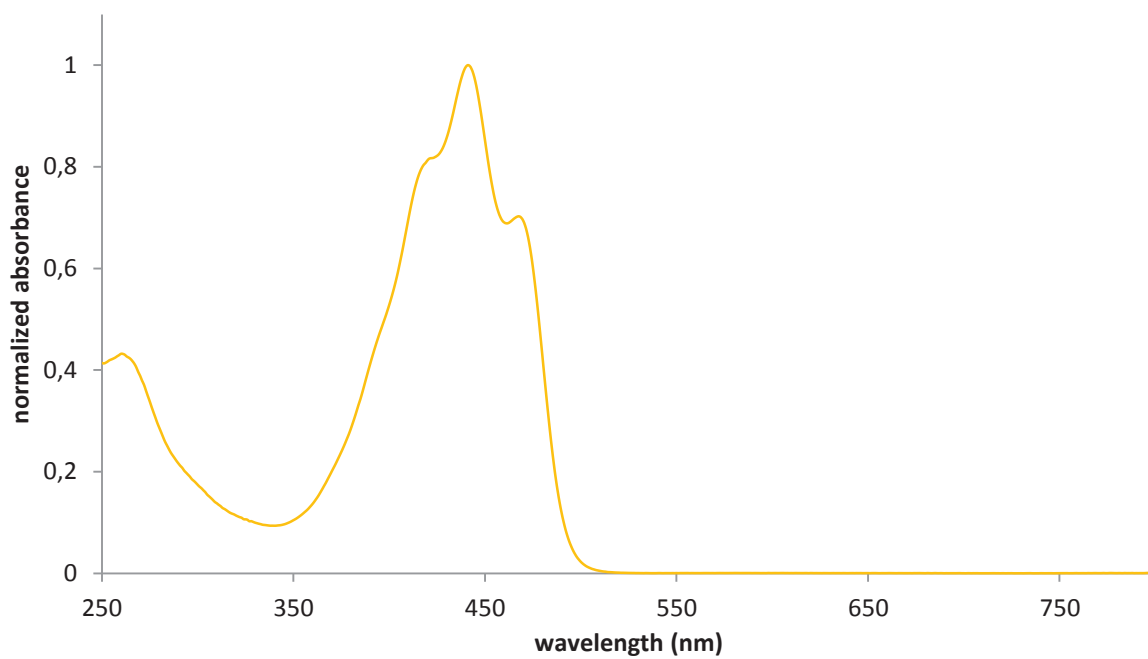
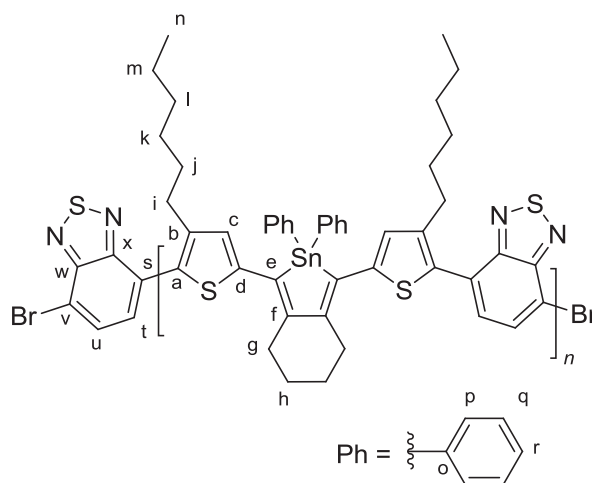


Figure 25. Full absorption spectrum of **3** in solution (chloroform).

5.5.3 7,7'-(5,5'-(2,2-Diphenyl-4,5,6,7-tetrahydro-2H-benzo[c]stannole-1,3-diyl)bis(3-hexylthiophene-5,2-diyl))bis(4-bromobenzo[c][1,2,5]thiadiazole) (TStTB with $n = 1$)



3 (160 mg, 154 μmol), $[\text{Pd}(\text{PPh}_3)_4]$ (8.9 mg, 7.7 μmol , 5 mol%), 4,7-dibromo-2,1,3-benzothiadiazole (45.0 mg, 154 μmol) and 3 drops of DMSO were dissolved in toluene (4 mL). The orange solution was heated to 120 $^\circ\text{C}$ in a microwave apparatus for 8 h. Then, the volatiles were removed *in vacuo* and TLC as well as NMR analysis showed that a mixture of starting material and low molecular weight oligomers was obtained. The crude product was purified by column chromatography (*n*-hexane/TEA 95:5; $R_f = 0.06$; the TEA was added to prevent decomposition) to obtain 10 mg (6 %) of a black solid, which was identified as **TStTB** with $n = 1$. Other fractions did not contain single compounds.

$^1\text{H NMR}$ (500 MHz, CDCl_3): $\delta = 7.87$ (d, $^3J = 7.6$ Hz, 2 H, t or u), 7.79–7.66 (m, 4 H, p)*, 7.44 (d, $^3J = 7.6$ Hz, 2 H, t or u), 7.42–7.38 (m, 6 H, q and r), 6.98 (s, 2 H, c), 2.96–2.89 (m, 4 H, g), 2.54–2.48 (t, $^3J = 7.6$ Hz, 4 H, i), 1.84–1.78 (m, 4 H, h), 1.48–1.38 (m, 4 H, j), 1.17–1.06 (m, 12 H, k, l and m), 0.82–0.75 (m, 6 H, n) ppm.

* the signal shows satellites due to coupling with tin.

$^{13}\text{C NMR}$ (126 MHz, CDCl_3): $\delta = 153.7$ (w and x)**, 150.5 (f), 146.2 (Tph), 141.8 (Tph), 138.3 (o), 137.4 (p, $^2J = 20.6$ Hz)*, 132.6 (Tph), 132.5 (Tph), 132.2 (t or u), 130.8 (e), 130.2 (t or u), 129.6 (r), 129.1 (q, $^3J = 27.0$ Hz)*, 128.1 (s), 113.2 (v), 32.1 (k or l or g), 31.7 (k or l or g), 30.6 (j), 29.3 (i or k or l), 29.1 (i or k or l), 23.3 (h), 22.6 (m), 14.2 (n) ppm.

Signals that show satellites due to coupling with tin are marked with *. Coupling constants $^nJ(^{119}\text{Sn}, ^{13}\text{C})$ are given in parentheses when signal to noise ratio allowed the determination.

** this signal consists of two overlapping signals.

^{119}Sn NMR (187 MHz, CDCl_3): $\delta = -79.9$ ppm.

λ_{max} (CHCl_3) = 507 nm.

M.p.: 177 °C.

IR (ATR): $\tilde{\nu} = 2923$ (s), 2855 (m), 1479 (s), 1426 (s), 1359 (m), 1259 (m), 1072 (m), 998 (w), 876 (s), 840 (s), 820 (s), 725 (s), 694 (s), 619 (m), 551 (m) cm^{-1} .

HRMS (MALDI, colloidal graphite matrix) m/z : Found 1138.0281; calcd. for $\text{C}_{52}\text{H}_{50}\text{Br}_2\text{N}_4\text{S}_4\text{Sn}$ 1138.0287.

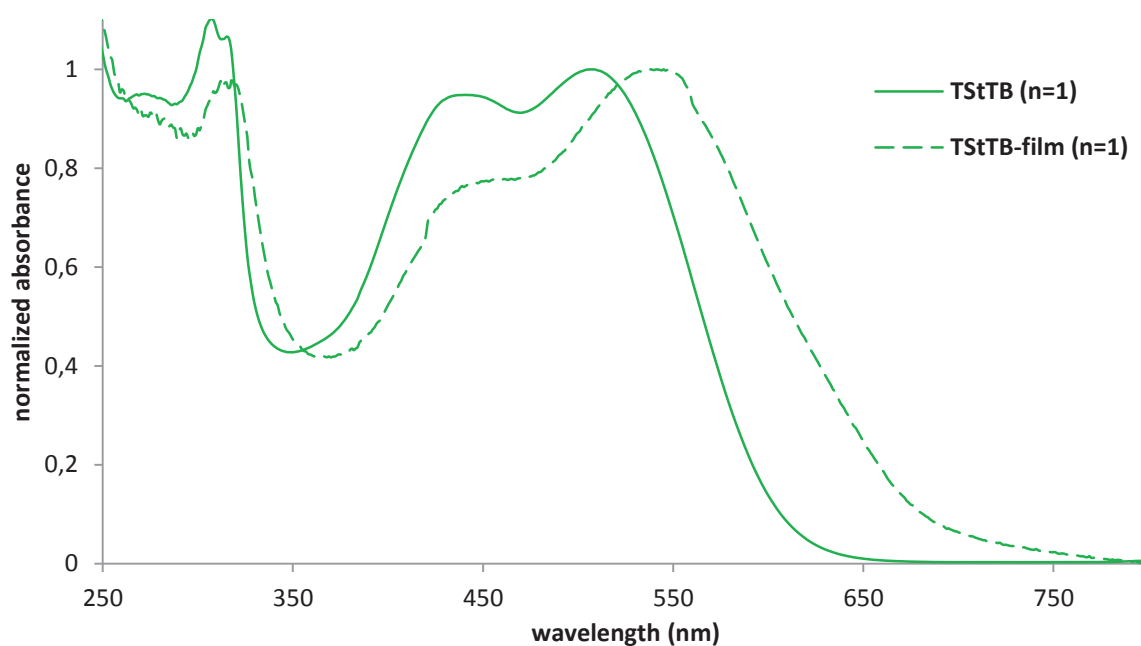
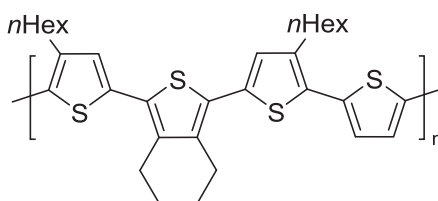


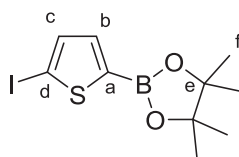
Figure 26. Full absorption spectra of **TStTB** ($n = 1$) in solution (chloroform) and as film.

5.5.4 Polymer TTTT



A yellow-orange solution of **4** (108.4 mg, 150.0 μmol), 2,5-bis(trimethylstannyl)thiophene (61.5 mg, 150 μmol) and $[\text{Pd}(\text{PPh}_3)_4]$ (8.7 mg, 7.5 μmol , 5 mol%) in toluene (5 mL), prepared in a glove box, was heated to reflux for 15 h. A red suspension was obtained and the volatiles were removed *in vacuo*. The resulting polymer was insoluble in common solvents (chloroform, dichloromethane, THF, toluene, chlorobenzene) at 20 °C and the corresponding reflux temperatures. Thus, a characterization was not possible.

5.5.5 2-(5-Iodothiophen-2-yl)-4,4,5,5-tetramethyl-1,3,2-dioxaborolane (6)



A solution of diisopropylamine (7.08 g, 70.0 mmol) in THF (200 mL) was cooled to $-78\text{ }^{\circ}\text{C}$ and *n*-butyllithium (20.0 mL, 50.0 mmol; 2.5 M in hexanes) was added dropwise within 30 min. The mixture was warmed to $0\text{ }^{\circ}\text{C}$, cooled back to $-78\text{ }^{\circ}\text{C}$ and stirring was continued for 5 min. 2-Iodothiophene (10.5 g, 50.0 mmol) in THF (20 mL) was added over the course of 25 min and the reaction mixture was stirred for 1 h at $-78\text{ }^{\circ}\text{C}$. *i*PrO-BPin (10.2 g, 55.0 mmol) was added dropwise to the orange-brown suspension and the reaction mixture was stirred for 19 h while it was allowed to warm to $20\text{ }^{\circ}\text{C}$ without removal of the cooling bath. The reaction was quenched with a saturated solution of ammonium chloride (50 mL) and the aqueous layer was extracted with ethyl acetate (3 x 100 mL). The combined organic layers were dried over magnesium sulfate. The volatiles were removed *in vacuo* to obtain 16.7 g (99 %) of an oil that crystallized after 18 h at $5\text{ }^{\circ}\text{C}$ to a pale yellow solid.

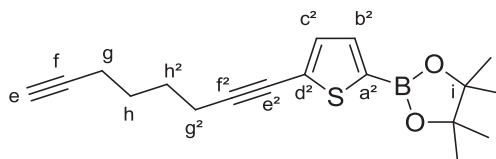
$^1\text{H NMR}$ (500 MHz, CDCl_3): δ = 7.29 (d, 1 H, 3J = 3.6 Hz, b or c), 7.27 (d, 1 H, 3J = 3.6 Hz, b or c), 1.33 (s, 12 H, f) ppm.

$^{13}\text{C NMR}$ (126 MHz, CDCl_3): δ = 138.5 (b or c), 138.3 (b or c), 84.3 (e), 81.5 (d), 24.7 (f) ppm.^[65]

$^{11}\text{B NMR}$ (160 MHz, CDCl_3): δ = 28.2 ppm.

The NMR data are in agreement with the data found in the literature.^[66]

5.5.6 4,4,5,5-Tetramethyl-2-(5-(octa-1,7-diyn-1-yl)thiophen-2-yl)-1,3,2-dioxaborolane (7)



A mixture of **6** (2.31 g, 6.88 mmol), 1,7-octadiyne (1.47 g, 13.8 mmol), [Pd(PPh₃)₄] (80.9 mg, 70.0 μmol, 1 mol%) and copper(I) iodide (13.3 mg, 70.0 μmol, 1 mol%) in TEA (1.5 mL) and DMF (4.5 mL) was stirred for 18 h at 55 °C. The reaction was quenched with brine (50 mL) and the aqueous layer was extracted with diethyl ether (3 x 80 mL). The combined organic layers were washed with water (50 mL) and then dried over magnesium sulfate. The volatiles were removed *in vacuo* and the residue was purified by column chromatography (gradient from cyclohexane to cyclohexane/diethyl ether 9:1; R_f = 0.59 for cyclohexane/diethyl ether 9:1) to obtain 1.20 g of a yellow oil (56 %).

¹H NMR (500 MHz, CDCl₃): δ = 7.44 (d, 1 H, ³J = 3.6 Hz, b²), 7.15 (d, 1 H, ³J = 3.6 Hz, c²), 2.47 (t, 2 H, ³J = 6.8 Hz, g²), 2.25 (td, 2 H, ³J = 6.8, ⁴J = 2.7 Hz, g), 1.96 (t, 1 H, ⁴J = 2.7 Hz, e), 1.77 – 1.65 (m, 4 H, h and h²), 1.33 (s, 12 H, j) ppm.

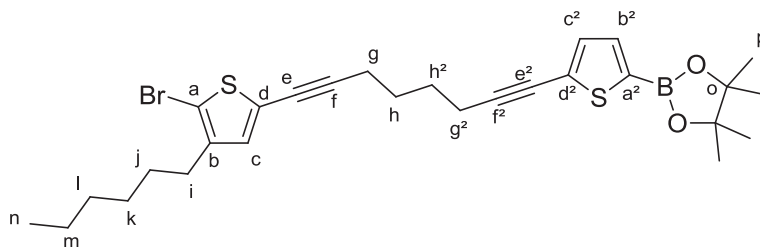
¹³C NMR (126 MHz, CDCl₃): δ = 136.8 (b²), 132.1 (c²), 130.7 (d²), 95.4 (f²), 84.2 (i), 84.0 (f), 74.2 (e²), 68.6 (e), 27.5 (h or h²), 27.4 (h or h²), 24.7 (j), 19.3 (g²), 18.0 (g) ppm.^[65]

¹¹B-NMR (160 MHz, CDCl₃): δ = 28.4 ppm.

IR (ATR): $\tilde{\nu}$ = 3298 (w), 2979 (w), 2934 (w), 1523 (m), 1456 (s), 1372 (m), 1352 (s), 1290 (m), 1270 (m), 1140 (s), 1065 (m), 852 (s), 812 (m), 664 (s), 633 (m) cm⁻¹.

HRMS (EI) *m/z*: Found 314.1515; calcd. for [M]⁺ C₁₈H₂₃BO₂S 314.1512.

5.5.7 2-(5-(8-(5-Bromo-4-hexylthiophen-2-yl)octa-1,7-diyn-1-yl)thiophen-2-yl)-4,4,5,5-tetramethyl-1,3,2-dioxaborolane (8)



A mixture of **7** (1.00 g, 3.18 mmol), **P2-4** (1.19 g, 3.18 mmol), [Pd(PPh₃)₄] (69.3 mg, 60.0 μmol, 2 mol%) and copper(I) iodide (11.4 mg, 60.0 μmol, 2 mol%) in TEA (1 mL) and DMF (3 mL) was stirred at 55 °C for 18 h. The reaction was quenched with brine (50 mL) and the aqueous layer was extracted with diethyl ether (3 x 80 mL). The combined organic layers were washed with water (50 mL) and then dried over magnesium sulfate. The volatiles were removed *in vacuo* and the residue was purified by column chromatography (gradient from *n*-pentane to *n*-pentane/diethyl ether 9:1; R_f = 0.26 for *n*-pentane/diethyl ether 95:5) to obtain 1.02 g (57 %) of a yellow oil.

¹H NMR (600 MHz, CDCl₃): δ = 7.45 (d, ³J = 3.6 Hz, 1 H, b²), 7.15 (d, ³J = 3.6 Hz, 1 H, c²), 6.81 (s, 1 H, c), 2.51–2.44 (m, 6 H, i, g and g²), 1.78–1.71 (m, 4 H, h and h²), 1.56–1.49 (m, 2 H, j), 1.33 (s, 12 H, p), 1.31–1.25 (m, 6 H, k, l and m), 0.88 (t, ³J = 6.7 Hz, 3 H, n) ppm.

¹³C NMR (151 MHz, CDCl₃): δ = 142.0 (b), 136.8 (b²), 132.1 (c and c²)*, 130.7 (d²), 123.7 (d), 108.3 (a), 95.4 (f²), 94.7 (f), 84.2 (o), 74.3 (e²), 73.8 (e), 31.6 (l), 29.6 (j), 29.4 (i), 28.8 (k), 27.6 (h and h²)*, 24.7 (p), 22.6 (m), 19.4 (g or g²), 19.3 (g or g²), 14.1 (n) ppm.^[65]

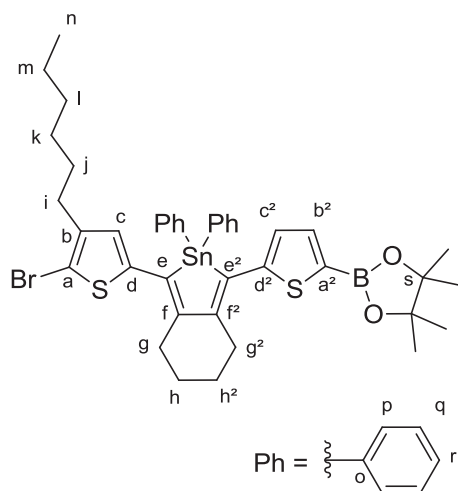
* two signals.

¹¹B NMR (160 MHz, CDCl₃): δ = 28.8 ppm.

IR (ATR): $\tilde{\nu}$ = 2926 (m), 2857 (w), 1522 (m), 1456 (s), 1379 (m), 1371 (m), 1352 (s), 1290 (m), 1270 (m), 1213 (w), 1166 (w), 1140 (s), 1064 (m), 1015 (w), 851 (s), 810 (m), 663 (s), 579 (w) cm⁻¹.

HRMS (EI) *m/z*: Found 558.1426; calcd. for [M]⁺ C₂₈H₃₆BBro₂S₂ 558.1433.

5.5.8 1-(5-Bromo-4-hexylthiophen-2-yl)-2,2-diphenyl-3-(5-(4,4,5,5-tetramethyl-1,3,2-dioxaborolan-2-yl)thiophen-2-yl)-4,5,6,7-tetrahydro-2H-benzo[c]-stannole (10)



In a nitrogen filled glovebox, **8** (71.6 mg, 128 μmol) and $\text{Cp}_2\text{Zr}(\text{pyr})(\text{Me}_3\text{SiC}\equiv\text{CSiMe}_3)$ (63.1 mg, 134 μmol) were dissolved in toluene (2 mL) and the solution was stirred for 20 h at 20 °C under nitrogen. Ph_2SnCl_2 (46.1 mg, 134 μmol), copper(I) chloride (12.7 mg, 128 μmol) and toluene (2 mL) were added to the dark solution in the glovebox. The reaction mixture was stirred at 20 °C for 4 h, was quenched with water (50 mL) and the aqueous layer was extracted with DCM (3 x 80 mL). The combined organic layers were dried over magnesium sulfate. The volatiles were removed *in vacuo* and the residue was purified by column chromatography (chloroform/*n*-pentane 40:60) to obtain 10 mg (9 %) of a yellow oil.

$^1\text{H NMR}$ (500 MHz, CDCl_3): δ = 7.66 – 7.54 (m, 4 H, p)*, 7.46 (d, 3J = 3.7 Hz, 1 H, b^2 or c^2), 7.39 – 7.35 (m, 6 H, q and r), 7.01 (d, 3J = 3.7 Hz, 1 H, b^2 or c^2), 6.65 (s, 1 H, c), 2.94 (t, 3J = 5.9 Hz, 2 H, g or g^2), 2.78 (t, 3J = 5.9 Hz, 2 H, g or g^2), 2.43 (t, 3J = 7.5 Hz, 2 H, i), 1.83 – 1.74 (m, 4 H, h and h^2), 1.48 – 1.39 (m, 2 H, j), 1.33 (s, 12 H), 1.24 – 1.18 (m, 6 H, k, l and m), 0.85 (t, 3J = 6.8 Hz, 3 H, n) ppm.

* the signal shows satellites due to coupling with tin.

$^{13}\text{C NMR}$ (126 MHz, CDCl_3): δ = 152.2 (d^2 or e^2 or f^2 or f), 151.7 (d^2 or e^2 or f^2 or f), 149.5 (d^2 or e^2 or f^2 or f), 144.7 (d or e), 141.6 (b), 137.8 (o), 137.1 (p, 2J = 20.6 Hz)*, 137.0 (b^2 or c^2), 131.4 (d or e), 131.1 (b^2 or c^2), 130.2 (c), 129.9 (d^2 or e^2 or f^2 or f), 129.5 (r), 128.9 (q, 3J = 26.8 Hz)*, 110.0 (a), 84.0 (s), 32.1 (g or g^2), 31.7 (g or g^2 or l or k), 31.6 (g or g^2 or l or k), 29.4 (j), 29.2 (i), 28.6 (k or l), 24.7 (t), 23.1 (h and h^2), 22.5 (m), 14.1 (n) ppm.^[65]

Signals that show satellites due to coupling with tin are marked with *. Coupling constants ${}^nJ({}^{119}\text{Sn}, {}^{13}\text{C})$ are given in parentheses when signal to noise ratio allowed the determination.

${}^{119}\text{Sn}$ NMR (187 MHz, CDCl_3): $\delta = -82.0$ ppm.

${}^{11}\text{B}$ NMR (160 MHz, CDCl_3): $\delta = 29.2$ ppm.

$\lambda_{\text{max}} = 439$ nm.^[67]

IR (ATR): $\tilde{\nu} = 2926$ (s), 2855 (m), 1513 (m), 1436 (s), 1354 (s), 1264 (m), 1184 (w), 1141 (s), 1073 (m), 854 (m), 801 (m), 728 (m), 697 (m), 664 (m), 588 (w) cm^{-1} .

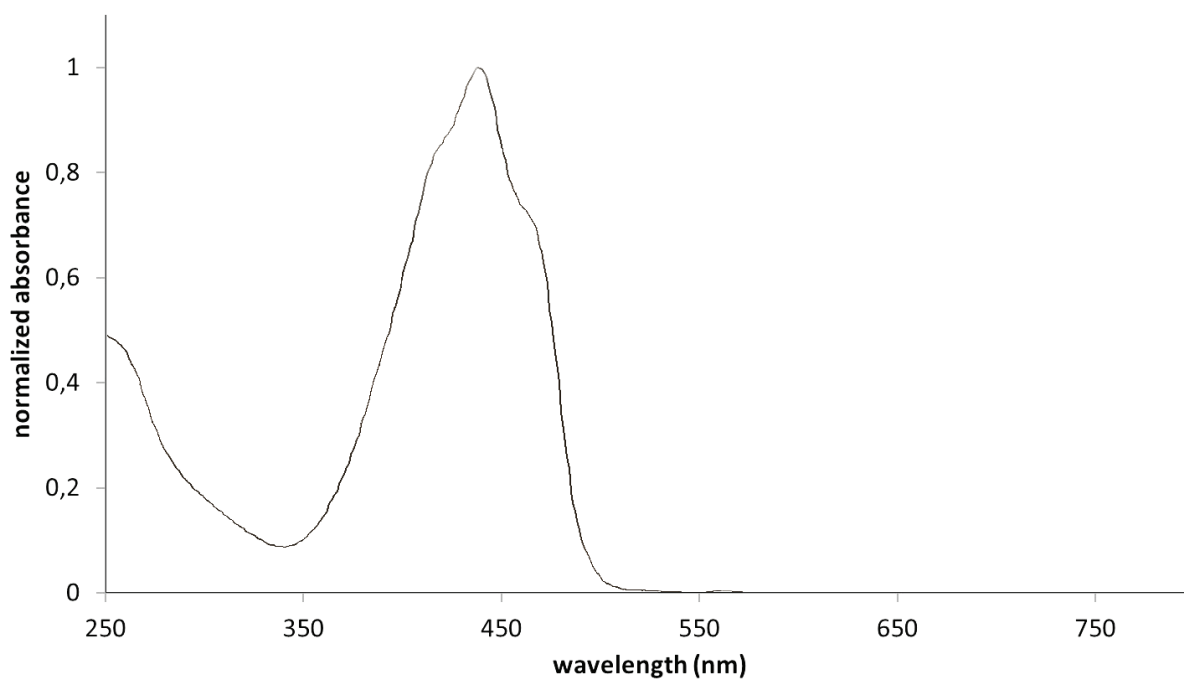
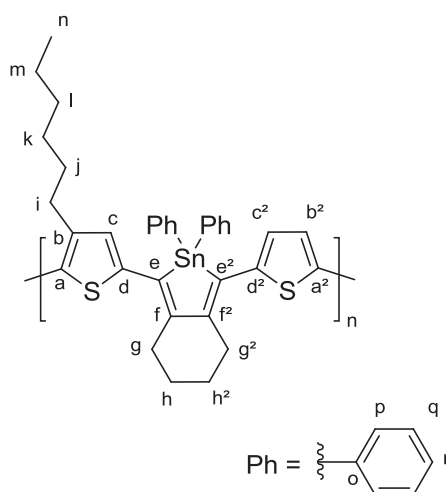


Figure 27. Absorption spectrum of **10** in solution (chloroform/*n*-pentane 40:60).^[67]

5.5.9 Polymer TStT



A yellow solution of **10** (14.0 mg, 16.8 μmol) and $[\text{Pd}(\text{PtBu}_3)_2]$ (0.9 mg, 1.7 μmol) in THF (5 mL) was prepared in a nitrogen filled glove box. The reaction vessel was sealed and brought out of the glove box. Tripotassium phosphate (2 M in water; 84.0 μL , 168 μmol) was added under argon at a Schlenk line, and the mixture was stirred for 20 h at 15 $^\circ\text{C}$. The deep blue-purple solution was precipitated into methanol (10 mL). The polymer was collected by centrifugation and dried *in vacuo* to yield 10 mg (95 %) of a dark blue-purple solid.

λ_{max} (CHCl_3) = 567 nm.^[68]

$^1\text{H NMR}$ (600 MHz, CDCl_3): δ = 7.71 – 7.60 (broad m, 4 H, p), 7.41 – 7.35 (broad m, 6 H, q and r), 7.00 – 6.95 (broad m, 1 H, c or c^2 or b^2), 6.93 – 6.88 (broad m, 1 H, c or c^2 or b^2), 6.80 – 6.75 (broad s, 1 H, c or c^2 or b^2), 2.97 – 2.84 (broad m, 4 H, g and g^2), 2.69 – 2.61 (broad m, 2 H, i), 1.86 – 1.77 (broad m, 4 H, h and h^2), 1.52 – 1.45 (broad m, 2 H, j), 1.24 – 1.15 (broad m, 6 H, k, l and m), 0.85 – 0.80 (broad m, 3 H, n) ppm.

Some additional signals that could correspond to e. g. different end groups and small molecular weight oligomers are present in the $^1\text{H NMR}$ spectrum.

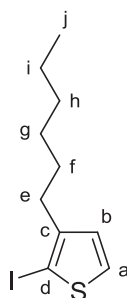
$^{13}\text{C NMR}$: Analysis by $^{13}\text{C NMR}$ was not possible due to the low solubility of the polymer.

$^{119}\text{Sn NMR}$ (187 MHz, CDCl_3): δ = -81.2 ppm.

IR (ATR): $\tilde{\nu}$ = 2924 (m), 2855 (m), 1645 (w), 1428 (w), 1060 (s), 974 (s), 850 (m), 724 (s), 695 (s), 668 (m), 467 (s) cm^{-1} .

Determination of the molecular weights by GPC was not possible due to the low solubility of the polymer.

5.5.10 3-Hexyl-2-iodothiophene (**11**)



3-Hexyl-2-iodothiophene (**11**) was synthesized similar to a method described in the literature^[69] and was modified as follows:

To a solution of 3-*n*-hexylthiophene (5.06 g, 30.1 mmol) in CHCl₃ (50 mL) and acetic acid (50 mL), NIS (6.77 g, 30.07 mmol) was added in portions within 3 min at 0 °C. The mixture was shielded from light and stirred for 18 h without removal of the cooling bath. The red solution was quenched with a saturated solution of sodium hydroxide (200 mL) and extracted with chloroform (3 x 70 mL). The combined organic layers were dried with magnesium sulfate and the volatiles were removed *in vacuo*. The crude product was distilled by Kugelrohr distillation (2·10⁻¹ mbar, 100 °C) to yield 6.62 g (75 %, Lit.^[69]: 90 % with impurities) of a pale yellow oil.

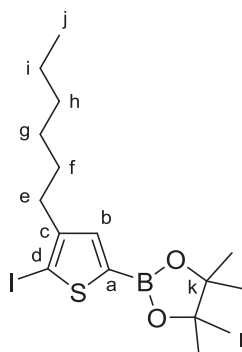
¹H NMR (500 MHz, CDCl₃): δ = 7.37 (d, ³J = 5.4 Hz, 1 H, a or b), 6.75 (d, ³J = 5.4 Hz, 1 H, a or b), 2.54 (t, ³J = 7.8 Hz, 2 H, e), 1.61 – 1.50 (m, 2 H, f), 1.38 – 1.27 (m, 6 H, g, h and i), 0.89 (t, ³J = 6.9 Hz, 3 H, j) ppm.

¹³C NMR (126 MHz, CDCl₃): δ = 147.2 (c), 130.3 (a or b), 127.9 (a or b), 73.9 (d), 32.1 (e), 31.6 (g or h), 30.0 (f), 28.9 (g or h), 22.6 (i), 14.1 (j) ppm.

IR (ATR): $\tilde{\nu}$ = 2953 (m), 2923 (s), 2854 (s), 1456 (m), 1397 (m), 963 (m), 828 (s), 713 (s), 684 (s), 634 (s) cm⁻¹.

The NMR data are in agreement with the data found in the literature.^[70]

5.5.11 2-(4-Hexyl-5-iodothiophen-2-yl)-4,4,5,5-tetramethyl-1,3,2-dioxaborolane (12)



2-(4-Hexyl-5-iodothiophen-2-yl)-4,4,5,5-tetramethyl-1,3,2-dioxaborolane (**12**) was synthesized similar to a method described in the literature^[70] and was modified as follows:

A solution of diisopropylamine (2.62 g, 25.9 mmol) in THF (120 mL) was cooled to $-78\text{ }^{\circ}\text{C}$ and *n*-butyllithium (7.40 mL, 18.5 mmol; 2.5 M in hexanes) was added dropwise within 5 min. The mixture was warmed to $0\text{ }^{\circ}\text{C}$ within 15 min, cooled back to $-78\text{ }^{\circ}\text{C}$ and stirring was continued for 5 min. 3-Hexyl-2-iodothiophene (**11**; 5.44 g, 18.5 mmol) in THF (5 mL) was added over the course of 10 min and the reaction mixture was stirred for 1 h at $-78\text{ }^{\circ}\text{C}$. *i*PrO-BPin (3.80 g, 20.4 mmol) was added dropwise and the orange-brown solution was stirred for 18 h while it was allowed to warm to $17\text{ }^{\circ}\text{C}$ without removal of the cooling bath. The dark brown reaction was quenched with a saturated solution of ammonium chloride (50 mL) and the aqueous layer was extracted with chloroform (3 x 70 mL). The combined organic layers were dried over magnesium sulfate. The volatiles were removed *in vacuo* and the residue was purified by column chromatography (gradient from *n*-pentane to *n*-pentane/ethyl acetate 95/5; $R_f = 0.68$ for 95/5 *n*-pentane/ethyl acetate) to obtain a red oil (6.70 g, 86 %, Lit.^[70]: 30 %).

¹H NMR (500 MHz, CDCl_3): $\delta = 7.24$ (s, 1 H, c), 2.57–2.52 (m, 2 H, e), 1.61–1.53 (m, 2 H, f), 1.36–1.27 (m, 18 H, g, h, i and l), 0.88 (t, $^3J = 6.9$ Hz, 3 H, j) ppm.

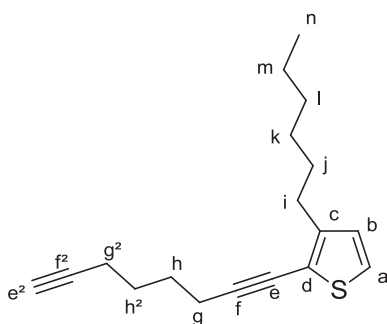
¹³C NMR (126 MHz, CDCl_3): $\delta = 148.6$ (c), 137.5 (b), 84.2 (k), 82.7 (d), 31.9 (e or g or h), 31.6 (e or g or h), 30.0 (f), 28.9 (g or h), 24.7 (l), 22.6 (i), 14.1 (j) ppm.^[65]

¹¹B NMR (160 MHz, CDCl_3): $\delta = 28.4$ ppm.

IR (ATR): $\tilde{\nu} = 2955$ (w), 2926 (m), 2855 (w), 1540 (m), 1428 (s), 1370 (m), 1327 (s), 1294 (s), 1267 (s), 1139 (s), 1025 (m), 956 (w), 851 (s), 662 (s) cm^{-1} .

The NMR data are in agreement with the data found in the literature.^[70]

5.5.12 3-Hexyl-2-(octa-1,7-diyn-1-yl)thiophene (14)



A mixture **11** (4.62 g, 15.7 mmol), 1,7-octadiyne (6.67 g, 62.8 mmol), [Pd(PPh₃)₄] (358 mg, 310 μmol, 2 mol%) and copper(I) iodide (59.0 mg, 310 μmol, 2 mol%) in TEA (10 mL) and DMF (30 mL) was stirred for 3 h at 55 °C. The brown suspension was quenched by opening the reaction vessel to air and adding water (50 mL). The aqueous layer was extracted with *n*-pentane (3 x 80 mL). The combined organic layers were dried over magnesium sulfate, the volatiles were removed *in vacuo* and the residue was purified by column chromatography (*n*-pentane; R_f = 0.24). The obtained oil was distilled by Kugelrohr distillation (4.4·10⁻² mbar, 135 °C) to yield 2.67 g (62 %) of a yellow oil.

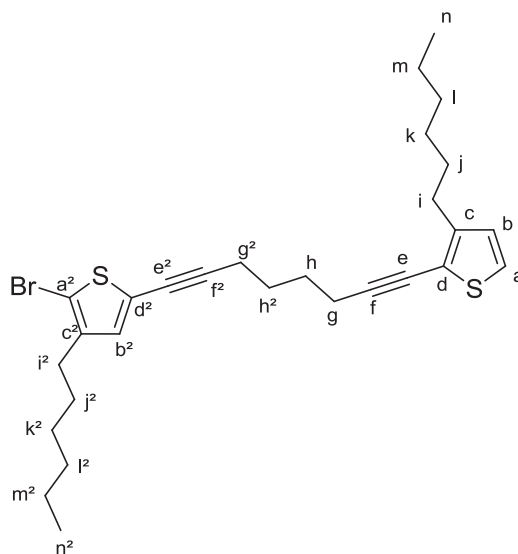
¹H NMR (600 MHz, CDCl₃): δ = 7.05 (d, ³J = 5.2 Hz, 1 H, a or b), 6.81 (d, ³J = 5.2 Hz, 1 H, a or b), 2.65 (t, ³J = 7.7 Hz, 2 H, i), 2.49 (t, ³J = 6.6 Hz, 2 H, g), 2.28 – 2.23 (m, 2 H, g²), 1.96 (t, ⁴J = 2.6 Hz, 1 H, e²), 1.76 – 1.69 (m, 4 H, h and h²), 1.62 – 1.56 (m, 2 H, j), 1.36 – 1.28 (m, 6 H, k, l and m), 0.88 (t, ³J = 6.8 Hz, 3 H, n) ppm.

¹³C NMR (151 MHz, CDCl₃): δ = 146.7 (c), 128.0 (a or b), 124.5 (a or b), 118.9 (d), 95.6 (f), 84.1 (f²), 73.7 (e), 68.5 (e²), 31.6 (k or l), 30.2 (j), 29.4 (i), 29.0 (k or l), 27.7 (h or h²), 27.5 (h or h²), 22.6 (m), 19.3 (g), 18.0 (g²), 14.1 (n) ppm.

IR (ATR): $\tilde{\nu}$ = 3302 (w), 2926 (s), 2857 (m), 1457 (m), 1428 (m), 1327 (w), 1237 (w), 1086 (w), 834 (m), 722 (m), 629 (s), 507 (w) cm⁻¹.

HRMS (EI) *m/z*: Found 272.1595; calcd. for C₁₈H₂₄S [M]⁺ 272.1599.

5.5.13 2-Bromo-3-hexyl-5-(8-(3-hexylthiophen-2-yl)octa-1,7-diyn-1-yl)thiophene (15)



A mixture **14** (2.53 g, 9.28 mmol), **P2-4** (3.81 g, 10.2 mmol), [Pd(PPh₃)₄] (220 mg, 0.19 mmol, 2 mol%) and copper(I) iodide (36 mg, 0.19 mmol, 2 mol%) in TEA (9 mL) and DMF (27 mL) was stirred for 40 h at 55 °C. The brown suspension was quenched by opening the reaction vessel to air and adding water (50 mL). The aqueous layer was extracted with *n*-pentane (3 x 80 mL). The combined organic layers were dried over magnesium sulfate, the volatiles were removed *in vacuo* and the residue was purified by column chromatography (*n*-pentane; R_f = 0.32) to obtain a yellow oil (4.12 g, 86 %).

¹H NMR (600 MHz, CDCl₃): δ = 7.06 (d, ³J = 5.2 Hz, 1 H, a or b), 6.82 (d, ³J = 5.2 Hz, 1 H, a or b), 6.80 (s, 1 H, b²), 2.66 (t, ³J = 7.7 Hz, 2 H, i), 2.54 – 2.41 (m, 6 H, g, g² and i²), 1.83 – 1.72 (m, 4 H, h and h²), 1.63 – 1.50 (m, 4 H, j and j²)*, 1.39 – 1.26 (m, 12 H, k, k², l, l², m and m²), 0.92 – 0.84 (m, 6 H, n and n²) ppm.

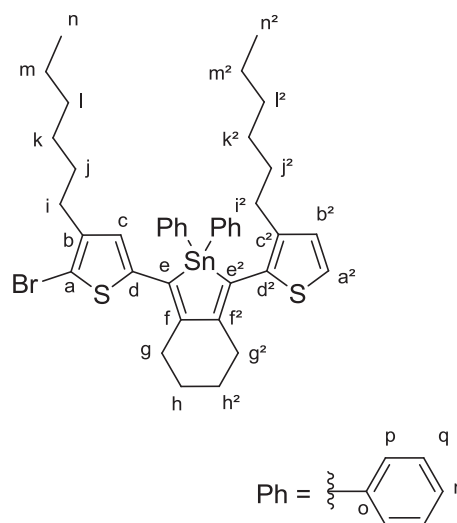
* overlapping with water signal.

¹³C NMR (151 MHz, CDCl₃): δ = 146.7 (c), 142.0 (c²), 132.0 (b²), 128.0 (a or b), 124.6 (a or b), 123.8 (d²), 118.9 (d), 108.3 (a²), 95.6 (f or f²), 94.7 (f or f²), 73.8 (e or e²), 73.7 (e or e²), 31.7 (k and k² or l and l²), 31.6 (k and k² or l and l²), 30.2 (j), 29.6 (j²), 29.4 (i and i²), 29.0 (k and k² or l and l²), 28.8 (k and k² or l and l²), 27.8 (h or h²), 27.6 (h or h²), 22.6 (m and m²)*, 19.3 (g and g²)*, 14.1 (n and n²)* ppm. * two signals.

IR (ATR): $\tilde{\nu}$ = 2924 (s), 2855 (s), 1546 (w), 1456 (m), 1325 (m), 1197 (m), 1007 (w), 834 (s), 722 (m), 695 (m), 656 (m), 535 (w) cm⁻¹.

HRMS (EI) *m/z*: Found 516.1517; calcd. for C₂₈H₃₇BrS₂ [M]⁺ 516.1520.

5.5.14 1-(5-Bromo-4-hexylthiophen-2-yl)-3-(3-hexylthiophen-2-yl)-2,2-diphenyl-4,5,6,7-tetrahydro-2H-benzo[*c*]stannole (16)



In a glovebox, **15** (518 mg, 1.00 mmol) and $\text{Cp}_2\text{Zr}(\text{pyr})(\text{Me}_3\text{SiC}\equiv\text{CSiMe}_3)$ (495 mg, 1.05 mmol) were dissolved in toluene (8 mL) and the dark solution was stirred for 20 h at 20 °C. Ph_2SnCl_2 (361 mg, 1.05 mmol), copper(I) chloride (9.9 mg, 100 μmol) and toluene (2 mL) were added in a glovebox and the dark mixture was stirred for 3 h at 20 °C, over which time the solution turned brown-yellow. The suspension was quenched with water (25 mL) and the aqueous layer was extracted with *n*-pentane (3 x 50 mL). The combined organic layers were dried over magnesium sulfate. The volatiles were removed *in vacuo* and the residue was purified by column chromatography (*n*-pentane; $R_f = 0.15$) to yield 85 mg (11 %) of a yellow oil.

$^1\text{H NMR}$ (500 MHz, CDCl_3): $\delta = 7.60 - 7.47$ (m, 4 H, p)*, 7.37 – 7.33 (m, 6 H, q and r), 7.08 (d, $^3J = 5.2$ Hz, 1 H, a² or b²), 6.81 (d, $^3J = 5.2$ Hz, 1 H, a² or b²), 6.58 (s, 1 H, c), 2.80 (t, $^3J = 6.6$ Hz, 2 H, g or g²), 2.56 (t, $^3J = 6.4$ Hz, 2 H, g or g²), 2.42 (t, $^3J = 7.5$ Hz, 2 H, i or i²), 2.26 (t, $^3J = 7.9$ Hz, 2 H, i or i²), 1.83 – 1.76 (m, 2 H, h or h²), 1.68 – 1.61 (m, 2 H, h or h²), 1.45 – 1.37 (m, 2 H, j or j²), 1.36 – 1.27 (m, 4 H, j or j², $-(\text{CH}_2)_3\text{CH}_3$), 1.24 – 1.13 (m, 6 H, $-(\text{CH}_2)_3\text{CH}_3$), 1.10 – 1.02 (m, 2 H, $-(\text{CH}_2)_3\text{CH}_3$), 1.02 – 0.94 (m, 2 H, $-(\text{CH}_2)_3\text{CH}_3$), 0.87 – 0.79 (m, 6 H, n and n²) ppm.

* the signal shows satellites due to coupling with tin.

$^{13}\text{C NMR}$ (126 MHz, CDCl_3): $\delta = 156.4$ (f or f²), 148.2 (f or f²), 144.5 (d or e), 141.6 (b), 139.3 (c² or d²), 138.0 (c² or d² or o), 137.8 (c² or d² or o), 137.1 (p, $^2J = 20.1$ Hz)*, 132.4 (d or e), 130.2 (c), 129.9 (e²), 129.4 (r), 128.8 (q, $^3J = 26.9$ Hz)*, 128.6 (a² or b²), 122.6 (a² or b²), 109.7 (a), 31.6 ($-(\text{CH}_2)_4\text{CH}_2\text{CH}_3$)**, 30.6 (g or g², $-(\text{CH}_2)_4\text{CH}_2\text{CH}_3$)**, 30.5 (g or g²), 29.4 ($-(\text{CH}_2)_4\text{CH}_2\text{CH}_3$)**, 29.2 ($-(\text{CH}_2)_4\text{CH}_2\text{CH}_3$), 29.1 ($-(\text{CH}_2)_4\text{CH}_2\text{CH}_3$), 28.6 ($-(\text{CH}_2)_4\text{CH}_2\text{CH}_3$), 23.3 (h or h²), 22.9 (h or h²), 22.6 (m or m²), 22.5 (m or m²), 14.1 (n and n²) ppm.

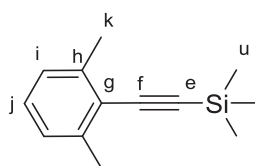
Signals that show satellites due to coupling with tin are marked with *. Coupling constants $^nJ(^{119}\text{Sn}, ^{13}\text{C})$ are given in parentheses when signal to noise ratio allowed the determination.

** two signals.

^{119}Sn NMR (187 MHz, CDCl_3): $\delta = -95.7$ ppm.

IR (ATR): $\tilde{\nu} = 2925$ (s), 2855 (m), 1641 (w), 1542 (w), 1481 (w), 1430 (s), 1378 (w), 1074 (m), 1022 (w), 998 (w), 727 (s), 696 (s), 450 (m) cm^{-1} .

HRMS (MALDI, colloidal graphite matrix) m/z : Found 791.1397; calcd. for $\text{C}_{40}\text{H}_{48}\text{BrS}_2\text{Sn} [\text{M} + \text{H}]^+$ 791.1397.

5.5.15 ((2,6-Dimethylphenyl)ethynyl)trimethylsilane (27)

A mixture of 2-iodo-1,3-dimethylbenzene (5.00 g, 21.5 mmol), [Pd(PPh₃)₄] (990 mg, 0.86 mmol, 4 mol%), copper(I) iodide (160 mg, 0.86 mmol, 4 mol%), triethylamine (30 mL), DMF (120 mL) and ethynyltrimethylsilane (2.53 g, 25.8 mmol) was heated to 100 °C for 3 d. The reaction mixture was quenched with a saturated solution of ammonium chloride (50 mL) and extracted with *n*-pentane (4 x 40 mL). The combined organic layers were dried over magnesium sulfate and concentrated *in vacuo*. The residue was distilled by Kugelrohr distillation (5 mbar, 100 °C) to obtain 3.85 g (89 %) of a colorless oil.

¹H NMR (500 MHz, CDCl₃): δ = 7.13 – 7.09 (m, 1 H, j), 7.07 – 7.01 (m, 2 H, i), 2.45 (s, 6 H, k), 0.29 (s, 9 H, u) ppm.

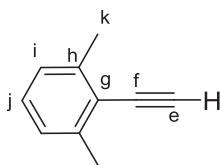
¹³C NMR (126 MHz, CDCl₃): δ = 140.5 (h), 127.7 (j), 126.4 (i), 122.9 (g), 102.7 (f, e)*, 20.9 (k), 0.2 (u) ppm.

*two signals.

²⁹Si NMR (99 MHz, CDCl₃): δ = -18.0 ppm.

IR (ATR): $\tilde{\nu}$ = 2959 (w), 2150 (m), 1468 (w), 1249 (s), 1209 (w), 861 (s), 938 (s), 758 (s), 700 (m), 626 (w), 415 (w) cm⁻¹.

HRMS (EI) *m/z*: Found 202.1175; calcd. for [M]⁺ C₁₃H₁₈Si 202.1178.

5.5.16 2-Ethynyl-1,3-dimethylbenzene (28)

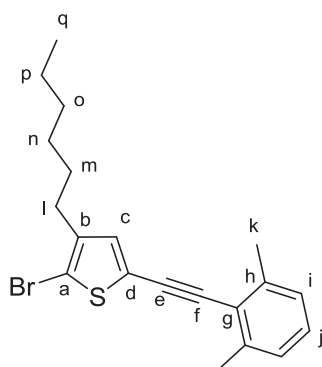
A mixture of **27** (3.85 g, 19.0 mmol) and potassium carbonate (11.8 g, 85.0 mmol) in methanol (30 mL) was stirred at 20 °C for 2 h under air. The reaction mixture was diluted with water (20 mL) and extracted with *n*-pentane (4 x 50 mL). The combined organic layers were dried over magnesium sulfate. The solvent was removed *in vacuo* and the residue was distilled (4 mbar, 100 °C) to obtain 2.38 g (96 %) of a colorless oil.

¹H NMR (500 MHz, CDCl₃): δ = 7.17 – 7.12 (m, 1 H, j), 7.07-7.04 (m, 2 H, i), 3.52 (s, 1 H, e), 2.47 (s, 6 H, k) ppm.

¹³C NMR (126 MHz, CDCl₃): δ = 140.9 (h), 128.8 (j), 126.7 (i), 121.9 (g), 85.3 (e), 81.1 (f), 20.9 (k) ppm.

IR (ATR): $\tilde{\nu}$ = 3297 (m), 2948 (w), 2919 (w), 1467 (m), 1379 (w), 1165 (w), 1086 (w), 1034 (w), 768 (s), 733 (m), 642 (s), 603 (s) cm⁻¹.

HRMS (EI) *m/z*: Found 130.0780; calcd. for [M]⁺ C₁₀H₁₀ 130.0783.

5.5.17 2-Bromo-5-((2,6-dimethylphenyl)ethynyl)-3-hexylthiophene (29)

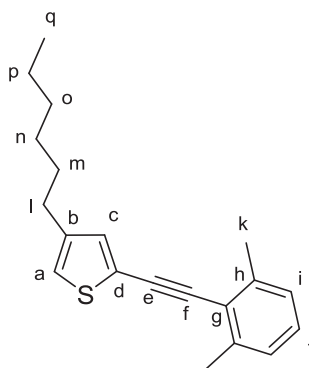
A mixture of **P2-4** (3.00 g, 8.04 mmol), **28** (1.05 g, 8.04 mmol), [Pd(PPh₃)₄] (159 mg, 160 μmol, 2 mol%), copper(I) iodide (30.5 mg, 160 μmol, 2 mol%), TEA (12 mL) and DMF (24 mL) was stirred at 60 °C for 24 h. The reaction mixture was quenched with water (50 mL) and extracted with *n*-pentane (4 x 40 mL). The combined organic layers were dried over magnesium sulfate and concentrated *in vacuo*. The crude product was purified by column chromatography (*n*-pentane, R_f = 0.67) to afford 2.04 g (68%) of a colorless oil.

¹H NMR (500 MHz, CDCl₃): δ = 7.18 – 7.14 (m, 1 H, j), 7.10 – 7.07 (m, 2 H, i), 6.98 (s, 1 H, c), 2.57 (t, ³J = 7.6 Hz, 2 H, l), 2.49 (s, 6 H, k), 1.66 – 1.58 (m, 2 H, m), 1.41 – 1.31 (m, 6 H, n, o and p) 0.93 (t, ³J = 6.9 Hz, 3 H, q) ppm.

¹³C NMR (126 MHz, CDCl₃): δ = 142.4 (b), 140.2 (h), 132.1 (c), 128.2 (j), 126.7 (i), 123.4 (d), 122.3 (g), 109.7 (a), 91.6 (e), 90.1 (f), 31.5 (o), 29.6 (l or m), 29.4 (l or m), 28.8 (n), 22.5 (p), 21.0 (k), 14.1 (q) ppm.

IR (ATR): $\tilde{\nu}$ = 2953 (s), 2923 (s), 2855 (s), 1544 (w), 1465 (m), 1440 (m) 1376 (m) 1241 (w), 1194 (w) 1162 (w), 1113 (w), 1002 (s), 832 (m), 767 (s), 729 (m), 528 (m), 414 (m) cm⁻¹.

HRMS (EI) *m/z*: Found 374.0703; calcd. for [M]⁺ C₂₀H₂₃BrS 374.0704.

5.5.18 2-((2,6-Dimethylphenyl)ethynyl)-4-hexylthiophene (30)

n-Butyllithium (1.52 mL, 3.80 mmol; 2.5 M in hexanes) was added dropwise within 15 min to a solution of **29** (1.00 g, 2.66 mmol) in THF (30 mL) at -78 °C. The yellow-green solution was stirred for 1 h and water (3 mL) was added dropwise within 5 min. The suspension was allowed to warm to 20 °C after removal of the cooling bath and a saturated solution of ammonium chloride (10 mL) was added. The mixture was extracted with *n*-pentane (4 x 60 mL) and the combined organic layers were dried over magnesium sulfate. The volatiles were removed *in vacuo* and the residue was filtered over a short plug of silica (2 x 4 cm; *n*-pentane) to obtain 700 mg (89 %) of a pale yellow oil.

¹H NMR (500 MHz, CDCl₃): δ = 7.14 – 7.09 (m, 2 H, c and j), 7.07 – 7.03 (m, 2 H, i), 6.87 (m, 1 H, a), 2.58 (t, ³J = 7.9 Hz, 2 H, l), 2.48 (s, 6 H, k), 1.66 - 1.60 (m, 2 H, m), 1.38 – 1.24 (m, 6 H, n, o and p), 0.89 (t, ³J = 6.9 Hz, 3 H, q) ppm.

¹³C NMR (126 MHz, CDCl₃): δ = 143.4 (b), 140.1 (h), 132.6 (c), 127.8 (j), 126.7 (i), 123.3 (d), 122.7 (g), 121.9 (a), 91.2 (e), 90.4 (f), 31.6 (o), 30.4 (l and m)*, 28.9 (n), 22.6 (p), 21.1 (k), 14.1 (q) ppm.

* two signals.

IR (ATR): $\tilde{\nu}$ = 2954 (m), 2925 (s), 2855 (m), 1542 (w), 1466 (s), 1377 (w), 1262 (w), 1243 (w), 1197 (w), 1164 (w), 838 (m), 767 (s), 748 (s), 730 (s), 635 (w), 584 (w), 519 (m), 408 (w) cm⁻¹.

HRMS (EI) *m/z*: Found 296.1599; calcd. for [M]⁺ C₂₀H₂₄S 296.1599.

5.6 Single Crystal Data

5.6.1 3,4-Bis(2,6-dimethylphenyl)-2,5-bis(4-hexylthiophen-2-yl)-Cp₂ZrC₄ (31)

Table 5.1 Crystal data and structure refinement.

Empirical formula	C ₅₀ H ₅₈ S ₂ Zr	
Formula weight	814.30	
Temperature	200(2) K	
Wavelength	0.71073 Å	
Crystal system	monoclinic	
Space group	P2/c	
Unit cell dimensions	a = 16.8665(4) Å	α = 90°.
	b = 10.8153(2) Å	β = 108.606(2)°.
	c = 24.7282(6) Å	γ = 90°.
Volume	4275.07(17) Å ³	
Z	4	
Density (calculated)	1.265 Mg/m ³	
Absorption coefficient	0.388 mm ⁻¹	
F(000)	1720	
Crystal size	0.04 x 0.1 x 0.2 mm ³	
Theta range for data collection	1.27 to 27.00°.	
Index ranges	-21 ≤ h ≤ 21, -13 ≤ k ≤ 13, -31 ≤ l ≤ 30	
Reflections collected	49666	
Independent reflections	9336 [R(int) = 0.0578]	
Completeness to theta = 27.00°	99.9 %	
Refinement method	Full-matrix least-squares on F ²	
Data / restraints / parameters	9336 / 7 / 529	
Goodness-of-fit on F ²	1.033	
Final R indices [I > 2σ(I)]	R1 = 0.0358, wR2 = 0.0860	
R indices (all data)	R1 = 0.0456, wR2 = 0.0902	
Largest diff. peak and hole	0.446 and -0.399 e.Å ⁻³	

Comments:

All non-hydrogen atoms were refined anisotropic. The C-H H atoms were positioned with idealized geometry (methyl H atoms allowed to rotate but not to tip) and refined isotropic with $U_{\text{iso}}(\text{H}) = 1.2 \cdot U_{\text{eq}}(\text{C})$ (1.5 for methyl H atoms) using a riding model. A numerical absorption correction was performed (Tmin/max: 0.8805/0.9856). There are two crystallographically independent molecules in the asymmetric unit, that are located on a 2-fold rotation axis. In one of these molecules 5 atoms of the alkyl chain are disordered and were refined with restraints using a split model (sof = 0.665 (6): 0.335 (6)).

Table 5.2 Atomic coordinates ($\times 10^4$) and equivalent isotropic displacement parameters ($\text{\AA}^2 \times 10^3$). $U(\text{eq})$ is defined as one third of the trace of the orthogonalized U_{ij} tensor.

	x	y	z	U(eq)
Zr(1)	5000	4154(1)	2500	33(1)
S(1)	6507(1)	4607(1)	1635(1)	47(1)
C(1)	6506(2)	4971(2)	958(1)	50(1)
C(2)	5945(2)	5867(2)	716(1)	45(1)
C(3)	5520(1)	6285(2)	1096(1)	42(1)
C(4)	5753(1)	5718(2)	1619(1)	36(1)
C(5)	5409(1)	5815(2)	2091(1)	33(1)
C(6)	5229(1)	6927(2)	2285(1)	33(1)
C(7)	5534(1)	8125(2)	2108(1)	36(1)
C(8)	6395(1)	8410(2)	2328(1)	44(1)
C(9)	6687(2)	9510(2)	2162(1)	59(1)
C(10)	6161(2)	10286(2)	1773(1)	66(1)
C(11)	5330(2)	9986(2)	1539(1)	56(1)
C(12)	5000(1)	8917(2)	1702(1)	43(1)
C(13)	7012(1)	7533(2)	2716(1)	52(1)
C(14)	4095(2)	8626(2)	1424(1)	55(1)
C(15)	5766(2)	6330(2)	111(1)	61(1)
C(16)	5687(2)	7721(2)	48(1)	68(1)
C(17)	6458(2)	8408(2)	362(1)	68(1)
C(18)	6344(2)	9810(3)	257(1)	70(1)
C(19)	7110(2)	10521(3)	551(2)	76(1)
C(20)	6989(2)	11909(3)	461(2)	94(1)
C(21)	3467(1)	4160(2)	1945(1)	52(1)
C(22)	3650(1)	2970(2)	2175(1)	50(1)
C(23)	4182(2)	2398(2)	1918(1)	56(1)
C(24)	4336(2)	3231(3)	1534(1)	60(1)
C(25)	3896(2)	4322(2)	1547(1)	56(1)
Zr(2)	0	2104(1)	2500	35(1)
S(2)	255(1)	2503(1)	4077(1)	58(1)
C(31)	869(2)	3016(2)	4734(1)	55(1)
C(32)	1321(2)	4024(2)	4692(1)	47(1)
C(33)	1161(1)	4390(2)	4114(1)	41(1)
C(34)	581(1)	3690(2)	3720(1)	38(1)
C(35)	261(1)	3757(2)	3098(1)	34(1)
C(36)	121(1)	4871(2)	2819(1)	32(1)
C(37)	146(1)	6067(2)	3139(1)	34(1)
C(38)	-497(1)	6302(2)	3376(1)	39(1)
C(39)	-476(2)	7383(2)	3686(1)	50(1)
C(40)	179(2)	8201(2)	3786(1)	55(1)
C(41)	826(2)	7955(2)	3574(1)	48(1)
C(42)	818(1)	6900(2)	3246(1)	38(1)
C(43)	-1195(1)	5394(2)	3327(1)	47(1)
C(44)	1550(1)	6663(2)	3043(1)	48(1)
C(45)	1889(2)	4734(2)	5184(1)	69(1)
C(46)	1489(3)	6099(4)	5145(2)	59(1)
C(47)	2013(2)	6965(3)	5596(1)	51(1)
C(48)	1701(3)	8292(4)	5492(2)	50(1)
C(49)	2204(3)	9202(6)	5933(2)	62(1)
C(50)	1883(4)	10515(6)	5808(4)	78(2)
C(46')	2104(6)	6067(7)	5174(3)	59(2)
C(47')	1313(6)	6624(8)	5203(4)	58(2)
C(48')	1354(6)	8053(7)	5238(4)	51(2)
C(49')	1928(7)	8543(11)	5808(4)	63(2)
C(50')	1841(9)	9918(13)	5884(6)	80(4)
C(51)	-1568(1)	2222(2)	2156(1)	60(1)
C(52)	-1351(2)	1125(3)	1933(1)	60(1)
C(53)	-996(2)	322(2)	2385(1)	55(1)
C(54)	-980(2)	912(2)	2888(1)	52(1)
C(55)	-1337(1)	2092(2)	2750(1)	55(1)

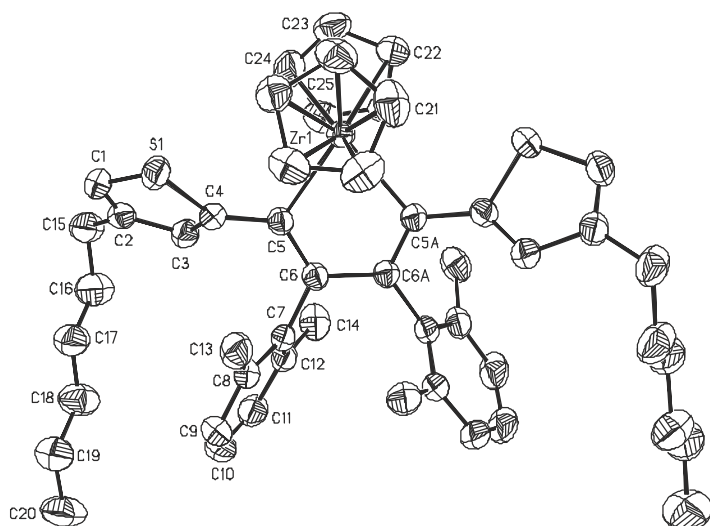


Table 5.3 Bond lengths [Å] and angles [°]. Symmetry code: A = -x+1,y,-z+1/2.

Zr(1)-C(5A)	2.2743(18)	Zr(1)-C(22)	2.510(2)
Zr(1)-C(5)	2.2743(18)	Zr(1)-C(22A)	2.510(2)
Zr(1)-C(24)	2.501(2)	Zr(1)-C(21)	2.511(2)
Zr(1)-C(24A)	2.501(2)	Zr(1)-C(21A)	2.511(2)
Zr(1)-C(25)	2.501(2)	Zr(1)-C(23)	2.512(2)
Zr(1)-C(25A)	2.501(2)	Zr(1)-C(23A)	2.512(2)
C(5A)-Zr(1)-C(5)	75.63(9)	C(25A)-Zr(1)-C(21)	147.38(8)
C(5A)-Zr(1)-C(24)	129.34(8)	C(22)-Zr(1)-C(21)	32.42(8)
C(5)-Zr(1)-C(24)	89.82(8)	C(22A)-Zr(1)-C(21)	147.87(8)
C(5A)-Zr(1)-C(24A)	89.82(8)	C(5A)-Zr(1)-C(21A)	99.20(7)
C(5)-Zr(1)-C(24A)	129.34(8)	C(5)-Zr(1)-C(21A)	80.57(7)
C(24)-Zr(1)-C(24A)	132.94(14)	C(24)-Zr(1)-C(21A)	126.34(9)
C(5A)-Zr(1)-C(25)	97.00(8)	C(24A)-Zr(1)-C(21A)	53.81(8)
C(5)-Zr(1)-C(25)	76.31(7)	C(25)-Zr(1)-C(21A)	147.38(8)
C(24)-Zr(1)-C(25)	32.51(9)	C(25A)-Zr(1)-C(21A)	32.58(8)
C(24A)-Zr(1)-C(25)	154.33(9)	C(22)-Zr(1)-C(21A)	147.87(8)
C(5A)-Zr(1)-C(25A)	76.31(7)	C(22A)-Zr(1)-C(21A)	32.42(8)
C(5)-Zr(1)-C(25A)	97.00(8)	C(21)-Zr(1)-C(21A)	179.70(11)
C(24)-Zr(1)-C(25A)	154.33(9)	C(5A)-Zr(1)-C(23)	131.51(7)
C(24A)-Zr(1)-C(25A)	32.51(9)	C(5)-Zr(1)-C(23)	122.10(8)
C(25)-Zr(1)-C(25A)	171.67(12)	C(24)-Zr(1)-C(23)	32.28(9)
C(5A)-Zr(1)-C(22)	99.96(7)	C(24A)-Zr(1)-C(23)	104.00(10)
C(5)-Zr(1)-C(22)	129.28(7)	C(25)-Zr(1)-C(23)	53.67(8)
C(24)-Zr(1)-C(22)	53.60(8)	C(25A)-Zr(1)-C(23)	134.60(9)
C(24A)-Zr(1)-C(22)	100.72(9)	C(22)-Zr(1)-C(23)	32.30(8)
C(25)-Zr(1)-C(22)	53.76(8)	C(22A)-Zr(1)-C(23)	94.25(8)
C(25A)-Zr(1)-C(22)	131.70(9)	C(21)-Zr(1)-C(23)	53.64(8)
C(5A)-Zr(1)-C(22A)	129.28(7)	C(21A)-Zr(1)-C(23)	126.64(8)
C(5)-Zr(1)-C(22A)	99.96(7)	C(5A)-Zr(1)-C(23A)	122.10(8)
C(24)-Zr(1)-C(22A)	100.72(9)	C(5)-Zr(1)-C(23A)	131.51(7)
C(24A)-Zr(1)-C(22A)	53.60(8)	C(24)-Zr(1)-C(23A)	104.00(10)
C(25)-Zr(1)-C(22A)	131.70(9)	C(24A)-Zr(1)-C(23A)	32.28(9)
C(25A)-Zr(1)-C(22A)	53.76(8)	C(25)-Zr(1)-C(23A)	134.60(9)
C(22)-Zr(1)-C(22A)	118.65(11)	C(25A)-Zr(1)-C(23A)	53.67(8)
C(5A)-Zr(1)-C(21)	80.57(7)	C(22)-Zr(1)-C(23A)	94.25(8)
C(5)-Zr(1)-C(21)	99.20(7)	C(22A)-Zr(1)-C(23A)	32.30(8)
C(24)-Zr(1)-C(21)	53.81(8)	C(21)-Zr(1)-C(23A)	126.64(8)
C(24A)-Zr(1)-C(21)	126.34(9)	C(21A)-Zr(1)-C(23A)	53.64(8)
C(25)-Zr(1)-C(21)	32.58(8)	C(23)-Zr(1)-C(23A)	81.81(12)

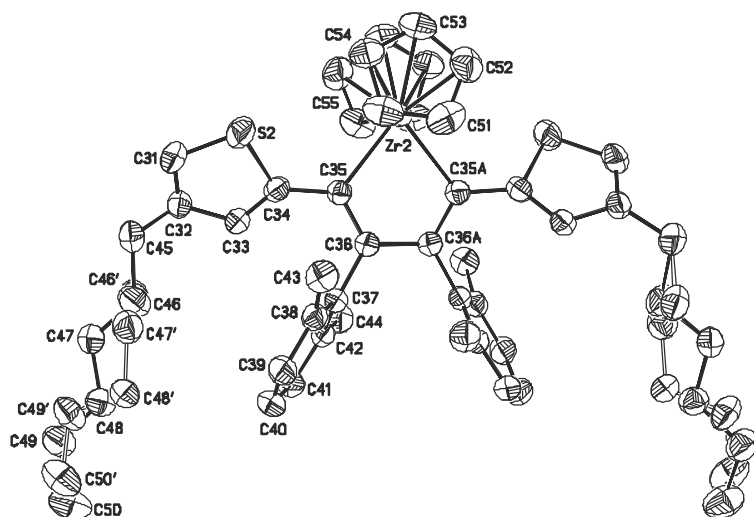


Table 5.4 Bond lengths [Å] and angles [°]. Symmetry code: A = -x,y,-z+1/2

Zr(2)-C(35A)	2.2723(18)	Zr(2)-C(53)	2.512(2)
Zr(2)-C(35)	2.2723(18)	Zr(2)-C(53A)	2.512(2)
Zr(2)-C(52)	2.498(2)	Zr(2)-C(54A)	2.515(2)
Zr(2)-C(52A)	2.498(2)	Zr(2)-C(54)	2.515(2)
Zr(2)-C(51)	2.509(2)	Zr(2)-C(55A)	2.522(2)
Zr(2)-C(51A)	2.509(2)	Zr(2)-C(55)	2.522(2)
C(35A)-Zr(2)-C(35)	76.18(9)	C(51A)-Zr(2)-C(54A)	53.58(8)
C(35A)-Zr(2)-C(52)	90.89(8)	C(53)-Zr(2)-C(54A)	93.47(8)
C(35)-Zr(2)-C(52)	130.65(8)	C(53A)-Zr(2)-C(54A)	32.12(8)
C(35A)-Zr(2)-C(52A)	130.65(8)	C(35A)-Zr(2)-C(54)	129.60(7)
C(35)-Zr(2)-C(52A)	90.89(8)	C(35)-Zr(2)-C(54)	99.75(7)
C(52)-Zr(2)-C(52A)	129.86(13)	C(52)-Zr(2)-C(54)	53.45(8)
C(35A)-Zr(2)-C(51)	76.98(7)	C(52A)-Zr(2)-C(54)	99.27(9)
C(35)-Zr(2)-C(51)	98.34(8)	C(51)-Zr(2)-C(54)	53.58(8)
C(52)-Zr(2)-C(51)	32.58(9)	C(51A)-Zr(2)-C(54)	130.24(9)
C(52A)-Zr(2)-C(51)	152.35(9)	C(53)-Zr(2)-C(54)	32.12(8)
C(35A)-Zr(2)-C(51A)	98.34(8)	C(53A)-Zr(2)-C(54)	93.47(8)
C(35)-Zr(2)-C(51A)	76.98(7)	C(54A)-Zr(2)-C(54)	118.33(11)
C(52)-Zr(2)-C(51A)	152.35(9)	C(35A)-Zr(2)-C(55A)	81.19(7)
C(52A)-Zr(2)-C(51A)	32.58(9)	C(35)-Zr(2)-C(55A)	99.25(8)
C(51)-Zr(2)-C(51A)	174.15(12)	C(52)-Zr(2)-C(55A)	125.96(9)
C(35A)-Zr(2)-C(53)	123.13(8)	C(52A)-Zr(2)-C(55A)	53.75(9)
C(35)-Zr(2)-C(53)	131.38(7)	C(51)-Zr(2)-C(55A)	147.68(9)
C(52)-Zr(2)-C(53)	32.26(8)	C(51A)-Zr(2)-C(55A)	32.38(9)
C(52A)-Zr(2)-C(53)	101.28(9)	C(53)-Zr(2)-C(55A)	125.91(8)
C(51)-Zr(2)-C(53)	53.61(8)	C(53A)-Zr(2)-C(55A)	53.56(8)
C(51A)-Zr(2)-C(53)	132.19(8)	C(54A)-Zr(2)-C(55A)	32.44(8)
C(35A)-Zr(2)-C(53A)	131.38(7)	C(54)-Zr(2)-C(55A)	147.03(8)
C(35)-Zr(2)-C(53A)	123.13(8)	C(35A)-Zr(2)-C(55)	99.25(8)
C(52)-Zr(2)-C(53A)	101.28(9)	C(35)-Zr(2)-C(55)	81.19(7)
C(52A)-Zr(2)-C(53A)	32.26(8)	C(52)-Zr(2)-C(55)	53.75(9)
C(51)-Zr(2)-C(53A)	132.19(8)	C(52A)-Zr(2)-C(55)	125.96(9)
C(51A)-Zr(2)-C(53A)	53.61(8)	C(51)-Zr(2)-C(55)	32.38(9)
C(53)-Zr(2)-C(53A)	79.80(11)	C(51A)-Zr(2)-C(55)	147.68(9)
C(35A)-Zr(2)-C(54A)	99.75(7)	C(53)-Zr(2)-C(55)	53.56(8)
C(35)-Zr(2)-C(54A)	129.60(7)	C(53A)-Zr(2)-C(55)	125.91(8)
C(52)-Zr(2)-C(54A)	99.27(9)	C(54A)-Zr(2)-C(55)	147.03(8)
C(52A)-Zr(2)-C(54A)	53.45(8)	C(54)-Zr(2)-C(55)	32.44(8)
C(51)-Zr(2)-C(54A)	130.24(9)	C(55A)-Zr(2)-C(55)	179.44(11)

Table 5.5 Bond lengths [Å] and angles [°].

S(1)-C(1)	1.719(2)	C(8)-C(9)	1.398(3)
S(1)-C(4)	1.7414(19)	C(8)-C(13)	1.505(3)
C(1)-C(2)	1.354(3)	C(9)-C(10)	1.369(4)
C(2)-C(3)	1.426(3)	C(10)-C(11)	1.374(4)
C(2)-C(15)	1.514(3)	C(11)-C(12)	1.396(3)
C(3)-C(4)	1.370(3)	C(12)-C(14)	1.494(3)
C(4)-C(5)	1.464(3)	C(15)-C(16)	1.514(4)
C(5)-C(6)	1.365(2)	C(16)-C(17)	1.485(4)
C(6)-C(6A)	1.500(3)	C(17)-C(18)	1.541(4)
C(6)-C(7)	1.510(2)	C(18)-C(19)	1.479(4)
C(7)-C(12)	1.405(3)	C(19)-C(20)	1.522(4)
C(7)-C(8)	1.413(3)		
C(2)-C(1)-S(1)-C(4)	92.59(10)	C(8)-C(7)-C(6)	118.64(17)
C(2)-C(1)-S(1)	112.27(16)	C(9)-C(8)-C(7)	119.2(2)
C(1)-C(2)-C(3)	111.26(19)	C(9)-C(8)-C(13)	119.2(2)
C(1)-C(2)-C(15)	124.4(2)	C(7)-C(8)-C(13)	121.62(19)
C(3)-C(2)-C(15)	124.3(2)	C(10)-C(9)-C(8)	121.2(2)
C(4)-C(3)-C(2)	115.26(19)	C(9)-C(10)-C(11)	119.7(2)
C(3)-C(4)-C(5)	130.76(18)	C(10)-C(11)-C(12)	121.4(2)
C(3)-C(4)-S(1)	108.59(14)	C(11)-C(12)-C(7)	119.2(2)
C(5)-C(4)-S(1)	120.21(14)	C(11)-C(12)-C(14)	118.9(2)
C(6)-C(5)-C(4)	122.21(16)	C(7)-C(12)-C(14)	121.87(18)
C(5)-C(6)-C(6A)	118.17(10)	C(2)-C(15)-C(16)	114.45(19)
C(5)-C(6)-C(7)	121.25(15)	C(17)-C(16)-C(15)	114.2(3)
C(6A)-C(6)-C(7)	120.43(10)	C(16)-C(17)-C(18)	111.3(3)
C(12)-C(7)-C(8)	119.20(18)	C(19)-C(18)-C(17)	112.7(3)
C(12)-C(7)-C(6)	122.01(17)	C(18)-C(19)-C(20)	112.6(3)
C(21)-C(22)	1.402(3)	C(23)-C(24)	1.394(4)
C(21)-C(25)	1.406(4)	C(24)-C(25)	1.400(4)
C(22)-C(23)	1.397(3)		
C(22)-C(21)-C(25)	107.6(2)	C(23)-C(24)-C(25)	108.2(2)
C(23)-C(22)-C(21)	108.2(2)	C(24)-C(25)-C(21)	107.9(2)
C(24)-C(23)-C(22)	108.1(2)		

Table 5.6 Bond lengths [Å] and angles [°].

S(2)-C(31)	1.717(2)	C(39)-C(40)	1.374(4)
S(2)-C(34)	1.744(2)	C(40)-C(41)	1.380(4)
C(31)-C(32)	1.353(3)	C(41)-C(42)	1.398(3)
C(32)-C(33)	1.424(3)	C(42)-C(44)	1.496(3)
C(32)-C(45)	1.498(3)	C(45)-C(46)	1.489(9)
C(33)-C(34)	1.367(3)	C(45)-C(46)	1.614(5)
C(34)-C(35)	1.461(3)	C(46)-C(47)	1.507(5)
C(35)-C(36)	1.370(3)	C(47)-C(48)	1.522(5)
C(36)-C(36A)	1.499(3)	C(48)-C(49)	1.513(6)
C(36)-C(37)	1.509(2)	C(49)-C(50)	1.516(6)
C(37)-C(42)	1.404(3)	C(46')-C(47')	1.487(10)
C(37)-C(38)	1.412(3)	C(47')-C(48')	1.548(11)
C(38)-C(39)	1.393(3)	C(48')-C(49')	1.527(11)
C(38)-C(43)	1.507(3)	C(49')-C(50')	1.512(12)
C(31)-S(2)-C(34)	92.77(10)	C(37)-C(38)-C(43)	122.24(18)
C(32)-C(31)-S(2)	111.84(16)	C(40)-C(39)-C(38)	121.2(2)
C(31)-C(32)-C(33)	111.8(2)	C(39)-C(40)-C(41)	119.7(2)
C(31)-C(32)-C(45)	125.5(2)	C(40)-C(41)-C(42)	121.0(2)
C(33)-C(32)-C(45)	122.7(2)	C(41)-C(42)-C(37)	119.43(19)
C(34)-C(33)-C(32)	115.09(19)	C(41)-C(42)-C(44)	118.50(19)
C(33)-C(34)-C(35)	131.44(18)	C(37)-C(42)-C(44)	122.00(18)
C(33)-C(34)-S(2)	108.50(14)	C(46')-C(45)-C(32)	125.4(4)
C(35)-C(34)-S(2)	119.98(15)	C(46')-C(45)-C(46)	38.0(4)
C(36)-C(35)-C(34)	121.35(17)	C(32)-C(45)-C(46)	105.9(3)
C(35)-C(36)-C(36A)	118.36(10)	C(47)-C(46)-C(45)	112.9(3)
C(35)-C(36)-C(37)	121.23(15)	C(46)-C(47)-C(48)	111.8(4)
C(36A)-C(36)-C(37)	120.27(9)	C(49)-C(48)-C(47)	114.1(4)
C(42)-C(37)-C(38)	119.16(17)	C(48)-C(49)-C(50)	112.4(4)
C(42)-C(37)-C(36)	122.34(17)	C(47')-C(46')-C(45)	99.5(7)
C(38)-C(37)-C(36)	118.30(17)	C(46')-C(47')-C(48')	112.4(8)
C(39)-C(38)-C(37)	119.44(19)	C(49')-C(48')-C(47')	113.7(8)
C(39)-C(38)-C(43)	118.27(19)	C(50')-C(49')-C(48')	113.5(9)
C(51)-C(55)	1.403(4)	C(53)-C(54)	1.390(3)
C(51)-C(52)	1.405(4)	C(54)-C(55)	1.407(3)
C(52)-C(53)	1.392(4)		
C(55)-C(51)-C(52)	107.9(2)	C(53)-C(54)-C(55)	108.3(2)
C(53)-C(52)-C(51)	108.1(2)	C(51)-C(55)-C(54)	107.4(2)
C(54)-C(53)-C(52)	108.3(2)		

Table 5.7 Hydrogen coordinates ($\times 10^4$) and isotropic displacement parameters ($\text{\AA}^2 \times 10^{-3}$).

		x	y	z	U(eq)	
Zr(1)	36(1)	29(1)	35(1)	0	11(1)	0
S(1)	50(1)	44(1)	55(1)	2(1)	27(1)	10(1)
C(1)	58(1)	45(1)	58(1)	-12(1)	36(1)	-6(1)
C(2)	61(1)	37(1)	46(1)	-9(1)	28(1)	-11(1)
C(3)	53(1)	37(1)	41(1)	-1(1)	22(1)	1(1)
C(4)	39(1)	32(1)	40(1)	-3(1)	17(1)	-1(1)
C(5)	32(1)	34(1)	36(1)	3(1)	13(1)	1(1)
C(6)	31(1)	34(1)	35(1)	2(1)	12(1)	0(1)
C(7)	42(1)	32(1)	41(1)	-2(1)	23(1)	0(1)
C(8)	45(1)	43(1)	51(1)	-10(1)	27(1)	-7(1)
C(9)	65(2)	51(1)	73(2)	-15(1)	41(1)	-22(1)
C(10)	98(2)	38(1)	83(2)	-6(1)	60(2)	-17(1)
C(11)	86(2)	35(1)	63(1)	8(1)	44(1)	8(1)
C(12)	56(1)	34(1)	47(1)	4(1)	29(1)	7(1)
C(13)	35(1)	62(1)	60(1)	-11(1)	17(1)	-2(1)
C(14)	55(1)	60(1)	53(1)	18(1)	20(1)	17(1)
C(15)	94(2)	52(1)	45(1)	-8(1)	34(1)	-17(1)
C(16)	106(2)	57(2)	43(1)	2(1)	26(1)	-11(1)
C(17)	92(2)	50(1)	72(2)	-4(1)	39(2)	-11(1)
C(18)	93(2)	59(2)	55(1)	3(1)	17(1)	-14(1)
C(19)	84(2)	63(2)	87(2)	-8(2)	35(2)	-14(2)
C(20)	108(3)	50(2)	125(3)	-7(2)	38(2)	-23(2)
C(21)	39(1)	49(1)	60(1)	-12(1)	5(1)	-1(1)
C(22)	49(1)	47(1)	56(1)	-9(1)	18(1)	-14(1)
C(23)	55(1)	42(1)	67(2)	-17(1)	16(1)	-7(1)
C(24)	58(1)	75(2)	49(1)	-26(1)	21(1)	-17(1)
C(25)	57(1)	57(1)	43(1)	1(1)	-1(1)	-14(1)
Zr(2)	35(1)	29(1)	42(1)	0	13(1)	0
S(2)	74(1)	54(1)	45(1)	11(1)	18(1)	-14(1)
C(31)	76(2)	53(1)	38(1)	11(1)	21(1)	3(1)
C(32)	62(1)	43(1)	34(1)	2(1)	13(1)	11(1)
C(33)	51(1)	36(1)	36(1)	4(1)	13(1)	3(1)
C(34)	42(1)	35(1)	38(1)	5(1)	15(1)	5(1)
C(35)	35(1)	34(1)	35(1)	-1(1)	14(1)	-1(1)
C(36)	31(1)	33(1)	35(1)	-1(1)	14(1)	-1(1)
C(37)	39(1)	32(1)	30(1)	2(1)	11(1)	3(1)
C(38)	44(1)	40(1)	35(1)	2(1)	14(1)	7(1)
C(39)	61(1)	48(1)	42(1)	-3(1)	20(1)	13(1)
C(40)	75(2)	40(1)	44(1)	-9(1)	12(1)	10(1)
C(41)	60(1)	35(1)	42(1)	0(1)	7(1)	-5(1)
C(42)	44(1)	35(1)	33(1)	4(1)	8(1)	-2(1)
C(43)	45(1)	51(1)	53(1)	3(1)	25(1)	5(1)
C(44)	42(1)	52(1)	50(1)	-1(1)	15(1)	-9(1)
C(45)	107(2)	58(2)	36(1)	-3(1)	12(1)	-10(2)
C(46)	56(3)	54(3)	58(2)	-14(2)	5(2)	7(2)
C(47)	56(2)	51(2)	42(2)	0(1)	10(2)	2(2)
C(48)	51(3)	44(2)	53(3)	-3(2)	16(2)	2(2)
C(49)	58(3)	57(3)	64(3)	-12(2)	12(2)	2(2)
C(50)	69(3)	55(3)	108(4)	-19(3)	28(3)	7(3)
C(46')	58(5)	67(5)	47(4)	-8(3)	11(3)	2(4)
C(47')	61(5)	61(6)	53(4)	-1(5)	20(4)	2(5)
C(48')	56(5)	44(4)	48(5)	-6(3)	12(4)	-5(4)
C(49')	62(5)	65(7)	56(6)	-22(5)	12(5)	-3(5)
C(50')	84(8)	72(9)	89(8)	-30(8)	35(6)	-15(9)
C(51)	37(1)	56(1)	82(2)	16(1)	13(1)	-2(1)
C(52)	52(1)	67(2)	56(1)	-6(1)	11(1)	-21(1)
C(53)	55(1)	39(1)	74(2)	-8(1)	26(1)	-11(1)
C(54)	51(1)	45(1)	62(1)	5(1)	23(1)	-10(1)
C(55)	46(1)	46(1)	83(2)	-9(1)	33(1)	-8(1)

Table 5.8 Hydrogen coordinates ($\times 10^4$) and isotropic displacement parameters ($\text{\AA}^2 \times 10^3$).

	x	y	z	U(eq)
H(1)	6858	4587	775	60
H(3)	5104	6913	994	50
H(9)	7261	9723	2323	70
H(10)	6370	11030	1664	79
H(11)	4971	10517	1261	68
H(13A)	7127	6851	2490	78
H(13B)	6777	7202	3001	78
H(13C)	7533	7974	2908	78
H(14A)	4013	7729	1418	83
H(14B)	3912	8945	1033	83
H(14C)	3766	9015	1641	83
H(15A)	5239	5948	-133	73
H(15B)	6221	6050	-33	73
H(16A)	5533	7932	-363	82
H(16B)	5225	8000	185	82
H(17A)	6928	8114	238	82
H(17B)	6599	8240	776	82
H(18A)	6184	9971	-158	84
H(18B)	5882	10103	390	84
H(19A)	7568	10247	409	91
H(19B)	7280	10341	965	91
H(20A)	7512	12336	662	141
H(20B)	6547	12190	610	141
H(20C)	6829	12095	52	141
H(21)	3116	4750	2040	62
H(22)	3448	2614	2457	60
H(23)	4400	1584	1993	67
H(24)	4681	3083	1302	72
H(25)	3889	5043	1326	68
H(31)	889	2638	5085	66
H(33)	1438	5070	4009	49
H(39)	-922	7558	3832	59
H(40)	185	8932	4000	66
H(41)	1285	8512	3652	57
H(43A)	-998	4745	3616	71
H(43B)	-1370	5021	2946	71
H(43C)	-1670	5826	3388	71
H(44A)	1623	5770	3011	72
H(44B)	2056	7015	3316	72
H(44C)	1451	7050	2669	72
H(45A)	2461	4777	5155	83
H(45B)	1918	4334	5550	83
H(46A)	1424	6452	4764	71
H(46B)	925	6034	5186	71
H(47A)	2601	6929	5598	61
H(47B)	2000	6692	5975	61
H(48A)	1713	8556	5111	59
H(48B)	1112	8318	5486	59
H(49A)	2796	9173	5945	74
H(49B)	2182	8955	6314	74
H(50A)	2225	11069	6106	116
H(50B)	1300	10552	5803	116
H(50C)	1917	10773	5437	116

Table 5.9 Hydrogen coordinates ($\times 10^4$) and isotropic displacement parameters ($\text{\AA}^2 \times 10^3$).

	x	y	z	U(eq)
H(46C)	2589	6299	5508	70
H(46D)	2218	6296	4818	70
H(47C)	1192	6297	5543	69
H(47D)	848	6376	4861	69
H(48C)	1553	8370	4928	61
H(48D)	783	8380	5173	61
H(49C)	1802	8101	6121	75
H(49D)	2516	8359	5837	75
H(50D)	2220	10172	6257	120
H(50E)	1263	10108	5861	120
H(50F)	1984	10365	5583	120
H(51)	-1825	2927	1941	72
H(52)	-1433	960	1541	72
H(53)	-798	-489	2355	65
H(54)	-764	575	3261	62
H(55)	-1409	2692	3011	66

References

- [1] a) C. D. Dimitrakopoulos, P. R. L. Malenfant, *Adv. Mater.* **2002**, *14*, 99-117; b) H. E. Katz, J. Huang, *Annu. Rev. Mater. Res.* **2009**, *39*, 71-92; c) A. Facchetti, *Chem. Mater.* **2011**, *23*, 733-758; d) A. P. Kulkarni, C. J. Tonzola, A. Babel, S. A. Jenekhe, *Chem. Mater.* **2004**, *16*, 4556-4573; e) N. Koch, *ChemPhysChem* **2007**, *8*, 1438-1455; f) Y. Shirota, *J. Mater. Chem.* **2000**, *10*, 1-25; g) R. R. Sondergaard, M. Hoesel, F. C. Krebs, *J. Polym. Sci., Part B: Polym. Phys.* **2013**, *51*, 16-34.
- [2] a) Z. Bao, J. A. Rogers, H. E. Katz, *J. Mater. Chem.* **1999**, *9*, 1895-1904; b) S. R. Forrest, *Nature* **2004**, *428*, 911-918.
- [3] a) N. R. Armstrong, W. Wang, D. M. Alloway, D. Placencia, E. Ratcliff, M. Brumbach, *Macromol. Rapid Commun.* **2009**, *30*, 717-731; b) D. Braun, *Mater. Today* **2002**, *5*, 32-39; c) O. Nuyken, S. Jungermann, V. Wiederhorn, E. Bacher, K. Meerholz, *Monatsh. Chem.* **2006**, *137*, 811-824.
- [4] <http://www.samsungmobilepress.com/2014/09/03/Samsung-Introduces-the-Latest-in-its-Iconic-Note-Series---The-Galaxy-Note-4,-and-Showcases-Next-Generation-Display-with-Galaxy-Note-Edge-1>, state 13.09.2014, 13:48.
- [5] a) W. Wu, Y. Liu, D. Zhu, *Chem. Soc. Rev.* **2010**, *39*, 1489-1502; b) H. Sirringhaus, N. Tessler, R. H. Friend, *Science* **1998**, *280*, 1741-1744.
- [6] C. M. Roberts, *Computers & Security* **2006**, *25*, 18-26.
- [7] a) G. Dennler, M. C. Scharber, C. J. Brabec, *Adv. Mater.* **2009**, *21*, 1323-1338; b) B. C. Thompson, J. M. J. Fréchet, *Angew. Chem., Int. Ed.* **2008**, *47*, 58-77; c) G. Li, V. Shrotriya, J. Huang, Y. Yao, T. Moriarty, K. Emery, Y. Yang, *Nat. Mater.* **2005**, *4*, 864-868; d) Z. He, C. Zhong, S. Su, M. Xu, H. Wu, Y. Cao, *Nat. Photon.* **2012**, *6*, 591-595.
- [8] http://www.heliatek.com/newscenter/latest_news/heliatek-erzielt-effizienzrekord-mit-40-transparenten-organischen-solarzellen/?lang=en, state 13.09.2014, 15:04.
- [9] <http://www.samsungmobilepress.com/2014/09/03/GALAXY-Note-Edge>, state 13.09.2014, 13:54.
- [10] <http://www.heliatek.com/newscenter/download/>, state 13.09.2014, 16:49.
- [11] a) A. J. Heeger, *Angew. Chem., Int. Ed.* **2001**, *40*, 2591-2611; b) A. G. MacDiarmid, *Angew. Chem., Int. Ed.* **2001**, *40*, 2581-2590; c) H. Shirakawa, *Angew. Chem., Int. Ed.* **2001**, *40*, 2575-2580.
- [12] H. Shirakawa, E. J. Louis, A. G. MacDiarmid, C. K. Chiang, A. J. Heeger, *J. Chem. Soc., Chem. Commun.* **1977**, 578-580.
- [13] G. Inzelt, *Conducting Polymers: A New Era in Electrochemistry*, 1. ed., Springer-Verlag, Berlin Heidelberg, **2008**.
- [14] M. Rehn, *Chem. unserer Zeit* **2003**, *37*, 18-30.
- [15] Y. Kanbur, M. Irimia-Vladu, E. D. Głowacki, G. Voss, M. Baumgartner, G. Schwabegger, L. Leonat, M. Ullah, H. Sarica, S. Erten-Ela, R. Schwödiauer, H. Sitter, Z. Küçükyavuz, S. Bauer, N. S. Sariciftci, *Org. Electron.* **2012**, *13*, 919-924.
- [16] E. V. Anslyn, D. A. Dougherty, *Modern Physical Organic Chemistry*, University Science Books, Sausalito, CA, **2006**.
- [17] P. Kovacic, M. B. Jones, *Chem. Rev.* **1987**, *87*, 357-79.

- [18] J. H. Burroughes, D. D. C. Bradley, A. R. Brown, R. N. Marks, K. Mackay, R. H. Friend, P. L. Burns, A. B. Holmes, *Nature* **1990**, *347*, 539-541.
- [19] I. Osaka, R. D. McCullough, *Acc. Chem. Res.* **2008**, *41*, 1202-1214.
- [20] A. F. Diaz, K. K. Kanazawa, G. P. Gardini, *J. Chem. Soc., Chem. Commun.* **1979**, 635-636.
- [21] D. Quintens, W. Fischer, F. Jonas, H. Ohst, H. Rehbein, *Agfa-Gevaert A.-G.*, EP570795A1, **1993**.
- [22] G. Barbarella, M. Melucci, G. Sotgiu, *Adv. Mater.* **2005**, *17*, 1581-1593.
- [23] R. Kroon, M. Lenes, J. C. Hummelen, P. W. M. Blom, B. d. Boer, *Polym. Rev.* **2008**, *48*, 531-582.
- [24] H. A. M. v. Mullekom, J. A. J. M. Vekemans, E. E. Havinga, E. W. Meijer, *Materi. Sci. Eng. R.* **2001**, *32*, 1-40.
- [25] a) N. Blouin, A. Michaud, M. Leclerc, *Adv. Mater.* **2007**, *19*, 2295-2300; b) Z. Zhu, D. Waller, R. Gaudiana, M. Morana, D. Mühlbacher, M. Scharber, C. Brabec, *Macromolecules* **2007**, *40*, 1981-1986; c) J. Hou, H.-Y. Chen, S. Zhang, G. Li, Y. Yang, *J. Am. Chem. Soc.* **2008**, *130*, 16144-16145.
- [26] T. Yamamoto, K. Sanechika, A. Yamamoto, *J. Polym. Sci., Polym. Lett. Ed.* **1980**, *18*, 9-12.
- [27] a) R. L. Elsenbaumer, K. Y. Jen, R. Oboodi, *Synth. Met.* **1986**, *15*, 169-174; b) R. Sugimoto, S. Takeda, H. B. Gu, K. Yoshino, *Chem. Express* **1986**, *1*, 635-638.
- [28] M. Leclerc, F. M. Diaz, G. Wegner, *Makromol. Chem.* **1989**, *190*, 3105-3116.
- [29] R. D. McCullough, R. D. Lowe, *J. Chem. Soc., Chem. Commun.* **1992**, 70-72.
- [30] a) A. Yokoyama, R. Miyakoshi, T. Yokozawa, *Macromolecules* **2004**, *37*, 1169-1171; b) E. E. Sheina, J. Liu, M. C. Iovu, D. W. Laird, R. D. McCullough, *Macromolecules* **2004**, *37*, 3526-3528; c) M. C. Iovu, E. E. Sheina, R. R. Gil, R. D. McCullough, *Macromolecules* **2005**, *38*, 8649-8656.
- [31] a) T. A. Chen, R. D. Rieke, *J. Am. Chem. Soc.* **1992**, *114*, 10087-10088; b) R. S. Loewe, S. M. Khersonsky, R. D. McCullough, *Adv. Mater.* **1999**, *11*, 250-253; c) T. Yokozawa, R. Suzuki, M. Nojima, Y. Ohta, A. Yokoyama, *Macromol. Rapid Commun.* **2011**, *32*, 801-806.
- [32] J. Liu, M. Arif, J. Zou, S. I. Khondaker, L. Zhai, *Macromolecules* **2009**, *42*, 9390-9393.
- [33] a) E. Elmalem, F. Biedermann, K. Johnson, R. H. Friend, W. T. S. Huck, *J. Am. Chem. Soc.* **2012**, *134*, 17769-17777; b) H.-H. Zhang, C.-H. Xing, Q.-S. Hu, *J. Am. Chem. Soc.* **2012**, *134*, 13156-13159; c) R. Grisorio, P. Mastrorilli, G. P. Suranna, *Polym. Chem.* **2014**, *5*, 4304-4310; d) A. Yokoyama, H. Suzuki, Y. Kubota, K. Ohuchi, H. Higashimura, T. Yokozawa, *J. Am. Chem. Soc.* **2007**, *129*, 7236-7237.
- [34] E. Elmalem, A. Kiriya, W. T. S. Huck, *Macromolecules* **2011**, *44*, 9057-9061.
- [35] a) T. Yokozawa, H. Kohno, Y. Ohta, A. Yokoyama, *Macromolecules* **2010**, *43*, 7095-7100; b) S. Kang, R. J. Ono, C. W. Bielawski, *J. Am. Chem. Soc.* **2013**, *135*, 4984-4987.
- [36] H. Braunschweig, T. Kupfer, *Chem. Commun.* **2011**, *47*, 10903-10914.
- [37] H. Braunschweig, T. Kupfer, *Chem. Commun.* **2008**, *37*, 4487-4489.
- [38] J. J. Eisch, N. K. Hota, S. Kozima, *J. Am. Chem. Soc.* **1969**, *91*, 4575-4577.
- [39] Other methods are known, but they all have their drawbacks compared to the tin-boron exchange.

- [40] J. J. Eisch, J. E. Galle, S. Kozima, *J. Am. Chem. Soc.* **1986**, *108*, 379-385.
- [41] H. Braunschweig, C.-W. Chiu, A. Damme, K. Ferkinghoff, K. Kraft, K. Radacki, J. Wahler, *Organometallics* **2011**, *30*, 3210-3216.
- [42] a) H. Braunschweig, C.-W. Chiu, A. Damme, B. Engels, D. Gamon, C. Hörl, T. Kupfer, I. Krummenacher, K. Radacki, C. Walter, *Chem. Eur. J.* **2012**, *18*, 14292-14304; b) H. Braunschweig, A. Damme, J. O. C. Jimenez-Halla, C. Hörl, I. Krummenacher, T. Kupfer, L. Mailänder, K. Radacki, *J. Am. Chem. Soc.* **2012**, *134*, 20169-20177; c) C.-W. So, D. Watanabe, A. Wakamiya, S. Yamaguchi, *Organometallics* **2008**, *27*, 3496-3501.
- [43] Boroles that do not show antiaromatic character were not considered in this short introduction.
- [44] a) T. Araki, A. Fukazawa, S. Yamaguchi, *Angew. Chem., Int. Ed.* **2012**, *51*, 5484-5487; b) C. Fan, W. E. Piers, M. Parvez, *Angew. Chem., Int. Ed.* **2009**, *48*, 2955-2958.
- [45] A. C. J. Heinrich, B. Thiedemann, P. J. Gates, A. Staubitz, *Org. Lett.* **2013**, *15*, 4666-4669.
- [46] a) N. Yuki, H. Ikuya, T. Norihiko, T. Kyozauro, *Jpn. J. Appl. Phys.* **2004**, *43*, 4248; b) N. Yuki, T. Kyozauro, *Jpn. J. Appl. Phys.* **2006**, *45*, 2628; c) H. Cao, J. Ma, G. Zhang, Y. Jiang, *Macromolecules* **2005**, *38*, 1123-1130; d) U. Salzner, J. B. Lagowski, P. G. Pickup, R. A. Poirier, *Synth. Met.* **1998**, *96*, 177-189.
- [47] G. L. Gibson, T. M. McCormick, D. S. Seferos, *J. Am. Chem. Soc.* **2011**, *134*, 539-547.
- [48] T. Yamamoto, Z.-h. Zhou, T. Kanbara, M. Shimura, K. Kizu, T. Maruyama, Y. Nakamura, T. Fukuda, B.-L. Lee, *J. Am. Chem. Soc.* **1996**, *118*, 10389-10399.
- [49] B. Pignataro, *Tomorrow's Chemistry Today*, 2nd ed., Wiley-VCH, Weinheim **2009**.
- [50] R. C. Coffin, J. Peet, J. Rogers, G. C. Bazan, *Nat. Chem.* **2009**, *1*, 657-661.
- [51] Due to the exocyclic trimethyl tin groups, **3** showed a sensitivity towards acidic conditions, and with TEA conditioned silica as well as dried and light protected deuterated chloroform should be used.
- [52] A. A. El-Shehawy, N. I. Abdo, A. A. El-Barbary, J.-S. Lee, *Eur. J. Org. Chem.* **2011**, *2011*, 4841-4852.
- [53] a) J. Kulhanek, F. Bures, O. Pytela, T. Mikysek, J. Ludvik, *Chem. Asian J.* **2011**, *6*, 1604-1612; b) P. Pawluc, A. Franczyk, J. Walkowiak, G. Hreczycho, M. Kubicki, B. Marciniak, *Tetrahedron* **2012**, *68*, 3545-3551; c) S.-L. Zheng, N. Lin, S. Reid, B. Wang, *Tetrahedron* **2007**, *63*, 5427-5436.
- [54] A. Alhaj Zen, J. W. Aylott, W. C. Chan, *Tetrahedron Lett.* **2014**, *55*, 5521-5524.
- [55] S. Hitosugi, D. Tanimoto, W. Nakanishi, H. Isobe, *Chem. Lett.* **2012**, *41*, 972-973.
- [56] The resolution of the used MALDI spectrometer was very low and can deviate up to several Da. Thus, end group analysis was impossible.
- [57] Because another type of monomer was needed, the synthesis of **10** was not optimized.
- [58] I. Osaka, R. D. McCullough, *Acc. Chem. Res.* **2008**, *41*, 1202-1214.
- [59] F. Ge, G. Kehr, C. G. Daniliuc, G. Erker, *J. Am. Chem. Soc.* **2014**, *136*, 68-71.
- [60] H. Braunschweig, C.-W. Chiu, K. Radacki, P. Brenner, *Chem. Commun.* **2010**, *46*, 916-918.
- [61] A. D. Miller, J. F. Tannaci, S. A. Johnson, H. Lee, J. L. McBee, T. D. Tilley, *J. Am. Chem. Soc.* **2009**, *131*, 4917-4927.

-
- [62] L.-Y. He, M. Schulz-Senft, B. Thiedemann, J. Linshoeft, P. J. Gates, A. Staubitz, *Chem. Commun.* **2014**, submitted.
- [63] C. V. Pham, H. B. Mark, H. Zimmer, *Synth. Commun.* **1986**, *16*, 689-696.
- [64] On two occasions, when the experiment was repeated, the microwave vial exploded for unknown reasons. This could be prevented by adding one drop of dry DMSO. Due to the high absorption coefficient for microwave irradiation, DMSO aids in the heating process.
- [65] The carbon atom bound to boron was not visible due to the high quadrupole moment of the boron nucleus.
- [66] G. A. Chotana, V. A. Kallepalli, R. E. Maleczka, M. R. Smith Iii, *Tetrahedron* **2008**, *64*, 6103-6114.
- [67] The absorption spectrum was recorded during the purification with the Interchim puriFlash system. Due to a very high scan speed (the exact value is unknown), the shape of the absorption spectrum differs slightly from the spectrum of the other stannole monomers which were recorded on the Perkin Elmer Lambda14 spectrometer.
- [68] The available substance amounts were too low for a precise determination of an extinction coefficient.
- [69] R. Tkachov, V. Senkovskyy, H. Komber, A. Kiriya, *Macromolecules* **2011**, *44*, 2006-2015.
- [70] T. Yokozawa, R. Suzuki, M. Nojima, Y. Ohta, A. Yokoyama, *Macromol. Rapid. Commun.* **2011**, *32*, 801-806.
- [71] Due to this sensitivity, the melting point, IR spectrum and mass spectrum were not obtained.